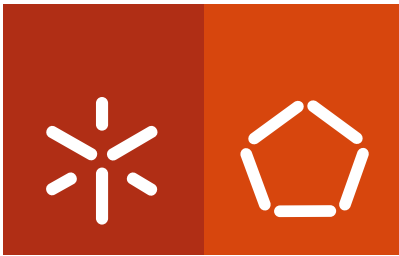Universidade do Minho
Escola de Engenharia

Susana Isabel Ribeiro Cerqueira

Cell targeted nanoparticle-based drug delivery systems for spinal cord injury regeneration

novembro de 2013

Universidade do Minho
Escola de Engenharia

Susana Isabel Ribeiro Cerqueira

Cell targeted nanoparticle-based drug delivery systems for spinal cord injury regeneration

Programa Doutoral em Engenharia de Tecidos, Medicina Regenerativa e Células Estaminais

Trabalho realizado sob a orientação do
Professor Doutor Rui Luís Gonçalves dos Reis
e do
Professor Doutor Nuno Jorge Carvalho de Sousa

novembro de 2013

Declaração

Nome: Susana Isabel Ribeiro Cerqueira

Endereço eletrónico: susana.cerqueira@dep.uminho.pt

Número de cartão do cidadão: 123089166ZZ7

Título da dissertação:

Cell targeted nanoparticle-based drug delivery systems for spinal cord injury regeneration

Programa Doutoral em Engenharia de Tecidos,
Medicina Regenerativa e Células Estaminais

Orientadores:

Professor Doutor Rui Luís Gonçalves dos Reis

Professor Doutor Nuno Jorge Carvalho de Sousa

Ano de conclusão: 2013

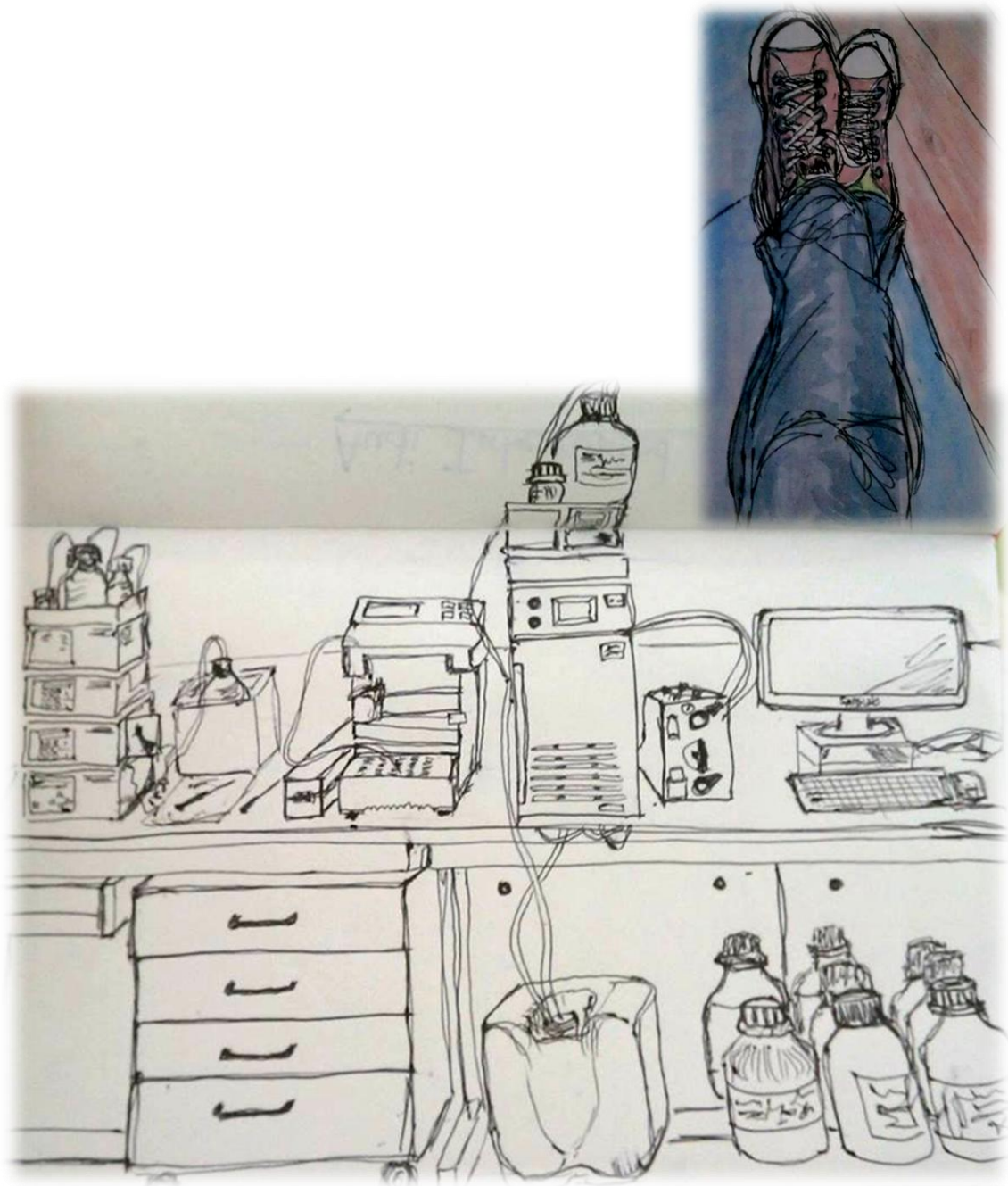Universidade do Minho,   /   / 2013

Assinatura:

Ao Manuel, à Anita e ao Luís,

os meus pilares.

"So many of our dreams at first seem impossible, then they seem improbable,

And then, when we summon the will, they soon become inevitable."

Christopher Reeve (1952 – 2004)

Inscription on the Lois Pope Life Center fountain.

Another way of looking at it.

(some personal sketches)

ACKNOWLEDGEMENTS

I present to you the result of my PhD work, compiled in this thesis. It is the product of an intense and enriching journey that brought me to where I am now. Naturally, a number of people walked along this path beside me, contributing in varied ways for this final product and I genuinely acknowledge all of them.

I would like to start expressing my appreciation to my supervisor Professor Rui L. Reis, for accepting me as his student in the 3B´s Research Group. I sincerely value your continuous support and promptness in relation to all my questions that always earned wise and frank replies. I cannot disregard the amazing opportunities of attending international conferences and collaborating with other international institutes, always with your incentive. I am very thankful, Professor Rui, for your continuous encouragement and mentorship, particularly in these last months.

Professor Nuno Sousa, my project co-supervisor, was an inspiring mentor. You showed me the different perspectives and directions I could pursue in my work whenever I needed and I deeply appreciate that. Thank you for being "the teacher who shows where to look, without telling what to see". I am also truly grateful for your warm and kind hugs, which were as motivating and helpful as the precious scientific input.

I am particularly grateful to Dr Miguel Oliveira for his generous and relentless guidance and support throughout all this work. Hopefully I did not disappoint you and "your" tiny dendrimers. My genuine appreciation for your constant availability and endless enthusiasm that turned out to be critical in my performance.

Dr António Salgado was also a key contributor and impellor in this work that started back when I was doing my BSc final project. You advised me to embrace this PhD project, and here I am. This thesis has your contributions and input, as well. I appreciate your assistance in the PhD project writing for my FCT fellowship.

I cannot properly express how privileged I feel to have had the opportunity to collaborate as well with Professor Mary Bartlett Bunge, in the Miami Project to Cure Paralysis, and Professor Robert Zorec, in the Pathophysiology Institute of the Faculty of Medicine of the University of Ljubljana. Dr Mary, you are an inspiration to me as a scientist and as a woman. Your strength and kindness are admirable. It was an honour to be part of your team. Professor Robert, thank you for welcoming me in your lab with such confidence in me and my skills, and giving me the amazing opportunity of collaborating with your group. Postojna and Pokljuka were amazing. *Hvala lepa.*

Helena Chowdhury was a precious co-supervisor in Ljubljana. I really appreciate all your efforts and assistance in organizing my stay and assisting me in the workplanning, making sure everything would go on smoothly. And it did. Thank you, Lenka.

CELL TARGETED NANOPARTICLE-BASED DRUG DELIVERY SYSTEMS FOR SPINAL CORD INJURY REGENERATION

ABSTRACT

Spinal cord injuries (SCI) afflict millions of people every year worldwide. Since no cure exists for such neurotraumatic episodes, patients thus experience highly debilitating symptoms. These comprehend partial to complete muscular weakness and sensory loss, and commonly lead to paraplegia or tetraplegia. The tremendous complexity of cellular and biochemical reactions that follow the initial trauma, along with the lack of specificity of the drugs used, are hindering the development of effective treatments for SCI. Current clinical options are thus mainly based on palliative care, and systemic high dose administration of methylprednisolone (MP), a powerful anti-inflammatory and antioxidant corticosteroid that has shown to lead to functional recovery. However, the unspecificity and deleterious side effects of MP are making some clinicians cautious towards its administration. Actually, this treatment is very controversial, therefore, new enhanced approaches are needed to repair the injured spine and provide SCI patients a better quality of life.

The most recent developments in nanotechnology show great promise for tissue engineering advanced solutions. Recently, poly(amido)amine (PAMAM) dendrimer nanoparticles grafted with CMCht have been proposed as intracellular nanocarriers for stem cell osteogenic differentiation. In this thesis, it was explored the application of the developed CMCht/PAMAM dendrimer nanoparticles for neuroprotection of the injured spinal cord tissue, ultimately contributing to regeneration and repair. Firstly, functionalization of CMCht/PAMAM dendrimer nanoparticles was performed covalently binding an antibody to its structure, and then incorporating a relevant drug, such as MP. Both modifications were confirmed using spectroscopic techniques and *in vitro* biological evaluation was performed in primary cortical glial cultures. No cytotoxicity associated with the multifunctional CMCht/PAMAM dendrimer nanoparticles was observed. *In vitro* internalization studies revealed a differential uptake, when the antibody was bond to the CMCht/PAMAM dendrimer nanoparticles. Therefore, the addition of targeting moieties to the nanoparticles contributed to a modulation of the nanoparticle uptake by glial cells. In order to analyze the intracellular trafficking, as well as internalization and clearance routes,

electrophysiology recordings of live astrocyte (single-cell) membrane capacitance were performed after incubation with MP-loaded CMCht/PAMAM dendrimer nanoparticles. The patch-clamp studies showed that nanoparticles do affect both endocytosis and exocytosis rates. In fact, these observations were further confirmed by confocal microscope visualization of astrocyte endocytotic and exocytotic vesicles. To our knowledge, this study clarified for the first time the endocytotic/exocytotic pathways that nanoparticles follow in primary nervous cells, demonstrating for the first time the exocytotic clearance of the nanoparticles. Following this, administration of FITC-labeled MP-loaded CMCht/PAMAM dendrimer nanoparticles in the cerebrospinal fluid (CSF) of healthy rats was performed. The distribution of the nanoparticles was widespread along several brain areas and layers, showing that once the blood-brain barrier (BBB) is overcome the nanoparticles are easily transported and retained in the brain tissue. Moreover, the drug was shown to be acting intracellularly by protein expression quantification. Subsequently, extensive investigation of the physico-chemical characteristics of the MP-loaded nanoparticles was carried out revealing its spherical 109 nm structure and zeta potential stability. Moreover, a preliminary therapeutic assessment of this system was analyzed *in vitro* in microglial cultures, and *in vivo* in an animal model of SCI. Promising results were obtained with the successful modulation of microglia proliferation, and significant locomotor improvements in the treated injured animals. Finnaly, biocompatibility and functionality studies were performed in Schwann cell pure cultures and co-cultures with dorsal root ganglia neurons, when in contact with the MP-loaded CMCht/PAMAM dendrimer nanoparticles. The presence of nanoparticles has not affected the cell morphology or typical distribution in culture. Moreover, extensive myelination was performed by Schwann cells that enveloped the axons of dorsal root ganglia neurons, showing normal viability and function. These results open new possibilities for therapeutic strategies, namely combination of Schwann cell transplantation and nanoparticle administration.

From these findings, new knowledge regarding nanoparticle interaction with nervous cells was obtained, along with the potential therapeutic value. For the first time, multifunctionalization of CMCh/PAMAM dendrimer nanoparticles was successfully accomplished and proved to modulate the cell uptake rates. Moreover, the innovative use of patch-clamp electrophysiology for the quantification of vesicle formation/fusion in the cell membrane following nanoparticle incubation proved to be useful in this type of studies. The promising locomotor improvements observed in nanoparticle-treated SCI animals, along with the biocompatibility of these nanoparticles for CNS applications, bring new hopes for the development of successful strategies for SCI repair.

SISTEMAS DE LIBERTAÇÃO DE FÁRMACOS BASEADOS EM NANOPARTÍCULAS PARA DIRECCIONAMENTO CELULAR E REGENERAÇÃO DE LESÕES DE ESPINAL MEDULA

RESUMO

Lesões traumáticas na espinal medula afetam anualmente milhões de pessoas em todo o mundo. Atualmente não existe cura para lesões neurotraumáticas, e os pacientes vivenciam sintomas altamente debilitantes. Estes vão desde parcial a total perda de força muscular e perceção sensorial, e comummente culminam em paraplegia ou tetraplegia. A elevada complexidade de reações celulares e bioquímicas que se seguem ao trauma inicial, associada à falta de especificidade das drogas em uso, têm vindo a dificultar o desenvolvimento de terapias eficazes para o tratamento de lesões na espinal medula. Como consequência, as opções clínicas atuais centram-se maioritariamente em cuidados paliativos e na administração sistémica aguda de metilprednisolona (MP), um poderoso corticosteroide anti-inflamatório e antioxidante que demonstrou melhorias funcionais em pacientes. No entanto, a falta de especificidade e os graves efeitos secundários associados à administração sistémica de MP estão a levar alguns especialistas a administrá-la com grande precaução. De facto, a aplicação desta terapêutica é bastante controversa logo, é essencial e urgente desenvolver novas estratégias mais eficazes e seguras para regenerar a espinal medula, de forma a poder proporcionar aos pacientes uma melhor qualidade de vida.

Os mais recentes desenvolvimentos na área da nanotecnologia têm mostrado grande potencial para aplicação em estratégias avançadas de engenharia de tecidos. Recentemente, nanopartículas dendriméricas de poliamidoamina (PAMAM) superficialmente modificadas com carboximetilquitosano (CMCht) foram propostas para transporte intracelular de fármacos. Nesta tese, a aplicação destas nanopartículas dendriméricas de CMCht/PAMAM é explorada para neuroprotecção da espinal medula após lesão, tendo como objetivo permitir a regeneração do tecido. Primeiramente procedeu-se à funcionalização das nanopartículas dendriméricas CMCht/PAMAM através da ligação covalente de um anticorpo à sua estrutura, e subsequente incorporação do corticosteroide MP. Ambas as modificações foram confirmadas por análise espectroscópica, e de seguida efetuou-se uma avaliação biológica *in vitro* em culturas primárias de células da glia. Não foi observado qualquer efeito citotóxico relacionado com a presença das nanopartículas multifuncionais nas culturas e a presença do anticorpo na sua estrutura originou

uma alteração do perfil de internalização das mesmas nas culturas de glia. Confirmou-se, assim, que a adição de agentes de direcionamento à estrutura das nanopartículas CMCht/PAMAM contribui para a alteração da distribuição da internalização celular. Com a finalidade de analisar a distribuição intracelular das nanopartículas, assim como as vias de internalização e remoção, efetuaram-se análises eletrofisiológicas para medir a capacitância de membrana de astrócitos viáveis após incubação com nanopartículas com MP. Os estudos de patch-clamp demonstraram que as nanopartículas afetam as taxas de endocitose e exocitose destas células. Estas observações foram também confirmadas por observação por microscopia confocal e quantificação de fluorescência. Este estudo clarifica pela primeira vez as vias que estas nanopartículas seguem em células nervosas, nomeadamente endocitose e exocitose. Seguidamente, administrou-se nanopartículas com MP e marcadas com o fluorocromo FITC no líquido cefalorraquidiano de ratos saudáveis e verificou-se uma distribuição ampla ao longo de várias regiões e camadas do cérebro, provando que uma vez ultrapassada a barreira hematoencefálica as nanopartículas facilmente são transportadas no tecido nervoso. Posteriormente, procedeu-se à caracterização físico-química das nanopartículas incorporadas com MP e efetuou-se uma avaliação preliminar do potencial terapêutico deste sistema em culturas de microglia e *in vivo* num modelo animal de lesão de espinal medula. A modulação da proliferação de microglias *in vitro*, assim como as melhorias locomotoras registadas nos animais lesionados tratados com nanopartículas são resultados bastante encorajadores. Finalmente, os estudos de biocompatibilidade e funcionalidade em células de Schwann expostas a nanopartículas incorporadas com MP não indicaram qualquer anomalia na morfologia celular ou na típica distribuição destas células em cultura. Quando em co-cultura com neurónios de gânglios espinais, as células de Schwann mielinizaram de forma extensa os axónios destas células, comprovando a sua normal viabilidade e funcionalidade.

Destes resultados, obteve-se novo conhecimento acerca da interação de nanopartículas dendriméricas CMCht/PAMAM multifuncionalizadas com células nervosas, assim como do seu potencial valor terapêutico em lesões de espinal medula. Efetuou-se com sucesso uma funcionalização que conduziu à alteração do perfil de internalização celular. O uso inovador de eletrofisiologia patch-clamp para quantificar a formação/fusão de vesículas na membrana celular após incubação com nanopartículas demostrou ter extrema utilidade neste tipo de estudos. Os resultados obtidos revelando melhorias locomotoras em animais lesionados e tratados com nanopartículas com metilprednisolona, associados à biocompatibilidade destas nanopartículas para aplicações do foro neurológico, traz renovada esperança na busca de melhores estratégias para tratar de forma eficaz as consequências de lesões na espinal medula.

TABLE OF CONTENTS

#
α – alpha

A
A/B - antibiotic
ANOVA – analysis of variance
ATP – adenosine-5'-phosphate

B
BBB – blood-brain barrier; or Basso, Beattie and Bresnahan locomotor test
BCSFB – blood-cerebrospinal fluid barrier
BDNF – brain-derved neurotrophic factor
BMSCs – bone marrow stromal cells
BrdU – 5-bromo-2'-deoxyuridine
BSCB – blood-spinal cord barrier

C
Ca – calcium
$CaCl_2$ – calcium chloride
CB - cerebellum
CD11b – cluster of differentiation 11b
Cht – chitosan
Cm – membrane capacitance
CMCht - carboxymethylchitosan
CNS – central nervous system
CP – choroid plexus
CO_2 – carbon dioxide
CSF – cerebrospinal fluid
CSPG – chondroitin sulfate proteoglycans

D
D_2O – deuterated water
Da – Dalton
DAPI – 4',6-diamino-2-phenylindole
DD – degree of deacetylation
DDS – drug delivery system
DLS – dynamic light scattering
DMEM – Dulbecco´s modified Eagle´s medium
DMEM-F12 - Dulbecco´s modified Eagle´s medium, nutrient mixture F-12

DMSO – dimethyl sulfoxide
DNA – deoxyribonucleic acid
DNAse - deoxyribonuclease
DPPC – dipalmitoylphosphatidylcholine
DRGN – dorsal root ganglia neurons
DS – degree of substitution

E
ECM – extracellular matrix
ECS – extracellular solution
EDA – ethylene diamine
EDC - 1-ethyl-3-(3-dimethylaminopropyl) carbodiimide
EDTA - ethylenediamine tetraacetic acid
ELISA - enzyme-linked immunosorbent assay
ESC – embryonic stem cells
EU – European Union

F
FBS – fetal bovine serum
FGF – fibroblast growth factor
FITC – fluorescein isothiocyanate
FL – forelimb
FTIR - Fourier transform infrared spectroscopy
FUDR - floxuridine

G
G – (dendrimer) generation
GDNF – glia-derived neurotrophic factor
GFAP – glial fibrillary acidic protein
GR – glucocorticoid receptor

H
H – hydrogen
[3]H - tritium
HAMC – hyaluronan/methylcellulose
HBSS - Hank's balanced salt solution
HCl – hydrochloric acid
He - helium

HEPES – 4-(2-hydroxyethyl)-1-piperazineethalnesulfonic acid
HL – hind limb
HPC – hippocampus
HPLC – high-performance liquid chromatography
hr - hour
HRP – horseradish peroxidase
Hz – hertz

I
I - internalization
i.e. – *id est*
IgG – immunoglobulin G
iPSCs – induced pluripotent stem cells

K
K^+ - potassium
KBr – potassium bromide
kDa – kilodalton
kg - kilogram
kHz – kilohertz

L
L-15 – Leibovitz
LDV - Laser Doppler velocimetry
LV – lateral ventriculus

M
M – molar
MAG – myelin-based glycoprotein
MAP-2 – microtubule-associatedprotein 2
MBP – myelin basic protein
mg – miligram
Mg – magnesium
MgCl – magnesium chloride
MHz – megahertz
min – minute
mL – mililiter
mm – milimeter
mM – milimolar
MΩ - megaohm
mOsm - miliosmole
MP – methylprednisolone
MS – multiple sclerosis
MSCs – mesenchymal stem cells
MTS – 3-(4,5 – dimethylthiazol-2-yl)-5-(3-carboxymethoxyphenol)-2H-tetrazolium

N
n – total number of data points
NAC – N-acetylcysteyne
NaCl – sodium chloride
Na_2CO_3 – sodium carbonate
NaOH – sodium hydroxide
Ne - neon
NGF – nerve growth factor
nm – nanometer
NMR – nuclear magnetic resonance
NP – nanoparticle
NPs – nanoparticles
NPY – neuropeptide Y
NSC – neural stem cells
NT-3 – neurotrophin-3

O
O4 – oligodendrocyte marker 4
OCT – optimal cutting temperature
OD – optical density
OECs – olfactory ensheating cells
OMgp – oligodendrocyte myelin protein
OsO_4 – osmium tetroxide

P
p – probability value
PAGE - polyacrilamide gel electrophoresis
PAMAM – poly(amido)amine
PAMAM-CT – carboxylic acid- terminated poly(amido)amine
PBS – phosphate buffered saline
PEG – polyethylene glycol
PFA – paraformaldehyde
PFC – pre-frontal córtex
PLA – polylactic acid
PLGA – poly(lactic-co-glycolic) acid
PMMA – poly(methyl) methacrylate
PNS – peripheral nervous system
PPV - polyphenylenevinylene

R
RIPA – radio immune precipitation assay
ROS – reactive oxygen species
rpm – revolutions per minute
RT – room temperature

S
s – second

SCs – Schwann cells
SCI – spinal cord injury
SD – standard deviation
SDS - sodium dodecyl sulfate
SEM – standard error of the mean, or
scanning electron microscopy
siRNA – small interference ribonucleic acid
SPCL – starch/ polycaprolactone
STEM – scanning-transmission electron
microscopy

T
T – thoracic level
TAC – tacrolimus
TBI – traumatic brain injury
TEM – transmission electron microscopy
TFA – trifluoroacetic acid
Tris - (hydroxymethyl)aminomethane

U
U – enzyme unit
UK – United kingdom
µL – microliter
µm - micrometer
USA – United States of America
UV - ultraviolet

V
v/v – volume per volume

W
w/v – weight per volume

X
x - times

SECTION I

CHAPTER I. Introduction – Nanotechnology advances in tissue engineering for drug delivery following neurotrauma

SECTION II

CHAPTER II. Materials and methods

SECTION III

CHAPTER III. Multifunctionalized CMCht/PAMAM dendrimer nanoparticles modulate the cellular uptake by astrocytes and oligodendrocytes in primary cultures of glial cells

CHAPTER IV. Electrophysiological quantification of cellular internalization, retention and exocytosis of drug-loaded nanoparticles in astrocytes

CHAPTER V. Dendrimer nanoparticle diffusion in the rat brain parenchyma following intracisternal administration

CHAPTER VI. Microglia response and *in vivo* therapeutic potential of methylprednisolone loaded dendrimer nanoparticles in spinal cord injury

CHAPTER VII. Biocompatibility and functionality studies of MP-loaded CMCht/PAMAM dendrimer nanoparticles with Schwann cell cultures

LIST OF TABLES

SECTION I

CHAPTER I. Introduction – Nanotechnology advances in tissue engineering for drug delivery following neurotrauma

SECTION II

CHAPTER II. Materials and methods

SHORT CURRICULUM VITAE

Susana Cerqueira was born in Braga, Portugal, in 1983. She obtained her BSc degree in Applied Biology from the School of Sciences at the University of Minho in 2008. Her final project was developed at the 3B´s Research Group in collaboration with the Life and Health Sciences Research Institute (ICVS) under the supervision of Dr António Salgado and Dr Miguel Oliveira. In 2009, Susana initiated her Doctoral Program in Tissue Engineering, Regenerative Medicine and Stem Cells at the ICVS/3B´s Associate Lab, under the supervision of Professor Rui L. Reis and Professor Nuno Sousa. During the course of her PhD she visited and collaborated with Prof. Robert Zorec from the University of Ljubljana, Slovenia, and Prof. Mary Bartlett Bunge from the Miami Project to Cure Paralysis, University of Miami, USA.

Susana was awarded a scholarship from the Portuguese Foundation for Science and Technology (FCT) to conduct her PhD project in 2009. She has received a fellowship to participate in the "Nanotechnology and Nanomedicine" course that took place in the International Nanotechnology Laboratory. In 2012, she was selected to attend the NIH/NINDS Spinal Cord Injury Research Training Program, taking place at the Ohio State University. She was also attributed a COST-NAMABIO grant for the execution of a Short Term Scientific Mission in the Faculty of Medicine of the University of Ljubljana, Slovenia in 2013.

She is a member of the Society for Neuroscience, Portuguese Society for Neuroscience, Tissue Engineering and Regenerative Medicine International Society, and the Portuguese Society of Stem Cells and Cellular Therapies.

As a result of her research efforts she is currently author of 4 publications, with 5 others submitted. Additionally, she has presented 20 communications (10 oral and 10 posters) in international conferences. She has been invited for 4 lectures.

LIST OF PUBLICATIONS

The research studies performed during the extent of this PhD, including collaborative work, resulted in the following publications:

Peer-reviewed journals

Cerqueira S. R., Oliveira J. M., Silva N. A., Leite-Almeida H., Samy S. M., Almeida A., Mano J. F., Sousa N., Salgado A. J., and Reis R. L., ''Microglia response and *in vivo* therapeutic potential of methylprednisolone-loaded dendrimer nanoparticles in spinal cord injury'', Small, vol. 9, issue 5, pp. 738-749, 2013.

Cerqueira S. R., Silva B. L., Oliveira J. M., Mano J. F., Sousa N., Salgado A. J., and Reis R. L., ''Multifunctionalized CMCht/PAMAM Dendrimer Nanoparticles Modulate the Cellular Uptake by Astrocytes and Oligodendrocytes in Primary Cultures of Glial Cells'', Macromolecular Bioscience, vol. 12, pp. 591–597, 2011.

Pojo M.,* **Cerqueira S. R.**,* Mota T., Xavier-Magalhães A., Oliveira J. M., Samy S. M., Mano J. F., Reis R. L., Costa B. M., Sousa N., and Salgado A. J., ''*In vitro* evaluation of the cytotoxicity and cellular uptake of CMCht/PAMAM dendrimer nanoparticles by glioblastoma cell models'', Journal of Nanoparticle Research (NANO), vol.15, pp.1621-1629, 2013 (*equally contributing authors*)

Pereira V. H., Salgado A. J., Oliveira J. M., **Cerqueira S. R.**, Frias A. M., Fraga J. S., Roque S., Falcão A. M., Marques F. M., Neves N. M., Mano J. F., Reis R. L., and Sousa N., ''*In Vivo* Biodistribution of Carboxymethylchitosan/Poly(amidoamine) Dendrimer Nanoparticles in Rats'', Journal of Bioactive and Compatible Polymers , vol. 26, issue 6, pp. 619–627, 2011.

Invited Lecture

Cerqueira S. R., Oliveira J. M., Mano J. F., Sousa N., Salgado A. J., and Reis R. L., ''Regeneration Strategies in the Central Nervous System'', 3rd 3B´s Symposium on Biomaterials and Stem cells in Regenerative Medicine, 2013.

Cerqueira S. R., Oliveira J. M., Salgado A. J., Sousa N., and Reis R. L., "Nanoparticle-mediated drug delivery systems for spinal cord injury repair", Miami Project Lecture Series, The Miami Project To Cure Paralysis, Miller School of Medicine, University of Miami, 2012.

Oliveira J. M., **Cerqueira S. R.**, Salgado A. J., Sousa N., Mano J. F., and Reis R. L., "Dendrimeric nanocarriers for intracellular cell- and tissue-engineering applications", 2nd IBB Meeting, University of Minho, 2010.

Cerqueira S. R., "Why using dendrimers modified with polyssacharides in cell engineering?", 3B's Short Workshop on Natural-Based Polymers for Biomedical Applications, 2009.

Presentations in international conferences

Cerqueira S. R., Chowdhury H. H., Mano J. F., Oliveira J. M., Sousa N., Zorec R., and Reis R. L., "Internalization, intracellular retention and release of drug-loaded dendrimer nanoparticles in astrocytes", TERM STEM 2013, 2013.

Cerqueira S. R., Oliveira J. M., Silva B. L., Silva N. A., Mano J. F., Sousa N., Salgado A. J., and Reis R. L., "Targeted intracellular delivery of methylprednisolone from a dendrimer nanoparticle-based delivery system for spinal cord injury applications", 8th FENS – Forum of Neuroscience, 2012.

Oliveira J. M., Cerqueira S. R., Pereira V. H., Mano J. F., Sousa N., Salgado A. J., and Reis R. L., "*In vitro* and *in vivo* biocompatibility of carboxymethylchitosan/PAMAM dendrimer nanoparticles with potential applications in intracellular delivery strategies for bone tissue engineering and CNS", 9th World Biomaterials Congress, 2012.

Cerqueira S. R., Oliveira J. M., Silva B. L., Silva N. A., Mano J. F., Sousa N., Salgado A. J., and Reis R. L., "Intracellular delivery of methylprednisolone by dendrimer-based nanoparticles improves locomotor outcomes after spinal cord injury", TERM STEM 2012, 2012.

Cerqueira S. R., Oliveira J. M., Silva N. A., Leite-Almeida H., Samy S. M., Almeida A., Sousa N., Reis R. L., and Salgado A. J., "Local sustained nanoparticle methylprednisolone delivery improves the locomotor activity of spinal cord injured rats", Neuroscience 2012, 2012.

Cerqueira S. R., Pereira V. H., Oliveira J. M., Sousa N., Salgado A. J., and Reis R. L., "Biodistribution and preliminary therapeutic potential of CMCht/PAMAM dendrimer nanoparticles administration in rats", 3rd TERMIS World Congress, 2012.

Cerqueira S. R., Oliveira J. M., Mano J. F., Salgado A. J., Sousa N., and Reis R. L., "Intracellular methylprednisolone release to glial cells using an engineered dendrimer nanoparticle system", XXXVIII Congress of the European Society for Artificial Organs (ESAO 2011) and IV Biennial Congress of the International Federation on Artificial Organs (IFAO 2011), 2011.

Cerqueira S. R., Oliveira J. M., Mano J. F., Sousa N., Salgado A. J., and Reis R. L., "Dendrimer-based nanoparticle delivery system for the sustained and intracellular delivery of methylprednisolone to CNS cells: potential application in spinal cord injury treatment", TERMIS-EU 2011, 2011.

Cerqueira S. R., Oliveira J. M., Mano J. F., Sousa N., Reis R. L., and Salgado A. J., "Intracellular Methylprednisolone Delivery to Glial Cells by a Surface Engineered Nanoparticle System for Spinal Cord Injury Therapies", XII Meeting of the Portuguese Society for Neurosciences, 2011.

Cerqueira S. R., Oliveira J. M., Mano J. F., Sousa N., Salgado A. J., and Reis R. L., "Microglial Specific Nanoparticle Based Drug Delivery System for Spinal Cord Injury Regeneration", Annual Tissue Engineering and Regenerative Medicine International Society - TERMIS-NA Meeting, 2010.

Cerqueira S. R., Oliveira J. M., Mano J. F., Sousa N., Salgado A. J., and Reis R. L., "Microglia specific dendrimer based drug delivery system", 2nd Scientific Meeting of the Institute for Biotechnology and Bioengineering, 2010.

Pereira V. H., Cerqueira S. R., Fraga J. S., Oliveira J. M., Mano J. F., Reis R. L., Sousa N., and Salgado A. J., "CMC/PAMAM Dendrimer Nanoparticles as Intracellular Drug Delivery Systems for Central Nervous System Applications: *In Vitro* and *In Vivo* Studies", 5th International Meeting of the Portuguese Society for Stem Cells and Cellular Therapies (SPCE-TC), 2010.

Cerqueira S. R., Oliveira J. M., Mano J. F., Sousa N., Salgado A. J., and Reis R. L., "CMC/PAMAM Dendrimer Nanoparticles as Intracellular Drug Delivery Systems for Spinal Cord Injury Applications ", TERMIS EU 2010, 2010.

Cerqueira S. R., Pereira V. H., Oliveira J. M., Mano J. F., Sousa N., Reis R. L., and Salgado A. J., "CMC/PAMAM Dendrimer Nanoparticles as Intracellular Drug Delivery Systems for Spinal Cord Injury Applications", 40th Annual Meeting of the Society for Neuroscience, 2010.

Cerqueira S. R., Oliveira J. M., Mano J. F., Sousa N., Salgado A. J., and Reis R. L., "Nanoparticle-Based Cellular Drug Delivery System for Spinal Cord Injury Therapies: Internalization Efficiency and Cytotoxicity Screening ", 5th Annual International Meeting of the Portuguese Society for Stem Cells and Cellular Therapies - SPCE-TC, 2010.

Pereira V. H., Cerqueira S. R., Fraga J. S., Oliveira J. M., Mano J. F., Salgado A. J., Reis R. L., and Sousa N., "Dose dependent effects of FITC-labeled CMC/PAMAM dendrimer nanoparticles

on central nervous system derived cells: *In vitro* and *in vivo* evaluation'', TERMIS 2nd World Congress 2009, 2009.

Cerqueira S. R., Oliveira J. M., Mano J. F., Sousa N., Salgado A. J., and Reis R. L., ''Cell Targeted Nanoparticle-Based Drug Delivery System for Spinal Cord Injury Regeneration'', 5th European Symposium on Biopolymers, 2009.

Cerqueira S. R., Oliveira J. M., Mano J. F., Sousa N., Salgado A. J., and Reis R. L., ''Cell Targeted Nano-Based Drug Delivery Systems for Spinal Cord Injury Regeneration'', TERMIS 2nd World Congress 2009, 2009.

Pereira V. H., Cerqueira S. R., Fraga J. S., Oliveira J. M., Mano J. F., Reis R. L., Sousa N., and Salgado A. J., ''Dose Dependent Effects of FITC-labeled CMC/PAMAM dendrimer Nanoparticles on Central Nervous System Derived Cells: *In Vitro* and *In Vivo* Evaluation'', 11th Meeting of the Portuguese Society for Neurosciences, 2009.

Pereira V. H., Cerqueira S. R., Fraga J. S., Oliveira J. M., Mano J. F., Salgado A. J., Reis R. L., and Sousa N., ''Dose Dependent Effects of FITC-labeled CMC/PAMAM dendrimer Nanoaparticles on Central Nervous System Derived Cells: *In Vitro* and *In Vivo* Evaluation'', 2nd TERMIS World Congress, Seoul, Korea (south), August 2009, 2009.

INTRODUCTION TO THE THESIS FORMAT

This thesis is divided into four sections that comprise a total of eight chapters. The body of the thesis chapters is based on a series of related articles published or submitted for publication in international peer-reviewed journals. Each of the chapters is presented in the manuscript form, i.e., starting with an abstract and followed by introduction, materials and methods, results, discussion and conclusions. A list of references is also provided in the end of each chapter. The contents of each chapter are summarized below.

Section I

Chapter I presents a comprehensive overview on the aims of this work. It starts elucidating the reader on the physiology of the central nervous system and pathophysiology of neurotrauma, focusing on spinal cord injury (SCI). Going through the current clinical options to treat this condition, some innovative tissue engineering approaches are reviewed, focusing on drug delivery strategies using nanoparticles.

Section II

Chapter II describes the experimental techniques and protocols used to obtain the herein presented results. Although each chapter is accompanied by the description of the materials and methods utilized, this chapter intends to assemble all the relevant information concerning this matter.

Section III

This section describes the experimental work conducted within the scope of this thesis.

Chapter III reports the functionalization of MP-loaded CMCht/PAMAM dendrimer nanoparticles with a targeting agent and evaluation of the uptake of functionalized nanoparticles by primary glial cells. The viability of glia and microglia primary cultures is also taken into account to assess possible cytotoxicity of the newly developed multifunctional nanoparticles.

Chapter IV presents the investigation of the MP-loaded CMCht/PAMAM dendrimer nanoparticle uptake mechanisms, intracellular trafficking and possible clearance routes. Two combined techniques are exploited to conduct the investigation: patch-clamp electrophysiology recordings and confocal microscopy of primary live astrocytes.

Chapter V describes the assessment of the brain distribution of MP-loaded CMCht/PAMAM dendrimer nanoparticles following intracisternal administration. Confocal microscopy is used to examine the preferential localization and distribution of the injected nanoparticles in healthy Wistar rats.

Chapter VI presents a detailed physico-chemical characterization of the MP-loaded nanoparticles and assesses their influence in the metabolic activity and proliferation of primary glial cultures. Moreover, preliminary therapeutic activity of the nanoparticle-system is assessed in microglia cultures and in a rat model of SCI.

Chapter VII depicts the analysis of the interaction of MP-loaded dendrimer nanoparticles with Schwann cells. The characterization of the nanoparticle uptake profile is done, along with fluorescence microscopy assessment of the cells. Electron micrographs are observed to analyse possible nanoparticle caused ultrastructural alterations. Also, the myelination capacity of Schwann cells is verified in co-cultures of these cells with dorsal root ganglia neuron co-cultures previously incubated with nanoparticles.

Section IV

Chapter VIII contains the general conclusions of the works carried out under the scope of this thesis. General remarks and future directions are also provided.

SECTION I

CHAPTER I

Introduction – Recent nanotechnology advances in tissue engineering for drug delivery following neurotrauma

CHAPTER I

Introduction – Recent nanotechnology advances in tissue engineering for drug delivery following neurotrauma

Abstract

Neurotraumatic conditions, such as spinal cord injury (SCI), are devastating and highly debilitating neurological disorders that tremendously affect our society. Although some remarkable advances have been made in the last decades concerning its pathophysiology, no similar translation has been achieved in terms of clinical treatments. In fact, there is no effective therapeutic option for SCI yet. This has been mainly associated with the extremely complex cascade of events following trauma, a highly inhibitory set that is established at the lesion site, as well as the natural barriers that prevent the entry of pharmaceutics into the CNS. Current clinical practices in SCI management involve column stabilization and decompression, and the administration of high dosage of the corticosteroid methylprednisolone, with sometimes only modest functional improvements, however. The main reasons for treatment failure are thus the restricted access and lack of specificity of therapeutic drugs to the spine. Nanotechnology and tissue engineering are bringing new possibilities for treatment and targeted drug delivery, engineering more refined and advanced strategies for SCI repair. Herein, the most recent advances in tissue engineering for SCI will be addressed, focusing particularly on the contributions of nanotechnology for the design of new and improved drug delivery systems following neurotrauma. Some fundamental aspects of CNS cellular organization will also be briefly discussed, as well as relevant hallmarks on the pathophysiology of SCI.

1. Introduction

Richard P. Feynman first proposed the direct manipulation of atoms as a more powerful chemical synthesis technique.[1] Since then, a vast number of nanoparticles has been developed for biomedical purposes, namely liposomes, fullerenes, magnetic, and natural-based and synthetic polymeric nanoparticles.[2] Many central nervous system (CNS) disorders still completely lack effective treatments, for example spinal cord injury (SCI), leading to an urgent demand for enhanced therapeutic strategies that will provide patients with a better quality of life.[3] Neurotraumatic ailments, comprising stroke and brain/spinal cord injuries currently affect millions of people worldwide and result in severe neurological deficits, commonly accompanied by other harsh disabilities.[4] In this review, the pathophysiology of SCI and the constraints for successful therapies, namely the existence of blood-CNS barriers associated with the extreme complexity of events following injury, will be briefly addressed along with the current clinical options. Afterwards, the most promising tissue engineering approaches for neurotrauma repair, focusing on the most recent advances of nanotechnology for intracellular drug delivery will be presented.

1.1. Glia: Cellular targets to restore nerve function after injury

Similarly to other systems in the mammalian organism, the nervous system is constituted by a set of specialized cells that perfectly combine and intricate to maintain the ideal conditions for the nerve impulse to occur. Neurons are responsible for the conduction of the nerve impulse along the organism, receiving and transmitting essential information in the form of electrical impulses.[5] Different categories of neurons have been defined, whether having inhibitory or excitatory actions and depending on the type and extent of the connections they make.[6] The ideal conditions for the perfect functioning of neurons, however, are assured by glial cells, which are divided in three major cell types and intimately interact with neurons, displaying a vast array of functions. Glial cells, often referred to as support cells, have however been recently accounted for

more active roles in neuronal processing and are now recognized as new potential therapeutic targets following CNS disorders.[7]

Astrocyte characterization is still incomplete, with some authors defending that they represent more than one cell type given the complexity and variety of morphological, molecular and functional profiles.[8] The accurate performance of astrocytes and its interactions with other cells is imperative for nervous tissue function, nevertheless astrocytes also play a central role following injury or during disease.[9] The formation of a glial scar, which has a primary protective role, aims at limiting the spread of inflammation or infection in the nervous tissue.[10] However, it can also bring some detrimental consequences restricting the establishment of neuronal re-connections following trauma, for example. Hence, astrocytes are an important therapeutic target concerning neuroinflammation and neurodegeneration, and the control and management of astrogliosis and scar formation have been attracting a great deal of attention in biomedical research.[11] Microglia functions in the healthy CNS are still to be completely understood, nonetheless it is known that these cells promptly respond to alterations in the environment with a very low threshold of activation.[12] Unlike astrocytes, microglia do not connect with each other therefore acting in a more individual manner and mainly based in autocrine and paracrine mechanisms.[13] The intrinsic neuroinflammatory and neuroprotective profiles of microglia are leading some researchers to attempt to modulate its action, trying to reinforce the neuroprotective effect in pathological conditions.[14] Finally, oligodendrocytes are the glial cells that most intimately interact with neurons, particularly axons, producing and wrapping them in a myelin sheath.[15] In pathology, oligodendrocytes are directly involved in some degenerating diseases, such as multiple sclerosis, and are particularly vulnerable cells if alterations in the neural environment occur.[16] Consequently, protection of oligodendrocytes should be a critical issue in therapeutic interventions following disease or trauma to the CNS.[17]

Thus, to restore the neuronal network following trauma, glial cells are important cellular targets to consider in an attempt to optimize and program neuronal and functional recovery.[18] As shown in Table 1, each glial cell type exerts particular functions in the maintenance of neural integrity and activity, both in health and disease. Therapies to restore and improve function should therefore aim at maximizing the neuroprotective and reparative intrinsic capacity of these cells, while modulating and minimizing potential deleterious actions and the progression of injury.

Nonetheless, drug access to the nervous tissue is restricted due to the presence of cellular barriers, which will be addressed in the next section.

Table 1 – Glial cells overview: characteristics and main functions.

Cell type	Characteristics	Main functions
Astrocytes	Most abundant CNS cells	Essential during development to the migration and guidance of neurons.[8]
	Variable morphology	Constituents of the BBB, in proximity to endothelial cells.[19]
	Usually star-shaped	Continuous monitoring of and modulation of neuronal activity.[20]
		Functional connection of distant cells and structures.[21]
		Gliotransmitter and other factor (glutamate, ATP) secretion.[22]
		Become reactive and hypertrophy following injury.[23]
		Formation of a glial scar (astrogliosis).[10]
Microglia	Very plastic	Removal of degenerating structures and cell debris.[24]
	Various mobile processes	Assist in the maintenance of neuronal cell activity.[25]
	Rod-shaped soma	Can become macrophage to perform immunological functions.[24]
	Resting ramified state	Sense the CNS environment.[26]
	Reactive amoeboid state.	Secrete pro-inflammatory/immunomodulatory mediators, and neurotrophic factors.[27]
Oligodendrocytes	Variable morphology	Production of myelin sheaths around axons.[15]
	Ramified processes	Essential in neuronal survival and integrity.[17,28,29]

1.2. The blood-CNS barriers limiting therapeutic intervention

Both the brain and the spinal cord need to be highly irrigated in order to obtain the nutrients that fulfill its high metabolic requirements for proper functioning. However, the blood vessels in the CNS have some particular characteristics as compared to the capillaries irrigating the rest of the body. It was in the 19th century that Ehrlich discovered that systemic administration of vital dyes in mammalians stained all organs of the organism, except the brain and the spinal cord.[30] Conversely, if a dye is injected in the cerebrospinal fluid (CSF), it would stain the CNS but none of the peripheral organs. Thus, a century ago it was discovered that a barrier exists between the blood and the CNS organs. More recently, it was shown that CNS vasculature presents distinctive physical and enzymatic properties, including association with cells that constitute this shield – designated as the neurovascular unit - and limit the entrance of solutes to the CNS.[31] The

neurovascular unit has four main functions: (i) regulation of CNS homeostasis; (ii) protection against potential environmental threats; (iii) provision of nutrients; and (iv) guidance of inflammatory cell response.[30] Although exceedingly important in healthy circumstances, both the blood-brain barrier (BBB) and blood-spinal cord barrier (BSCB) dramatically limit the penetration of pharmaceutics in case of disease.[32] Simultaneously, some impairments in the BBB are closely associated with neuropathological conditions.[31] Essentially, the BBB is composed by the microvascular endothelial cells surrounded by an extracellular base membrane in close interaction with adjacent astrocyte end-feet, pericytes and neurons. Its selective permeability is mainly due to the lack of endothelial cell fenestrations and the presence of tight junctions, allowing the transport of substances only if the respective transporters are present in the membrane (e.g., glucose, transferrin and insulin).[32] The spinal cord possesses similar features in its neurovascular unit.

Although most of the present studies focus on the BBB, there is an additional blood-CNS barrier at the choroid plexus level. This additional barrier is needed since the capillaries that irrigate this area do not possess tight junctions. In this case, the brain protection is assured by the presence of a monolayer of epithelial cells with tight juntions on its apical side.[33] This interface in the choroid plexus is known as the blood-CSF barrier (BCSFB).[34] Consequently, if one intends to therapeutically target the CNS administrating a drug aimed at healing a damaged tissue, these barriers present serious obstacles to that purpose.

1.3.   Current local delivery options to circumvent the BSCB

Safely delivering optimal doses of drugs to the CNS is one of the most challenging problems faced in the treatment of neurotraumatic diseases. Generally, therapies directed to the nervous tissue need high dosage systemic administration of compounds in order to reach beneficial effects. This is necessary due to the short half-life of drugs and often results in undesired deleterious side effects.[35] More importantly, most of the pharmaceutics do not even pass the barriers that protect the CNS due to the neurovascular unit properties that limit passage to the CNS.[36] Consequently, and since systemic administration of pharmaceuticals has proven most of the times to be inefficacious in the treatment of CNS conditions, with additional problems of drug degradation and rapid renal clearance, local delivery methods have been attempted as alternative options.[37] Local routes for spinal cord delivery include: epidural, intrathecal and

intraspinal.[38] Epidural injection refers to fluid introduction in the epidural space, between the vertebrae and the dura, while intrathecal administrations are made in the sub-arachnoid region. These two methods are clinically performed, particularly for pain and spasticity management.[39] Intraspinal delivery, on the other hand is a more invasive route that can damage the nervous tissue and is not usually used in the clinics, although it is being investigated in research to directly introduce therapeutic compounds or cells in damaged areas.[40] From these options, it is possible to select between single bolus injection and continuous infusion using appropriate devices. Bolus injections provide local short-term delivery, while continuous infusion presents some advantages with the possibility of controlled administration over periods of weeks, using for that purpose mini-pumps.[41] Although advantageous as compared to systemic administration, the use of implantable devices for the continuous sustained delivery to the intrathecal or epidural spaces has been associated with infections, as well as some scarring and compression of the spinal cord.[42] Moreover, the invasive character of mini-pump implantation associated with the subsequent inflammatory response is undermining its use in human patients. Thus, improved means of delivery are required to tackle the deleterious reactions that occur following injury and lead to degeneration and loss of function.

2. Consequences of neurotrauma: Neurodegeneration and axon failure

Several causes can impair the integrity of the CNS organs causing subsequent devastating costs to the patient's life. Among neurotraumatic ailments, stroke can occur as a result of partial or total obstruction of the cerebral blood flow in the brain, while brain and spinal cord injuries are usually a consequence of mechanical insults.[43] Not only severe neurological deficits arise from these type of injuries, but also peripheral organs can be seriously affected following neurotrauma.[4] In terms of incidence, it is estimated that 10 million people are afflicted every year worldwide from traumatic brain injuries (TBI), while the figures can ascend to 15 million suffering from stroke, and 80 million in the case of spinal cord injuries (SCI).[44]

The temporal cascade of events that follow these incidents is similar independently of the cause and affected organ.[45,46] The immediate result of such occurrences is massive cell death, generally followed by a series of biochemical and cellular events, designated as secondary injury reactions that contribute to the degeneration and progressive death of neuronal cells.[47] In order to re-establish function in the affected tissue it is imperative to restore neuronal connections, which is

currently difficult to accomplish. The post-injury environment becomes very aggressive for axonal re-growth and even neuronal survival. In the case of neuronal injury, the affected areas can become permanently demyelinated and an anterograde degenerative process, designated as Wallerian degeneration, can arise leading to complete neuronal loss.[48] In this section, particular focus will be given to SCI providing an overview on the pathophysiology, current options for drug delivery and future therapeutic trends for the field.

2.1. Epidemiology and pathophysiology of SCI

According to recent health epidemiological studies, traumatic SCI afflicts primarily young adults and the elderly population, still resulting in high mortality rates in developing countries and devastating personal and societal costs.[49] The main causes of these injuries are associated with: vehicle accidents, violence/self-harm acts, falls and sports-related activities.[50] Nonetheless, non-traumatic SCI can also develop from congenital or developmental disorders, infection, inflammation and tumors, with equally devastating outcomes.[51] The level and intensity of the lesion determines the extent of damage and the neurological deficits, giving rise to clinical signs that go from partial to complete muscular weakness and sensory loss at and below that level, potentially resulting in paraplegia or tetraplegia.[52] Cervical injuries are the most common SCI in humans, followed by thoracic, lumbar and sacral injuries.[53] Since there is no effective treatment for this condition, SCI patients experience besides the highly debilitating neurological deficits, frequent bladder, bowel and kidney infections, along with cardiac and respiratory problems, in addition to autonomic dysreflexia.[54] As a result, the life of SCI patients suffers drastic alterations in their daily routines, which become conditioned by a series of mandatory regimens to ensure proper body function and commonly the dependence on assistive devices, such as wheelchairs or ventilators.

When the primary insult distresses the spinal cord generally there is a compression of neural elements and the blood vessels resulting in axon disruption. Immediately after, hemorrhage, swelling and ischemia occur triggering a series of secondary reactions that exacerbate the extent of the initial primary injury.[55] The secondary injury is actually the first opportunity for therapeutic interventions aiming at managing and minimizing the overall impact of the damage, sparing the neurologic tissue as much as possible. In order to do that, accurate knowledge on the ongoing reactions is imperative for successful interventions. Diverse cellular and biochemical reactions

occur simultaneously at this stage (Figure 1), making SCI a complex pathology to deal with.[56] Secondary reactions include: (i) excitotoxicity, as a result of excess glutamate release;[57] (ii) apoptotic cell death, predominantly neurons and oligodendrocytes;[46] (iii) oxidative stress, with free radical production and lipid peroxidation;[58] (iv) further edema, hypoxia and ischemia;[59] and (v) inflammation, with the production of pro-inflammatory cytokines, microglia activation and leukocyte infiltration.[60] Thereby, the lesion area becomes a very harsh environment for repair and functional recovery.[61] The demyelination that initiates after injury is also responsible for the production of a series of myelin-related inhibitory molecules that obstruct regeneration, such as Nogo, myelin-based glycoprotein (MAG) and oligodendrocyte myelin protein (OMgp).[62] Eventually, a chronic phase is established comprising irreversible white matter demyelination and the formation of a glial scar around the lesion, creating a barrier that inhibits axon regeneration.[63] The glial scar is predominantely composed of proliferating astrocytes and inflammatory and fibrotic cells, and often surrounds a fluid-filled cystic cavity.[10] These two structures are highly inhibitory for repair and reconnection, both physically and by expressing inhibitory molecules, such as chondroitin sulphate proteoglycans (CSPG).[64]

Primary injury	Secondary injury	Chronic phase
Mechanical damage	Excitotoxicity	Glial scar
Vascular leakage	Ischemia	Demyelination
Glutamate release	ROS production	
Edema	Lipid peroxidation	
Inflammation	Apoptosis	
	Ionic imbalance	
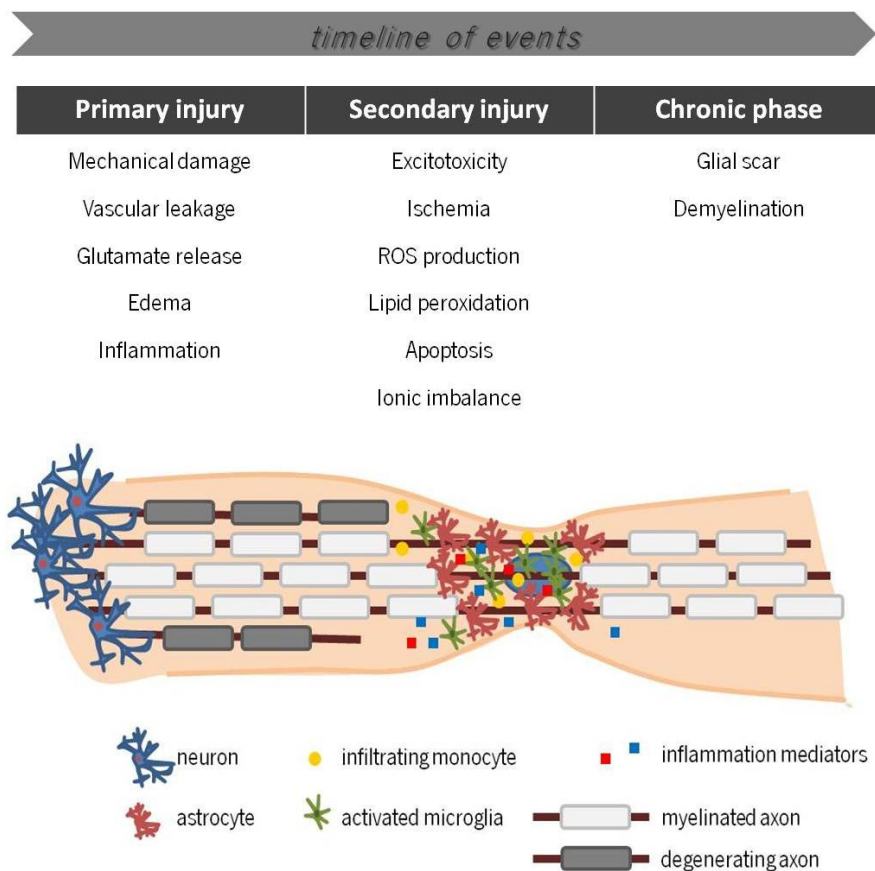
Figure 1 – Schematic representation of the main cellular and biochemical events following SCI.

Therapeutic interventions tackling neuroprotection after SCI have to take into consideration this entire set of reactions, in an attempt to modulate the secondary events and attain a molecular balance where ideally regeneration is possible and more likely to occur than degeneration. However, the complexities of the spatio-temporal event sequence in SCI make it difficult to repair the tissue, and classical drugs and current treatments are very limited with few options for clinical intervention.[65]

3. Current clinical practices to minimize the impact of the secondary injury

The first supportive actions following SCI are crucial in the progression of damage. Presently, the current medical procedures involve three main actions: (i) stabilization of the spinal column; (ii) pharmacological management for prevention of the secondary injury; and (iii) enhancement of spinal cord perfusion.[66] As for spinal perfusion procedures, selective perfusion of the injured spine has been accounted to maintain the blood flow in the cord and reduce the incidence of ischemic episodes during surgery.[67] Early surgical intervention is usually performed to realign and stabilize the column, often associated with decompression that has also been recommended based on reported neurological and functional benefits.[68,69] The basis of this decompression surgery focuses on prevention of secondary injury mechanisms, while stabilization has been reported to reduce the incidence and severity of sepsis and respiratory failure, improving survival in patients undergoing surgery.[70]

Following these initial surgical procedures, the management of secondary injury by pharmacological means is pursued. The therapeutic agent recommended for clinical use in SCI patients is the corticosteroid MP, which was tested in three multicenter, randomized and double-blinded clinical trials.[71,72] Motor improvements were observed when a high dosage of the drug was administered 3 to 8 hours after injury and with 48-hour continued administration. However, severe undesired effects were simultaneously reported, as patients were showing higher incidence of gastrointestinal hemorrhage, wound infection, pulmonary embolism, severe pneumonia and sepsis, and even death due to respiratory complications, as a result of the necessary systemic high dose of the steroid.[73] Consequently, its use has become extremely controversial with some clinicians arguing that the benefits are not significant enough to compensate for the occasionally drastic harmful side effects.[74] MP is an anti-inflammatory and

antioxidant drug, also known to inhibit lipid peroxidation and maintain the integrity of the BSCB.[75] Though the precise molecular mechanisms of action through which MP exerts its actions remain undisclosed, some oligodendrocyte-specific anti-apoptotic effects have recently been discovered.[76] Moreover, reactive astrocyte CSPG expression has recently been reported to be inhibited by MP administration, as well as pro-inflammatory cytokine secretion by microglia.[77,78] So, if appropriate means of delivering MP in a cell-targeted manner are developed, the drug beneficial actions can be maximized with elimination of the current negative side effects that systemic administration causes. Other drugs are also being tested or under pre-clinical investigations, such as riluzole, minocycline, erythropoietin and rolipram, but none of them has still proven effective clinical improvements.[79]

4. Promising tissue engineering approaches in SCI repair

While no successful therapeutic options exist yet to repair the damaged cord since none of the treatments so far can tackle all the factors that arise after damage, several advances in biomedical research and regenerative medicine are bringing new hopes for people suffering from SCI.[80] Emerging therapies from tissue engineering involve areas from biomolecular therapies to cell transplantation and advanced strategies based in biomaterials. Tissue engineering applies the principles of biology and engineering to the development of functional substitutes for damaged tissue.[81] These approaches are used to alter the local chemical and physical environment around the lesion site to facilitate tissue repair and modulate biochemical distresses. Lately, some combinatorial approaches have also been considered to tackle the complexity of SCI (Figure 2).[82] Herein, we will briefly discuss the most recent developments in neural tissue engineering for SCI repair, giving a particular and more careful consideration to the design of targeted drug delivery systems for neuroprotection of the spinal cord following injury. Each of the tissue engineering strategies will be presented separately, nonetheless combination of two or more approaches can be advantageous and some examples of combinatorial approaches will also be presented.
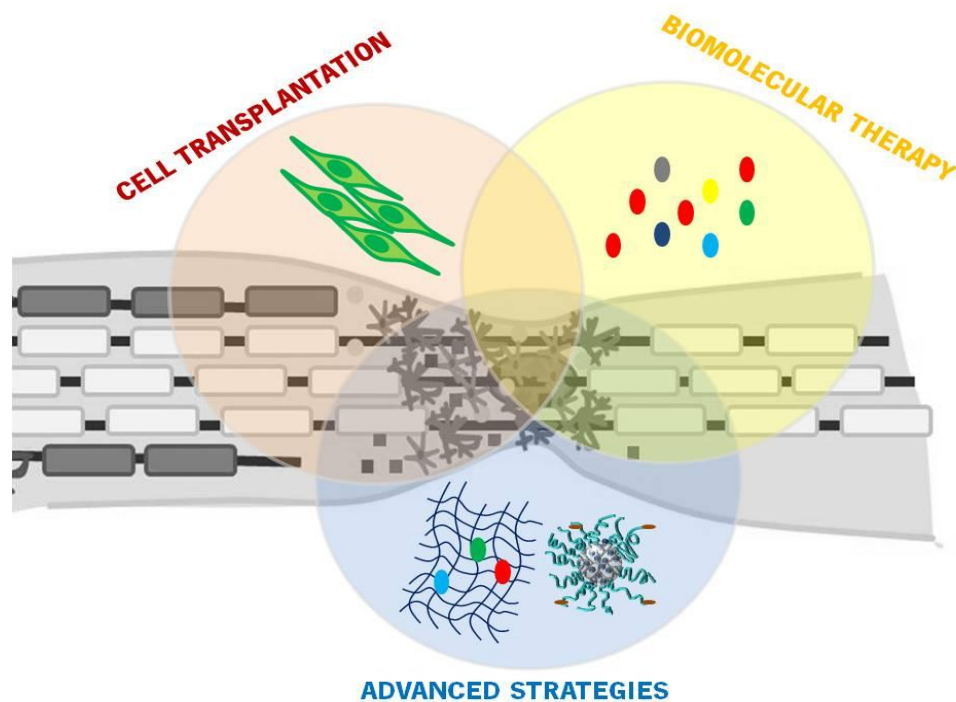
Figure 2 – Representation of the main tissue engineering strategies for spinal cord injury repair.

4.1. Cellular transplantation

Cell therapies currently being considered to repair the spinal cord address the use of Schwann cells (SCs), olfactory ensheathing cells (OECs) and embryonic and adult neural stem cells (NSCs), bone marrow stromal cells (BMSC) and, more recently, induced pluripotent stem cells (iPSCs).[83,84] The use of cell therapy in the injured spinal cord usually involves cell transplantation and the rationale behind its application focuses on cell replacement (mainly neurons and oligodendrocytes) and trophic factor delivery, modulating the environment in the lesion area to facilitate axon regeneration.[84] Schwann cells produce extracellular matrix (ECM) and adhesion molecules, as well as neurotrophins and integrins that can support axon growth. The ability of SCs to promote nerve regeneration has been investigated since highly pure cultures of these cells can be obtained from nerve autografts, for future transplantation purposes.[85] Recent studies have been focusing on combining SC transplantation with other strategies that provide a more prone environment for regeneration. For instance, Pearse *et al.* transplanted SCs grafts in combination with rolipram and cAMP administration in a rat contusion model.[86] The results have shown enhanced axonal sparing and myelination, as seen in Figure 3, with additional significant

15

locomotor improvements. In another study, co-grafting of glia-restricted precursor cells and SCs resulted in synergistic actions, with robust oligodendrocyte differentiation, consequent improved axonal myelination and recovery of function following SCI.[87] The other glia-derived cell type being considered in SCI cell therapies is OEC transplantation. OECs migrate along axons to support their growth and survival in the olfactory epithelium, thus providing permissive conditions for repair.[88] Transplantation of OECs into spinal cord transected rats has shown to ameliorate autonomic dysreflexia symptoms.[89] Additionally, in a clinical trial involving 6 patients with chronic complete SCI resulted in improvements in neurological function with no further clinical complications following autologous OEC transplantation.[90] For more detailed information, SC and OEC transplantation following SCI has been recently reviewed and explored elsewhere.[91,92]
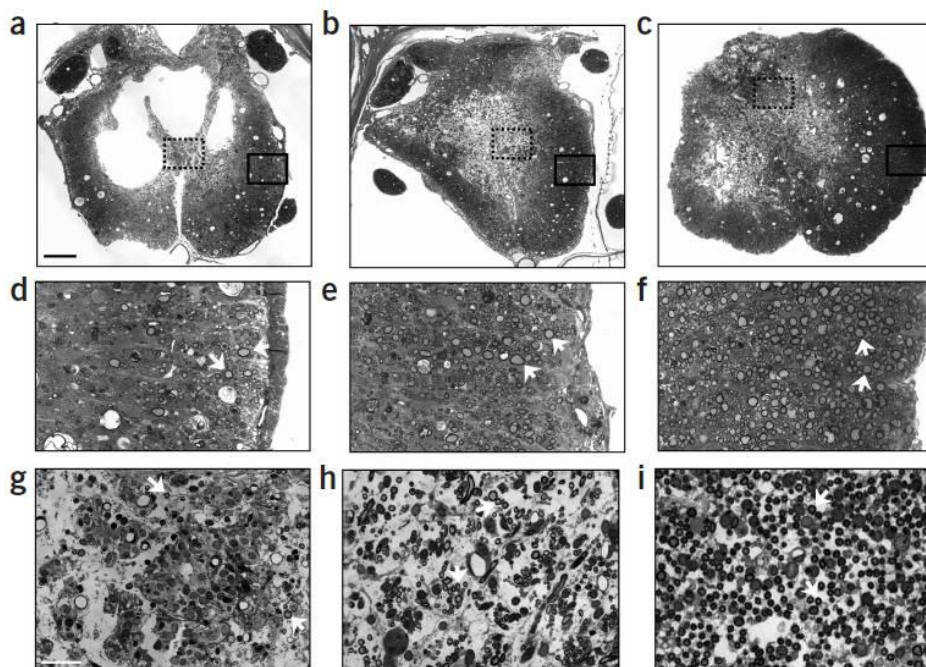
Figure 3 – Photomicrographs of transverse sections of rat spinal cords 11 weeks after contusion injury. Pictured are: a) control; b) SC transplantation; and c) SC transplantation combined with rolipram and db-cAMP. Scale bar = 250 μm. Higher magnification images (d-f) illustrate differences in spared central myelinated axon density. Scale bar = 50 μm. Higher magnifications (g-i) demonstrate differences in peripheral myelinated axon density within the site of injury and transplant. Scale bar = 50 μm.[86]

Stem cells are also under extensive evaluation, regarding transplantation into the injured cord. However, more profound evaluations need to be performed when using stem cells, due to the potential risk of tumor formation or abnormal circuit arrangement.[93] Nevertheless, the potential benefits linked to these cells ability to self-renew and differentiate into different cell types, makes

them attractive for therapeutic use in neural regeneration strategies. Human embryonic stem cell (ESC)-derived oligodendrocyte and motor neuron progenitor cells transplanted into spinal transected rats have induced locomotor recovery, along with survival, migration and differentiation of the stem cells into mature oligodendrocytes and neurons.[94] Similar results were described by Kerr *et al.* transplanting human ESCs in a contusion model, with extensive survival and migration of the stem cells from the lesion site to surrounding areas, and successful integration of newly differentiated oligodendrocytes into the spinal cord.[95] NSCs, in turn, are more committed than ESCs while still having the ability to differentiate into neurons, oligodendrocytes and astrocytes. Moreover, these are the naturally occurring stem cells of the nervous system and can be efficiently propagated *in vitro.*[96] NSCs embedded in fibrin matrices containing growth factor cocktails and implanted in the SCI transection site have successfully differentiated into functional neurons, inducing functional recovery.[97] In another study, sub-acute NSC transplantation in severely contused mice not only has led to locomotor recovery, but it has shown that inflammation was being re-programmed by interaction of NSC with macrophages.[98] Finally, the recently described iPSCs are also being evaluated for therapeutic use in neurotraumatic conditions promising additional sources of autologous cells for transplantation.[99] iPSCs are pluripotent stem cells that were obtained from fibroblasts in a retrovirus-mediated gene transfer.[100] They do not entail ethical or immunological concerns, that can be associated to the use of ESCs or NSCs, and some authors believe they will become the preferred cell source for regenerative medicine.[101] Human iPSCs-derived neurospheres have proven to differentiate in all neural lineages, as well as increased axonal re-growth, angiogenesis and myelination in the injured mice spinal cord .[102]

A common issue with cell transplantation into the injured cord is the extremely inhibitory environment for survival and cell proliferation. Thus, cell transplantation should be considered in conjunction with complimentary strategies, such as the administration of therapeutic biomolecules that modulate the lesion area providing more permissive conditions for cell survival and consequent tissue repair.

4.2. Biomolecular therapies to enhance regeneration

Biomolecular therapies to regenerate the spinal cord focus on the supply of biochemical cues that influence cell behavior so as to overcome the growth inhibitory nature of the injured spine.

This can be achieved with the delivery of growth promoting ECM molecules, adhesion molecules and trophic factors.[82,103] Examples of ECM molecules are collagen, laminin and fibronectin, all commonly used *in vitro* for the promotion of neural cell adhesion. In association with other compounds or constructs, adhesion molecules can help achieve better integration in the host neural tissue. Yoo *et al.* developed an engineered human neural cell line expressing L1, a regenerative conducive adhesion molecule and tested its implantation in an acute compression injury in mice.[104] Treated animals have shown locomotor improvements, lower CSPG expression and migration of cells in the target tissue. A similar approach was examined with transduced SCs expressing L1, and the transplanted mice have exhibited faster locomotor recovery that was attributed to enhanced myelination and increased serotonergic fiber sprouting.[105] Other biomolecules act in the soluble form and influence neural cells activating secondary messenger pathways. Neurotrophic factor adequate spatial and temporal expression patterns have shown to contribute to successful regeneration (as seen in the peripheral nervous system),[106] and numerous studies are exploiting the use of these molecules to achieve effective repair in the CNS.[107] Nerve growth factor (NGF) is the most studied trophic factor and is up-regulated following injury.[108] Along with brain-derived neurotrophic factor (BDNF) and neurotrophin-3 (NT-3) they bind to surface receptors activating intracellular signaling cascades, such as cAMP. Single exogenous administration of NGF has demonstrated increased regeneration in CNS, however it also induced significant sprouting of uninjured axons which lead to chronic pain symptoms and inappropriate reflexes.[109] Similar studies with BDNF proved to be inconclusive, and corroborated that a local and high dosage administration of the factor is needed for regeneration to occur.[110,111] A multifunctional NT-3/D15A neurotrophin has been recently created and combined with SC transplantation revealing enhanced SC survival, as well as sensory and supra-spinal fiber extension.[112] Thus, combined administration of neurotrophic factors seems to be the best approach assembling the varied neural responses as it can promote simultaneously: nerve outgrowth, survival and plasticity; spinal cord and peripheral nerve regeneration; dendritic arborization and synapse formation.[113] Nonetheless, a critical point is the controlled delivery of these compounds, since these natural cues usually are presented in neural tissue in specific spatial and temporal distributions. Biodegradable polymers processed as micro- and nanoparticle systems can be useful carriers due to their versatile properties that can be designed to accomplish precise spatiotemporal control over drug release, and are one of the recent advanced tissue engineering strategies for neural repair.[114]

4.3.　Advanced regenerative strategies

Advanced tissue engineering strategies rely on trying to mimic the natural repair and regeneration in the organism, focusing on creating complex guidance channels and/or combining multiple stimuli in a single therapy. Physical, chemical and electrical guidance cues are essential to neural cells during development, and these are being considered in tissue engineering strategies for neuronal repair.[115] Guidance channels are one of the strategies and have been produced using several different techniques, aiming at creating intricate structures that accurately imitate the nerve architecture. Prang *et al.* developed an alginate-based anisotropic hydrogel that has elicited oriented axon re-growth and appropriate reinnervation in organotypic cultures.[116] Chitosan scaffolds seeded with NSCs have also been tested and implanted in spinal cord transected rats revealing NSCs survival and host axon re-growth.[117] Silva *et al.* engineered a hybrid scaffold tubular structure composed of a starch/poly-ε-caprolactone (SPCL) surrounding a gellan gum hydrogel and shown efficient integration of the scaffold in a rat hemisection model, with no inflammatory reaction.[118] Other recent constructs made of poly-L-lactic acid (PLLA) and polylactic-co-glycolic acid (PLGA) were cultured with olfactory bulb derived cells and have shown up-regulation of NGF and BDNF, along with stimulation of endothelial cell networks.[119] Several other types of conduits have been produced for nerve repair, and these have been reviewed elsewhere.[120,121]

Refined multifunctional drug delivery systems (DDS) are another recently explored advanced tissue engineering strategy to overcome the current impenetrability of SCI therapy.[122] Nanoparticle-based systems are being suggested for use as DDS due to the possibility to engineer these molecules, fine-tuning its properties for more effective delivery of therapeutics to CNS.[123] In the next section we will review the more recent reports on the use of nanocarriers for SCI drug delivery.

5.　Nanocarriers for the effective delivery of neurotherapeutics

In face of the present constraints and challenges in delivering drugs to the nervous tissue, there is an evident need to pursue more sophisticated and thus efficient DDS. Nanotechnology, as the scientific field dealing with the synthesis, characterization and application of materials comprised

within dimensions from few to about 100 nanometers, is promising unique benefits in biomedical applications for CNS.[124] Ranging from improved means of diagnostics and imaging to targeted therapies, nanomedicine applied in neuroscience is a growing field in research. There are several advantages that nanomaterials present for use as drug carriers in regenerative strategies, namely: (i) increased drug bioavailability, with extended circulation times; (ii) the possibility to overcome the blood-CNS barriers; and (iii) the possibility to be functionalized, adding targeting, imaging or therapeutic features to the nanoparticle systems (Figure 4); while making use of traditional routes of administration, as intravenous injection.[125] Moreover, some nanoparticles still present intrinsic therapeutic features, such as reactive oxygen species scavenging,[126] anti-angiogenic properties,[127] peroxidase-like activity,[128] and other interesting qualities that can be used for therapeutic purposes. Additionally, the design of successful nanocarriers for SCI will allow the use of current classical drugs in more effective manners, directing its actions to the desired sites.

| | BIOCOMPATIBLE POLYMER | | TARGETING AGENT | | THERAPEUTIC FACTORS |
| | PENETRATING PEPTIDE | | IMAGING MOLECULE | | GENETIC MATERIAL |
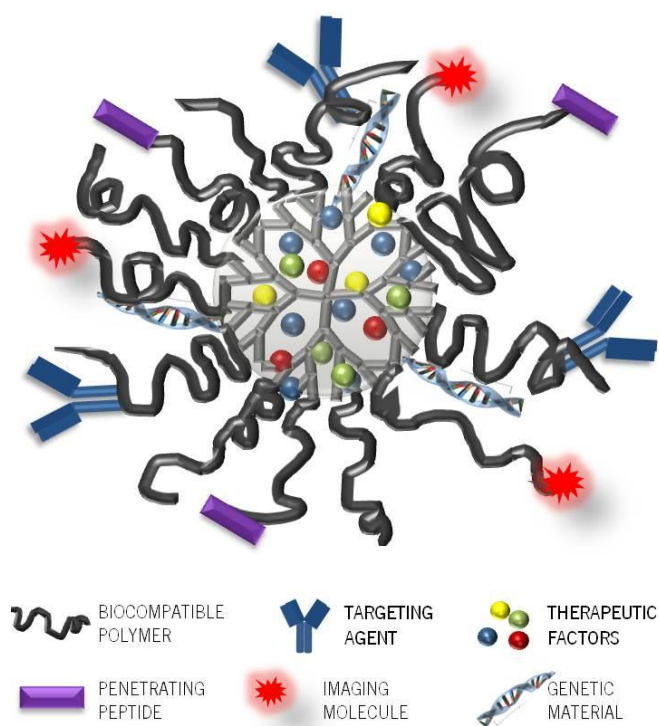
Figure 4 – Illustrative example of a dendrimer-based multifunctional nanoparticle system.

There is therefore an immense set of nanoparticles recently proposed for use as nanocarriers for therapeutic applications, from classical linear polymers to novel spherical molecules.[129] Nanoparticles can be made from various materials, including proteins, peptides, polymers, lipids,

metals and carbon, among others.[130] The most relevant structures have the ability to be functionalized with targeting moieties, therapeutic and/or contrast agents. The developed nanoparticles for drug delivery in the CNS will be addressed, and the most recent examples of use in SCI related applications are provided in Table 2.

Table 2 – Recent nanomedicine examples for drug/gene delivery applications in the injured CNS.

Nanocarrier type	CNS injury model	Administration route	Main results
Liposomes			
Hydroxycamptothecin-loaded liposomes Yang *et al.*[131]	L4-L6 laminectomies with L5 disc injury on adult New Zealand white rabbits.	Local administration	Reduced fibrosis and epidural adhesion.
PEG-TAT modified liposomes Liu *et al.*[132]	T10 severe contusion injury in Wistar rats.	Systemic (intravenous, tail)	Modified liposomes cross the BSCB and accumulate at lesion site.
Clodronate-loaded liposomes Ianotti *et al.*[133]	T8 moderate contusion in adult Sprague-Dawley rats.	Systemic (intraperitoneal)	Enhanced neuroprotection, tissue sparing and hindlimb functional recovery.
DNA-loaded mesoporous silica-supported lipid bilayers Dengler *et al.*[134]	Chronic constriction injury to the sciatic nerve of adult Sprague-Dawley rats	Local (intrathecal)	Functional suppression of pain-related behavior (successful spinal gene delivery).
Polymeric nanoparticles			
Chitosan nanoparticles Cho *et al.* [135]	Mid-thoracic crush/compression injury in adult Hartley guinea pigs	Systemic (subcutaneous)	Restoration of the nerve impulse transmission; membrane sealing properties.
Methylprednisolone-encapsulated PLGA-based nanoparticles Kim*et al.*[136]	T9-10 thoracic dorsal hemisection injury in adult Sprague-Dawley rats	Local (topical delivery)	Lesion volume reduction and improved functional outcomes (grid and beam walking).
BSA or GDNF-loaded PLGA nanoparticles Wang *et al.*[137]	T9-10 moderate and severe injuries in adult Sprague-Dawley rats	Local (intraspinal)	Improved neuronal survival and hindlimb locomotion.
PEGylated silica nanoparticles Chen *et al.*[138] Cho *et al.*[139]	*Ex vivo* compression injury in adult Hartley guinea pig	_____	Selective targeting of injured tissue
	In vivo mid-thoracic crush injury in adult Hartley guinea pig	Systemic (subcutaneous)	Specific targeting of damaged tissue Reduction in ROS production and lipid peroxidation Nerve impulse re-conduction
Chitosan-DNA/ hyaluronic acid nanoparticles Gwak *et al.*[140]	*In vitro* NSC cultures Organotypic SC slices	_____	Low cytotoxicity and high transgene expression

Nanocarrier type	CNS injury model	Administration route	Main results
Poly(methyl methacrylate) nanoparticles Rossi *et al.*[141]	In vivo T11 laminectomy in C57BL/6 mice	Local (embedded in agarose hydrogel)	Sustained and tunable drug release
FGF2-loaded PLGA nanoparticles Kang *et al.*[142]	T2 clip compression injury in Sprague-Dawley rats	Local (embedded in HAMC hydrogel)	Enhanced blood vessel density in the lesioned area
SOD and NR1 antibody conjugated PBCA nanoparticles Reukov *et al.*[143]	*In vitro* primary neuronal cultures		Control of the composition and activity of the NP conjugates Neuroprotection of the neuronal cultures
Prostaglandin E$_1$-loaded PEG-PDLLA nanoparticles Takenaga *et al.*[144]	T10 severe contusion injury in adult Sprague-Dawley rats	Systemic (intravenous)	Improved neuroprotection and anti-apoptotic action; Functional recovery.
Dendrimers			
Methylprednisolone-loaded CMCht/PAMAM dendrimers Cerqueira *et al.*[145]	*In vitro* glia cultures *In vivo* T8 lateral hemisection in adult Wistar rats	Local (intraspinal)	Microglia proliferation modulation; Locomotor improvement
Polyphenylenevinylene(PPV)-PAMAM dendrimers Rodrigo *et al.*[146]	*In vitro* primary rat cerebellar neuronal cultures		Non toxic Efficient siRNA delivery (cofilin-1 gene silencing)
Anti-H1F1-α siRNA carbosilane dendrimers Posadas *et al.*[147]	*In vitro* primary rat cortical neuronal cultures		High transfection levels Selective H1F1 synthesis blocking Neuroprotective in hypoxia conditions
pBDNF-IRES-hrGFP PAMAM dendrimers Shakhbazau *et al.*[148]	*In vitro* human MSCs		Successful transfection and expression of BDNF
Magnetic nanoparticles			
Iron oxide nanoparticles Pal *et al.*[149]	*In vitro* GMB-U87 cell line *In vivo* T11 complete transection in adult Wistar rats	Local (embedded in agarose hydrogel)	Low cytotoxicity Antioxidant and neuroprotective properties Lesion volume reduction and siginificant functional recovery
Aminosilane-coated iron oxide nanoparticles Zhizhi *et al.*[150]	*In vitro* Brain-derived microvessel endothelial cell line (bEnd.3) Primary cortical neurons and astrocytes		Low toxicity Intracellular accumulation High biocompatibility
Superparamagnetic iron oxide nanoparticles Vanecek *et al.*[151]	*In vitro* MSC cultures *In vivo* T8-9 ballon compression lesion in adult Wistar rats	Local (intrathecal, nanoparticle-labeled MSC transplantation)	Efficient MSC labeling Targeting of the lesion site
Commercial magnetic nanoparticles (Chemicell) Pinkernelle *et al.*[152]	*In vitro* cerebellar primary cultures SC/ fibroblast cultures PC12 cell line Organotypic co-culture of spinal cord and peripheral nerve graft		Preferential uptake by microglia cells Differential uptake in PC12 cells and primary neurons

Nanocarrier type	CNS injury model	Administration route	Main results
Superparamagnetic iron oxide nanoparticles Lei *et al.*[153]	Spinal cord NSCs cultures		Successful labeling of NGF-transfected NSCs
Micelles			
mPEG-PDLLA micelle nanoparticles Shi *et al.*[154]	*Ex vivo* spinal cord crush model T10 compression injury adult Long-Evans rats	Systemic (intravenous, tail)	No cytotoxicity Decreased lesion volume and macrophage infiltration Improved locomotor recovery
Methylprednisolone-loaded PEO-PPO-PEO triblock copolymer micelles Chen *et al.*[155]	New Zealand adult rabbits T10 severe contusion injury in adult mice	Systemic (intravenous)	Increased bioavailability Anti-apoptotic effects
Colloidal			
NogoR/ Fc-conjugated gold nanoparticles Wang *et al.*[156]	*In vitro* DRG cultures *In vivo* T10 dorsal hemisection injury in Sprague-Dawley rats		Stimulation of anti-NgR production; Inhibition of myelin inhibitors, promotion of axon growth, tissue protection and functional recovery. No detectable toxicity.
Carbon-based NP			
PEG-functionalized single-walled carbon nanotubes Roman *et al.*[157]	T9 complete transection injury in adult Sprague-Dawley rats	Local	Decreased lesion volume Enhanced neurofilament and CST positive fibers Modest hidlimb motor recovery

Liposomes are unilamellar or multilammelar phospholipid bilayer vesicles comprising an aqueous inner core, and have sizes usually around 50 to 100 nm.[158] They can be engineered controlling lipid composition to possess more fluid or rigid properties, positive or negative net charge, and can be further surface functionalized with targeting molecules.[159] Due to their similarity to lipid membranes, liposomes have remarkable cell penetration and diffusion properties. They have been recently examined for use in the management of oxidative stress-induced diseases, by intravenous administration of N-acetylcysteyne (NAC) containing dipalmitoylphosphatidylcholine (DPPC) liposomes, and no toxicity has been associated to the treatment.[160] In another strategy, implantation of tacrolimus (TAC) liposomal pellets has been presented as an effective immunosupressive DDS that allowed long-term survival of human NSC grafts in healthy and SCI rats.[161] As nanocarriers for the injured spinal cord, liposomes have been tested both as drug or

DNA delivery agents in animal models of the injury. Local administration of hydroxycamptothecin in laminectomized rabbits has significantly reduced the subsequent fibrosis and epidural adhesion.[131] Iannotti *et al.*, in turn, have investigated the effect of systemic administration of clodronate-loaded liposomes in contused rats and verified that the treated animals presented improved tissue sparing and limb functional recovery, due to enhanced neuroprotection.[133] Additionally, functionalization of liposomes with the cell penetrating peptide TAT (Figure 5) has allowed efficient transport of these nanocarriers along the BSCB.[162] Moreover, this TAT-liposomes tend to accumulate at the lesion site which can be helpful in therapeutic applications.[132] Finally, intrathecal injection of DNA-loaded loaded liposomes in a sciatic nerve constriction model has shown suppression of pain-relating behavior in rats, proving successful gene delivery.[134]
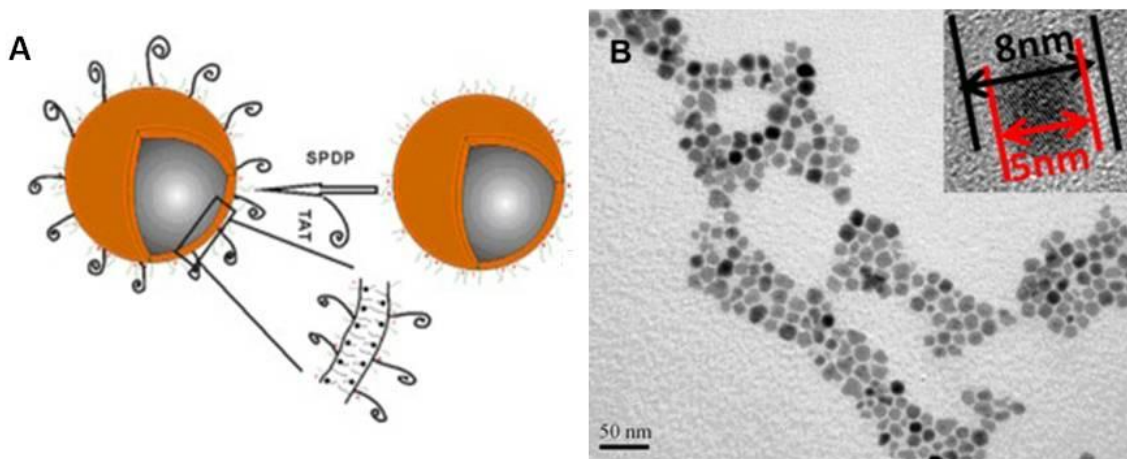
Figure 5 – A. Schematic illustration of the TAT-PEG liposomes/magnetic NPs used by Wang *et al.* **B.** A transmission electron microscopy (TEM) image shows the nanostructure of the TAT-PEG liposomes/ magnetic NPs.[162]

Polymeric nanoparticles have been produced from a variety of materials, either natural-based or synthetic materials. Natural-based nanoparticles are mainly derived from proteins (e.g., silk,[163] collagen,[164] and albumin[165]) or polysaccharides (e.g., chitosan,[166] alginate,[167] and heparin[168]). The use of natural-based nanoparticles is based on the lower immunogenicity of these molecules that leads to enhanced biocompatibility, associated with the possibility of nanoparticle biodegradation and clearance by the organism. However, the increasing control in the synthesis of polymers is allowing the design of more sophisticated systems, with the ability to mimic some of the natural

biopolymers.[169] Some of the most common synthetic polymers under investigation for their therapeutic properties are poly(ethylene glycol) (PEG), poly(lactic acid) (PLA), and poly (lactic acid-glycolic acid) (PLGA).[170] PEG is a polyether that is very often covalently attached to the surface of nanoparticles since PEGylation grafting masks the nanoparticle from the host immune system, reducing potential immunogenicity, and also increases the nanoparticle hydrodynamic size which confers longer circulation times to the molecules.[171] Systemic administration of PEGylated silica nanoparticles in spinal cord crushed guinea pig models, has revealed low immunogenicity, as well as preferential targeting for the damaged tissue, with further reduced ROS production and lipid peroxidation.[139] Drug encapsulated synthetic nanoparticles have also been tested in animal models of SCI. Methylprednisolone and GDNF were incorporated in PLGA nanoparticles and administered locally in the lesion site, as represented in Figure 6, both resulting in improved functional recovery.[136] [137] A general approach that has been recently tested in nanoparticle drug delivery to the spinal cord is the embedding of the trophic-factor loaded nanoparticles in hydrogels and implantation of the material in the lesion area, since most hydrogels can be produced as injectable materials.[172] Hydrogels are biodegradable water-swollen polymers that can be designed with tissue-like properties.[173] These systems can be natural or synthetic-based and used for the controlled and sustained release of factors locally *in vivo*. Rossi *et al.* have tested the embedding of poly(methyl methacrylate) (PMMA) nanoparticles in an agarose gel and following implantation in mice subjected to a laminectomy, the tunable and sustained drug release in the injury site has been confirmed.[141] A different study with growth factor FGF-2-loaded PLGA nanoparticles included in a hyaluronan/methyl cellulose (HAMC) hydrogel has revealed enhanced blood vessel density in a rat compression injury model, suggesting beneficial effects of the FGF-2 release.[142] As for natural-based polymeric nanoparticles, chitosan nanoparticles have been widely used for these applications.[174] DNA-loaded chitosan/hyaluronan nanoparticles have been tested in NSC cultures and organotypic spinal cord slices, revealing in both cases low cytotoxicity and high transgene expression.[140] In *in vivo* compression models, Chen *et al.* have also described restoration of nerve impulse transmission and membrane sealing occurrence following chitosan nanoparticle administration.[135]
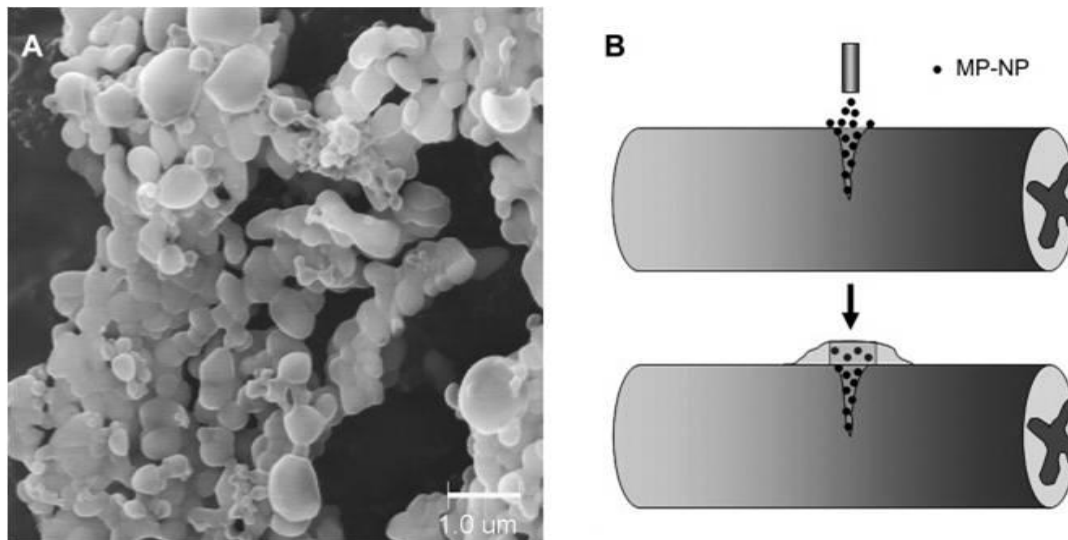
Figure 6 - Methylprednisolone-encapsulating PLGA nanoparticles (MP-NP) for hydrogel inclusion and SCI implantation. **A.** A SEM image of the lyophilized MP-NPs. Scale bar = 1 μm. **B.** Schematic of topical and local delivery of the MP-NPs onto dorsal hemisection lesioned spinal cord.[136]

Magnetic nanoparticles are spherical nanocrystals of about 10 to 20 nm with an iron core and they have been traditionally used for imaging, due to their intrinsic magnetic properties.[175] The recent possibilities of nanoparticle functionalization have also applied to magnetic nanoparticles thus broadening its range of applications, namely as targeted DDS. Pal *et al.* have investigated the potential of iron oxide magnetic nanoparticles *in vitro* and in spinal cord complete transected rats, embedding the nanoparticles in an agarose gel.[149] The authors have reported interesting intrinsic antioxidant and neuroprotective properties, associated with low toxicity profiles and lesion volume reduction. Furthermore, significant functional recovery has also been reported from the same study, supporting the therapeutic potential of these magnetic nanoparticles. Other studies, using aminosilane-coated iron oxide nanoparticles and super-paramagnetic nanoparticles (Figure 7) have also demonstrated efficient targeting of the lesion and high biocompatibility *in vitro* in endothelial and cortical cell cultures.[150,151]
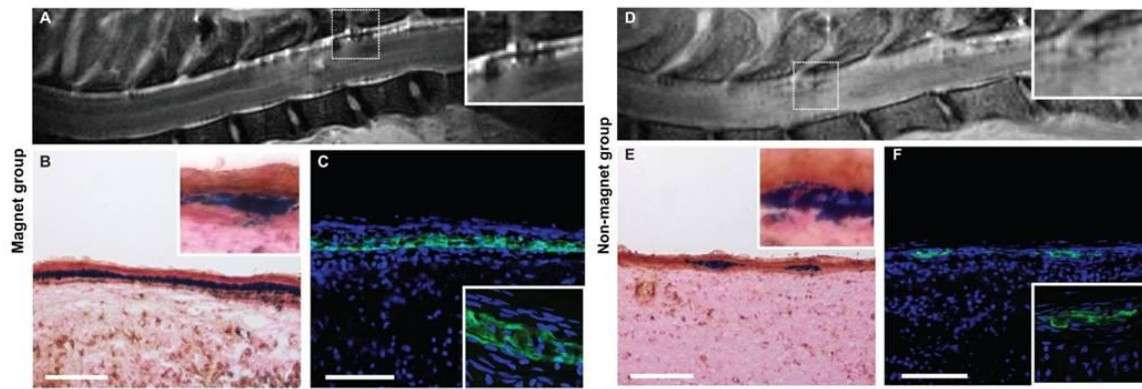
Figure 7 - Magnetic resonance signal of superparamagnetic iron oxide NP-labeled MSCs in SCI animals: in a magnet group after intrathecal application (**A),** in contrast to the non-magnet group (**D**). Intense Prussian blue staining (**B**) co-localized with the GFP signal (**C**) in the area under the magnet. Cell nuclei are stained with DAPI (blue) (**C** and **F**).[151] Scale bars = 100 μm.

One of the most recently developed nanoparticle types are dendrimers, which possess unique branched and spherical architecture, and form a new class of polymers after the classical linear, crosslinked and branched polymers.[176] Dendrimers can be synthesized in a defined manner, with precise control over its molecular weight, branching structure and composition, while allowing several additional surface modifications.[177] Due to its structural similarities with proteins, dendrimers are sometimes referred to as "artificial proteins". Their multiple functionalization possibilities, associated with high drug payloads and monodispersity are making them attractive molecules for use in biomedical and pharmaceutical applications.[178] For CNS applications, dendrimers have mainly been proposed as gene delivery carriers. For instance, siRNAs have been incorporated in polyphenylenevinylene (PPV)-poly(amidoamine) (PAMAM) and carbosilane dendrimers and tested in primary neuron cultures with successful gene silencing and no associated cytotoxicity.[146,147] Shakhbazau *et al.,* in turn, have coupled a BDNF plasmid to PAMAM dendrimers and tested the transfection rates in human bone marrow MSC cultures, envisioning a BDNF-secreting MSC transplantation strategy following neural system injuries.[148] The results have indicated successful transfection and expression of the neurotrophic factor, suggesting a safer method than viral approaches to engineer autologous stem cells to produce relevant factors. Oliveira *et al.,* have recently focused on the application of a non-toxic carboxymethylchitosan (CMCht) grafted PAMAM dendrimer (Figure 8) for neurotrauma therapies as an intracellular drug nanocarrier.[179] The successful incorporation of MP into the nanoparticles has proven to be beneficial following hemisection in rat models, originating functional improvements.[145]
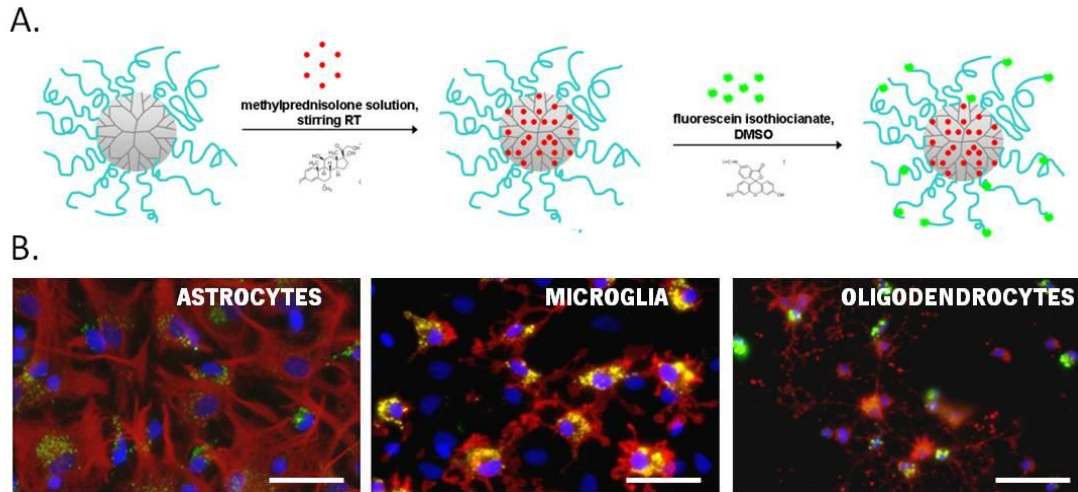
Figure 8 – A. Structural representation of MP incorporation and FITC conjugation to CMCht/PAMAM dendrimer nanoparticles. **B.** Intracellular retention of FITC-labeled MP-loaded CMCht/PAMAM dendrimer nanoparticles in primary glial cultures.[145]

Moreover, a multifunctional dendrimer has also been designed and produced coupling the MP-loaded dendrimers with an antibody that conferred altered uptake in primary glial cultures.[180] With this strategy, the enhanced use of a classical drug in SCI is proposed, maximizing its beneficial actions in glial cells following injury. Moreover, a targeted delivery to the injury site is expected to eliminate the deleterious side effects provoked by systemic high dosage administration.

As herein presented, significant advances in therapeutics are expected to continue to occur derived from nanotechnology progress; nonetheless, particular attention should also be given to the toxicology of nanoparticles. When materials are used as nanoformulations, may present different toxicological profiles than the bulk materials.[181] Although routine assays are currently performed evaluating *in vitro* and *in vivo* nanoparticle toxicity, and emphasizing on pharmacokinetics and distribution, long-term studies should also be considered to assess potential chronic toxicity.

6. Conclusions and future perspectives

The advent of nanotechnology brought a whole new range of possibilities in biomedical engineering, bringing improved means of therapeutics, imaging and diagnostics, which can even be combined in a single system. The possibility to design nano-polymers to attain desired properties and functions and be able to enter the organism, execute a determined action and exit

whenever the task is completed is making R. Feynman suggestion of "swallowing the surgeon" a reality. The complexities of the events that follow SCI, both at the cellular and molecular levels, associated with the presence of BSCB, have been hindering the successful establishment of an effective treatment for SCI. However, tissue engineering and nanotechnology recent advances are enabling the development of more complex approaches that are bringing new hopes for SCI repair. Most of the nanoparticle-based systems that have been herein described enclose multiple functionalities, such as: (i) drug/gene incorporation; (ii) surface grafting to confer enhanced biocompatibility, penetration and/or targeting; and (iii) imaging properties. For SCI applications, nanoparticles have been recently pointed out as systems that have the potential to effectively act on the modulation of the harsh secondary injury environment, providing a more suitable environment for successful nerve regeneration and tissue repair to occur.

Given its intrinsic properties, magnetic nanoparticles have been mainly investigated as imaging agents contributing to the identification and *in vivo* tracking of relevant cells with demonstrated therapeutic potential. Liposomes, as drug and gene nanocarriers, have shown some interesting improvements in SCI animal models, both with local or systemic administrations. Notwithstanding, a more recent class of nanoparticles has brought additional advantageous properties for theranostics prospective uses. Dendrimers display superior drug payloads and control over its structure, along with further functionalization possibilities. The use of a PAMAM dendrimer grafted with CMCht has shown superior loading capability and therapeutic properties when loaded with MP. Additionally, high transfection efficiency has also been described using PAMAM dendrimers. Conjugation of multiple functionalization in the same nanoparticle system, have tremendous potential for strategies envisioning combined actions in damaged areas. For instance, inclusion of a cocktail of relevant factors in a nanoparticle system targeting the modulation of glial cell activity or transplanted cells, in a specific and differential manner, may finally bring exciting and reasonable hopes in the management of such a complex ailment as SCI. Although more exhaustive investigations are needed regarding nanoparticle administration for SCI repair, namely analysis of intracellular trafficking and clearance routes, as well as long-term toxicity studies, these newly developed strategies are bringing promising hopes for the development of an effective therapy for neurotrauma.

References

1   Feynman, R. P. There's plenty of room at the bottom - An invitation to enter a new field of physics. *Engineering and Science* 23, 22-26 (1960).

2   Sanvicens, N. & Marco, M. P. Multifunctional nanoparticles–properties and prospects for their use in human medicine. *Trends in biotechnology* 26, 425-433 (2008).

3   Shah, L., Yadav, S. & Amiji, M. Nanotechnology for CNS delivery of bio-therapeutic agents. *Drug Delivery and Translational Research*, 1-16 (2013).

4   Catania, A., Lonati, C., Sordi, A. & Gatti, S. Detrimental consequences of brain injury on peripheral cells. *Brain, behavior, and immunity* 23, 877-884 (2009).

5   Llinás, R. R. The intrinsic electrophysiological properties of mammalian neurons: insights into central nervous system function. *Science* 242, 1654-1664 (1988).

6   van Vreeswijk, C. & Sompolinsky, H. Chaos in neuronal networks with balanced excitatory and inhibitory activity. *Science* 274, 1724-1726 (1996).

7   Kimelberg, H. K. & Nedergaard, M. Functions of Astrocytes and their Potential As Therapeutic Targets. *Neurotherapeutics* 7, 338-353 (2010).

8   Volterra, A. & Meldolesi, J. Astrocytes, from brain glue to communication elements: the revolution continues. *Nature Reviews Neuroscience* 6, 626-640 (2005).

9   Middeldorp, J. & Hol, E. GFAP in health and disease. *Progress in Neurobiology* 93, 421-443 (2011).

10   Wanner, I. B. *et al.* Glial Scar Borders Are Formed by Newly Proliferated, Elongated Astrocytes That Interact to Corral Inflammatory and Fibrotic Cells via STAT3-Dependent Mechanisms after Spinal Cord Injury. *The Journal of Neuroscience* 33, 12870-12886 (2013).

11   Hamby, M. E. & Sofroniew, M. V. Reactive Astrocytes As Therapeutic Targets for CNS Disorders. *Neurotherapeutics* 7, 494-506 (2010)

12   Graeber, M. B. Changing face of microglia. *Science* 330, 783-788 (2010).

13   Pocock, J. M. & Liddle, A. C. in *Progress in brain research* Vol. Volume 132 (ed M. Nieto-Sampedro B. Castellano Lopez) 555-565 (Elsevier, 2001).

14   Polazzi, E. & Monti, B. Microglia and neuroprotection: From in vitro studies to therapeutic applications. *Progress in Neurobiology* 92, 293-315 (2010).

15   Pfeiffer, S. E., Warrington, A. E. & Bansal, R. The oligodendrocyte and its many cellular processes. *Trends in cell biology* 3, 191-197 (1993).

16   Chang, A., Tourtellotte, W. W., Rudick, R. & Trapp, B. D. Premyelinating oligodendrocytes in chronic lesions of multiple sclerosis. *New England Journal of Medicine* 346, 165-173 (2002).

17   Wilkins, A., Majed, H., Layfield, R., Compston, A. & Chandran, S. Oligodendrocytes promote neuronal survival and axonal length by distinct intracellular mechanisms: a novel role for oligodendrocyte-derived glial cell line-derived neurotrophic factor. *The Journal of Neuroscience* 23, 4967-4974 (2003).

18   Becker, D., Sadowsky, C. L. & McDonald, J. W. Restoring function after spinal cord injury. *Neurologist* 9, 1-15 (2003).

19   Abbott, N. J., Rönnbäck, L. & Hansson, E. Astrocyte–endothelial interactions at the blood–brain barrier. *Nature Reviews Neuroscience* 7, 41-53 (2006).

20   Fellin, T. Communication between neurons and astrocytes: relevance to the modulation of synaptic and network activity. *Journal of neurochemistry* 108, 533-544 (2009).

21   Hansson, E. & Ronnback, L. Glial neuronal signaling in the central nervous system. *The FASEB Journal* 17, 341-348 (2003).

22   Araque, A., Carmignoto, G. & Haydon, P. G. Dynamic signaling between astrocytes and neurons. *Annual Review of Physiology* 63, 795-813 (2001).

23   Pekny, M., Porritt, M., de Pablo, Y., Pekna, M. & Wilhelmsson, U. in *The Cytoskeleton* 299-319 (Springer, 2013).

24   Hanisch, U.-K. & Kettenmann, H. Microglia: active sensor and versatile effector cells in the normal and pathologic brain. *Nature neuroscience* 10, 1387-1394 (2007).

25   Béchade, C., Cantaut-Belarif, Y. & Bessis, A. Microglial control of neuronal activity. *Frontiers in Cellular Neuroscience* 7 (2013).

26   Kreutzberg, G. W. Microglia: a sensor for pathological events in the CNS. *Trends in Neurosciences* 19, 312-318 (1996).

27   Kettenmann, H., Hanisch, U.-K., Noda, M. & Verkhratsky, A. Physiology of microglia. *Physiological reviews* 91, 461-553 (2011).

28   Griffiths, I. *et al.* Axonal swellings and degeneration in mice lacking the major proteolipid of myelin. *Science* 280, 1610-1613 (1998).

29   Fünfschilling, U. *et al.* Glycolytic oligodendrocytes maintain myelin and long-term axonal integrity. *Nature* 485, 517-521 (2012).

30   Cardoso, F. L., Brites, D. & Brito, M. A. Looking at the blood–brain barrier: molecular anatomy and possible investigation approaches. *Brain research reviews* 64, 328-363 (2010).

31   Persidsky, Y., Ramirez, S. H., Haorah, J. & Kanmogne, G. D. Blood–brain barrier: structural components and function under physiologic and pathologic conditions. *Journal of Neuroimmune Pharmacology* 1, 223-236 (2006).

32   Pardridge, W. M. Blood–brain barrier delivery. *Drug discovery today* 12, 54-61 (2007).

33   Marques, F., Sousa, J. C., Sousa, N. & Palha, J. A. Blood–brain-barriers in aging and in Alzheimer's disease. *Molecular Neurodegeneration* 8, 38 (2013).

34   Sharma, H. S. *Blood-spinal cord and brain barriers in health and disease*. (Access Online via Elsevier, 2003).

35   Pathan, S. A. *et al.* CNS drug delivery systems: novel approaches. *Recent patents on drug delivery & formulation* 3, 71-89 (2009).

36   Abbott, N. J., Patabendige, A. A., Dolman, D. E., Yusof, S. R. & Begley, D. J. Structure and function of the blood–brain barrier. *Neurobiology of disease* 37, 13-25 (2010).

37   Jain, A., Kim, Y.-T., McKeon, R. J. & Bellamkonda, R. V. In situ gelling hydrogels for conformal repair of spinal cord defects, and local delivery of BDNF after spinal cord injury. *Biomaterials* 27, 497-504 (2006).

38   Deer, T. R. in *Atlas of Implantable Therapies for Pain Management*   139-141 (Springer, 2011).

39   Amar, A. P., Larsen, D. W. & Teitelbaum, G. P. Percutaneous Spinal Interventions. *Neurosurgery Clinics of North America* 16, 561-568 (2005).

40   Peljto, M., Dasen, J. S., Mazzoni, E. O., Jessell, T. M. & Wichterle, H. Functional diversity of ESC-derived motor neuron subtypes revealed through intraspinal transplantation. *Cell stem cell* 7, 355-366 (2010).

41   Young, Y. *et al.* Sustained delivery of pro-inflammatory growth factors via a mini osmotic pump to an experimental spinal cord injury in rats. *Journal of Bone & Joint Surgery, British Volume* 94-B, 110 (2012).

42   Jones, L. L. & Tuszynski, M. H. Chronic intrathecal infusions after spinal cord injury cause scarring and compression. *Microscopy research and technique* 54, 317-324 (2001).

43   Farooqui, A. A. in *Neurochemical Aspects of Neurotraumatic and Neurodegenerative Diseases*   383-397 (Springer, 2010).

44   Bragge, P. *et al.* An overview of published research about the acute care and rehabilitation of traumatic brain injured and spinal cord injured patients. *Journal of neurotrauma* 29, 1539-1547 (2012).

45   Bazan, N. G., de Turco, E. B. R. & Allan, G. Mediators of injury in neurotrauma: intracellular signal transduction and gene expression. *Journal of neurotrauma* 12, 791-814 (1995).

46   Grossman, S., Rosenberg, L. & Wrathall, J. Temporal–spatial pattern of acute neuronal and glial loss after spinal cord contusion. *Experimental neurology* 168, 273-282 (2001).

47   Adamchik, Y., Frantseva, M., Weisspapir, M., Carlen, P. & Perez Velazquez, J. Methods to induce primary and secondary traumatic damage in organotypic hippocampal slice cultures. *Brain Research Protocols* 5, 153-158 (2000).

48   Vargas, M. E. & Barres, B. A. Why is Wallerian degeneration in the CNS so slow? *Annu. Rev. Neurosci.* 30, 153-179 (2007).

49   Van den Berg, M., Castellote, J., Mahillo-Fernandez, I. & de Pedro-Cuesta, J. Incidence of spinal cord injury worldwide: a systematic review. *Neuroepidemiology* 34, 184-192 (2010).

50   Lee, B., Cripps, R., Fitzharris, M. & Wing, P. The global map for traumatic spinal cord injury epidemiology: update 2011, global incidence rate. *Spinal cord* (2013).

51   McDonald, J. W. & Sadowsky, C. Spinal-cord injury. *The Lancet* 359, 417-425 (2002).

52   Jacobs, W. B. & Nguyen, R. Acute spinal cord injury: clinical evaluation, diagnosis and classification. *Critical Care in Spinal Cord Injury* (2013).

53   Bransford, R. J., Chapman, J. R., Skelly, A. C. & VanAlstyne, E. M. What do we currently know about thoracic spinal cord injury recovery and outcomes? A systematic review. *Journal of Neurosurgery: spine* 17, 52-64 (2012).

54   Sarhan, F., Saif, D. & Saif, A. An overview of traumatic spinal cord injury: part 2. Acute management. *British Journal of Neuroscience Nursing* 9, 138-144 (2013).

55   Wilson, I. R. & Fehlings, M. G. Spinal cord injury: pathophysiology and prospect of decompressive. *Traumatic Brain and Spinal Cord Injury: Challenges and Developments*, 242 (2012).

56   Kwon, B. K., Tetzlaff, W., Grauer, J. N., Beiner, J. & Vaccaro, A. R. Pathophysiology and pharmacologic treatment of acute spinal cord injury. *The Spine Journal* 4, 451-464 (2004).

57   Park, E., Velumian, A. A. & Fehlings, M. G. The role of excitotoxicity in secondary mechanisms of spinal cord injury: a review with an emphasis on the implications for white matter degeneration. *Journal of neurotrauma* 21, 754-774 (2004).

58   Azbill, R. D., Mu, X., Bruce-Keller, A. J., Mattson, M. P. & Springer, J. E. Impaired mitochondrial function, oxidative stress and altered antioxidant enzyme activities following traumatic spinal cord injury. *Brain research* 765, 283-290 (1997).

59   Martirosyan, N. L. *et al.* Blood supply and vascular reactivity of the spinal cord under normal and pathological conditions: A review. *Journal of Neurosurgery: spine* 15, 238-251 (2011).

60   Alexander, J. K. & Popovich, P. G. Neuroinflammation in spinal cord injury: therapeutic targets for neuroprotection and regeneration. *Progress in brain research* 175, 125-137 (2009).

61   Fitch, M. T. & Silver, J. CNS injury, glial scars, and inflammation: Inhibitory extracellular matrices and regeneration failure. *Experimental neurology* 209, 294-301 (2008).

62   Schwab, M. E. Repairing the injured spinal cord. *Science* 295, 1029-1031 (2002).

63   Sofroniew, M. V. Molecular dissection of reactive astrogliosis and glial scar formation. *Trends in Neurosciences* 32, 638-647 (2009).

64   Tyler, J. Y., Xu, X.-M. & Cheng, J.-X. Nanomedicine for treating spinal cord injury. *Nanoscale* 5, 8821-8836 (2013).

65   Domingo, A. *et al.* A systematic review of the effects of pharmacological agents on walking function in people with spinal cord injury. *Journal of neurotrauma* 29, 865-879 (2012).

66   Markandaya, M., Stein, D. M. & Menaker, J. Acute treatment options for spinal cord injury. *Current treatment options in neurology* 14, 175-187 (2012).

67   Kawaharada, N. *et al.* Spinal cord protection with selective spinal perfusion during descending thoracic and thoracoabdominal aortic surgery. *Interactive CardioVascular and Thoracic Surgery* 10, 986-991 (2010).

68   Furlan, J. C., Noonan, V., Cadotte, D. W. & Fehlings, M. G. Timing of decompressive surgery of spinal cord after traumatic spinal cord injury: an evidence-based examination of pre-clinical and clinical studies. *Journal of neurotrauma* 28, 1371-1399 (2011).

69   Dimar 2nd, J., Glassman, S., Raque, G., Zhang, Y. & Shields, C. The influence of spinal canal narrowing and timing of decompression on neurologic recovery after spinal cord contusion in a rat model. *Spine* 24, 1623 (1999).

70   Bellabarba, C., Fisher, C., Chapman, J., Dettori, J. & Norvell, D. Does early fracture fixation of thoracolumbar spine fractures decrease morbidity or mortality? *Spine* 35, S138 (2010).

71   Bracken, M. B. *et al.* A Randomized, Controlled Trial of Methylprednisolone or Naloxone in the Treatment of Acute Spinal-Cord Injury. *New England Journal of Medicine* 322, 1405-1411 (1990).

72   Bracken, M. B. *et al.* Administration of Methylprednisolone for 24 or 48 Hours or Tirilazad Mesylate for 48 Hours in the Treatment of Acute Spinal Cord InjuryResults of the Third National Acute Spinal Cord Injury Randomized Controlled Trial. *JAMA: the journal of the American Medical Association* 277, 1597-1604 (1997).

73   Short, D., El Masry, W. & Jones, P. High dose methylprednisolone in the management of acute spinal cord injury: a systematic review from a clinical perspective. *Spinal cord* 38, 273-286 (2000).

74   Hurlbert, R. J. Methylprednisolone for acute spinal cord injury: an inappropriate standard of care*. *Journal of Neurosurgery: spine* 93, 1-7 (2000).

75   Kuffler, D. P. Combinatorial techniques for enhancing neuroprotection. *Annals of the New York Academy of Sciences* 1199, 164-174 (2010).

76   Xu, J. *et al.* STAT5 mediates antiapoptotic effects of methylprednisolone on oligodendrocytes. *The Journal of Neuroscience* 29, 2022-2026 (2009).

77   Liu, W. L. *et al.* Methylprednisolone inhibits the expression of glial fibrillary acidic protein and chondroitin sulfate proteoglycans in reactivated astrocytes. *Glia* 56, 1390-1400 (2008).

78   Xu, J. *et al.* Methylprednisolone inhibition of TNF-α expression and NF-kB activation after spinal cord injury in rats. *Molecular brain research* 59, 135-142 (1998).

79   Rabchevsky, A. G., Patel, S. P. & Springer, J. E. Pharmacological interventions for spinal cord injury: where do we stand? How might we step forward? *Pharmacology & therapeutics* 132, 15-29 (2011).

80   Madigan, N. N., McMahon, S., O'Brien, T., Yaszemski, M. J. & Windebank, A. J. Current tissue engineering and novel therapeutic approaches to axonal regeneration following spinal cord injury using polymer scaffolds. *Respiratory physiology & neurobiology* 169, 183-199 (2009).

81   Langer, R. & Vacanti, J. Tissue engineering. *Science* 260, 920-926 (1993).

82   Karumbaiah, L. & Bellamkonda, R. in *Neural Engineering*   765-794 (Springer, 2013).

83   Tetzlaff, W. *et al.* A systematic review of cellular transplantation therapies for spinal cord injury. *Journal of neurotrauma* 28, 1611-1682 (2011).

84   Sahni, V. & Kessler, J. A. Stem cell therapies for spinal cord injury. *Nature Reviews Neurology* 6, 363-372 (2010).

85   Morrissey, T. K., Kleitman, N. & Bunge, R. P. Isolation and functional characterization of Schwann cells derived from adult peripheral nerve. *The Journal of Neuroscience* 11, 2433-2442 (1991).

86   Pearse, D. D. *et al.* cAMP and Schwann cells promote axonal growth and functional recovery after spinal cord injury. *Nature medicine* 10, 610-616 (2004).

87   Hu, J. G. *et al.* Co-transplantation of glial restricted precursor cells and Schwann cells promotes functional recovery after spinal cord injury. *Cell transplantation* (2013).

88   Higginson, J. R. & Barnett, S. C. The culture of olfactory ensheathing cells (OECs)—a distinct glial cell type. *Experimental neurology* 229, 2-9 (2011).

89   Kalinčík, T. *et al.* Olfactory ensheathing cells reduce duration of autonomic dysreflexia in rats with high spinal cord injury. *Autonomic Neuroscience* 154, 20-29 (2010).

90   Rao, Y. *et al.* Long-term Outcome of Olfactory Ensheathing Cell Transplantation in Six Patients with Chronic Complete Spinal Cord Injury. *Cell transplantation* (2013).

91   Wiliams, R. R. & Bunge, M. Schwann cell transplantation: a repair strategy for spinal cord injury? *Progress in brain research* 201, 295-312 (2011).

92   Mackay-Sim, A. & St John, J. A. Olfactory ensheathing cells from the nose: clinical application in human spinal cord injuries. *Experimental neurology* 229, 174-180 (2011).

93   Sahni, V. & Kessler, J. A. Stem cell therapies for spinal cord injury. *Nat Rev Neurol* 6, 363-372 (2010).

94   Erceg, S. *et al.* Transplanted Oligodendrocytes and Motoneuron Progenitors Generated from Human Embryonic Stem Cells Promote Locomotor Recovery After Spinal Cord Transection. *STEM CELLS* 28, 1541-1549 (2010).

95   Kerr, C. L. *et al.* Efficient Differentiation of Human Embryonic Stem Cells into Oligodendrocyte Progenitors for Application in a Rat Contusion Model of Spinal Cord Injury. *International Journal of Neuroscience* 120, 305-313 (2010).

96   Ronaghi, M., Erceg, S., Moreno-Manzano, V. & Stojkovic, M. Challenges of Stem Cell Therapy for Spinal Cord Injury: Human Embryonic Stem Cells, Endogenous Neural Stem Cells, or Induced Pluripotent Stem Cells? *STEM CELLS* 28, 93-99 (2010).

97   Lu, P. *et al.* Long-Distance Growth and Connectivity of Neural Stem Cells after Severe Spinal Cord Injury. *Cell* 150, 1264-1273 (2012).

98   Cusimano, M. *et al.* Transplanted neural stem/precursor cells instruct phagocytes and reduce secondary tissue damage in the injured spinal cord. *Brain* 135, 447-460 (2012).

99   Nakamura, M., Tsuji, O., Nori, S., Toyama, Y. & Okano, H. Cell transplantation for spinal cord injury focusing on iPSCs. *Expert Opinion on Biological Therapy* 12, 811-821 (2012).

100   Takahashi, K. & Yamanaka, S. Induction of pluripotent stem cells from mouse embryonic and adult fibroblast cultures by defined factors. *Cell* 126, 663-676 (2006).

101   Nori, S. *et al.* Therapeutic potential of induced pluripotent stem cells for spinal cord injury. *Brain and nerve= Shinkei kenkyū no shinpo* 64, 17 (2012).

102   Nori, S. *et al.* Grafted human-induced pluripotent stem-cell–derived neurospheres promote motor functional recovery after spinal cord injury in mice. *Proceedings of the National Academy of Sciences* 108, 16825-16830 (2011).

103   Giger, R. J., Hollis, E. R. & Tuszynski, M. H. Guidance molecules in axon regeneration. *Cold Spring Harbor perspectives in biology* 2 (2010).

104   Yoo, M., Lee, G. A., Park, C., Cohen, R. I. & Schachner, M. Analysis of human embryonic stem cells with regulatable expression of the cell adhesion molecule L1 in regeneration after spinal cord injury. *Journal of neurotrauma* (2013).

105   Lavdas, A. A. *et al.* Schwann cells engineered to express the cell adhesion molecule L1 accelerate myelination and motor recovery after spinal cord injury. *Experimental neurology* 221, 206-216 (2010).

106   Madduri, S. & Gander, B. Schwann cell delivery of neurotrophic factors for peripheral nerve regeneration. *Journal of the Peripheral Nervous System* 15, 93-103 (2010).

107   McCall, J., Weidner, N. & Blesch, A. Neurotrophic factors in combinatorial approaches for spinal cord regeneration. *Cell and tissue research* 349, 27-37 (2012).

108   Krenz, N. R. & Weaver, L. C. Nerve growth factor in glia and inflammatory cells of the injured rat spinal cord. *Journal of neurochemistry* 74, 730-739 (2000).

109   Romero, M. I., Rangappa, N., Garry, M. G. & Smith, G. M. Functional regeneration of chronically injured sensory afferents into adult spinal cord after neurotrophin gene therapy. *The Journal of Neuroscience* 21, 8408-8416 (2001).

110   Mamounas, L. A. *et al.* BDNF promotes the regenerative sprouting, but not survival, of injured serotonergic axons in the adult rat brain. *The Journal of Neuroscience* 20, 771-782 (2000).

111   Boyd, J. & Gordon, T. A dose-dependent facilitation and inhibition of peripheral nerve regeneration by brain-derived neurotrophic factor. *European Journal of Neuroscience* 15, 613-626 (2002).

112   Enomoto, M., Bunge, M. B. & Tsoulfas, P. A multifunctional neurotrophin with reduced affinity to p75NTR enhances transplanted Schwann cell survival and axon growth after spinal cord injury. *Experimental neurology* 248, 170-182 (2013).

113   Hollis II, E. R. & Tuszynski, M. H. Neurotrophins: potential therapeutic tools for the treatment of spinal cord injury. *Neurotherapeutics* 8, 694-703 (2011).

114   Thorne, R. G. & Frey II, W. H. Delivery of neurotrophic factors to the central nervous system. *Clinical pharmacokinetics* 40, 907-946 (2001).

115   Wilkinson, A. E., McCormick, A. M. & Leipzig, N. D. Central Nervous System Tissue Engineering: Current Considerations and Strategies. *Synthesis Lectures on Tissue Engineering* 3, 1-120 (2011).

116   Prang, P. *et al.* The promotion of oriented axonal regrowth in the injured spinal cord by alginate-based anisotropic capillary hydrogels. *Biomaterials* 27, 3560-3569 (2006).

117   Nomura, H. *et al.* Extramedullary chitosan channels promote survival of transplanted neural stem and progenitor cells and create a tissue bridge after complete spinal cord transection. *Tissue Engineering Part A* 14, 649-665 (2008).

118   Silva, N. A. *et al.* Development and characterization of a Novel Hybrid Tissue Engineering–based scaffold for spinal cord injury repair. *Tissue Engineering Part A* 16, 45-54 (2009).

119   Blumenthal, J., Cohen-Matsliah, S. I. & Levenberg, S. Olfactory bulb-derived cells seeded on 3D scaffolds exhibit neurotrophic factor expression and pro-angiogenic properties. *Tissue Engineering Part A* (2013).

120   Cao, H., Liu, T. & Chew, S. Y. The application of nanofibrous scaffolds in neural tissue engineering. *Advanced Drug Delivery Reviews* 61, 1055-1064 (2009).

121   Wrobel, M. R. & Sundararaghavan, H. G. Directed Migration in Neural Tissue Engineering. *Tissue Engineering Part B: Reviews* (2013).

122   Modi, G., Pillay, V. & Choonara, Y. E. Advances in the treatment of neurodegenerative disorders employing nanotechnology. *Annals of the New York Academy of Sciences* 1184, 154-172 (2010).

123   Patel, T., Zhou, J., Piepmeier, J. M. & Saltzman, W. M. Polymeric nanoparticles for drug delivery to the central nervous system. *Advanced Drug Delivery Reviews* 64, 701-705 (2012).

124   Silva, G. A. Nanotechnology applications and approaches for neuroregeneration and drug delivery to the central nervous system. *Annals of the New York Academy of Sciences* 1199, 221-230 (2010).

125   Lee, D.-E. *et al.* Multifunctional nanoparticles for multimodal imaging and theragnosis. *Chemical Society Reviews* 41, 2656-2672 (2012).

126   Kajita, M. *et al.* Platinum nanoparticle is a useful scavenger of superoxide anion and hydrogen peroxide. *Free radical research* 41, 615-626 (2007).

127   Mukherjee, P. *et al.* Antiangiogenic properties of gold nanoparticles. *Clinical cancer research* 11, 3530-3534 (2005).

128   Gao, L. *et al.* Intrinsic peroxidase-like activity of ferromagnetic nanoparticles. *Nature nanotechnology* 2, 577-583 (2007).

129   Petros, R. A. & DeSimone, J. M. Strategies in the design of nanoparticles for therapeutic applications. *Nature Reviews Drug Discovery* 9, 615-627 (2010).

130   Janib, S. M., Moses, A. S. & MacKay, J. A. Imaging and drug delivery using theranostic nanoparticles. *Advanced Drug Delivery Reviews* 62, 1052-1063 (2010).

131   Yang, J., Ni, B., Liu, J., Zhu, L. & Zhou, W. Application of liposome-encapsulated hydroxycamptothecin in the prevention of epidural scar formation in New Zealand white rabbits. *The Spine Journal* 11, 218-223 (2011).

132   Liu, Y. *et al.* Novel multifunctional polyethylene glycol-transactivating-transduction protein-modified liposomes cross the blood-spinal cord barrier after spinal cord injury. *Journal of Drug Targeting* 18, 420-429 (2010).

133   Iannotti, C. A. *et al.* A combination immunomodulatory treatment promotes neuroprotection and locomotor recovery after contusion SCI. *Experimental neurology* 230, 3-15 (2011).

134   Dengler, E. C. *et al.* Mesoporous silica-supported lipid bilayers (protocells) for DNA cargo delivery to the spinal cord. *Journal of Controlled Release* 168, 209-224 (2013).

135   Cho, Y., Shi, R. & Borgens, R. B. Chitosan produces potent neuroprotection and physiological recovery following traumatic spinal cord injury. *The Journal of experimental biology* 213, 1513-1520 (2010).

136   Kim, Y.-t., Caldwell, J.-M. & Bellamkonda, R. V. Nanoparticle-mediated local delivery of methylprednisolone after spinal cord injury. *Biomaterials* 30, 2582-2590 (2009).

137   Wang, Y.-C. *et al.* Sustained intraspinal delivery of neurotrophic factor encapsulated in biodegradable nanoparticles following contusive spinal cord injury. *Biomaterials* 29, 4546-4553 (2008).

138   Chen, B., Zuberi, M., Borgens, R. B. & Cho, Y. Affinity for, and localization of, PEG-functionalized silica nanoparticles to sites of damage in an ex vivo spinal cord injury model. *J Biol Eng* 6, 18 (2012).

139   Cho, Y., Shi, R., Ivanisevic, A. & Ben Borgens, R. Functional silica nanoparticle-mediated neuronal membrane sealing following traumatic spinal cord injury. *Journal of Neuroscience Research* 88, 1433-1444 (2010).

140   Gwak, S.-J. *et al.* Chitosan/TPP-hyaluronic acid nanoparticles: a new vehicle for gene delivery to the spinal cord. *Journal of Biomaterials Science, Polymer Edition* 23, 1437-1450 (2012).

141   Rossi, F. *et al.* Tunable hydrogel—Nanoparticles release system for sustained combination therapies in the spinal cord. *Colloids and Surfaces B: Biointerfaces* 108, 169-177 (2013).

142   Kang, C. E., Baumann, M. D., Tator, C. H. & Shoichet, M. S. Localized and sustained delivery of fibroblast growth factor-2 from a nanoparticle-hydrogel composite for treatment of spinal cord injury. *Cells Tissues Organs* 197, 55-63 (2012).

143   Reukov, V., Maximov, V. & Vertegel, A. Proteins conjugated to poly(butyl cyanoacrylate) nanoparticles as potential neuroprotective agents. *Biotechnology and Bioengineering* 108, 243-252 (2011).

144   Takenaga, M. *et al.* Nano PGE1 promoted the recovery from spinal cord injury-induced motor dysfunction through its accumulation and sustained release. *Journal of Controlled Release* 148, 249-254 (2010).

145   Cerqueira, S. R. *et al.* Microglia Response and In Vivo Therapeutic Potential of Methylprednisolone-Loaded Dendrimer Nanoparticles in Spinal Cord Injury. *Small* 9, 738-749 (2013).

146   Rodrigo, A. C. *et al.* Efficient, Non-Toxic Hybrid PPV-PAMAM Dendrimer as a Gene Carrier for Neuronal Cells. *Biomacromolecules* 12, 1205-1213 (2011).

147   Posadas, I. *et al.* Highly Efficient Transfection of Rat Cortical Neurons Using Carbosilane Dendrimers Unveils a Neuroprotective Role for HIF-1α in Early Chemical Hypoxia-Mediated Neurotoxicity. *Pharm Res* 26, 1181-1191 (2009).

148   Shakhbazau, A. *et al.* Use of polyamidoamine dendrimers to engineer BDNF-producing human mesenchymal stem cells. *Mol Biol Rep* 37, 2003-2008 (2010).

149   Pal, A. *et al.* Iron oxide nanoparticles and magnetic field exposure promote functional recovery by attenuating free radical-induced damage in rats with spinal cord transection. *International Journal of Nanomedicine* 8, 2259-2272 (2013).

150   Zhizhi, S. *et al.* Characterization of cellular uptake and toxicity of aminosilane-coated iron oxide nanoparticles with different charges in central nervous system-relevant cell culture models. *Int J Nanomedicine* 8, 961-970 (2013).

151   Vaněček, V. *et al.* Highly efficient magnetic targeting of mesenchymal stem cells in spinal cord injury. *International Journal of Nanomedicine* 7, 3719 (2012).

152   Pinkernelle, J., Calatayud, P., Goya, G. F., Fansa, H. & Keilhoff, G. Magnetic nanoparticles in primary neural cell cultures are mainly taken up by microglia. *BMC neuroscience* 13, 32 (2012).

153   Lei, D. *et al.* Superparamagnetic iron oxide labeling of spinal cord neural stem cells genetically modified by nerve growth factor-β. *J. Huazhong Univ. Sci. Technol. [Med. Sci.]* 29, 235-238 (2009).

154   Shi, Y. *et al.* Effective repair of traumatically injured spinal cord by nanoscale block copolymer micelles. *Nat Nano* 5, 80-87 (2010).

155   Chen, C.-L. *et al.* Bioavailability Effect of Methylprednisolone by Polymeric Micelles. *Pharm Res* 25, 39-47 (2008).

156   Wang, Y.-T. *et al.* The use of a gold nanoparticle-based adjuvant to improve the therapeutic efficacy of hNgR-Fc protein immunization in spinal cord-injured rats. *Biomaterials* 32, 7988-7998 (2011).

157   Roman, J. A., Niedzielko, T. L., Haddon, R. C., Parpura, V. & Floyd, C. L. Single-walled carbon nanotubes chemically functionalized with polyethylene glycol promote tissue repair in a rat model of spinal cord injury. *Journal of neurotrauma* 28, 2349-2362 (2011).

158   Sahoo, S. K. & Labhasetwar, V. Nanotech approaches to drug delivery and imaging. *Drug discovery today* 8, 1112-1120 (2003).

159   Malam, Y., Loizidou, M. & Seifalian, A. M. Liposomes and nanoparticles: nanosized vehicles for drug delivery in cancer. *Trends in pharmacological sciences* 30, 592-599 (2009).

160   Alipour, M., Smith, M. G., Pucaj, K. & Suntres, Z. E. Acute toxicity study of liposomal antioxidant formulations containing N-acetylcysteine, α-tocopherol, and γ-tocopherol in rats. *Journal of Liposome Research* 22, 158-167 (2012).

161   Sevc, J. *et al.* Effective long-term immunosuppression in rats by subcutaneously implanted sustained-release tacrolimus pellet: Effect on spinally grafted human neural precursor survival. *Experimental neurology* 248, 85-99 (2013).

162   Wang, H. *et al.* PEGlated magnetic polymeric liposome anchored with TAT for delivery of drugs across the blood-spinal cord barrier. *Biomaterials* 31, 6589-6596 (2010).

163   Numata, K., Yamazaki, S. & Naga, N. Biocompatible and biodegradable dual-drug release system based on silk hydrogel containing silk nanoparticles. *Biomacromolecules* 13, 1383-1389 (2012).

164   Papi, M. *et al.* Controlled self assembly of collagen nanoparticle. *Journal of Nanoparticle Research* 13, 6141-6147 (2011).

165   Wagner, S. *et al.* Enhanced drug targeting by attachment of an anti αv integrin antibody to doxorubicin loaded human serum albumin nanoparticles. *Biomaterials* 31, 2388-2398 (2010).

166   Nagpal, K., Singh, S. K. & Mishra, D. N. Chitosan nanoparticles: a promising system in novel drug delivery. *Chemical and Pharmaceutical Bulletin* 58, 1423-1430 (2010).

167   Zhang, C. *et al.* Doxorubicin-loaded glycyrrhetinic acid-modified alginate nanoparticles for liver tumor chemotherapy. *Biomaterials* 33, 2187-2196 (2012).

168   Eidi, H. *et al.* Cytotoxicity assessment of heparin nanoparticles in NR8383 macrophages. *International journal of pharmaceutics* 396, 156-165 (2010).

169   Cunliffe, D., Pennadam, S. & Alexander, C. Synthetic and biological polymers––merging the interface. *European Polymer Journal* 40, 5-25 (2004).

170   Sokolsky-Papkov, M., Agashi, K., Olaye, A., Shakesheff, K. & Domb, A. J. Polymer carriers for drug delivery in tissue engineering. *Advanced Drug Delivery Reviews* 59, 187-206 (2007).

171   Jevševar, S., Kunstelj, M. & Porekar, V. G. PEGylation of therapeutic proteins. *Biotechnology Journal* 5, 113-128 (2010).

172   Katz, J. S. & Burdick, J. A. Hydrogel mediated delivery of trophic factors for neural repair. *Wiley Interdisciplinary Reviews: Nanomedicine and Nanobiotechnology* 1, 128-139 (2009).

173   Zhu, J. & Marchant, R. E. Design properties of hydrogel tissue-engineering scaffolds. *Expert review of medical devices* 8, 607-626 (2011).

174   Chen, B., Bohnert, D., Borgens, R. B. & Cho, Y. Pushing the science forward: chitosan nanoparticles and functional repair of CNS tissue after spinal cord injury. *J Biol Eng* 7, 1-9 (2013).

175   Veiseh, O., Gunn, J. W. & Zhang, M. Design and fabrication of magnetic nanoparticles for targeted drug delivery and imaging. *Advanced Drug Delivery Reviews* 62, 284-304 (2010).

176   Menjoge, A. R., Kannan, R. M. & Tomalia, D. A. Dendrimer-based drug and imaging conjugates: design considerations for nanomedical applications. *Drug discovery today* 15, 171-185 (2010).

177   Svenson, S. & Tomalia, D. A. Dendrimers in biomedical applications—reflections on the field. *Advanced Drug Delivery Reviews* (2012).

178   Oliveira, J. M., Salgado, A. J., Sousa, N., Mano, J. F. & Reis, R. L. Dendrimers and derivatives as a potential therapeutic tool in regenerative medicine strategies—a review. *Progress in Polymer Science* 35, 1163-1194 (2010).

179   Salgado, A. J. *et al.* Carboxymethylchitosan/Poly(amidoamine) Dendrimer Nanoparticles in Central Nervous Systems-Regenerative Medicine: Effects on Neuron/Glial Cell Viability and Internalization Efficiency. *Macromolecular Bioscience* 10, 1130-1140 (2010).

180   Cerqueira, S. R. *et al.* Multifunctionalized CMCht/PAMAM Dendrimer Nanoparticles Modulate the Cellular Uptake by Astrocytes and Oligodendrocytes in Primary Cultures of Glial Cells. *Macromolecular Bioscience* 12, 591-597 (2012).

181   De Jong, W. H. & Borm, P. J. Drug delivery and nanoparticles: applications and hazards. *International Journal of Nanomedicine* 3, 133 (2008).

SECTION II

CHAPTER II

Materials and Methods

CHAPTER II

Materials and methods

The main aim of this chapter is to describe the experimental work and protocols used in the scope of this thesis and related to the obtained results, which will be provided in more detail in Section 3. Along with Chapter I, it aims to provide the reader a more comprehensive overview of the experimental and analytical tools used, as well as the rationale behind its use.

1. Materials

1.1. Poly(amido)amine dendrimers

Poly(amido)amine (PAMAM) dendrimers are the most common class of dendrimers and are used nowadays for several biotechnology applications.[1] Dendrimers were first described in 1978, introducing a new class of nanoscale synthetic polymers with branched spherical architectures, inspired in nature (*dendron* is the greek word for tree).[2] These molecules present an extremely precise and controlled structure, and therefore have tuneable sizes and molecular weights, with further functionalization possibilities.
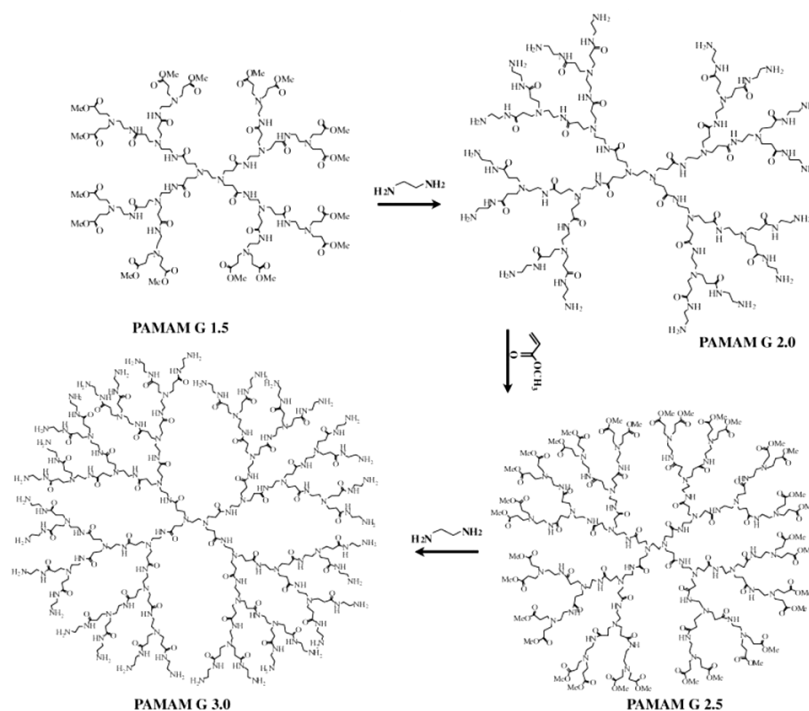
Figure 1 - Structures of generations 1.5 to 3 poly(amidoamine) dendrimers.

The typical dendrimer structure comprises three main parts: the inner core that ramifies in branching units and eventually ends in external capping groups.[3] To each layer of the branching units it is attributed the designation of generation (G). The PAMAM dendrimers consist of an alkyl-diamine core with tertiary amine branching units. It is commercially available and the PAMAM dendrimers used throughout this work were obtained from Sigma, USA.

1.2. Chitosan and its derivative carboxymethylchitosan

Chitin and chitosan (Cht) are interesting macromolecules for biomedical uses; however, they present some limitations due to its poor water solubility. Some chemical modifications in the chitosan structure can be performed in order to overcome this, and taking advantage of its reactive functional groups (e.g., amine -NH_2 and hydroxyl -OH) the degradation profile can be controlled, thus broadening its range of applications.[4] Modification of Cht structure has been done introducing acetyl, carboxymethyl, sulfuryl or phosphoryl groups, among others.[5] Carboxymethylchitosan (CMCht) is a water-soluble biomacromolecule derived from deacetylation and insertion of carboxylic groups in Cht (Figure 2). CMCht is soluble in a wide range of pH and its properties, namely low toxicity and antimicrobial activity, are attractive in medical and pharmaceutical areas, mainly for the controlled release of drugs.[5]
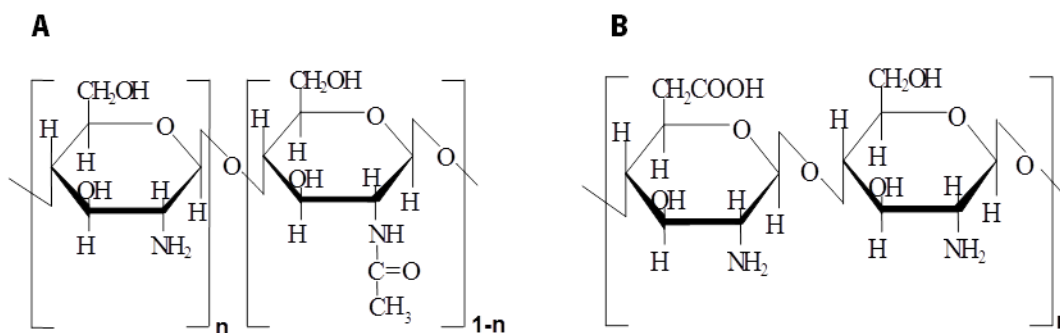
Figure 2 - Schematic representation of chitosan (A), and carboxymethylchitosan (B) molecular structure.

For the purpose of this thesis, reagent grade chitosan particles with a degree of deacetylation (DD) of ≈91% were used for the preparation of CMCht. The methodology used has been previously reported by Chen *et al.*[6] Succinctly, chitosan was dissolved in 40% sodium hydroxide (NaOH, Sigma, Germany) solution at room temperature for 1 hour. Then, monocloroacetic acid ($ClCH_2COOH$, Sigma, Germany) was added into the reaction vessel drop-wise and let react for 2

hours, in a water bath at 60°C. The reaction was stopped by adding 70% ethanol and the resulting pellet filtered and rinsed in sequential 70 to 90% ethanol. Finally, the H-form of CMCht was obtained by re-suspending the filtrate in 80% ethanol solution and 37% hydrochloric acid (HCl, Sigma, Germany) for 30 minutes, under agitation. New filtration was performed followed by de-hydration. CMCht was obtained by freeze-drying at -80°C (Telstar-Cryodos -80, Spain). CMCht with a DD of 80% and a degree of substitution (DS) of 47% was used for the surface modification of the dendrimers, as previously reported.[7]

1.3. Methylprednisolone

Methylprednisolone (MP) is a synthetic corticosteroid drug clinically used for its potent anti-inflammatory and antioxidant properties.[8] MP is currently recommended for use in a variety of CNS disorders involving white matter injuries, such as spinal cord injury (SCI) and multiple sclerosis (MS).[9] Nonetheless, its use has been shown to be highly unspecific, leading to a series of undesired side effects in patients following intravenous administration, such as gastric bleedings and pneumonia.[10] Therefore, the blurred balance between the benefits and drawbacks of MP administration has led some clinicians to abandon its use. In fact, its precise mechanisms of action are still being uncovered and it is becoming clearer that according to the target cell MP exerts differential effects.[11]
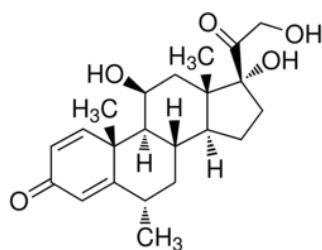
Figure 3 - Schematic representation of the methylprednisolone molecule.

1.4. Reagents

Chemicals used for the synthesis and purification of CMCht, CMCht/PAMAM dendrimer nanoparticles as well as their processing and characterization, were bought from the following companies: Fluka (Slovakia), Merck (Germany), Panreac (Spain), Pronalab (Portugal), Riedel-de Haën (Germany) and Sigma (Germany).

2. Nanoparticle synthesis and functionalization

2.1. Dendrimer nanoparticle synthesis: overview

Dendrimer synthesis has been suggested through two alternative methodologies: the divergent and the convergent synthesis. The divergent method has been described by Tomalia *et al.,*[12] and it involves the *in situ* assembly of each branching unit in a step-by-step manner around the central core (Figure 4A). In the convergent approach, developed by Fréchet and colleagues, the building blocks are first prepared (as dendrons) and afterwards put together from the outside to the core (Figure 4b).[13]
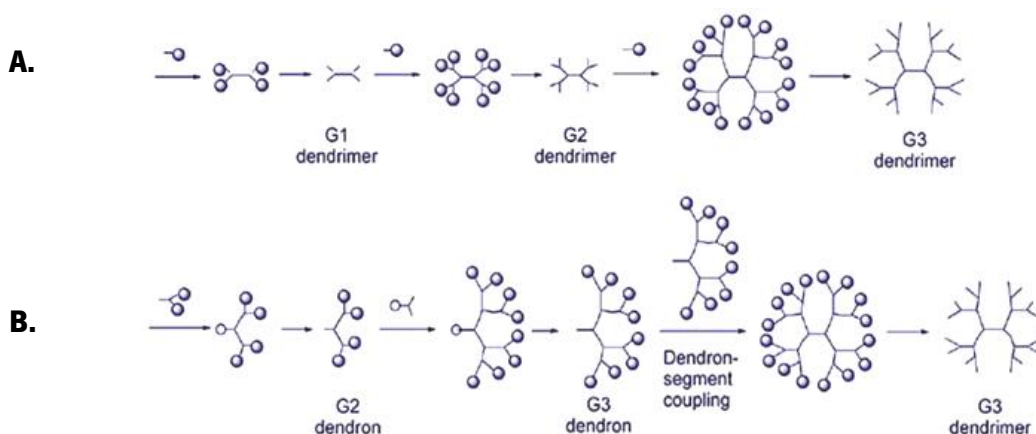
Figure 4 – Schematic representation of the divergent (A) and convergent (B) synthesis approaches.

In this thesis, the dendrimer nanoparticle systems were obtained following the divergent route, expanding a PAMAM G1.5 dendrimer to a PAMAM G3 molecule.[14] The drug delivery systems (DDS) were herein produced for applications in CNS tissue repair, namely for spinal cord injury drug delivery.

2.2. Carboxymethylchitosan/poly(amido)amine dendrimer nanoparticles

In the present thesis we applied a nanoparticle system with novel capabilities and performance for CNS drug delivery purposes. Investigation of this system applicability should address concurrently: (i) the prevention of opsonization or early NP clearance; (ii) the ability to enter cells

and cross biological barriers, such as the BBB; (iii) intracellular trafficking of the nanostructures; (iv) toxicity assessment, both *in vitro* and *in vivo*; (v) *in vivo* biodistribution; and (vi) the therapeutic activity of the DDS. The techniques herein described were used with the aim of evaluating these parameters, allowing a relevant and complete understanding of the developed DDS. In the herein presented approach, surface grafted amine-terminated PAMAM dendrimers with water-soluble CMCht were produced in order to neutralize the amine groups of PAMAM, which have been described to be accountable for some toxicity.[15,16]

2.3 CMCht/PAMAM dendrimer nanoparticle synthesis

For the surface modification of the PAMAM dendrimers, CMCht with a DD of 80% and DS of 47% was used. Starburst® poly(amido)amine-carboxylic terminated dendrimers (PAMAM-CT) (generation 1.5, 20% (w/v)) in a methanolic solution with an ethylenediamine core were purchased (Sigma, Germany). CMCht/PAMAM nanoparticles were prepared in a step-by-step method starting with the increase of the PAMAM-CT G 1.5 to a G 3 dendrimer. To achieve this, the methanol was evaporated from the PAMAM dendrimers under nitrogen gas to completely remove it. The remaining compound was re-dissolved in ultra-pure water to a final concentration of 10 mg.mL^{-1}, and the pH was adjusted with HCl to 6.5. Afterwards, 1-ethyl-3(3-dimethylaminopropyl) carbodiimide hydrochloride (EDC, Fluka, Slovakia) was added to the solution to modify the carboxylate residues. The reaction was let occur for 30 minutes at room temperature (RT) and under agitation. Following this, ethylenediamine (EDA, Sigma, Germany) was added and let react for 4 hours. The exceeding EDC was removed by dialysis in ultrapure water using a cellulose tubing (benzoylated for separating compounds with a molecular weight of ≤1,200, Sigma, Germany). The obtained amine-terminated PAMAM dendrimers (PAMAM-AT) were mixed with methanol (Sigma, Germany) and methyl methacrylate (Fluka, Germany) and kept under agitation in a water bath at 50°C for 24 hours, to perform alkylation of its primary amines (Michael addition).[12] Finally, in order to perform a condensation reaction between the CMCht and the PAMAM groups, hydrochloric acid (HCl, Panreac, Portugal) and trifluoroacetic acid (TFA, Sigma, Germany) were added to the solution. Meanwhile, 1 g of CMCht was dissolved in 50 mL of water. The PAMAM methyl esther terminated dendrimers were dissolved in a 20/80 water/methanol solution and the CMCht was added and kept under agitation for 72 hours, after which the CMCht/ PAMAM dendrimer nanoparticles with carboxylic-terminated groups were

obtained. The nanoparticles were then precipitated with the addition of an appropriate volume of a saturated sodium carbonate (Na$_2$CO$_3$, Sigma, Germany) solution and acetone (Pronalab, Portugal). CMCht/PAMAM dendrimer nanoparticles were obtained by freezing the solution at -80°C and freeze-drying (Telstar-Cryodos -80, Spain) for 5 days, until the solvent was completely removed.

2.4. Incorporation of methylprednisolone into CMCht/PAMAM dendrimer nanoparticles

The corticosteroid MP was physically incorporated into the CMCht/PAMAM dendrimer nanoparticle branches. Firstly, CMCht/PAMAM dendrimer nanoparticles were mixed with an ethanolic MP solution in a final concentration of 5×10^{-4} M (w/w) under agitation. The mixture was then added to precipitation media consisting of a saturated Na$_2$CO$_3$ (Sigma, Germany) and acetone (Pronalab, Portugal) solution, under vigorous agitation. Precipitates were collected by filtration and dispersed in ultrapure water for dialysis against ultrapure water (cellulose tubing, benzoylated for separating compounds with a molecular weight of ≤1,200, Sigma, Germany) during 48 hours. MP-loaded CMCht/PAMAM dendrimer nanoparticles were obtained by freezing the solution at -80°C and freeze-drying (Telstar-Cryodos -80, Spain) until the solvent was completely removed.

2.5. Labeling CMCht/PAMAM dendrimer nanoparticles with fluorescein isothiocyanate

In order to track the intracellular localization of the NPs, conjugation with a fluorescent probe was performed. A derivative of fluorescein was used to label the NPs, fluorescein isothiocyanate (FITC, Sigma, Germany). FITC-labeled dendrimer nanoparticle conjugates were prepared by covalently bonding the amine group of CMCht and the isothiocyanate group from FITC. To perform the reaction, a 10 mg.mL^{-1} FITC solution was prepared in dimethyl sulfoxide anhydrous (DMSO, Riedel-de Haen, Germany) in the dark. Concurrently, a 10 mg.mL^{-1} CMCht/PAMAM dendrimer nanoparticle solution was prepared in a carbonate/bicarbonate coupling buffer (pH 9.2) and 50 μL of FITC/DMSO solution were added per each mL of CMCht/PAMAM dendrimer nanoparticle buffered solution, under agitation. The resulting solution was kept in the dark at 4°C for 8 hours. The obtained FITC-labeled CMCht/PAMAM dendrimer nanoparticle solution was then dialyzed against ultra-pure water (cellulose tubing, benzoylated for separating compounds with a

molecular weight of ≤1,200, Sigma, Germany) for 48 hours in order to remove unbonded FITC molecules. The final product was obtained by freezing the solution at -80°C and freeze-drying (Telstar-Cryodos -80, Spain) for 5 days, until the solvent was completely removed.
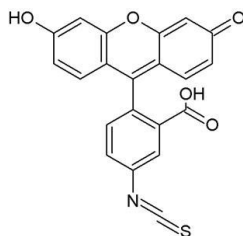
Figure 5 - Chemical structure of the FITC molecule.

2.6. Surface functionalization with CD11b antibody

One of the most exciting features of nanoparticles in drug delivery is the possibility to design a DDS that can act specifically in a certain cell type or tissue, for instance. The drug delivery efficiency would subsequently be maximized while unwanted side reactions in other tissues would be significantly lessened.[17] To assess the possibility of functionalization of CMCht/PAMAM dendrimer NPs with a targeting agent that might confer altered uptake, we performed a crosslinking reaction with an antibody. Along with other moieties, such as low molecular weight molecules, peptides, proteins, polysaccharides, DNA and plasmids, antibodies have been suggested to confer selectivity in NP uptake.[18] Antibodies, also known as immunoglobulins (Ig), are recognition proteins used as part of the immune system to specifically identify and neutralize foreign bodies in the organism. Antibodies identify a distinctive part of the foreign body, called antigen, to which they bind with high affinity (Figure 8).
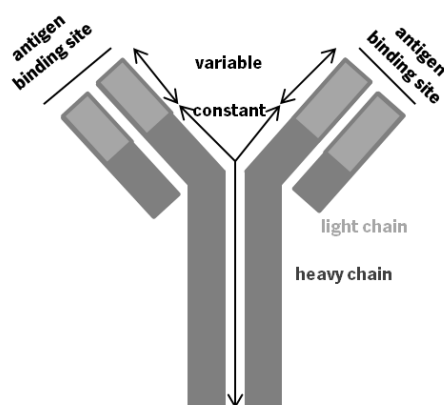
Figure 6 - Structural representation of an antibody and its main parts.

In order to conjugate anti-mouse CD11b antibody (BD Biosciences, USA) which identifies microglial cells to the dendrimer nanoparticles a crosslinking reaction was performed.[19] A 20 mg.mL^{-1} solution of nanoparticles in phosphate buffered saline (PBS, pH 7.4) was mixed with 1 mg.mL^{-1} of 1-ethyl-3(3-dimethylaminopropyl) carbodiimide hydrochloride (EDC, Fluka, Slovakia) and let react for 30 minutes at RT. The remaining solution was dialysed against ultrapure water (cellulose tubing, benzoylated for separating compounds with a molecular weight of ≤1,200, Sigma, Germany) for 24 hours to remove the excess EDC. Afterwards, the pH was corrected to 7.4 and the 4 nmol of CD11b antibody were added under agitation. The crosslinking reaction was let occur for 1 hour, after which the solution was frozen at -80°C and freeze-dried (Telstar-Cryodos-80, Spain) for 5 days, until the solvent was completely removed.

3. Physicochemical characterization techniques

3.1. Scanning-transmission electron microscopy

The morphology and average diameter distribution of NPs were investigated under a scanning-transmission electron microscope (Nova™ NanoSEM 50 series, FEI Company, The Netherlands). Conventional electron microscopy allows examination of the samples via a beam of electrons that either scan the surface of the sample (scanning electron microscope, SEM) or are transmitted through it (transmission electron microscope, TEM) providing high magnification detailed images of its morphology.[20] Novel advanced electron microscopy techniques, especially scanning transmission electron microscopy (STEM) techniques are becoming indispensable for characterizing nanosystems. STEM microscopes present higher versatility, with atomic resolution imaging, diffraction patterns and spectroscopy data being obtained simultaneously or sequentially by this method from the same region of the specimen.[21] STEM is therefore considered one of the most powerful microscopy techniques for use in the physicochemical characterization of nanosystems. To have high resolution images of the nanoparticles produced during this work, lyophilized NPs were dispersed in ultrapure water to a final concentration of 1 mg.mL^{-1}, stained with 1% phosphotungstic acid and placed on copper grids for further observation.

3.2. Fourier-transform infra-red spectroscopy

Fourier-transform infra-red (FTIR) analysis allows to determine the presence of functional groups in organic molecules in a non destructive manner by registering the vibrational spectra of the compounds.[22] It is a spectroscopic technique in which a beam containing the selected frequencies is pointed out to a pellet containing the specimen and a measure of the absorption at each frequency is made, resulting in specific spectra for each compound analyzed.[23] To validate the synthesis of CMCht/PAMAM dendrimer NPs, as well as the MP incorporation and antibody bonding, the obtained spectra for each sample were analyzed. Transparent potassium bromide (KBr) pellets were prepared by mixing in the sample in KBr, and the analysis was performed using a Perkin-Elmer spectroscope (Perkin-Elmer 1600 series equipment). All transmission spectra were recorded in the region of 4400-450 cm^{-1}, using a minimum of 32 scans and a 2 cm^{-1} resolution.

3.3. Nuclear magnetic resonance spectroscopy

Nuclear magnetic resonance (NMR) is a physical phenomenon that occurs when the nuclei of certain atoms absorb and re-emit electromagnetic radiation.[24] Some nuclei experience this phenomenon depending upon whether they possess a property called spin. ^{1}H NMR is the application of nuclear magnetic resonance spectroscopy with respect to hydrogen nuclei within the molecules of a compound and allows the resolution of the structure of organic compounds. Unlike other NP characterization techniques, such as electron microscopy, it does not require sample preparation with the risk of causing artifacts or sample deterioration.[25] Moreover, NMR spectroscopy renders simultaneous information on the chemical composition as well as the molecular mobility of components in a complex non-homogenous mixture. In this thesis, ^{1}H NMR analysis of the CMCht/PAMAM, MP-loaded CMCht/PAMAM, FITC-labeled CMCht/PAMAM and CD11b antibody-conjugated CMCht/PAMAM dendrimer NPs was carried out in order to confirm the performed functionalization. For this purpose, NPs were dissolved in deuterated water (D_2O) and the ^{1}H NMR spectra were obtained in a Varian Unity Plus spectrometer at 300 MHz and 20°C. The one-dimensional ^{1}H spectra were acquired using a 45° pulse, a spectral width of 6.3 kHz and an acquisition time of 2.001 seconds.

3.4. Zeta potential and particle size analysis

Zeta potential and particle size of the CMCht/PAMAM dendrimer nanoparticles and MP-loaded CMCht/PAMAM dendrimer nanoparticles were measured in a particle size analyzer (Zetasizer Nano ZS, Malvern Instruments, UK). The zeta potential is calculated by determining the electrophoretic mobility, which is obtained by performing an electrophoresis experiment on the sample and measuring the velocity of the particles using a Laser Doppler Velocimetry (LDV).[26] Zeta potential has proven to be a central index which reflects the intensity of repulsive forces among the NPs, and consequently its stability when dispersed in solution.[27] Studies have shown that zeta potential depends on the chemical composition of the NPs, the surrounding solvent, the pH of the media and the ions in the suspension.[28] Electrophoretic determinations of zeta potential were investigated using the universal 'dip' cell, at pH 5.0; 7.4 and 10.0, in citrate buffer, phosphate buffered saline (PBS) and bicarbonate buffer solutions, respectively.

Using the same equipment, diameter determinations were made using dynamic light scattering (DLS). DLS utilizes time variation of scattered light from suspended particles under Brownian motion to obtain their hydrodynamic size.[29] It is a reliable technique that has been used to measure macromolecules and small particles in dilute suspensions. Thus, for the present study, particle size analyses were performed using the DLS technique. The analyses were carried out in different aqueous solutions (PBS pH 7.4; citrate buffer pH 5.0; and bicarbonate buffer pH 10.0) with low concentration of nanoparticles and using disposable sizing cuvettes.

3.5. High performance liquid chromatography

High performance liquid chromatography (HPLC) is an analytical technique used to identify, quantify and purify the individual components of a solution. The compounds are separated passing through a column at different rates due to differential affinity and interaction of the mobile phase (comprising the sample) and the stationary phase of the column.[30] The MP release from the NPs was quantified using HPLC (Knauer Smartline, Germany), with an UV detector set at 250 nm. The mobile phase consisted of acetonitrile:ammonium phosphate buffer (0.1 M, pH 4.6) (50:50 v/v) at a flow rate of 1 mL.min^{-1}. MP release was studied after dissolution of 10 mg of MP-loaded CMCht/PAMAM dendrimer nanoparticles in 10 mL of PBS (pH 7.4, Sigma, USA) solution. Simultaneously, the absence or presence of 15% fetal bovine serum (FBS) was also

tested in order to assess protein interaction in the drug release rates. To avoid external biological contaminations sodium azide 0.01% (w/v) (Sigma, Germany) was added to the buffer solutions. The *in vitro* release studies were performed at 37°C and 60 rpm for times ranging from 1 hour to 14 days. At set time intervals, 1 mL of sample was collected for analysis and the same volume replaced by the respective buffer solution. Prior analysis, samples were centrifuged at 2,000 rpm for 10 minutes. A solution with sample:acetonitrile:ammonium phosphate buffer (50:25:25, v/v) was prepared for further analysis. A C18 analytical column (Atlantis T3, Waters, USA) was used. The MP retention time was approximately 3 minutes. A calibration curve was acquired preparing relevant standard solutions.

4. Primary cell isolation and culture establishment

Cell culture studies are a fundamental step in biotechnological product evaluation before *in vivo* testing, particularly if biomedical applications are envisioned. Frequently, *in vitro* studies in cell culture models of neuropathologies are used to test possible therapies, namely for brain tumor,[31] neurotrauma,[32] and neurodegeneration.[33] Particular focus has also been given recently to modelling the BBB *in vitro* cell trafficking and substance permeability studies.[34] In this thesis, fresh primary cultures were used in an attempt to more closely mimic the *in vivo* conditions and generate physiologically relevant data. In order to assess the NP effect on cell viability and its uptake profile, mixed glial cell cultures were established. Further purification of these cultures was executed to obtain pure microglia and astrocyte cultures, allowing the assessment of intracellular MP action and NP intracellular trafficking, respectively. Additionally, Schwann cell (SC) and dorsal root ganglia neuron (DRGN) cultures were done to verify the NPs effect on the SCs ability to myelinate DRGN axons. All the cultures were derived from Wistar or Fischer rats. Animal handling and experiments were conducted in accordance with the guidelines for the care and handling of laboratory animals in the Directive 2010/63/EU of the European Parliament and Council.

4.1. Primary cultures of cortical glial cells

Cortical glial cells were isolated from P4 newborn Wistar rats. Upon careful dissection to remove the skin and the skull, the cortices were collected and maintained in ice-cold Hanks' balanced

salt solution (HBSS, Gibco, USA) to be mechanically dissected. Afterwards, the cortical fragments were incubated in an enzymatic medium of 30 mg.mL^{-1} DNAse solution (Sigma, Germany) with 0.25% trypsin (Sigma, Germany) in Ca^{2+}/Mg^{2+} free HBSS solution for 30 minutes at 37°C. The trypsin reaction was blocked adding 40% foetal bovine serum (FBS, Gibco, USA) and the resulting tissue was centrifuged at 800 rpm for 2 minutes. Glial cells were then plated out on coverslips previously coated with poly-L-lysine (Sigma, USA) at a density of 4x10^4 cells.cm^{-2}. Cells were maintained for one week at 37°C in 5% CO$_2$, in Dulbecco's modified Eagle's medium (DMEM, Gibco, USA) supplemented with 1% antibiotic (A/B) and 10% fetal bovine serum (FBS, Gibco, USA) with periodical media renewal. All the procedure was performed under aseptic conditions. These mixed cultures are constituted mainly by astrocytes, followed by microglia and oligodendrocytes. Therefore, these cell types are representative of the environment that surrounds neurons in the CNS. The glial cultures were used to assess the NP influence in these cells viability and also to have an uptake profile of the NP in each cell type.
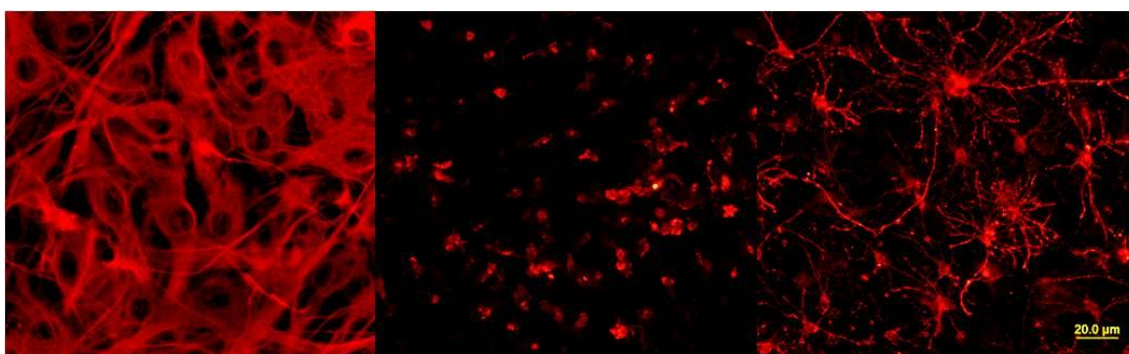
Figure 7 - Primary cultures of cortical glial cells. Immunocytochemistry was done for astrocytes (GFAP), microglia (CD11b) and oligodendrocytes (O4), respectively.

4.2. Primary cultures of microglial cells

Microglia cultures were purified from the mixed glial cell cultures. A physical separation is on the basis of this isolation procedure, since microglial cells are known to grow on top of astrocytes and can be isolated by physical separation without trypsinization. Consequently, after the isolation procedure glial cells were plated out at a density of 1×10^6 cells.cm^{-2} in polystyrene T$_{75}$ flasks (Thermo Scientific, USA) previously coated with poly-L-lysine (Sigma, USA). The glial primary cultures were kept at 37°C in 5% CO$_2$, in DMEM (Gibco, USA) supplemented with 1% A/B and 10% FBS (Gibco, USA) for two weeks, with periodical media renewal. After this period, the

cell flasks were agitated in an orbital shaker at 240 rpm during 4 hours at 37°C. Following this, the medium containing detached microglia cells was collected, centrifuged at 800 rpm for 5 minutes and the pellet re-suspended in DMEM medium (Gibco, USA) and plated out at a density of 4×10^4 cells.cm^{-2}. Microglial cell primary cultures were then maintained at 37°C in a 5% CO_2 atmosphere, in DMEM medium (Gibco, USA) supplemented with 10% FBS (Gibco, USA) and 1% A/B (Sigma, USA) for 3 days for further testing. All the procedure was performed under aseptic conditions. The purity of these cultures was verified by immunocytochemistry with CD11b antibody and proved to be superior to 95%. The microglial cell cultures were herein used to assess the intracellular action of MP, while being intracellularly released from the NPs.

4.3. Primary cultures of astrocytes

For astrocyte isolation, the same concept of microglial isolation was on the basis of astrocyte purification. After microglial cell detachment and discarding pure cultures of astrocytes were obtained. The isolated glial cells were plated out at a density of 1×10^6 cells.cm^{-2} in polystyrene T_{75} flasks (Thermo Scientific, USA) previously coated with poly-L-lysine (Sigma, USA), and kept at 37°C in 5% CO_2. The cultures were maintained in DMEM (Gibco, USA) supplemented with 1% A/B and 10% FBS (Gibco, USA) for two weeks, with periodical media renewal. After this period, the cell flasks were agitated in an orbital shaker at 240 rpm during 4 hours at 37°C, after which the media was discarded. The remaining cells from the agitation procedure were grown in high glucose DMEM and supplemented with 10% FBS (Gibco, USA), 2 mM L-glutamine (Sigma, Germany), 1 mM sodium pyruvate (Sigma, Germany) and penicillin/streptomycin (Sigma, Germany). The cultures were kept at 37°C and 95% air and 5% CO_2. The astrocytes were then sub-cultured onto 22 mm diameter poly-L-lysine (Sigma, USA) coated glass coverslips at low densities. All the procedure was performed under aseptic conditions. These cells were used in electrophysiological membrane capacitance readings for investigation of endocytosis/exocytosis frequency following NP incubation. Moreover, confocal imaging of live astrocytes was also performed.

4.4. Primary cultures of Schwann cells

Schwann cells (Figure 8) were obtained from sciatic nerves of adult female Fischer rats. Upon dissection, the sciatic nerves were cut into small 1-2 mm pieces and incubated in DMEM-F12 (Gibco, USA) with 10% FBS (Gibco, USA) and 1% A/B (Gibco, USA) onto uncoated culture dishes. The cultures were kept at 37°C and 95% air and 5% CO_2. Every week the nerve segments were transferred to new 35 mm dishes until, after 3 weeks in culture, the nerve segments, essentially depleted from fibroblasts, were mechanically and enzymatically dissociated with collagenase solution (320 U, Sigma, Germany) containing 5 $U.mL^{-1}$ DNase (Worthington, UK).
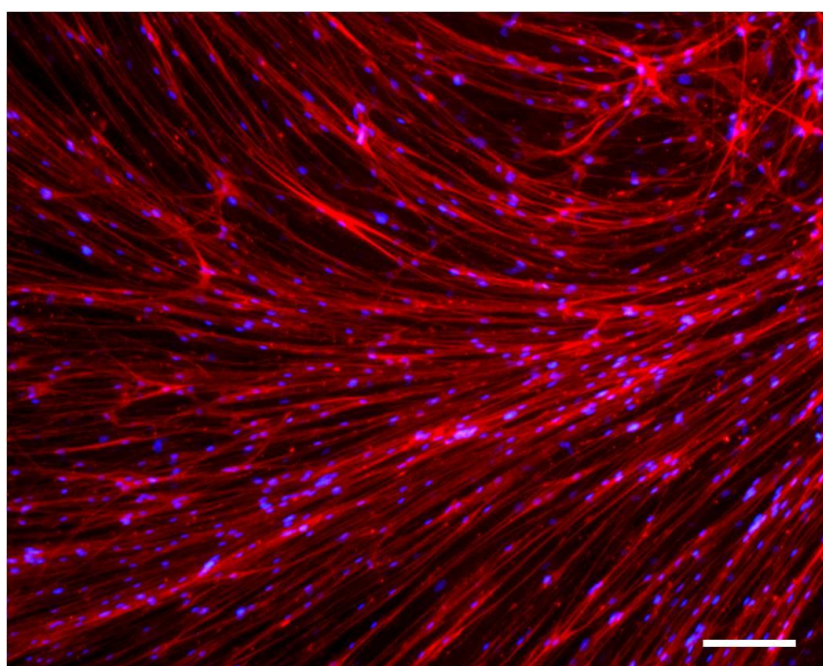
Figure 8 - Primary cultures of rat Schwann cells, with the nuclei stained with Hoescht (blue), and SCs labeled with GFAP (red) (10x). Scale bar represents 100 μm.

Cells were then transferred to new dishes for SC expansion in the presence of mitogens: 20 μg/mL bovine pituitary extract (Gibco, USA) and 2 μM forskolin (Sigma, Germany). SC purity was between 95 and 98%. All the procedure was performed under aseptic conditions. The obtained SCs were used for NP biocompatibility assessment and also for co-culturing with DRGN to evaluate the SC myelinating capacity in the presence of NPs.

4.5 Dorsal root ganglia neurons

The DRGs were dissected from embryonic day 15 Fischer rats and incubated in trypsin (Worthington Biochemical Corporation, USA). Trypsin activity was stopped by the addition of L-15 medium (Sigma, Germany) containing 10% FBS (Gibco, USA). The suspension was centrifuged and the pellet was re-suspended in serum-containing medium. Mechanical dissociation was done with a pipette until the neurons were dispersed and the volume increased to 5 mL. The cell suspension was mixed and centrifuged, and the pellet re-suspended in NLA medium containing: neurobasal medium (Invitrogen, USA), B27 neural supplement (Invitrogen, USA) and 10 ng/mL nerve growth factor (Invitrogen, USA). One drop of DRGN suspension in NLA medium was plated in the middle of dry, ammoniated collagen-coated dishes. Approximately 5,000 to 7,000 neurons were plated per culture. After the cells attached to the collagen overnight, the cultures were filled and subsequently treated with NLA medium containing fluorodeoxyuridine (FUDR, Sigma, Germany) on days 2 to 4, 6 to 8, and 10 to 12 to eliminate non-neuronal cells. After this anti-mitotic treatment, the resulting DRGN cultures were maintained on NLA medium for at least 1 week to ensure that no residual FUDR remained when SCs were added. The cultures were kept at 37°C and 95% air and 5% CO_2, and all the procedures were performed under aseptic conditions.

5. *In vitro* biological testing

5.1. Metabolic activity assay

The colorimetric 3-(4,5-dimethylthiazol-2-yl)-5-(3-carboxymethoxyphenyl)-2-(4-sulfophenyl)-2H-tetrazolium (MTS) viability test was performed to determine the potential cytotoxicity of MP-loaded CMCht/PAMAM dendrimer nanoparticles when incubated with glial cells. This assay has been widely used to measure cellular viability and it is based on the bioreduction of the MTS substrate into a brown formazan compound by dehydrogenase enzymes in metabolically active cells.[35] Glial cells were incubated with 200 µg.mL^{-1} MP-loaded CMCht/PAMAM dendrimer nanoparticles for a week with periodical renewal every 48 hours. Then, the cells were placed in serum-free culture medium containing MTS in a 5:1 ratio and incubated in a humidified atmosphere at 37°C and 5%

CO_2. After three hours of incubation 100 μL of solution from each well were transferred to a 96-well plate and the optical density for triplicates of each sample was determined at 490 nm.

5.2. Cell proliferation assay

The 5-bromo-2'-deoxyuridine (BrdU) assay (Roche, Switzerland) was used for DNA quantification as a measure of cell proliferation. Cell replication is commonly assessed analysing thymidine (^{3}H) incorporation into DNA.[36] BrdU is the equivalent non-radioactive method that evaluates DNA synthesis and cell proliferation. This ELISA-based assay measures the amount of BrdU incorporated into newly synthesized DNA of replicating cells. To perform the test, BrdU was added to the cell cultures for 24 hours and the cells were then fixed and its DNA denatured in a single step with FixDenat (Roche, Switzerland), after which the anti-BrdU peroxidase antibody (Roche, Switzerland) was added. The formed immune complexes were detected quantifying the substrate reaction product in a multiplate reader (BioRad) set at 370 nm (reference filter at 492 nm).

5.3. Assessment of FITC-labeled CMCht/PAMAM dendrimer nanoparticle internalization

In this thesis, the internalization of the FITC-labeled MP-loaded CMCht/PAMAM dendrimer nanoparticles was investigated in glia and Schwann cell cultures, both by fluorescence and confocal microscopy analyses. The glial cultures were incubated with 200 μg.mL^{-1} of FITC-labeled MP-loaded CMCht/PAMAM dendrimer nanoparticles for periods of 1, 3, 12, 18 and 24 hours (n=3/ time point). After each incubation time, the cells were washed in 0.1 M PBS and fixed in a 4% paraformaldehyde solution for 30 minutes. The nuclei were stained with 4',6-diamidino-2-phenylindole (DAPI, Invitrogen, USA), for the assessment of possible morphological changes. Immunocytochemistry was performed in order to co-localize the NPs within the cells with the following primary antibodies: rabbit GFAP antibody (Dako, Denmark, 1:500, v/v) for astrocytes recognition; mouse CD11b antibody (BD Biosciences Pharmingen, USA, 1:100, v/v) was used in microglial cells identification; and mouse O4 antibody (R&D Systems, 1:50, v/v) for oligodendrocytes detection. The FITC-labeled MP-loaded CMCht/PAMAM dendrimer nanoparticles internalization levels for each cell population were determined according to Equation (1) (n=3, 3 random fields/coverslip):

Equation (1): $I = \dfrac{Pc}{Tc} \times 100$

I: percentage of internalization;

Pc: number of positive cells for FITC-labeled MP-loaded CMCht/PAMAM dendrimer nanoparticles;

Tc: total number of each cell type.

For Schwann cell (SCs) cultures, 200 µg.mL^{-1} FITC-labeled MP-loaded CMCht/PAMAM dendrimer nanoparticles were incubated for periods of 3, 6, 16 and 24 hours. The samples for fluorescence microscopy were then washed with 1 mL of PBS, and cells fixed with 4% PFA for 10 minutes at 4°C followed by washing each well twice with PBS. After that SCs were incubated with 0.5 mL of PBS containing Hoechst 33258 (Invitrogen, USA) for cell nuclei staining. Immunocytochemistry was performed in order to co-localize the NPs within SCs with the primary antibody rabbit S100 antibody (Dako, Denmark, 1:500, v/v). The FITC-labeled MP-loaded CMCht/PAMAM dendrimer nanoparticles internalization levels for each cell population were determined according to Equation (1) (n=3, 3 random fields/coverslip).

5.4. Immunocytochemistry

Imunocytochemistry is a method for determining the presence, subcellular localization and relative abundance of a specific antigen in cultured cells. For internalization studies using glial cells and SCs, immunocytochemistry studies were performed in the scope of this thesis. The cells were fixed in 4% PFA for 30 minutes, permeabilized by incubation with 100% triton-X for 4 minutes and washed 3 times in PBS. Cells were then blocked with 10% FBS (Gibco, USA), followed by incubation with the following primary antibodies: rabbit anti-rat glial fibrillary acid protein (GFAP) (Dako, Denmark, 1:500) for astrocytes, mouse anti-CD11b (BD Biosciences Pharmigen, USA, 1:100) for microglial cells and mouse anti-O4 (R&D systems, USA, 1:50) for oligodendrocytes and rabbit anti-S100 (Dako, Denmark, 1:500) for SCs. Cells were then washed in PBS and incubated with the secondary antibodies: Alexa Fluor 594 goat anti-mouse immunoglobulin G (IgG) and Alexa Fluor goat anti-rabbit 594 (Molecular Probes, USA). The primary antibody was omitted to produce negative controls. Samples were further observed under an Olympus BX-61 Fluorescence Microscope (Olympus, Germany). Levels of FITC-labeled CMCht/PAMAM dendrimer nanoparticles internalization by the different cell populations were

quantified by determining the ratio between the number of positive cells for FITC-labeled CMCht/PAMAM internalization and the total number of cells.

5.5 Myelination in Schwann cell and dorsal root ganglia neuron co-cultures

For myelination experiments, co-cultures were prepared by adding 50,000 SC to purified DRGN cultures. The DRGN cultures and the co-cultures, represented in Figure 9, were fed every 2–3 days with NLA medium for 2 weeks at 37°C and 95% air and 5% CO_2. For the induction of myelination, NLA medium containing ascorbic acid (Sigma, Germany) was added to the co-cultures. All cultures were then maintained for an additional 2 week period, with replacement of the appropriate medium every 2–3 days.

Figure 9 - Co-cultures of primary rat Schwann cells and dorsal root ganglia neurons (Sudan black staining). Scale bar = 100 μm.

To quantify the myelination of axons two methods were used: immunocytochemistry and Sudan black staining. Immunocytochemistry procedure was done as already described (see 5.4) using mouse anti-myelin basic protein (MBP) SMI 94 (Sternberger Monoclonals, Inc., USA, 1:1000) or mouse anti-neurofilament SMI 31 (Sternberger Monoclonals, Inc., USA, 1:1000). Concomitantly, Sudan black was used to stain the myelin for bright field microscopy observation. Sudan black is a non-fluorescent lysocrome dye used for lipid staining, such as myelin, resulting in a blue-black

labeling.[37] To prepare the cell cultures for Sudan black staining, cells were fixed for at least 15 minutes in 4% PFA, rinsed in 0.1 M PBS and further fixed in 0.1% osmium tetroxide (OsO_4) for 1 hour. The cultures were then dehydrated in sequential 25%, 50% and 70% ethanol solutions for 5 minutes each. A 0.5% Sudan black in 70% ethanol solution was prepared and filtered before staining for 1 hr. The cultures were rehydrated in the following solutions sequentially: ethanol 70% for 1 minute; 50% ethanol for 5 minutes; and 25% ethanol for 5 minutes. The cultures were finally rinsed in 0.1 M PBS and mounted for further observation and counting. Myelinated axons were counted using a square grid eyepiece during three scans across the coverslip. The number of Sudan black-stained myelin sheaths crossing the scan line was counted.

6. Investigation of the mechanism of FITC-labeled MP-loaded CMCht/PAMAM dendrimer nanoparticle intracellular trafficking

For the investigation of the mechanisms by which dendrimer nanoparticles are internalized by cells, two different techniques were used complimentarily, i.e. patch-clamp membrane capacitance electrophysiological recording and confocal live astrocyte imaging. For endocytotic vesicle examination labeled dextrans were incubated in the astrocyte cultures, while for exocytotic vesicle observation astrocytes were transfected with neuropeptide-Y (NPY) plasmid for further visualization.

6.1. Electrophysiological analysis

Electrophysiology techniques allow the study of the electrical properties of cells and tissues, involving the placement of electrodes into the biological preparations to measure the flow of ions. In this thesis we used the patch-clamp technique in the cell-attached mode, where a micropipette approaches the cell membrane in order to form a "patch" by suction and a microelectrode records the cell membrane ion flow. This approach allows the monitoring of discrete alterations in the membrane capacitance (Cm) that reflect unitary endocytotic and exocytotic events and allow its quantification, as well as vesicle diameter and fusion pore opening time. The equipment used to analyze and record the membrane response is represented in Figure 10. In order to perform the electrophysiological readings, astrocyte coverslips were bathed in extracellular solution (ECS) containing: 130 mM NaCl, 5 mM KCl, 1 mM MgCl, 2 mM $CaCl_2$, 10 mM Na-

HEPES and 10 mM D-glucose at pH 7.4. The fire-polished 3–4 MΩ glass patch-clamp pipettes were coated with Sylgard resin and the recordings were all performed in a SWAM IIB (Celica, Ljubljana, Slovenia).[38] Single astrocytes revealing the typical star-like morphology were chosen for the patch-clamp analysis. To stimulate exocytosis ATP was added to the extracellular solution. The secretory activity of single cells was measured from the membrane capacitance (Cm). Off-line data analysis was performed using the software MATLAB (MathWorks Inc.). Quantification of the number of events was determined from the obtained recordings.
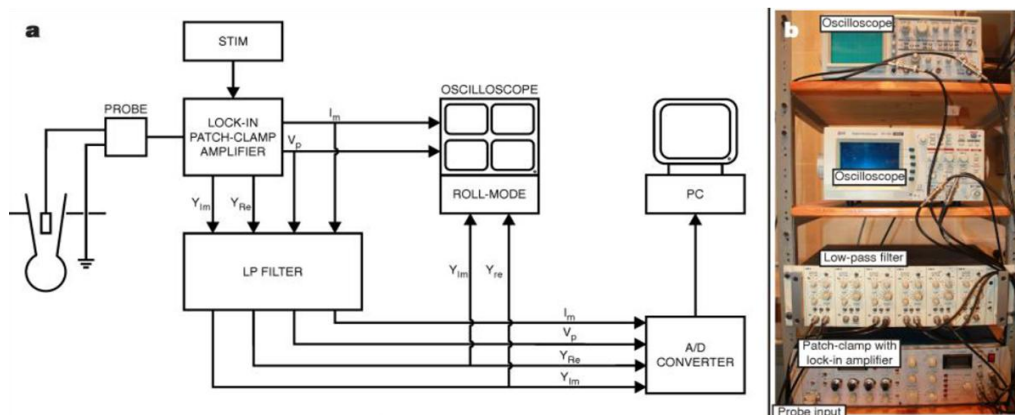
Figure 10 - Apparatus used for the electrophysiological recordings. **a.** Schematic representation of the circuit. **b.** Patch-clamp amplifier, low-pass filter and auxiliary oscilloscopes used. [38]

6.2. Endocytotic and exocytotic vesicle labeling

Co-localization studies in live astrocytes were performed in order to identify both the endocytotic and exocytotic vesicles involved in the nanoparticle cellular dynamics, namely its intracellular trafficking. For endocytotic vesicle labeling, low dense astrocyte cultures were incubated with Alexa Fluor® 546 Dextran (Molecular Probes, USA) for 1.5 hours and thoroughly washed in ECS prior to observation. To observe the exocytotic vesicles sub-confluent astrocyte cultures were used and transfected with the plasmid DNA encoding Neuropeptide Y (NPY) tagged with mCherry fluorescent protein (NPY-mCherry, a kind gift from Dr. Ronald W. Holz, University of Michigan, USA). Briefly, the cells to be transfected were incubated in lipofection media (DMEM, 1 mM sodium piruvate, 2 mM L-glutamine) and mixed with transfecting reagent (Fugene, Promega, USA) with 1 µg of plasmid DNA for 15 minutes, at 37°C. After that, culture medium was added and supplemented with 3% UltraSerG serum (Life Technologies, USA) and the cells were observed past 24 hours of incubation.

6.3. Confocal microscopy imaging of live astrocytes

Confocal imaging of live astrocytes following incubation with fluorescently labeled NPs along with vesicle staining enabled to track possible co-localization of NPs and vesicles, validating NP intracellular vesicle transport. Confocal imaging microscopy overcomes some of the limitations of conventional wide-field fluorescence microscopy by increasing resolution and contrast by making use of point illumination and a spatial pinhole to eliminate out-of-focus light outside the focal plane. The images were acquired with a confocal inverted microscope (Zeiss LSM META 510, Germany) equipped with a 63.2× oil-immersion objective. FITC molecules bonded to the NPs were excited by the 488-nm line of the argon laser and the emission light was collected through the bandpass filter (505–530 nm). Alexa Fluor 546 labeling the vesicles was excited with the He/Ne laser (543 nm) and the emission light was filtered with the long-pass filter, with the cutoff below 560 nm. To eliminate possible bleed through, the green and red emission fluorescence were acquired sequentially. Time series images were recorded in 20 seconds intervals during 45 minutes. All the recordings were performed in 300 mOsm ECS.

6.4. Fluorescence quantification of co-localization of internalized nanoparticles with vesicles

Co-localization spots refer to the observation of the spatial overlap between two different fluorescent labels each having separate emission wavelengths, to define if the different targets are located in the same area of the cell or very near to one another. Relative co-localization of FITC-labeled NPs with Alexa Fluor® 546 Dextran or NPY-mCherry was quantified using ColocAna software (Celica, Slovenia). The co-localization was calculated as a percentage of co-localized pixels versus all pixels of the respective labeled protein. The threshold intensity for the co-localized pixel count was 20% of the maximal fluorescence.

7. *In vivo* studies

In vivo studies presented in this thesis including animal handling and all the experiments were conducted in accordance with the guidelines for the care and handling of laboratory animals in the Directive 2010/63/EU of the European Parliament and Council. To have a more relevant

response on the effect of MP-loaded CMCht/PAMAM dendrimer NPs administration *in vivo* studies were performed. Firstly, NPs were administered in healthy Wistar rats to have insights on its diffusion and distribution in the brain tissue. Secondly, a spinal cord injury (SCI) animal model was established in order to test the possible therapeutic effects of the drug-loaded NPs following injury.

7.1. Animals

Eight and ten week-old male Wistar rats (Charles River, Spain) were used for the therapeutic and biodistribution studies, respectively. The animals were housed in light and temperature controlled rooms and fed with the recommended standard diet. The Animal Care Committee of the research Institute approved the animal protocols in accordance with standardized Animal Care Guidelines.[39] Following surgery the animals were kept under heat lamps and received vitamins and antibiotics, to prevent infections. Bladder evacuation was done manually whenever necessary. Throughout the recovery period the animals were examined for symptoms of illness or adverse reaction to the treatment.

7.2. Intracisternal administration of MP-loaded CMCht/PAMAM dendrimer nanoparticles

Administration of the NPs directly in the CSF of the animals was done in order to assess its biodistribution in the brain. All experiments were carried out using male ten week-old Wistar rats (Charles River, Spain). Before the surgery, the animals were anesthetized by intraperitoneal injection of 150 mg.Kg^{-1} ketamine hydrochloride (Dorbene Vet, Laboratorios SYVA SA, Spain) and 0.3 mg.Kg^{-1} medetomidine (Imalgen, Merial, France). The animals were placed in a stereotaxic frame with the head curved 45° downwards and the dorsal base of the skull was shaved and soaked with ethanol and chlorohexidin (AGB, UK). An occipital-cerebral midline incision was made with a blade and the muscles retracted until the meninges were visible. A small amount of CSF was withdrawn from the cistern magna and afterwards 15 μL of solution were injected with a Hamilton syringe (Hamilton, Switzerland). Following surgery, rats received analgesic (Butorphanol tartrate, 1 mg.mL^{-1}, Fort Dodge, Spain) and antibiotic (Enrofloxacine, 1 mg.mL^{-1}, Bayer, Germany) and were kept for 72 hours.

7.3. Spinal cord injury surgery

To have an insight of the possible therapeutic effects of MP-loaded CMCht/PAMAM dendrimer NPs, local administration of the nanocarriers was performed following thoracic hemisection of the cord. Eight week-old male Wistar rats (Charles River, Spain) were anesthetized by intraperitoneal injection of 150 mg.Kg^{-1} ketamine hydrochloride (Dorbene Vet, Laboratorios SYVA SA, Spain) and 0.3 mg.Kg^{-1} medetomidine (Imalgen, Merial, France). The surgical area was shaved and soaked with ethanol and chlorohexidin (AGB, UK). A laminectomy at T8-T9 level was performed to expose the spinal cord. After that, a unilateral defect was made on the cord by removing approximately 2 mm of the tissue. Immediately after the lesion, 5 µL of solution was injected circa 1 mm rostral and 1 mm caudal to the lesion (the content of the solution varied according to the experimental group). All solutions were prepared in 5 mg. mL^{-1} stocks. To stabilize the vertebral column in the lesion area, a semi-tubular starch/polycaprolactone (SPCL) scaffold was implanted in alignment with the vertebrae in all the animals.[40] The muscles and skin were separately sutured with Vicryl sutures (Johnson and Johnson, USA) and disinfection was carried out with chlorohexidin (AGB, UK). The animals were maintained for 4 weeks.

7.4. Basso, Beattie and Bresnahan locomotor test

The locomotor behavior of the animals was assessed using the Basso, Beattie and Bresnahan (BBB) locomotor rating scale.[41] The test was performed weekly after the surgery, for a month. The BBB test consists on a 21 point scale to evaluate the hindlimb motor recovery following a thoracic spinal injury. A BBB score of 0 indicates no hindlimb movement. From 1 to 8 the scores designate some joint movement, still with no weight support. BBB scores from 9 to 20 already demonstrate the animal ability to support weight and use the limbs for locomotion, although in the presence of some abnormalities such as the lack of coordination. Finally, a BBB score of 21 corresponds to the locomotion profile of a normal healthy rat (Table 1). To evaluate the rat locomotion, animals were allowed to move freely in the open-field arena and scored during a 4 minute period for their ability to use their hindlimbs by two independent blinded observers. Joint movements, paw placement, weight support, and fore/hindlimb coordination were judged according to the 21-point BBB locomotion scale. Scores obtained by 2 independent observers were averaged for the left hindlimb.

Table 1. Basso, Beattie and Bresnahan locomotor rating scale.[41]

Score	Operational Definition
0	No observable hindlimb (HL) movement
1	Slight movement of one or two joints (ankle, hip or knee) of the HL
2	Extensive movement of one joint OR extensive movement in one joint and slight movement in on other joint
3	Extensive movement in two joints
4	Slight movement of all three joints
5	Slight movement of all two joints and extensive movement of the third
6	Extensive movement of two joints and slight movement of the third
7	Extensive movement of all three joints
8	Sweeping with no weight support OR plantar placement of the paw with no weight support
9	Plantar placement of the paw with weight support in stance only (i.e., when stationary) OR occasional, frequent, or consistent weight supported dorsal stepping and no plantar stepping
10	Occasional weight supported plantar steps, no forelimb (FL)-HL coordination
11	Frequent to consistent weight supported planter steps and no FL-HL coordination
12	Frequent to consistent weight supported planter steps and occasional FL-HL coordination
13	Frequent to consistent weight supported planter steps and frequent FL-HL coordination
14	Consistent weight supported plantar steps, consistent FL-HL coordination and predominant paw position during locomotion is rotated (internally or externally) when it makes initial contact with the surface as well as just before it is lifted off at the end of stance OR frequent plantar stepping, consistent FL-HL coordination and occasional dorsal stepping
15	Consistent plantar stepping and consistent FL-HL coordination and no toe clearance or occasional toe clearance during forward limb advancement; predominant paw position is parallel to the body at initial contact
16	Consistent plantar stepping and consistent FL-HL coordination during gait and toe clearance occurs frequently during forward limb advancement, predominant paw position is parallel at initial contact and rotated at lift-off
17	Consistent plantar stepping and consistent FL-HL coordination during gait and toe clearance occurs frequently during forward limb advancement, predominant paw position is parallel at initial contact and lift-off
18	Consistent plantar stepping and consistent FL-HL coordination during gait and toe clearance occurs consistently during forward limb advancement, predominant paw position is parallel at initial contact and rotated at lift-off
19	Consistent plantar stepping and consistent FL-HL coordination during gait and toe clearance occurs consistently during forward limb advancement, predominant paw position is parallel at initial contact and lift-off, tail is down part or all the time
20	Consistent plantar stepping and consistent coordinated gait, consistent toe clearance, predominant paw position is parallel at initial contact and lift-off, trunk instability, tail consistently up
21	Consistent plantar stepping and consistent coordinated gait, consistent toe clearance, predominant paw position is parallel throughout stance, consistent trunk stability, tail consistently up

8. Histological and western blot analysis

8.1. Tissue preparation for immunohistochemistry

Following the *in vivo* experiments, once reaching the pre-established time-points animals were deeply anesthetized with an intraperitonial injection of sodium pentobarbital. Then, rats were perfused through the ascending aorta artery first with 0.9% NaCl saline solution and once the blood was cleared from the organism, with 4% PFA in PBS. Brains were collected for NP biodistribution studies and dissected to obtain the pre-frontal cortex, hippocampus and cerebellum. The tissues were immediately frozen at -80°C for further analysis. The remaining brains were carefully placed in OCT embedding compound (ThermoScientific, USA) and frozen at -20°C for posterior cutting in a cryostat at a thickness of 10 μm. The brain slices were then subjected to an immunohistochemical protocol. First the coverslips were covered in PBS (pH 7.4) and let stay for 15 minutes. Blocking solution composed of 5% FBS (Gibco, USA) in 0.5% Triton was applied to the brain slices for 1 hour at RT. Following that, primary antibodies were incubated overnight at 4°C: rabbit anti-rat glial fibrillary acid protein (GFAP) (Dako, Denmark, 1:500) for astrocyte labeling. The following day 3 washes in PBS were executed and then incubation with the secondary antibody Alexa Fluor goat anti-rabbit 594 (Molecular Probes, USA) in blocking solution was done, along with DAPI staining (1:1000, Invitrogen, USA). Samples were further observed under a confocal microscope (FV1000; Olympus, Germany). The coverslips were once again washed 3 times in PBS and then mounted in Vectashield (ThermoScientific, USA). The coverslips were kept at 4°C until further observation.

8.2. Western blot analysis

For protein expression analysis, three distinct brain areas were carefully dissected: the hippocampus (HPC), the pre-frontal cortex (PFC) and the cerebellum (CB). Proteins were extracted from the CB, HPC and PFC and homogenized in RIPA buffer (NaCl 0.1 M; tris(hydroxymethyl)aminomethane (Tris) pH 8.0, 0.01 M; EDTA pH 8.0, 0.001 M and complete protease inhibitor cocktail; Roche, Switzerland). Afterwards, sonication for 30 seconds in Laemmli buffer (SDS 4%, Tris pH 8, 0.12 M, glycerol 20% and dithiothreitol 0.2 M) was performed. Proteins were then quantified using the Bio-Rad protein assay (Bio-Rad, Hercules,

USA). Samples were separated by SDS-PAGE (50 μg/lane) and then transferred into a nitrocellulose membrane. Membranes were then stained with Ponceau S (Sigma) to confirm transfer efficiency; blocked with 5% skim milk in PBS and probed with anti-glucocorticoid receptor (GR) antibody (M-20) (Santa Cruz Biotechnology, USA, dilution 1:1000) at 4°C overnight. Membranes were washed and incubated with goat anti-rabbit IgG-HRP (Santa Cruz Biotechnology) and diluted to 1:10000. The blot was developed using the SuperSignal West Pico Chemiluminescent Substrate (PIERCE, USA) and exposed to X-ray film. Finally, the membranes were stripped with 2% SDS and 100 mM β-mercaptoetanol solution, warmed to 50°C for 30 minutes, thoroughly washed, blocked, re-blotted with mouse anti-alpha-tubulin (Santa Cruz Biotechnology) and diluted to 1:5000 to normalize for protein load.

9. Statistical analysis

Statistical evaluation was performed using GraphPad Prism v5.0 for Windows (GraphPad Software, USA). Statistical differences amongst groups were assessed either by one way ANOVA or two way ANOVA tests, followed by Tukey or the Bonferroni post-hoc tests, respectively. Statistical significance was defined as $p < 0.05$ for a 95% confidence interval.

References

1   Menjoge, A. R., Kannan, R. M. & Tomalia, D. A. Dendrimer-based drug and imaging conjugates: design considerations for nanomedical applications. *Drug Discovery Today* 15, 171-185 (2010).

2   Buhleier, E., Wehner, W. & Vögtle, F. Cascade and nonskid-chain-like synthesis of molecular cavity topologies. *Synthesis* 2, 155-158 (1978).

3   Fadhel, B., Hearn, M. & Chaffee, A. CO_2 adsorption by PAMAM dendrimers: Significant effect of impregnation into SBA-15. *Microporous and Mesoporous Materials* 123, 140-149 (2009).

4   Alves, N. M. & Mano, J. F. Chitosan derivatives obtained by chemical modifications for biomedical and environmental applications. *International Journal of Biological Macromolecules* 43, 401-414 (2008).

5   Mourya, V., Inamdar, N. & Tiwari, A. Carboxymethyl chitosan and its applications. *Advanced Materials Letters* 1, 11-33 (2010).

6   Chen, L., Tian, Z. & Du, Y. Synthesis and pH sensitivity of carboxymethyl chitosan-based polyampholyte hydrogels for protein carrier matrices. *Biomaterials* 25, 3725-3732 (2004).

7   Oliveira, J. M. *et al.* Surface engineered carboxymethylchitosan/poly (amidoamine) dendrimer nanoparticles for intracellular targeting. *Advanced Functional Materials* 18, 1840-1853 (2008).

8   Bracken, M. B. *et al.* Efficacy of methylprednisolone in acute spinal cord injury. *JAMA: the journal of the American Medical Association* 251, 45-52 (1984).

9   Hall, E. D. & Springer, J. E. Neuroprotection and Acute Spinal Cord Injury: A Reappraisal. *NeuroRX* 1, 80-100 (2004).

10   Bracken, M. B. *et al.* Administration of Methylprednisolone for 24 or 48 Hours or Tirilazad Mesylate for 48 Hours in the Treatment of Acute Spinal Cord InjuryResults of the Third National Acute Spinal Cord Injury Randomized Controlled Trial. *JAMA: the journal of the American Medical Association* 277, 1597-1604 (1997).

11   Lee, J.-M. *et al.* Methylprednisolone protects oligodendrocytes but not neurons after spinal cord injury. *The Journal of Neuroscience* 28, 3141-3149 (2008).

12   Tomalia, D. A. *et al.* Dendritic macromolecules: synthesis of starburst dendrimers. *Macromolecules* 19, 2466-2468 (1986).

13   Jayaraman, M. & Fréchet, J. M. A convergent route to novel aliphatic polyether dendrimers. *Journal of the American Chemical Society* 120, 12996-12997 (1998).

14   Boas, U. & Heegaard, P. M. H. Dendrimers in drug research. *Chemical Society Reviews* 33, 43-63 (2004).

15   Domanski, D. M., Klajnert, B. & Bryszewska, M. Influence of PAMAM dendrimers on human red blood cells. *Bioelectrochemistry* 63, 189 (2004).

16   Jevprasesphant, R., Penny, J., Attwood, D., Mckeown, N. B. & D'Emanuele, A. Engineering of dendrimer surfaces to enhance transepithelial transport and reduce cytotoxicity. *Pharmaceutical Research* 20, 1543-1550 (2003).

17   Arruebo, M., Valladares, M. & González-Fernández, Á. Antibody-conjugated nanoparticles for biomedical applications. *Journal of Nanomaterials* 2009, 37 (2009).

18   Petros, R. A. & DeSimone, J. M. Strategies in the design of nanoparticles for therapeutic applications. *Nature Reviews Drug Discovery* 9, 615-627 (2010).

19   Xu, C., Wang, B. & Sun, S. Dumbbell-like Au–Fe3O4 Nanoparticles for Target-Specific Platin Delivery. *Journal of the American Chemical Society* 131, 4216-4217 (2009).

20   Reddy, L. H., Arias, J. L., Nicolas, J. & Couvreur, P. Magnetic Nanoparticles: Design and Characterization, Toxicity and Biocompatibility, Pharmaceutical and Biomedical Applications. *Chemical Reviews* 112, 5818-5878 (2012).

21   Ponce, A., Mejía-Rosales, S. & José-Yacamán, M. in *Nanoparticles in Biology and Medicine* Vol. 906 *Methods in Molecular Biology* (ed Mikhail Soloviev) Ch. 37, 453-471 (Humana Press, 2012).

22   Furer, V. L. *et al.* FTIR spectroscopy studies of dendrimers built from cyclophosphazene core. *Vibrational Spectroscopy* 44, 89-93 (2007).

23   Albert, S., Albert, K. K. & Quack, M. in *Handbook of High-resolution Spectroscopy* (John Wiley & Sons, Ltd, 2011).

24   Hu, J., Xu, T. & Cheng, Y. NMR Insights into Dendrimer-Based Host–Guest Systems. *Chemical Reviews* 112, 3856-3891 (2012).

25   Mayer, C. in *Annual Reports on NMR Spectroscopy* Vol. Volume 55 (ed G. A. Webb) 205-258 (Academic Press, 2005).

26   Biricova, V. & Laznickova, A. Dendrimers: Analytical characterization and applications. *Bioorganic chemistry* 37, 185-192 (2009).

27   Liao, D. L., Wu, G. S. & Liao, B. Q. Zeta potential of shape-controlled TiO2 nanoparticles with surfactants. *Colloids and Surfaces A: Physicochemical and Engineering Aspects* 348, 270-275 (2009).

28   Attard, P., Antelmi, D. & Larson, I. Comparison of the zeta potential with the diffuse layer potential from charge titration. *Langmuir* 16, 1542-1552 (2000).

29   Jans, H., Liu, X., Austin, L., Maes, G. & Huo, Q. Dynamic light scattering as a powerful tool for gold nanoparticle bioconjugation and biomolecular binding studies. *Analytical chemistry* 81, 9425-9432 (2009).

30   Islam, M. T., Majoros, I. J. & Baker Jr, J. R. HPLC analysis of PAMAM dendrimer based multifunctional devices. *Journal of Chromatography B* 822, 21-26 (2005).

31   Barth, R. F. & Kaur, B. Rat brain tumor models in experimental neuro-oncology: the C6, 9L, T9, RG2, F98, BT4C, RT-2 and CNS-1 gliomas. *Journal of neuro-oncology* 94, 299-312 (2009).

32   Effgen, G. B. *et al.* A multiscale approach to blast neurotrauma modeling: part II: methodology for inducing blast injury to in vitro models. *Frontiers in neurology* 3, 23 (2012).

33   Reglodi, D., Kiss, P., Lubics, A. & Tamas, A. Review on the protective effects of PACAP in models of neurodegenerative diseases in vitro and in vivo. *Current pharmaceutical design* 17, 962-972 (2011).

34   Cucullo, L., Marchi, N., Hossain, M. & Janigro, D. A dynamic in vitro BBB model for the study of immune cell trafficking into the central nervous system. *Journal of Cerebral Blood Flow & Metabolism* 31, 767-777 (2010).

35   Tominaga, H. *et al.* A water-soluble tetrazolium salt useful for colorimetric cell viability assay. *Anal. Commun.* 36, 47-50 (1999).

36   Lappalainen, K., Jääskeläinen, I., Syrjänen, K., Urtti, A. & Syrjänen, S. Comparison of cell proliferation and toxicity assays using two cationic liposomes. *Pharmaceutical research* 11, 1127-1131 (1994).

37   Plant, G. W. *et al.* Purified adult ensheathing glia fail to myelinate axons under culture conditions that enable Schwann cells to form myelin. *The Journal of Neuroscience* 22, 6083-6091 (2002).

38   Rituper, B. *et al.* High-resolution membrane capacitance measurements for the study of exocytosis and endocytosis. *Nature protocols* 8, 1169-1183 (2013).

39   Zutphen, L. v., Baumans, V. & Beynen, A. C. *Principles of laboratory animal science: a contribution to the humane use and care of animals and to the quality of experimental results*. (Elsevier Science Publishers, 2001).

40   Silva, N. A. *et al.* Development and characterization of a Novel Hybrid Tissue Engineering–based scaffold for spinal cord injury repair. *Tissue Engineering Part A* 16, 45-54 (2009).

41   Basso, D. M., Beattie, M. S. & Bresnahan, J. C. A sensitive and reliable locomotor rating scale for open field testing in rats. *Journal of neurotrauma* 12, 1-21 (1995).

SECTION III

CHAPTER III

Multifunctionalized CMCht/PAMAM dendrimer nanoparticles modulate the cellular uptake by astrocytes and oligodendrocytes in primary cultures of glial cells

CHAPTER III

Multifunctionalized CMCht/PAMAM dendrimer nanoparticles modulate the cellular uptake by astrocytes and oligodendrocytes in primary cultures of glial cells

Abstract

The efficiency of the treatments involving CNS disorders is commonly diminished by the toxicity, reduced stability and lack of targeting of the administered neuroactive compounds. In this study, we have successfully multifunctionalized CMCht/PAMAM dendrimer nanoparticles by coupling the CD11b antibody and loading MP into the nanoparticles. The modification of the new antibody-conjugated nanoparticles was confirmed by S-TEM observation and ^{1}H NMR and FTIR spectroscopy. Cytotoxicity assays revealed that the conjugates did not affect the viability of both primary cultures of glial and microglial cells. Trace analyses of FITC-labeled nanoparticles revealed that the uptake of antibody-conjugated nanoparticles was conserved in microglial cells but significantly decreased in astrocytes and oligodendrocytes. Thus, this study demonstrates that antibody conjugation contributes to a modulation of the internalization of these nanocarriers by different cell types, which might be of relevance for specific targeting of CNS cell populations.

1. Introduction

Drug delivery to the central nervous system (CNS) has been a considerable challenge in biomedical research in the past decades.[1,2] Neurological disorders such as Alzheimer´s and Parkinson's diseases, stroke, multiple sclerosis and also neurotraumatic conditions, such as spinal cord injury (SCI), are amongst the main debilitating disorders of our times.[3] The unique environment and the complexity of the mechanisms involved in these conditions, some of which still poorly understood, have hindered the development of new and efficient treatments. The systemic administration of neuroactive molecules poses several intrinsic issues, particularly its toxicity and reduced stability in the organism.[4] Thus, there is an urgent demand not only for more detailed knowledge of the pathophysiology of CNS disorders, but also for more specific and effective drug delivery strategies.[5,6] In addition, the presence of biological barriers such as the blood-brain barrier (BBB) and the blood-cerebrospinal fluid barrier (B-CSF) that can obstruct the entry of therapeutic molecules to the nervous tissues, is a common limiting factor in the success of treatments.[7,8] Nonetheless, one must distinguish diseases that do not affect the BBB integrity from those which compromise it.[9] In the first case, the major obstacle to an effective cure of the disease is the BBB presence itself and its characteristics. However, when this barrier has been compromised, for instance, after neurotraumatic events, the delivery of compounds is clearly eased.[10] In brain and SCI physical damage occurs and the CNS barriers are disrupted opening a 'window of opportunity' for the entry of drugs that can limit the extent of following potential secondary damage.[10,11] Still, efficient drug delivery to the target cells remains a crucial task for the success of these therapies, since most of these drugs are often highly unspecific.[12]

The use of nanoparticle-based systems has gained increasing interest in drug delivery with exciting prospects.[13] These nanoscale materials present unique and advantageous features in comparison to the classical drug formulations, regarding its solubility, biodistribution, release characteristics and immunogenicity.[14] In addition, nanoparticles are amenable to further modifications that can provide higher functionalization degrees, namely cell or tissue targeting.[15] Fundamentally, nanoparticle-mediated selective drug delivery would offer a mean to minimize delivery to unintended sites, allowing higher doses of drug to be administered when reaching a precise target site, thereby lowering peripheral cytoxicity. A critical step in such a strategy is the internalization of nanoparticles into specific cells, and a way to overcome it would be the

modification of the nanoparticle surface with a ligand, that would be efficiently taken up by target cells.[16,17] A vast range of nanoparticles is being developed and investigated for specific drug delivery purposes although from these only a small percentage is being directed to CNS.[18]

A new surface engineered macromolecular carrier was recently proposed to be used in CNS applications, showing high internalization levels and no significant cytotoxicity over neurons and glial cells.[19] Moreover, it has also shown to be non-cytotoxic *in vivo*, revealing a wide biodistribution after intravenous injections, being simultaneously able to cross the B-CSF.[20] This system was firstly described as a new surface engineered nanoparticle based on a polyamidoamine (PAMAM) dendrimer core grafted with the natural polymer carboxymethylchitosan (CMCht).[21] The sphere-like CMCht/PAMAM dendrimer nanoparticles were proposed to be used as targeted drug delivery carriers for the modulation of the cells' behaviour by efficient intracellular uptake upon its functionalization via: (i) drug incorporation; (ii) fluorescent labelling; and (iii) ligand conjugation.[22] Furthermore, an anti-inflammatory corticosteroid clinically used in SCI related cases - methylprednisolone (MP) - has already shown to be efficiently incorporated and released from these nanoparticles, leading to important alterations on the viability of primary cultures of microglial cells.[23]

Therefore, following recent developments of these previous works the aim of this study was to achieve a higher functionalization level of the CMCht/PAMAM dendrimer nanoparticles by conjugating to the latter a targeting ligand, in order to determine a possible modulation of their internalization behaviour in glial cells. From the variety of potential ligands to nanoparticles surfaces, monoclonal antibodies are attractive molecules due its high specificity.[24] Therefore, the MP-loaded CMCht/PAMAM dendrimer nanoparticles were conjugated to the CD11b antibody which recognizes specific receptors on microglial cells' membranes. The multifunctional modification of the CMCht/PAMAM dendrimer nanoparticles was confirmed by Fourier transform infrared spectroscopy (FTIR) and proton nuclear magnetic resonance (^{1}H NMR). Then, we have investigated its effects in the normal viability of glial and microglial cells, *in vitro*. Finally, an assessment and comparison of the two types of nanoparticles uptake in mixed glial cultures was done following immunocytochemistry and fluorescence microscopy observation. Results revealed that conjugated nanoparticles were not deleterious to both glial and microglial cells. Moreover, the internalization profile of the new nanoparticles in a mixed glial culture was indeed altered when compared to the unmodified nanoparticles. This study demonstrates that by following the

above referred strategy it is possible to modulate the internalization of MP-loaded CMCht/PAMAM dendrimer nanoparticles by different glial cell populations, rendering them with a cell targeted profile for future CNS applications.

2. Materials and methods

2.1. Dendrimer nanoparticle preparation

2.1.1. CMCht/PAMAM dendrimer nanoparticles synthesis

Carboxymethylchitosan/polyamidoamine dendrimer nanoparticles were produced as previously reported by Oliveira *et al.*[21] Starburst® PAMAM-carboxylic acid terminated dendrimer solution (PAMAM-CT) (generation 1.5, 20% (w/v)) was purchased (Sigma, Germany). The following reactions were carried out: (i) increase in the PAMAM-CT generation; (ii) production of a PAMAM-methyl esther terminated dendrimer; (iii) condensation reaction between the methyl esther and amine groups of PAMAM and CMCht; and (iv) conversion of the non-reacting methyl esther groups into carboxylic ones in the CMCht/PAMAM dendrimer nanoparticles. Initially, the methanol was removed from the PAMAM-CT dendrimers by evaporation under nitrogen gas. The remaining compound was re-dissolved in ultra-pure water in a final concentration of 10 mg.mL^{-1} and the pH was corrected to 6.5. Then, 1-ethyl-3-(3-dimethylaminopropyl) carbodiimide hydrochloride (EDC, Fluka, Slovakia) was added under agitation for 30 minutes at room temperature. Ethylenediamine (EDA, Sigma, Germany) was included at the same molar ratio and reacted for 4 hours. The solution was subsequently dialyzed against ultrapure water in order to remove the exceeding EDC (cellulose tubing, benzoylated for separating compounds with a molecular weight of ≤1,200, Sigma, Germany). The obtained amine terminated PAMAM dendrimers (PAMAM-AT) were mixed with methanol (Sigma, Germany) and methyl methacrylate (Fluka, Germany) and kept under agitation in a water bath at 50°C for 24 hours. After methanol removal under nitrogen gas, appropriate volumes of hydrochloric acid (HCl, Panreac, Portugal) and trifluoroacetic acid (TFA, Sigma, Germany) were added to the solution. Meanwhile, 1 g of CMCht was dissolved in 50 mL of water. The PAMAM methyl esther terminated dendrimers were dissolved in a 20/80 water/methanol solution and the CMCht was added and kept under

agitation for 72 hours, after which the CMCht/ PAMAM dendrimer nanoparticles with carboxylic-terminated groups were obtained.

2.1.2. Methylprednisolone incorporation into CMCht/PAMAM dendrimer nanoparticles

Methylprednisolone (MP) was incorporated in the nanoparticles by mixing an aqueous solution of CMCht/PAMAM dendrimer nanoparticles with an ethanolic methylprednisolone solution with a final concentration of 5×10^{-4} M (w/w) and kept under vigorous agitation. Saturated sodium carbonate solution (Na_2CO_3, Aldrich, Germany) and acetone (Pronalab, Portugal) were then added to the mixture. The resulting precipitates were collected by filtration and then dispersed in ultrapure water. Extensive dialysis (cellulose tubing, benzoylated for separating compounds with a molecular weight of $\leq 1,200$, Sigma, Germany) was performed during 48 hours. Both CMCht/PAMAM dendrimer nanoparticles and MP-loaded CMCht/PAMAM dendrimer nanoparticles were obtained by freezing the final solution at -80°C and freeze-drying (Telstar-Cryodos-80, Spain) the samples for approximately 7 days, until the solvents were completely removed.

2.1.3. Fluorescent labelling of MP-loaded CMCht/PAMAM dendrimer nanoparticles

Fluorescein isothiocyanate (FITC, Sigma, Germany) labeled MP-loaded CMCht/PAMAM dendrimer nanoparticles conjugates were prepared by covalently bonding the amine group of CMCht and the isothiocyanate group from FITC. A 10 mg.mL^{-1} FITC solution was prepared in dimethyl sulfoxide anhydrous (DMSO, Riedel-de Haen, Germany) in the dark. Simultaneously, a 10 mg.mL^{-1} MP-loaded CMCht/PAMAM dendrimer nanoparticles solution was set in carbonate-bicarbonate coupling buffer (pH=9.2). Afterwards, 50 μL of the FITC/DMSO solution were added per each mL of the MP-loaded CMCht/PAMAM dendrimer nanoparticles buffered solution, under agitation. The resulting solution was kept in the dark at 4°C for 8 hours. The FITC-labeled MP-loaded CMCht/PAMAM dendrimer nanoparticles solution was then dialyzed (cellulose tubing, benzoylated for separating compounds with a molecular weight of $\leq 1,200$, Sigma, Germany) for

48 hours against ultrapure water in order to remove the FITC molecules that did not react. Finally, the solution was frozen at -80°C and subsequently freeze-dried (Telstar-Cryodos-80, Spain) until the solvents were completely removed.

2.1.4. CD11b antibody conjugation to CMCht/PAMAM dendrimer nanoparticles

In order to conjugate anti-mouse CD11b antibody (BD Biosciences, USA) to the dendrimer nanoparticles a crosslinking reaction was performed.[25] A 20 mg.mL^{-1} solution of nanoparticles in PBS was mixed with 1 mg.mL^{-1} EDC (Fluka, Slovakia) and let react for 30 minutes. The remaining solution was dialysed against ultrapure water for 24 hours to remove the excess EDC. Afterwards, the pH was corrected to 7.4 and 4 nmol of CD11b antibody were added under agitation. One hour after CD11b addition, the solution was frozen at -80°C and subsequently freeze-dried (Telstar-Cryodos-80, Spain).
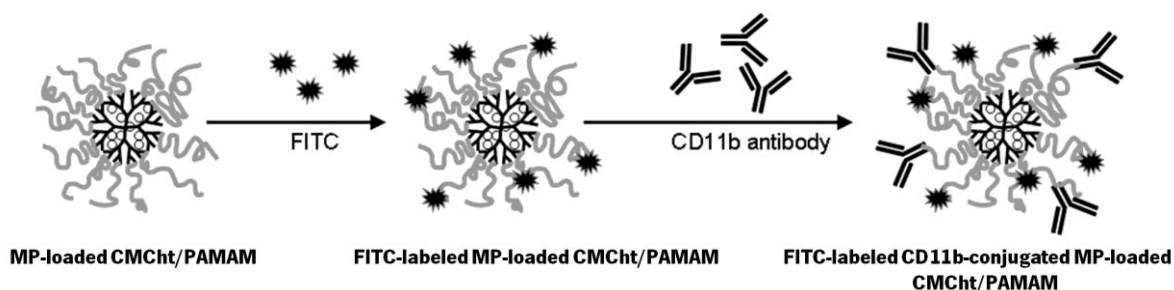
Figure 1. Surface modification of MP-loaded CMCht/PAMAM dendrimer nanoparticles with a fluoresecnt probe (FITC) and a targeting ligand (CD11b antibody).

2.2. Characterization of the CD11b antibody conjugated dendrimer nanoparticles

The conjugation effectiveness was analyzed by Fourier transform infrared spectroscopy (FTIR) and proton nuclear magnetic resonance (^{1}H NMR). The morphology of the new conjugated nanoparticles was assessed by scanning-transmission electron microscopy (S-TEM). To obtain the FTIR spectra of the samples, transparent potassium bromide (KBr, Pike Technologies, USA)

pellets were prepared containing the samples to be analyzed. The readings were run in an infrared spectroscope (IR Prestige-21, Shimadzu, Japan). For the ^{1}H NMR analyses the samples were dispersed in deuterium oxide (D$_2$0, Aldrich, Germany) at a final concentration of 10 mg.mL^{-1}. The one-dimensional ^{1}H spectra were acquired in a Varian Unity Plus spectrometer at 300 MHz and 20°C. The morphology was then verified by S-TEM (Nova™ NanoSEM 50 series, FEI Company, The Netherlands). For that purpose, the lyophilized CD11b-antibody conjugated MP-loaded CMCht/PAMAM dendrimer nanoparticles were dispersed in ultrapure water to a final concentration of 1 mg.mL^{-1}, stained with 1% phosphotungstic acid and placed on copper grids for further observation.

2.3. *In vitro* cell culture studies

2.3.1. Isolation and culturing of rat cortical glial cells

Neonatal rat cortices were isolated from P4 Wistar rat pups as previously described.[26] Upon removal under aseptic conditions, cortices were maintained in Hanks' balanced salt solution (HBSS, Gibco, USA) and mechanically dissected. Afterwards, the cortical fragments were incubated in an enzymatic medium of 30 mg.mL^{-1} DNAse solution (Sigma, Germany) with 0.25% trypsin (Sigma, Germany) in Ca^{2+}/Mg^{2+} free HBSS solution for 30 minutes at 37°C. The trypsin reaction was blocked adding 40% foetal bovine serum (FBS, Gibco, USA) and the resulting tissue was centrifuged at 800 rpm for 2 minutes and the cells were then plated out at a density of 4×10^4 cells.cm^{-2} on poly-L-lysine (Sigma, USA) coated coverslips. Glial cells primary cultures were then maintained at 37°C in a 5% CO$_2$ atmosphere, in Dulbecco's modified Eagle medium (DMEM, Gibco, USA) supplemented with 10% FBS and 1% antibiotic/antimycotic for 7 days.

2.3.2. Purification of rat cortical microglial cells

After the glial cells isolation procedure, these were plated out at a density of 1×10^6 cells.cm^{-2} in polystyrene T75 flasks (Thermo Scientific, USA) previously coated with poly-L-lysine (Sigma, USA). The glial primary cultures were maintained at 37°C in a 5% CO_2 atmosphere in Dulbecco's modified Eagle medium (DMEM, Gibco, USA) supplemented with 10% FBS and 1% antibiotic/antimycotic for two weeks, with periodical medium renewal. After that, the flasks were agitated in an orbital shaker at 240 rpm during 4 hours. Following this, the medium containing detached microglia cells was collected and the obtained suspension was centrifuged at 1200 rpm for 5 minutes. The pellet was re-suspended in DMEM medium (Gibco, USA) supplemented with 10% FBS and 1% antibiotic/antimycotic and plated out at a density of 4×10^4 cells.cm^{-2} on coverslips previously coated with poly-L-lysine (Sigma, USA). Microglia cells primary cultures were then maintained at 37°C in a 5% CO_2 atmosphere, in DMEM medium (Gibco, USA) supplemented with 10% FBS and 1% antibiotic/antimycotic for 4 days for further testing.

2.3.3. *In vitro* cytotoxicity assays

Unmodified and CD11b antibody-conjugated MP-loaded CMCht/PAMAM dendrimer nanoparticles were evaluated regarding its influence in the primary cell cultures' viability. For that purpose, two concentrations of nanoparticles were tested: 200 and 400 μg.mL^{-1} and the cultures were exposed to these conditions for a week. For both glial and microglial cell cultures the cell viability was verified after incubation of the cells at 37°C for 3 hours with (3-(4,5-dimethylthiazol-2-yl)-5-(3-carboxymethoxyphenyl)-2(4-sulfophenyl)-2H tetrazolium) (MTS, Promega, USA) in a 5:1 ratio. This compound is bioreduced by active dehydrogenase enzymes into a brown formazan product that is released to the medium. After the incubation, the optical density of each sample was read in a multiplate reader (Tecan Sunrise, Switzerland) at 490 nm.

2.3.4. Internalization assessment following immunocytochemistry

After a week, the glial cultures were incubated with 200 µg.mL⁻¹ of CD11b antibody-conjugated and the unmodified FITC-labeled MP-loaded CMCht/PAMAM dendrimer nanoparticles to assess their internalization rates, one week after its addition. After this time period, immunocytochemistry was performed. The cells were washed in 0.1 M PBS and fixed in a 4% paraformaldehyde solution for 30 minutes. For astrocytes recognition the wells were permeabilized with Triton-X-100 (Merck, Germany) 0.3% for 5 minutes, following a new wash in PBS 0.1 M. Afterwards, a 10% FCS solution in PBS was added to the cells for 1 hour and a new wash with PBS 0.1 M was carried out. The next step consisted on the incubation with the corresponding primary antibody diluted in 10% FCS in PBS. The following antibodies were used: rabbit anti-rat glial fibrillary protein (GFAP, Dako, Denmark, 1:500) for astrocytes recognition; mouse anti-CD11b (BD Biosciences Pharmingen, USA, 1:100) in microglial cells identification; and mouse anti-O4 (R&D Systems, 1:50) for oligodendrocytes detection. After 1 hour incubation, the cells were washed in 0.5% FCS in PBS (v/v) for further 1 hour incubation with the secondary antibodies: Alexa Fluor 594 anti-mouse and Alexa Fluor 568 anti-rabbit (both Molecular Probes, USA, 1:2000) were incubated for 1 hour. Negative controls were used performing the same treatment but omitting the primary antibody addition. The cells were then stained with 4',6-diamidine-2-phenyl indole (DAPI, Thermo Scientific, USA, 1:2000), for 5 minutes in the dark. The coverslips were finally mounted for posterior observation under an Olympus BX-61 Fluorescence Microscope (Olympus, Germany). The FITC-labeled dendrimer nanoparticles internalization levels for each cell population were determined according to Equation 1 (n=3, 3 random fields/ coverslip):

Equation 1: $I = \dfrac{Pc}{Tc} \times 100$

I: percentage of internalization;

Pc: number of positive cells for FITC-labeled dendrimer nanoparticles;

Tc: number of positive cells for FITC-labeled dendrimer nanoparticles.

2.4. Statistical analysis

Statistical evaluation was performed using the one-way analysis of variance test followed by the Tukey's post-test to assess the statistical differences between groups in the viability and internalization tests. Statistical significance was defined for p<0.05.

3. Results and discussion

The partial failure in CNS disorders' pharmacological treatments often resides in the lack of targeting of the administered therapeutic molecules.[4] Even in conditions where the BBB has been compromised and the delivery of compounds is considerably facilitated, as in SCI, efficient drug delivery to target cells should be carefully considered. Due to the massive inflammatory episodes that follow these injuries, a cell-specific drug delivery could be highly advantageous in the control and modulation of these deleterious events.[9] For instance, MP clinical administration as an anti-inflammatory drug aggravates a cascade of side effects that could be minimized in a targeted delivery strategy.[27] Following previous works by our group focusing on the development of a CNS targeted dendrimer-based macromolecular carrier,[19-21,23] we aimed at further modifying the CMCht/PAMAM dendrimer nanoparticles to achieve a higher functionalization degree.[28] For this purpose, we tested a new surface modification by conjugating a CD11b antibody to the MP-loaded CMCht/PAMAM dendrimer nanoparticles. The latter had already shown to be easily internalized by astrocytes, oligodendrocytes and microglial cells present in a mixed primary culture. All these cell types revealed maximum internalization levels 24 hours after exposure to these nanoparticles, being microglial cells the ones with faster uptakes.[23] If we intend to target the delivery of the drug to microglial cells, for instance, minimum amounts should reach the other cell types in order to maximize the desired drug actions while minimizing possible side effects. Therefore, it was investigated whether this generalized internalization intake would be affected by the presence of CD11b antibody, which is specific for microglial cell recognition. The CD11b antibody was chosen to facilitate the permeation of the nanoparticles through the microglial cells membrane by specifically interacting with an integrin chain expressed only in this type of cells.

Thus, the nanoparticles could be preferentially targeted to microglial cells, affecting the availability for entrance in the other cell types.

In the present study, it was initially investigated the conjugation of the CD11b antibody to the CMCht/PAMAM dendrimer nanoparticles. FTIR spectra of the unmodified and antibody-conjugated CMCht/PAMAM dendrimer nanoparticles are represented in Figure 2.A. From Figure 2, it is visible that the antibody-conjugated nanoparticles disclose an altered FTIR spectrum as compared to the unmodified nanoparticles. The 520 cm^{-1} free amino acid peak and the 1120 cm^{-1} NH_3^+ vibration appear after modification of the nanoparticles in the antibody-conjugated nanoparticles spectrum. Consequently, the comparative FTIR spectra analysis of the unmodified and CD11b conjugated dendrimer nanoparticles seems to suggest that the antibody was, in fact, successfully conjugated to the nanoparticles. Also the ^{1}H NMR spectra of CD11b antibody-conjugated and unmodified CMCht/PAMAM dendrimer nanoparticles (Figure 2.B) revealed new proton signals which indicate that the conjugation actually occurred. Some characteristic peaks of the CMCht/PAMAM dendrimer nanoparticles are maintained in both spectra, such as the 2.17 ppm CH_2 protons from the PAMAM dendrimer and the 4.07 ppm CH_2COO^- protons from CMCht.
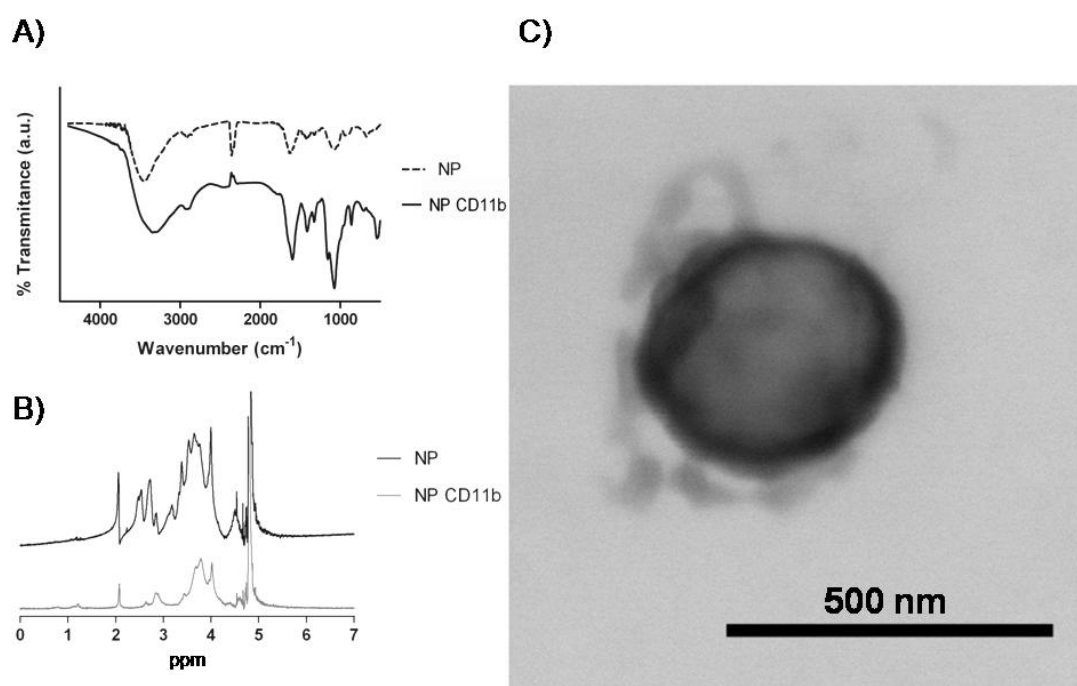
Figure 2. Characterization of the CD11b-conjugated CMCht/PAMAM dendrimer nanoparticles. **A.** FTIR spectra of unmodified (NP) and CD11b-conjugated (NP CD11b) CMCht/PAMAM dendrimer nanoparticles. Appearance of new peaks in the conjugated molecule confirms the effective conjugation of the antibody to the dendrimer nanoparticles. **B.** ^{1}H NMR spectra of unmodified (NP) and CD11b-conjugated (NP CD11b) CMCht/PAMAM dendrimer nanoparticles. **C.** S-TEM micrograph of CD11b-conjugated MP-loaded CMCht/PAMAM dendrimer nanoparticles evidencing its spherical morphology.

Also new signals were observed at 1.26 ppm and 2.71 ppm which are attributed to new $COCH_3$ and NCH_3 protons from the newly formed bonds. These new signals strongly suggest that the conjugation of CD11b antibody to the nanoparticles actually occurred. Additionally, STEM analysis (Figure 2.C) also revealed the nanosphere-like morphology of these nanoparticles.

Regarding the biological assays, both the glial and microglial cell cultures were incubated with two different concentrations of the CD11b-conjugated and the unmodified MP-loaded CMCht/PAMAM dendrimer nanoparticles. The metabolic activity was then quantified by means of performing an MTS assay. In all the tested conditions no negative effect in the normal cell activity was observed (Figure 3). Both cell populations reduced detectable amounts of MTS in similar ways to those of control cultures, showing normal cell viability and metabolism. Only a significant increase in the metabolic activity of glial cells after 200 µg addition of CD11b-conjugated MP-loaded CMCht/PAMAM dendrimer nanoparticles was observed while not being a drastic difference, in relation to the control cells. These data suggest that there is no cytotoxicity derived from the exposure of these cells to the multifunctionalized nanoparticles.
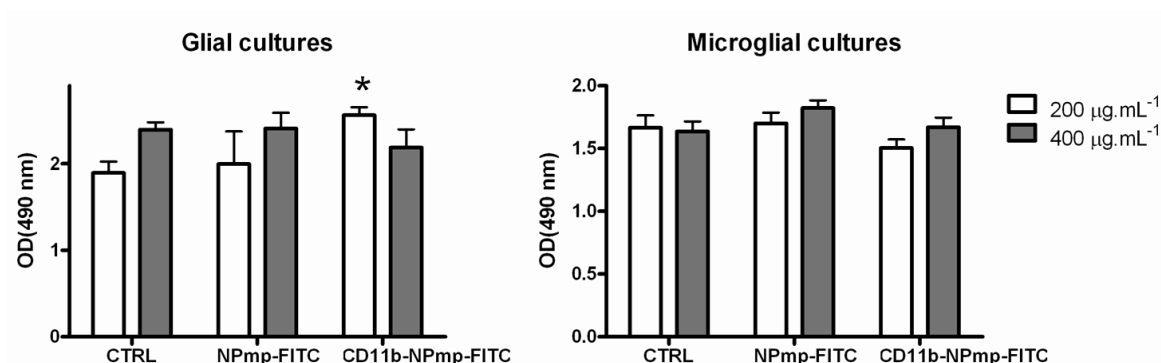
Figure 3. Metabolic activity measured with MTS assay of glial and microglial cultures after exoposure to the unmodified (NPmp-FITC) and CD11b-conjugated (CD11b-NPmp-FITC) CMCht/PAMAM dendrimer nanoparticles. Values are shown as mean±SD (n=3), *p<0.05.

The internalization of the nanoparticles by each cell type in the mixed primary culture of glial cells was then further investigated. To allow both a qualitative and a quantitative evaluation, cells were immunostained for observation and the number of cells containing fluorescently labeled internalized nanoparticles was determined. A previous study has shown that microglial cells presented maximum MP-loaded CMCht/PAMAM dendrimer nanoparticles internalization levels,

with all cells evidencing nanoparticles within its cytoplasmic compartment 24 hours after nanoparticles addition.[23] Moreover, astrocytes also reached high internalization levels around 90% followed by oligodendrocytes, which presented a slightly lower percentage of nanoparticles internalizing cells (around 80%). As observed in Figure 4, the CD11b conjugation to the MP-loaded CMCht/PAMAM dendrimer nanoparticles did not alter the percentage of microglial cells internalizing the nanoparticles as compared to cultures exposed to MP-loaded CMCht/PAMAM dendrimer nanoparticles. Interestingly, this observation was not verified for the other glial cell types cultured in the presence of the multifunctionalized nanoparticles. Regarding astrocytes, a drastic and significant decrease in the antibody-conjugated nanoparticles uptake was observed (around 50%), as seen in Figure 4. Similar to what it was observed in astrocytes, oligodendrocytes also revealed a significant decrease regarding the CD11b-conjugated MP-loaded CMCht/PAMAM dendrimer nanoparticles uptake. Again, the number of oligodendrocytes internalizing the modified nanoparticles was drastically reduced to 40% when compared to the unmodified nanoparticles condition.

The endocytosis pathway is believed to be the major route for dendrimer nanoparticles internalization, [21,29] and it was already shown that surface modifications modulate this mechanism.[30] Our strategy to modify the nanoparticles with an antibody that is efficiently taken up by microglial cells via receptor-mediated endocytosis seems to be advantageous in the non-specific uptake modulation by other cell types, such as astrocytes and oligodendrocytes. The yield of nanoparticles internalization by microglial cells did not improve, since maximum percentage figures were already being reached. However, the receptor-mediated endocytosis facilitation to microglial cells, due to the interaction of CD11b antibody-conjugated nanoparticles, indeed contributed to the improvement of their intracellular uptake and conferred a targeted profile to the system, drastically reducing the uptake by astrocytes and oligodendrocytes.

Thus, we demonstrate that the CD11b antibody-conjugated MP-loaded CMCht/PAMAM dendrimer nanoparticles can be beneficial when envisioning the development of targeted therapies aimed at applications in CNS disorders, namely by carrying anti-inflammatory drugs such as MP to inflammation mediator cells.
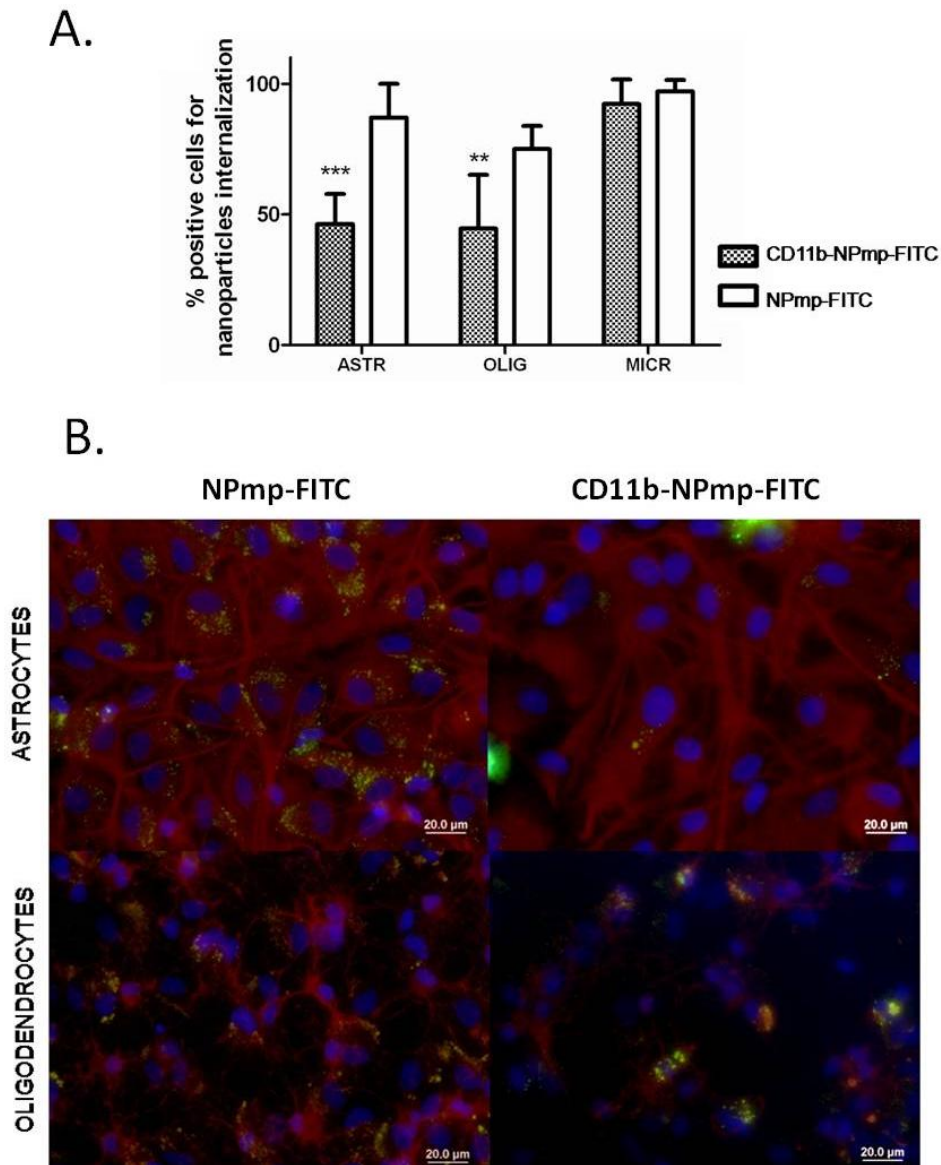
Figure 4. Nanoparticle cell uptake by primary glial cell cultures. A. The presence of the CD11b antibody in the nanoparticles induced a significant decrease in the number of astrocytes and oligodendrocytes internalizing nanoparticles 7 days after exposure. (n=3; 5 fields/coverslip; mean±SD).

4. Conclusions

Within the present study it was possible to describe for the first time the successful functionalization of MP-loaded CMCht/PAMAM dendrimer nanoparticles with a microglia-specific antibody, acting as a targeting ligand. The new sphere-like CD11b antibody-conjugated nanoparticles revealed no cytotoxicity when added to glial and microglial primary cell cultures.

Furthermore, a novel nanoparticle uptake profile by astrocytes and oligodendrocytes was achieved with the new modified nanoparticles. These cells significantly reduced the levels of CD11b antibody-conjugated nanoparticles internalization, while maintaining maximum uptake by microglial cells. Further studies will focus on the potential selective anti-inflammatory action of these nanoparticles, namely for spinal cord injury applications.

5. Acknowledgements

References

1   Pardridge, W. M. CNS drug design based on principles of blood-brain barrier transport. Journal of neurochemistry 70, 1781-1792 (1998).

2   Maysinger, D. & Morinville, A. Drug delivery to the nervous system. *Trends in biotechnology* 15, 410-418 (1997)

3   Kabanov, A. & Gendelman, H. Nanomedicine in the diagnosis and therapy of neurodegenerative disorders. *Progress in Polymer Science* 32, 1054-1082 (2007).

4   Begley, D. J. Delivery of therapeutic agents to the central nervous system: the problems and the possibilities. *Pharmacology & therapeutics* 104, 29-45 (2004).

5   Modi, G., Pillay, V. & Choonara, Y. E. Advances in the treatment of neurodegenerative disorders employing nanotechnology. *Annals of the New York Academy of Sciences* 1184, 154-172 (2010).

6   Nowacek, A. & Gendelman, H. E. NanoART, neuroAIDS and CNS drug delivery. *Nanomedicine* 4, 557-574 (2009).

7   Zlokovic, B. V. The blood-brain barrier in health and chronic neurodegenerative disorders. *Neuron* 57, 178-201 (2008).

8   Pardridge, W. M. Blood–brain barrier delivery. *Drug discovery today* 12, 54-61 (2007).

9   Donnelly, D. J. & Popovich, P. G. Inflammation and its role in neuroprotection, axonal regeneration and functional recovery after spinal cord injury. *Experimental neurology* 209, 378-388 (2008).

10   Habgood, M. *et al.* Changes in blood–brain barrier permeability to large and small molecules following traumatic brain injury in mice. *European Journal of Neuroscience* 25, 231-238 (2007).

11   Popovich, P. G., Horner, P. J., Mullin, B. B. & Stokes, B. T. A quantitative spatial analysis of the blood–spinal cord barrier: I. Permeability changes after experimental spinal contusion injury. *Experimental neurology* 142, 258-275 (1996).

12   Dommergues, M.-A., Plaisant, F., Verney, C. & Gressens, P. Early microglial activation following neonatal excitotoxic brain damage in mice: a potential target for neuroprotection. *Neuroscience* 121, 619-628 (2003).

13   Sanvicens, N. & Marco, M. P. Multifunctional nanoparticles–properties and prospects for their use in human medicine. *Trends in biotechnology* 26, 425-433 (2008).

14   Wang, A. Z. *et al.* Biofunctionalized targeted nanoparticles for therapeutic applications. *Expert Opin. Biol. Ther* 8, 1063-1070 (2008).

15   Chandrasekar, D., Sistla, R., Ahmad, F. J., Khar, R. K. & Diwan, P. V. The development of folate-PAMAM dendrimer conjugates for targeted delivery of anti-arthritic drugs and their pharmacokinetics and biodistribution in arthritic rats. *Biomaterials* 28, 504-512 (2007).

16   Kocbek, P., Obermajer, N., Cegnar, M., Kos, J. & Kristl, J. Targeting cancer cells using PLGA nanoparticles surface modified with monoclonal antibody. *Journal of controlled release* 120, 18-26 (2007).

17   Hughes, G. A. Nanostructure-mediated drug delivery. *Nanomedicine: nanotechnology, biology and medicine* 1, 22-30 (2005).

18   Zhang, L. *et al.* Nanoparticles in medicine: therapeutic applications and developments. *Clinical Pharmacology & Therapeutics* 83, 761-769 (2007).

19   Salgado, A. J. *et al.* Carboxymethylchitosan/Poly (amidoamine) Dendrimer Nanoparticles in Central Nervous Systems-Regenerative Medicine: Effects on Neuron/Glial Cell Viability and Internalization Efficiency. *Macromolecular bioscience* 10, 1130-1140 (2010).

20   Pereira, V. H. *et al.* In vivo biodistribution of carboxymethylchitosan/poly (amidoamine) dendrimer nanoparticles in rats. *Journal of Bioactive and Compatible Polymers* 26, 619-627 (2011).

21   Oliveira, J. M. *et al.* Surface engineered carboxymethylchitosan/poly (amidoamine) dendrimer nanoparticles for intracellular targeting. *Advanced Functional Materials* 18, 1840-1853 (2008).

22   Oliveira, J. M., Salgado, A. J., Sousa, N., Mano, J. F. & Reis, R. L. Dendrimers and derivatives as a potential therapeutic tool in regenerative medicine strategies—a review. *Progress in Polymer Science* 35, 1163-1194 (2010).

23   Cerqueira, S. R. *et al.* Microglia Response and In Vivo Therapeutic Potential of Methylprednisolone-Loaded Dendrimer Nanoparticles in Spinal Cord Injury. *Small* 9, 738-749 (2013).

24   Waldmann, T. A. Monoclonal antibodies in diagnosis and therapy. *Science* 252, 1657-1662 (1991).

25   Xu, C. *et al.* Au–Fe3O4 Dumbbell Nanoparticles as Dual-Functional Probes. *Angewandte Chemie International Edition* 47, 173-176 (2008).

26   Chen, Y. *et al.* Isolation and culture of rat and mouse oligodendrocyte precursor cells. *Nature protocols* 2, 1044-1051 (2007).

27   Baptiste, D. C. & Fehlings, M. G. Update on the treatment of spinal cord injury. *Progress in brain research* 161, 217-233 (2007).

28   Thanh, N. T. & Green, L. A. Functionalisation of nanoparticles for biomedical applications. *Nano Today* 5, 213-230 (2010).

29   Albertazzi, L., Serresi, M., Albanese, A. & Beltram, F. Dendrimer internalization and intracellular trafficking in living cells. *Molecular Pharmaceutics* **7**, 680-688 (2010).

30   Saovapakhiran, A.; D'Emanuele, A.; Attwood, D.; Penny, J., *Bioconjugate chemistry* 2009, *20* (4), 693-701.

CHAPTER IV

Electrophysiological quantification of cellular internalization, retention and exocytosis of drug-loaded dendrimer nanoparticles in astrocytes

CHAPTER IV

Electrophysiological quantification of cellular internalization, retention and exocytosis of drug-loaded dendrimer nanoparticles in astrocytes

Abstract

Engineered dendrimers are emerging as potentially safer and more effective nanocarriers to deliver therapeutic molecules to damaged tissues. Understanding the mechanisms involving NP interaction with cells and its intracellular dynamics are of the utmost importance for future clinical use. In this study, the uptake, retention time and clearance routes of MP-loaded CMCht/PAMAM dendrimer NPs in astrocytes were investigated using two methodologies: (i) patch-clamp electrophysiology to measure alterations in the membrane capacitance following NP exposure; and (ii) confocal imaging, in order to track the NP fate in live astrocytes following vesicle staining and incubation with fluorescent NPs. Interestingly, the electrophysiology data reveals fluctuations in the frequency of endo- and exocytotic events in astrocytes following NP incubation, revealing that NPs induce the formation of both endocytotic and exocytotic vesicles. Endocytosis is slightly increased when NPs are in contact with the astrocyte membrane, while exocytosis is significantly enhanced following 24 hour incubation. NPs also induce the formation of larger endosomes, while in the case of exocytotic vesicles NP exposure induces the formation of smaller ones. Concurrently, live confocal imaging confirms that NPs are transported within astrocytes via endocytotic and exocytotic vesicles. Macropinocytosis is shown to contribute to the NP cell uptake mechanism. Additionally, NPs are retained intracellularly in astrocytes for a week, while still being co-localized with exocytotic vesicles. These findings confirm the potential and suitability of CMCht/PAMAM dendrimer NPs for neurotherapeutics, particularly as intracellular drug delivery systems. Moreover, future studies on nanoparticle-cell interaction and fate may benefit from our findings involving the combination of these two techniques.

1. Introduction

Nanoparticle (NP) systems with diverse surface chemistries and tunable biological properties are emerging as prominent delivery carriers for biomedical applications.[1] Envisioned as key players with major roles in improving current means of diagnostics, imaging and therapeutics, NPs are being engineered to allow, for instance, passage through different biological barriers and deliver low molecular weight molecules to particular tissues, damaged sites or sub-cellular compartments, thus maximizing the healing effects while reducing inconvenient side effects.[2] Some of the conditions that would urgently benefit from improved therapeutic moieties are related to central nervous system (CNS) degeneration such as Parkinson and Alzheimer's diseases, amyotrophic lateral sclerosis and others, as well as neurotraumatic condition management. CNS-related diseases still present serious challenges in diagnostics and treatment being most of them therefore still classified as non-curable. Due to its importance in regulating the homeostasis of the nervous tissue, astrocytes were pointed out as ideal targets to be considered when dealing with therapies for CNS disorders.[3] Besides being essential constituents of the blood-brain barrier (BBB), astrocytes play important roles in signaling and intercellular communication, both in health and disease, and are critical contributors for the support and integration of several CNS functions.[4-6] In fact, astrocytes significantly outnumber any other cell type in the CNS, thus targeting its protection and repair following traumatic or degenerative progression is fundamental for any successful therapeutic intervention.

Dendrimers are a class of polymeric NPs with unique architectures, exhibiting highly branched nano-spherical structures that differ from linear classical polymers in its precise and controlled synthesis.[7,8] These synthetic polymers seem ideal nanocarriers for drugs and other molecules of interest owing to its tunable chemistries, drug payload and pharmacokinetics. An additional and quite interesting feature of dendrimers is the intrinsic multivalency that enables several types of functionalization and surface engineering.[9] Nonetheless, despite the immense amount of research presently being conducted involving dendrimer synthesis, functionalization and biological evaluation, basic knowledge on the interactions of these NPs with the living systems is still scarce. There are still few reports focusing this issue, and not many methodologies have been proposed to address NP interplay with the cell membrane and its intracellular trafficking.[10] It is essential that the mechanisms involving dendrimer internalization and cellular dynamics, in addition to cytosolic retention and further clearance, are carefully clarified if an effective and safe

therapeutic action is desired. It has recently become clear that dendrimer physical and chemical properties affect its interaction with cells, particularly the internalization and trafficking mechanisms.[11-13] Ideally, NPs would have such characteristics to allow straightforward entrance in the target cells, and once inside the intracellular milieu its cargo would be released and delivered to the sub-compartments where its action is desired.[14] Finally, after providing increased bioavailability of the therapeutic agent in the site of action the NPs and the cargo would enter the exocytotic pathway to be cleared out from the cells, and eventually from the organism when no longer needed.

Conventional methods employed in NP uptake studies involve confocal microscopy observation, often coupled with electron microscopy (EM) or flow cytometry (FC).[14] Typically, either specific cell structures are labeled to visualize co-localization with the NPs or inhibition of the endocytosis/exocytosis pathways is performed and its effects investigated. More recently, other techniques such as atomic force microscopy (AFM),[15] mathematical correlations from confocal laser scanning microscopy (CLSM) and high-throughput fluorescence-activated cell sorting (FACS)[16] were also suggested for more precise quantification of NP uptake and sub-cellular localization. Alternative quantitative methods using electrophysiological measurements to assess single-cell real-time quantitative evaluation of the NP internalization dynamics, retention and exocytosis have not been reported to our knowledge. Complementing high-resolution patch-clamp capacitance measurements with live confocal imaging renders the possibility to both quantify the frequency of membrane events, monitoring endocytosis and exocytosis in live cells, and to visualize co-localization of NPs with endocytotic and exocytotic vesicles. Patch-clamp electrophysiology capacitance measurements consist of real-time evaluation of the membrane capacitance (C_m) in living cells, a parameter that is linearly related to the membrane area.[17,18] It allows the precise live quantification of single endocytotic and exocytotic events and calculation of a variety of parameters, such as vesicle diameter and fusion pore properties. As for vesicle tracking using confocal observation, there is a vast number of fluorescent probes available that label specific compartments within the live cell (e.g., early endosomes, late endosomes, lysosomes, and others) allowing co-localization studies to be carried out.[19] Both pulse-chase or cell transfection experiments can be designed and performed for this end.[14]

Our group has recently reported on the surface modification of poly(amidoamine) (PAMAM) dendrimers with carboxymethylchitosan (CMCht) increasing its overall surface area and

conferring improved biocompatibility and solubility to the PAMAM dendrimers.[20] It has been confirmed the successful incorporation of lipophilic drugs, such as dexamethasone and methylprednisolone (MP) that display a sustained release *in vitro* and proved to exert actions over cell functions.[20,21] Moreover, we have devised CMCht/PAMAM dendrimer molecules conjugated to targeting molecules, conferring altered cell uptake profiles to these dendrimers.[22] These NPs are thus being proposed to be used in CNS conditions as therapeutic nanocarriers to be transported to the damaged nervous cells.[23,24]

In the present study, we investigated the interaction of MP-loaded CMCht/PAMAM dendrimer NPs with the astrocyte membrane (single-cell) using real-time patch-clamp electrophysiology capacitance measurements to quantify with high sensitivity the endocytotic and exocytotic events occurring following incubation with NP. Along with the electrophysiological data, the endocytotic and exocytotic vesicles were tracked in live astrocytes following fluorescent labeling, under a confocal microscope, to assess possible co-localization of the NPs with these structures. To the best of our knowledge, it is the first time that such a study is being conducted using these two techniques in combination for purposes of investigating NP uptake, intracellular fate and interaction in living CNS cells.

2. Materials and methods

2.1. CMCht/PAMAM dendrimer nanoparticle synthesis and functionalization

Carboxymethylchitosan/poly(amidoamine) (CMCht/PAMAM) dendrimer NP were produced as previously reported.[20] In brief, Starburst® PAMAM-carboxylic acid terminated dendrimers (PAMAM-CT) (generation 1.5, 20% w/v in methanolic solution) with an ethylenediamine core were purchased (Sigma, Germany) and a series of step-by-step reactions were performed. Firstly, the PAMAM-CT generation was doubled and a PAMAM-methyl ester terminated dendrimer was produced. Subsequently, a condensation reaction between the methyl ester and amine groups of PAMAM and CMCht was made. Finally, the non-reacting methyl ester groups were converted into carboxylic ones. Methylprednisolone (MP) was incorporated in the CMCht/PAMAM dendrimer NP combining a CMCht/PAMAM dendrimer NP aqueous solution with an ethanolic MP solution with

a final concentration of 5×10^4 M (w/w), under vigorous agitation. Saturated sodium carbonate solution (Na_2CO_3, Aldrich, Germany) and acetone (Pronalab, Portugal) were added to precipitate the mixture. The precipitate was collected by filtration and dispersed in ultrapure water to undergo dialysis (cellulose tubing, benzoylated for separating compounds with a molecular weight of ≤1,200, Sigma, Germany) for 48 hours. MP-loaded CMCht/PAMAM dendrimer NP were obtained by freeze-drying (Telstar-Cryodos-80, Spain). To label the NP, fluorescein isothyocianate (FITC, Sigma, Germany) was added and a covalent bonding reaction was carried out between the amine group of CMCht and the isothyocianate group from FITC. The obtained molecules were freeze-dried (Telstar-Cryodos-80, Spain).

2.2. Primary astrocyte cultures

Primary cultures of cortical astrocytes were prepared from P3 Wistar rat newborns.[25] The care for experimental animals was in accordance with International Guiding Principles for Biomedical Research Involving Animals which was developed by the Council for International Organizations of Medical Sciences and Directive on Conditions for issue of License for Animal Experiments for Scientific Research Purposes (Official Gazette of the Republic of Slovenia, No. 38/13). Following the tissue dissection, the isolated cells were plated out and grown in high glucose Dulbecco's modified Eagle's medium (DMEM), supplemented with 10% fetal bovine serum (FBS), 2 mM L-glutamine, 1 mM sodium pyruvate and penicillin/streptomycin. The cultures were kept at 37°C and 95% air/ 5% CO_2. The astrocytes were then sub-cultured onto 22 mm diameter poly-L-lysine coated glass coverslips at low densities. Control cultures were grown in normal astrocyte culture medium while stimulated cells were incubated with astrocyte media supplemented with 200 µg.mL^{-1} MP-loaded CMCht/PAMAM dendrimer nanoparticles for 6, 12 or 24 hours prior to analysis. All reagents were purchased from Sigma-Aldrich, Germany.

2.3. Electrophysiology recordings

For the electrophysiological recordings the coverslips were bathed in extracellular solution (ECS) containing: 130 mM NaCl, 5 mM KCl, 1 mM MgCl, 2 mM CaCl2, 10 mM Na-HEPES and 10 mM

D-glucose at pH 7.4. The fire-polished 3–5 MΩ glass pipettes were considerably coated with Sylgard (Midland, USA). Cell-attached high resolution membrane capacitance measurements were performed using two-phase lock-in amplifier (SWAM IIB; Celica, Slovenia) incorporated into a patch-clamp amplifier to record the real and imaginary parts of the admittance of equivalent electrical circuit.[17] In the compensated mode of recording, one of the two outputs of the dual-phase lock-in amplifier signal is directly proportional to changes in C_m.[26] Signals were filtered (10 Hz, -3 dB, low pass, Bessel 4-pole) and acquired with an analog-to-digital converter (National Instruments BNC-2110, National Instruments, USA) using a custom software (Cell, Celica, Slovenia). Membrane patches were voltage-clamped at a holding potential of 0 mV, to which a sine wave voltage (111.1 mV rms) was applied (800 Hz). Positive steps in C_m were interpreted as single exocytotic and negative steps as single endocytotic events. Steps were resolved by progressive filtering of records. The amplitude and frequency of steps in C_m were measured. Single astrocytes revealing the typical star-like morphology were chosen for the patch-clamp analysis. Recordings were made considering three different conditions: (i) control astrocytes grown in regular media and recorded in ECS; (ii) astrocytes cultured in regular media and recorded with the membrane exposed to a MP-loaded CMCht/PAMAM dendrimer NP solution filled pipette, which was designated as acute NP exposure; and (iii) astrocytes incubated with MP-loaded CMCht/PAMAM dendrimer nanoparticles for 24 hours and analyzed in ECS. Adenosine triphosphate (ATP, Sigma, Germany) was added as a batch solution to the ECS to assess its effect in the exocytosis frequency. Off-line data analyses were performed using the software MATLAB (MathWorks Inc.). Quantification of the frequency and amplitude of events was determined from the obtained recordings.

2.4. Vesicle labeling and live confocal imaging of astrocytes

Co-localization studies in live astrocytes were performed in order to identify both the endocytotic and exocytotic vesicles involved in the nanoparticle cellular dynamics. For endocytotic vesicle labeling, low dense astrocyte cultures were incubated with Alexa Fluor® 546 Dextran (Molecular Probes, USA) for 1.5 hours and thoroughly washed in ECS prior to observation. To observe the exocytotic vesicles sub-confluent astrocyte cultures were used and transfected with the plasmid DNA encoding Neuropeptide Y (NPY) tagged with mCherry fluorescent protein (NPY-mCherry, a kind gift from Dr. Ronald W. Holz, University of Michigan, USA). Briefly, the cells were incubated

in lipofection media (DMEM, 1 mM sodium piruvate, 2 mM L-glutamine) and mixed with transfecting reagent (Fugene, Promega, USA) with 1 µg of plasmid DNA for 15 minutes, at 37°C. After that, culture medium was added and supplemented with 3% UltraSerG serum (Life Technologies, USA) and the cells were observed past 24 hours of incubation.

Live confocal microscopy images were acquired with an inverted microscope (Zeiss LSM META 510, Germany) equipped with a 63.2× oil-immersion objective. FITC molecules bonded to the NPs were excited by the 488-nm line of the argon laser and the emission light was collected through the bandpass filter (505–530 nm). Alexa Fluor 546 labeling the vesicles was excited with the He/Ne laser (543 nm) and the emission light was filtered with the long-pass filter, with the cutoff below 560 nm. To eliminate possible bleed through, the green and red emission fluorescence were acquired sequentially. Time series images were recorded in 20 seconds intervals during 45 minutes. All the recordings were performed in 300 mOsm ECS. Cells were stimulated with 1 mM ATP to assess alterations in exocytosis.

2.5.   Data analysis

Electrophysiological analysis was performed in CellAnn software for MatLab (MathWorks, USA). Individual steps, both positive and negative, in the imaginary part of the admittance signal (with no projections in the direct current trace) were registered and accounted as endocytotic, transient or full fusion exocytotic events for the frequency determination. Vesicle diameters were calculated using a specific membrane capacitance of 8 fF.μm^{-2}. Values are presented as mean ± SEM, unless stated otherwise. Two-way analysis of variance with Bonferroni post-test was used to assess statistical significance.

3. Results and discussion

The physico-chemical properties of engineered nanomaterials including size, shape, surface charge and chemistry have been recognized to robustly modulate its cellular internalization efficiency and fate.[10] In our lab, MP-loaded CMCht/PAMAM dendrimer NPs have been previously characterized displaying negative zeta potential when dispersed in physiological buffer and a

globular structure of about 109 nm in hydrodynamic diameter. Despite the lack of information regarding the cellular inward and outward mechanisms, the MP-loaded CMCht/PAMAM dendrimer NPs were reported to be easily internalized by primary nervous cells in a time-dependent manner without altering their viability or metabolic activity.[27] Additional *in vivo* assays have also confirmed that no morphological alterations in the liver, kidney or lungs of Wistar rats following NP intravenous administration were present, confirming their suitability to be used as therapeutic nanocarriers.[23] Therefore, in order to fully devise these NPs as optimal drug delivery systems a comprehensive understanding of the interaction with the target cell membrane, as well as its intracellular trafficking has been investigated herein.

To further elucidate the uptake and clearance mechanisms, two distinct methods in cultured astrocytes were used complementarily. Firstly, we used cell-attached patch clamp electrophysiology to monitor discrete alterations in the membrane capacitance (C_m) that reflect unitary endocytotic and exocytotic events and allow the quantification of the later, as well as vesicle diameter and fusion pore opening time.[28] Afterwards, confocal imaging of live astrocytes following incubation with fluorescently labeled NPs along with vesicle staining enabled to track its co-localization, which demonstrates NP vesicle transport. The cell-attached patch-clamp C_m measurements are directly correlated to the plasma membrane surface area, which dynamically fluctuates due to exocytosis and endocytosis. We questioned whether any differences in the frequency of occurring events was present between control astrocytes and NP-stimulated cells, both acute or chronically. In the acute NP stimulus, the astrocyte membrane was exposed to the NPs in solution inside the patch pipette during the analysis; whereas the chronically stimulated cells were incubated previously with the NPs for 24 hours. In both cases a dose of 200 µg.mL^{-1} was used taking into account previous studies reporting no cytotoxicity at this concentration.[27] A total of 62 astrocyte membrane patches were recorded, each of which being analysed for about 1000 seconds. In all cells, three types of alterations were detected in the C_m: (i) discrete irreversible upward steps, representing full fusion exocytotic events; (ii) single irreversible downward steps, indicating the occurrence of endocytosis; and (iii) reversible upward steps illustrating transient exocytotic events. [17,18,29] These events are schematically represented in Figure 1.
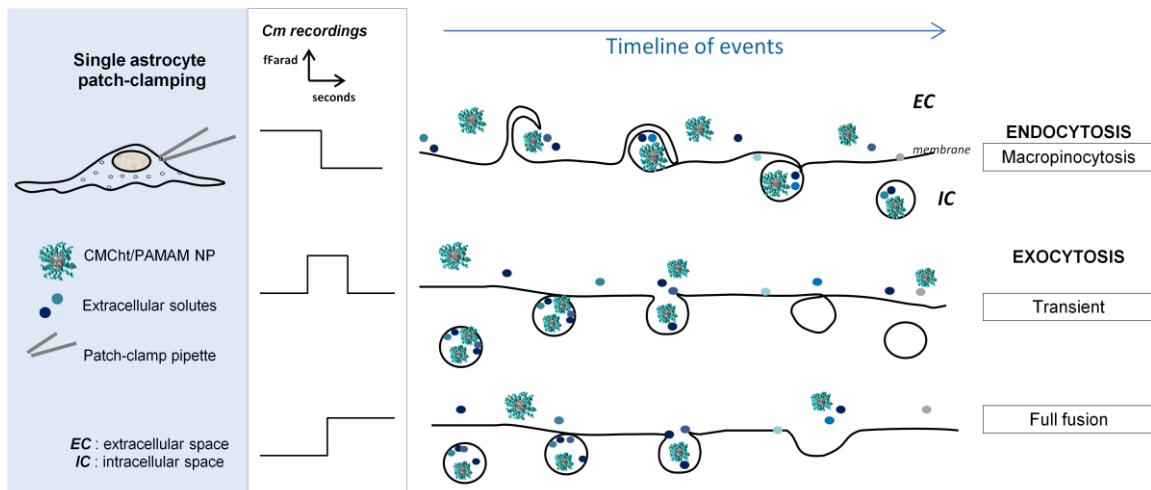
Figure 1 – Schematic representation of the membrane capacitance recordings by patch-clamp technique in astrocytes. Each of the possible alterations in the membrane is represented, namely: (i) endocytosis, with discrete downward steps in the recording; (ii) and exocytosis, with reversible (transient) or irreversible (full fusion) upward steps in the membrane capacitance.

Interestingly, our data revealed slight and similar increases in the frequency of endocytotic vesicles (Figure 2A) formed in the astrocyte membrane following NP incubation, both acute or chronically, in relation to control cells that had no exposure to NPs (Figure 2B). Although no statistical significance was determined between the groups, a slight amplification tendency is observed in the frequency of endocytotic events when NPs are present in the media. To our knowledge, it is the first time that endocytosis is analyzed following drug-loaded NP stimulation using the patch-clamp electrophysiological technique. Herein, it is suggested the use of this technique for similar studies, for its high sensitivity and resolution allow a precise quantification of the cell secretory activity. Moreover, the amplitude of the detected discrete steps allows the calculation of the vesicle diameter, assuming a spherical geometry, which provides singular insights on the vesicle properties. The vesicle diameter distribution revealed no significant differences between the control conditions (146±6 nm) and the astrocytes that were incubated with NPs for 24 hours (138±5 nm) (Figures 2C,E). Both the frequency and diameter figures were equivalent in these two situations. As seen in Figure 2D, however, when NPs are in solution inside the patch pipette, thus in contact with the astrocyte membrane, there is a small shift in the vesicle diameter distribution resulting in the formation of larger endosomes (173±6 nm). This is most likely due to the activation of a specific endocytic pathway that is carrying the 109 nm NPs inward to the astrocyte cytosol. The typical behavior of macropinocytosis vesicles seems coherent

and attributable to CMCht/PAMAM NP transport, namely due to the determined average vesicle size. PAMAM dendrimers have already been accounted to follow multiple endocytotic pathways to enter cells,[11,14] from receptor-mediated endocytosis (e.g., clathrin-mediated endocytosis) to non-specific uptake by macropinocytosis, depending on the surface modification and dendrimer generation.[30] The CMCht-grafted PAMAM dendrimers have been recently denoted to follow an endocytotic uptake mechanism, following a blocking study with colchicine, although no more detailed investigations were done.[20] Inhibition studies like the one before mentioned are often used to investigate the specific endocytotic route associated to the NP uptake, however some inhibitors have shown not to be that selective, actually affecting more than a single pathway.[31] Therefore, additional studies are crucial for a better understanding of the cell trafficking mechanisms.
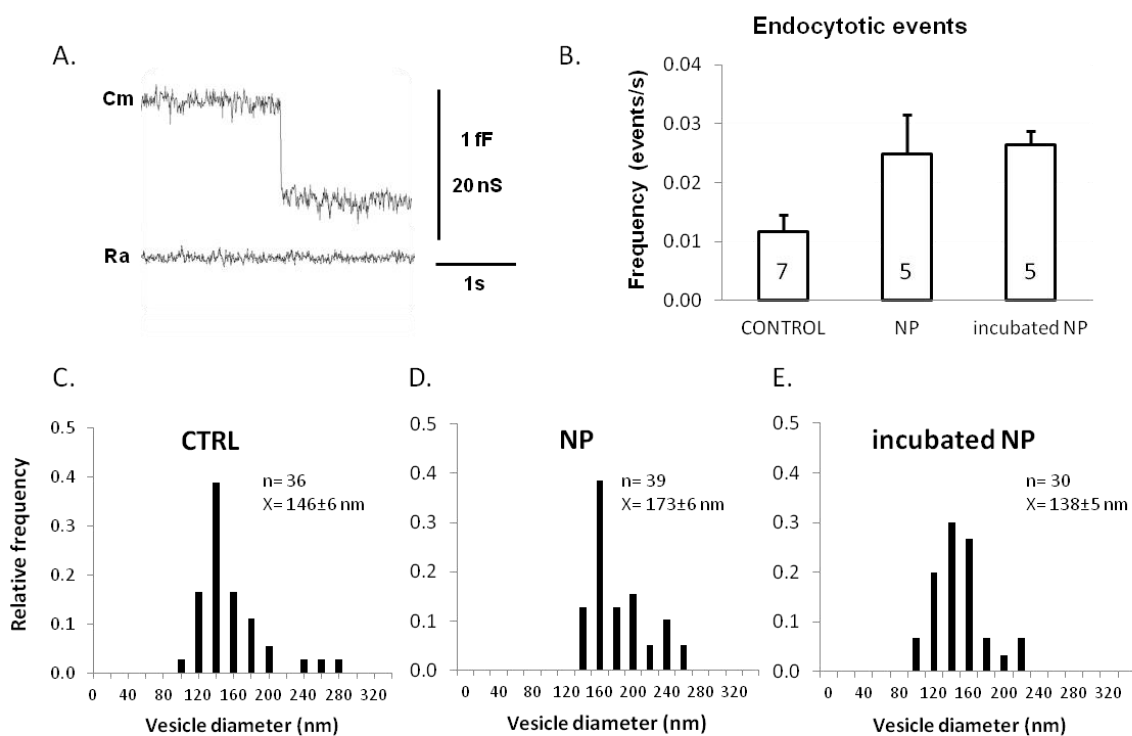
Figure 2 – A. Representative recording of an irreversible downward step in the imaginary admittance trace (Cm) proportional to membrane capacitance, and the corresponding real part of the admittance trace (Ra) proportional to access conductance, of a cell-attached recording indicative of the formation of an endocytotic vesicle. **B.** Graphical representation of the average frequency of endocytotic events in single astrocytes: (i) cultured in regular media (CONTROL); (ii) cultured in regular media but exposed to NP in the patch pipette solution, during the analysis (NP); and (iii) following 24 hours of incubation in NP (incubated NP) and analyzed in ECS. Values are presented as mean ± SEM. **C-E.** Endocytotic vesicle diameter distribution, calculated from the vesicle capacitance amplitude and assuming spherical morphology and a specific membrane capacitance of 8 fF/μm^2.

The endocytosis frequency determination from C_m readings does not allow to completely distinguish the different internalization routes, however the vesicle diameter determination can provide some insights regarding this.[32] In addition, a major gain of using this technique is the straightforward assessment of vesicle fusion and fission with temporal resolution, measuring events in the live membrane in real-time. From the present study, it appears that the interaction of NPs present in the vicinity of astrocyte plasma membranes induces, although to a limited extent, not only the formation of new endocytotic vesicles but also larger ones (Fig.2D). In view of the fact that no morphological alterations were observed in the cultured astrocytes and previous studies have demonstrated that the concentration used is not deleterious to primary nervous cells,[27] these variations have not been associated with any pathological alteration. However, a more detailed analysis dissecting all the endocytotic possible mechanisms occurring would better confirm this analysis.

We have hypothesized that a significant part of the NPs enters the astrocytes via macropinocytosis, based on the fact that the NPs possess a diameter that seems to be adequate to be transported by this type of vesicles. Nevertheless, we do not exclude the simultaneous occurrence of receptor-mediated endocytosis, as it is known that NPs interact with proteins present in the media and this corona may react with plasma membrane receptors, inducing specific endocytotic pathways. Nevertheless, we have focused our interest on the investigation of macropinocytosis given its anticipated relevance in the NP transport to the astrocyte cytosol. As a result, pulse-chase experiments were conducted adding labeled dextrans exogenously to primary astrocyte cultures, for the specific staining of macropinosomes.[11] Simultaneously, FITC-labeled MP-loaded NPs were incubated to track its intracellular trafficking and distribution. Confocal live imaging revealed extensive uptake of the FITC-labeled MP-loaded NPs after 24 hours of incubation with privileged perinuclear localization (Figure 3A), comparable to what has been previously reported.[21] Co-localization of NPs with the dextran-labeled macropinosomes was thoroughly observed evidencing directly and for the first time that the NPs are internalized via endocytosis, with an important contribution from the macropinocytic pathway. Confocal sequential live imaging allowed us to visualize the continuous trafficking of the endosomes in the cytoplasm, and more importantly to validate the co-localization findings with these vesicles. FITC-labeled NPs were observed circulating concurrently with labeled macropinosomes in the astrocyte cytosol. Regardless of the NP incubation times (6, 12 or 24 hours) co-localization of FITC-labeled NPs and dextran-labeled macropinosomes was always observed and apparently with

no significant differences (Figure 3B). Accordingly, similar co-localization coefficients were measured along time, implying that this uptake process is relatively fast (43±9% at 6h; 42±11% at 12h; and 36±7% at 24h incubation). Additionally in this study, it was noted that the NPs are able to be retained intracellularly in astrocytes for 24 hours, when present in the culture media.
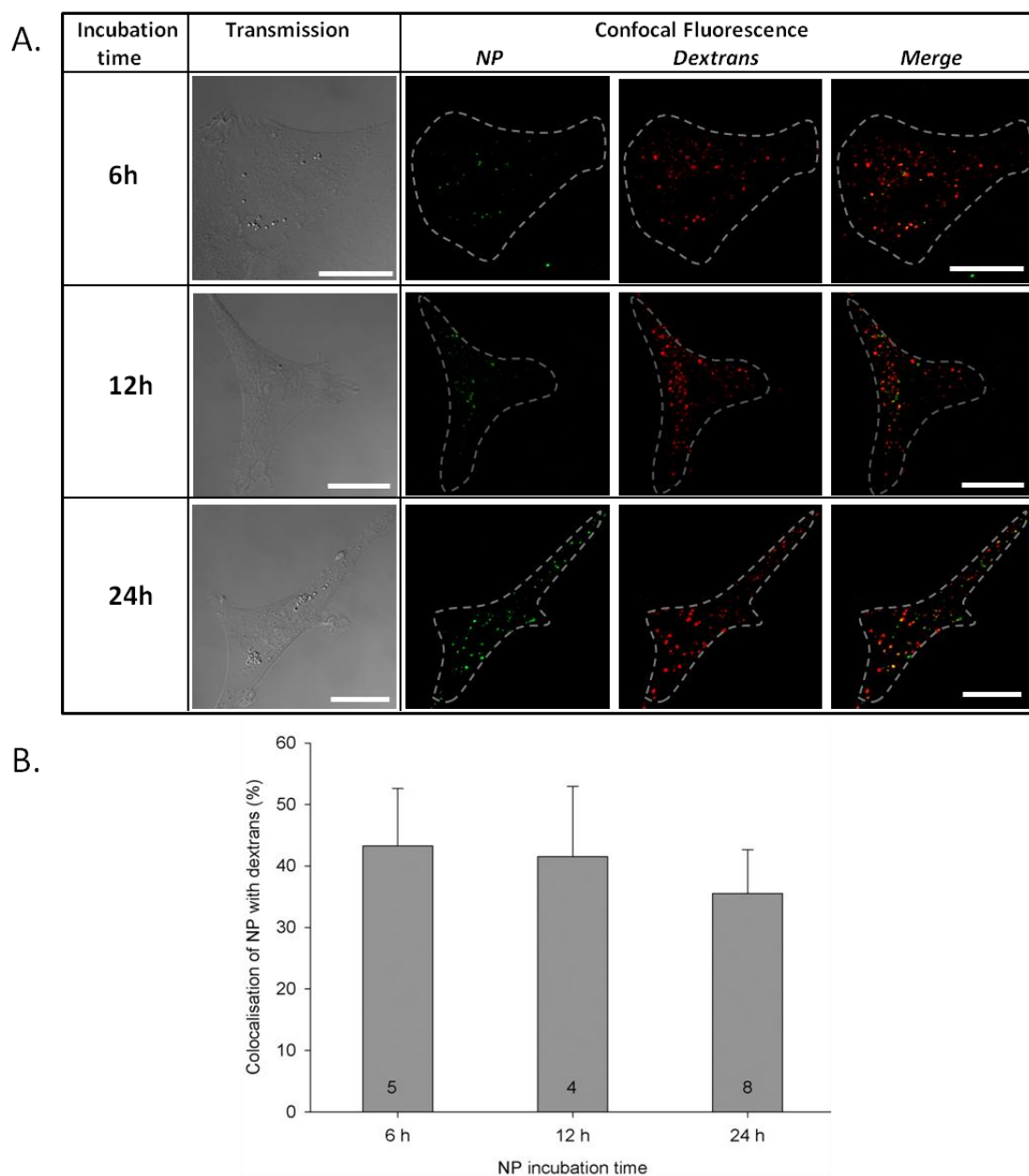
Figure 3 – A. Confocal micrographs of live astrocytes following Alexa Fluor® 546-dextran labeling (macropinosomes, in red) and incubation with FITC-labeled MP-loaded CMCht/PAMAM dendrimer NPs (in green). Co-localizations can be seen in yellow. The corresponding transmission light microscopy images are shown. Three different times of NP incubation were investigated: 6, 12 and 24 hours. Scale bars represent 20 µm. **B.** Relative co-localization of NPs with the dextran labeled macropinosomes (in %), relative to above threshold NP fluorescence in the cell, at different incubation period of cells with NPs. Threshold was 20 %. Error bars denote SEM; numbers in the columns indicate number of cells tested.

Notwithstanding, it was noted that the co-localization coefficients between NPs and endocytotic vesicles were slightly superior following shorter incubation times, rather than longer exposure to the NP, as 24h. We speculate that this is most likely due to a saturation effect and an endocytotic recycling regulatory mechanism. The initial input in the NP uptake is indeed the most relevant if we consider its therapeutic application; and we are showing that NPs are able to be rapidly transported to and retained inside astrocytes. Once in the cytosol, the NPs are expected to be retained long enough to allow the drug release, either by passive drug diffusion or as a result of NP degradation. Either way, after the therapeutic drug is released from the dendrimers, the NPs should be cleared out from the astrocytes.

Astrocytes, as other eukaryotic cells, contain secretory vesicles that exhibit a variety of diameters and serve for luminal cargo release, as well as membrane-associated receptors and transporters.[33] Comparing to neurons, exocytosis is much slower in astrocytes but it appears that, as in neurons, two types of exocytosis can occur (as shown in Figure 1): (i) full fusion, if the vesicle fuses in the cell membrane becoming part of the membrane; and (ii) transient, if the vesicle remains associated with the membrane, transiently opening the fusion pore and eventually returning to the cytosol.[33] Not many studies have focused on exocytosis of NPs regardless of its relevance, which eventually dictates the NP intracellular retention times and a potential chronic toxicity if NPs are not excreted from the cells. These two parameters are critical when considering therapeutic applications for NPs.[34-37] Ideally, after the NP desired action is accomplished intracellularly, extensive exocytosis of the latter should follow leaving the cells repaired and intact. To gain further insights into the clearance process of the MP-loaded CMCht/PAMAM dendrimer NPs, the frequency of formation of secretory vesicles was monitored once more by means of patch-clamp electrophysiology (Figure 4A), together with live confocal observation. In order to visualize the exocytotic vesicles and possible co-localization with NPs, transfection of astrocytes with mCherry-neuropeptide Y (NPY) was performed. NPY is a neurotransmiter that is broadly exocytosed by astrocytes, thus commonly serving as a marker for exocytosis.[38] The electrophysiological quantification of the exocytotic events occurring in the cell membranes revealed remarkable differences amongst the conditions tested (Figure 4B). Surprisingly, both the acute and chronic exposure to the NPs suggest an up-regulation of exocytosis in astrocytes, albeit at clearly different extents.
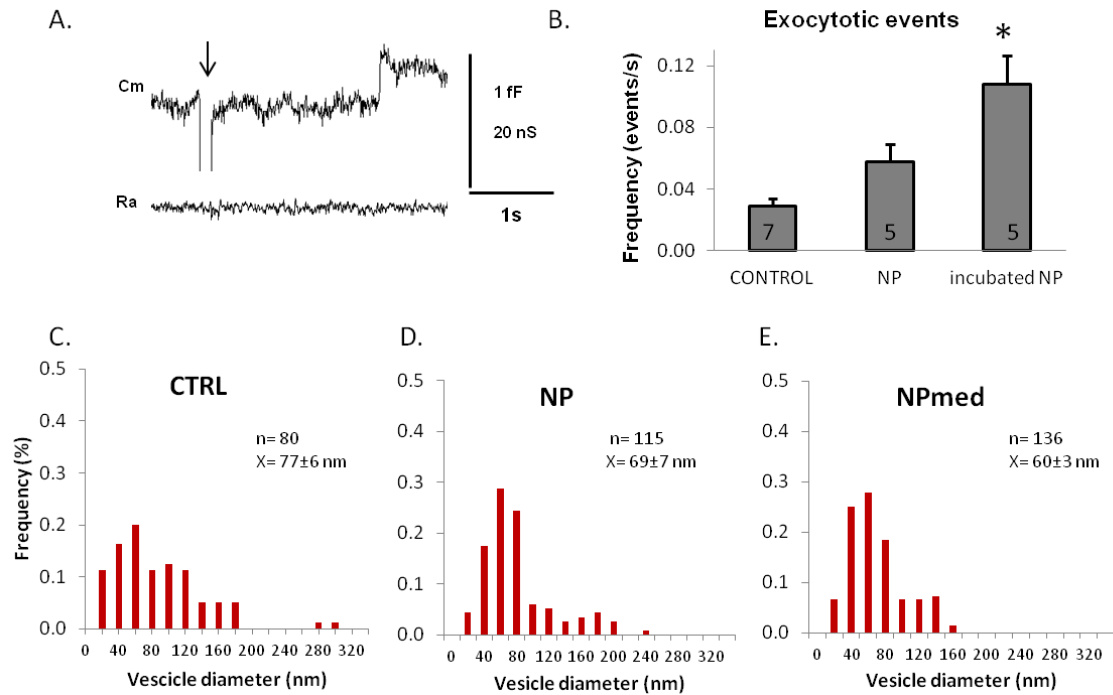
Figure 4 – A. Representative recording of an irreversible upward step in the imaginary admittance trace (Cm) and the corresponding real part of the admittance trace (Ra), indicative of the formation of an exocytotic vesicle. Arrow indicates a calibration pulse. **B.** Graphical representation of the average frequency of total exocytotic events in single astrocytes: (i) cultured in regular media (CONTROL); (ii) cultured in regular media and exposed to NP in the patch pipette solution during the recording (NP); and (iii) following 24 hours of incubation in MP-loaded CMCht/PAMAM dendrimer NP (incubated NP). Values are presented as mean ± SEM. * $p < 0.05$ **C-E.** Endocytotic vesicle diameter distribution, calculated from the vesicle capacitance amplitude and assuming spherical morphology and a specific membrane capacitance of 8 fF/ μm^2.

The total frequency of exocytotic events in astrocytes in the immediate NP contact (0.05±0.01 events/s) was above the basal levels (0.030±0.005 events/s); however, despite an almost 2-fold increase in the frequency, no statistical significance was detected (Figure 4B). Considering that a noticeably similar tendency was observed in the endocytosis rates in the acute NP exposure, we might infer that these two figures are related assuming, as suggested in the literature, that both endocytosis and exocytosis are occurring simultaneously and in a dynamic fashion as a result of NP interaction.[36] More importantly, a significant statistical difference was verified following a longer incubation time of 24 hours (0.11±0.02 events/s) revealing an unquestionable increase in the exocytosis frequency in astrocytes. To the best of our knowledge, it is the first time that such

an increase in exocytosis is reported from electrophysiological quantification of the secretory vesicle frequency after incubation of NPs in live astrocytes. The herein reported data reveals that following 24 hours of incubation with MP-loaded CMCht/PAMAM dendrimer NPs a drastic ≈4-fold increase in the frequency of exocytosis is detected in the astrocyte membrane patches (Figure 4B). Some authors suggest the occurrence of a recycling process of the membrane when in interaction with particulate systems, with the formation of exocytotic vesicles in response to the endocytosis of NPs.[39] Nonetheless, the frequencies of exocytosis we have measured are significantly superior to the endocytosis rates seen after chronic NP stimulation. However, if we take into account the vesicle diameter distributions (Figure 4C-E) it is evident that the exocytotic vesicles are significantly smaller in size than the endosomes, with an average diameter of 77±6 nm in basal conditions. Moreover, there is an additional shift in the exocytotic vesicle size distribution following NP acute or chronic exposure that indicates the formation of smaller vesicles, averaging 69±7 nm for acute NP exposure and 60±3 nm after prolonged 24 hour incubation. This might suggest that some NPs are being cleared out already with some extent of degradation.

A regulated balance between the endocytosis and exocytosis events occurring in the cells is of extreme importance, otherwise there would be a significant change in the membrane area and consequently in the cell volume that could be disturbing for the homeostasis and normal cell functioning. As corroborated by others, when macropinocytosis occurs there is a momentary increase in the cellular fluid uptake,[40] result of liquid and solutes engulfing from the extracellular media. Following this process, up-regulation of exocytosis may occur as a compensatory mechanism. Besides, since exocytosis is slower in astrocytes, its fluctuations in frequency are most likely to be noticed later, as it was observed after 24 hours of exposure to the NPs. We further confirmed that the NPs were indeed being exocytosed 24 hours after incubation, identifying co-localization spots of FITC-labeled NPs with the NPY-mCherry labeled exosomes, under a confocal microscope. Unlike endocytosis, the number of co-localized NPs with exocytotic vesicles found in astrocytes, visibly increased with time (Figure 5) corroborating the obtained electrophysiological data. Lower incubation times (6 hours) revealed the lowest percentage of co-localization (14±4%), while the higher incubation times (12 and 24 hours) uncovered significantly higher degrees of co-localization (38±10% and 40±6%, respectively). Thus, our findings indicate the direct dependence of this process with the time of exposure to NPs. For the first time, we are

confirming that the MP-loaded CMCht/PAMAM dendrimer NPs are cleared out from astrocytes via exocytosis, by two complimentary techniques that show compliant results.
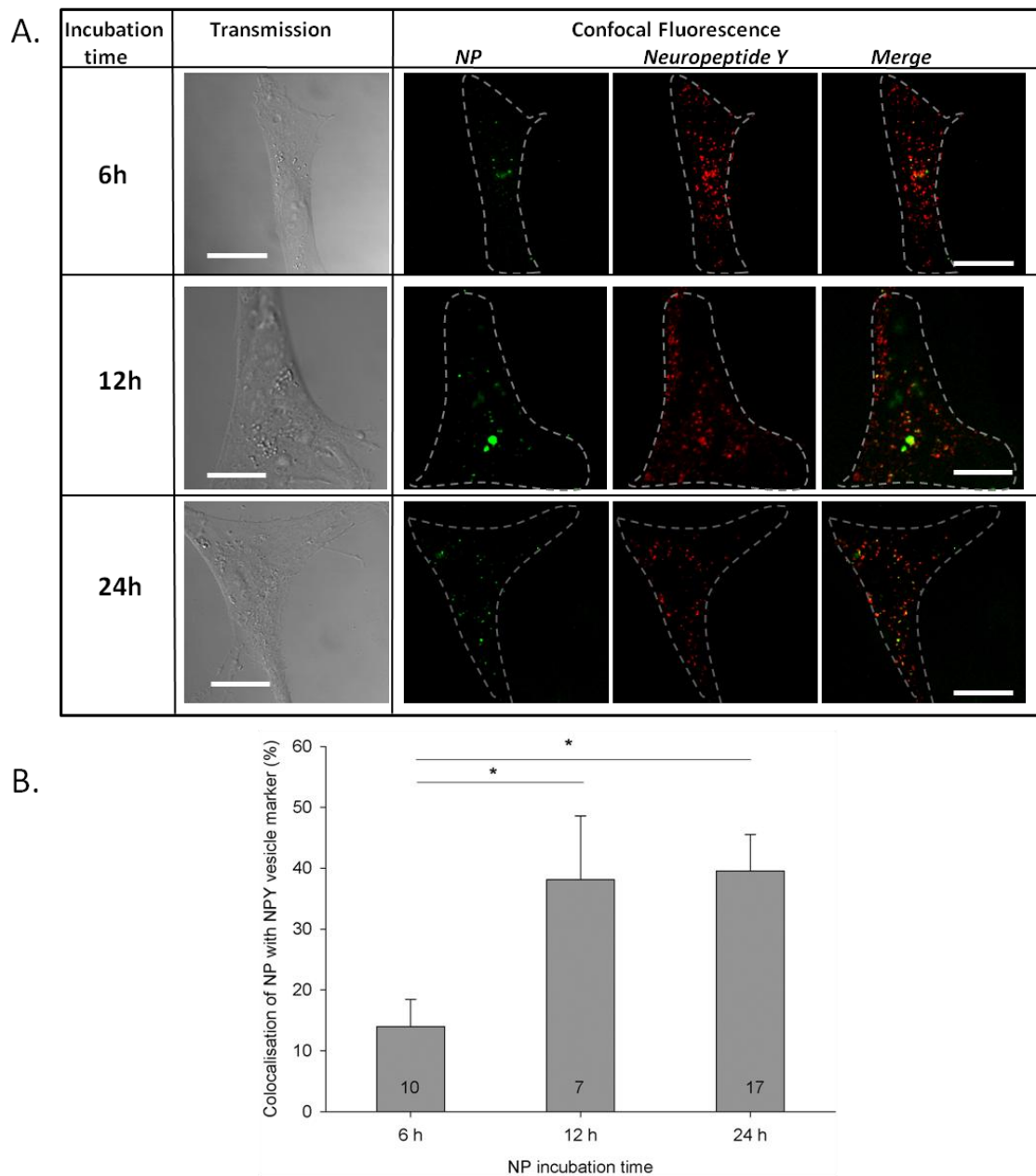
Figure 5 – A. Confocal micrographs of live astrocytes following mCherry-NPY transfection (exocytotic vesicles, in red) and incubation with FITC-labeled MP-loaded CMCht/PAMAM dendrimer NP (in green). Co-localizations can be seen in yellow. The corresponding transmission microscopy images are shown. Three different periods of NP incubation were investigated: 6, 12 and 24 hours. Scale bars represent 20 μm. **B.** Relative co-localization of NPs with the NPY exocytotic vesicle marker (in %), relative to above threshold NP fluorescence in the cell at different incubation period of cells with NPs. Threshold was 20 %. Bars denote SEM, asterisks indicate statistically significant differences between groups (* p<0.05), numbers in the columns indicate the number of cells tested.

The detailed investigation of the exocytotic mechanism occurrence after NP internalization in astrocytes was also considered (Figure 6A), as well as the influence of ATP as an exocytotic stimulant (Figure 6B). Intracellular ATP has been described as one of the energy sources for the formation of exocytotic vesicles inducing this process, and also functioning as an astrocytic transmitter.[33] We studied whether the astrocytes still respond as expected after ATP stimulation when NPs are also present. The patch-clamp C_m readings after addition of physiological solution of ATP (1 mM) to control astrocytes have revealed induced levels of exocytosis, as anticipated (Figure 6B). The same trend occurred after acute exposure to NPs, indicating that the NP interaction with the plasma membrane does not affect the response to this exocytosis stimulant.
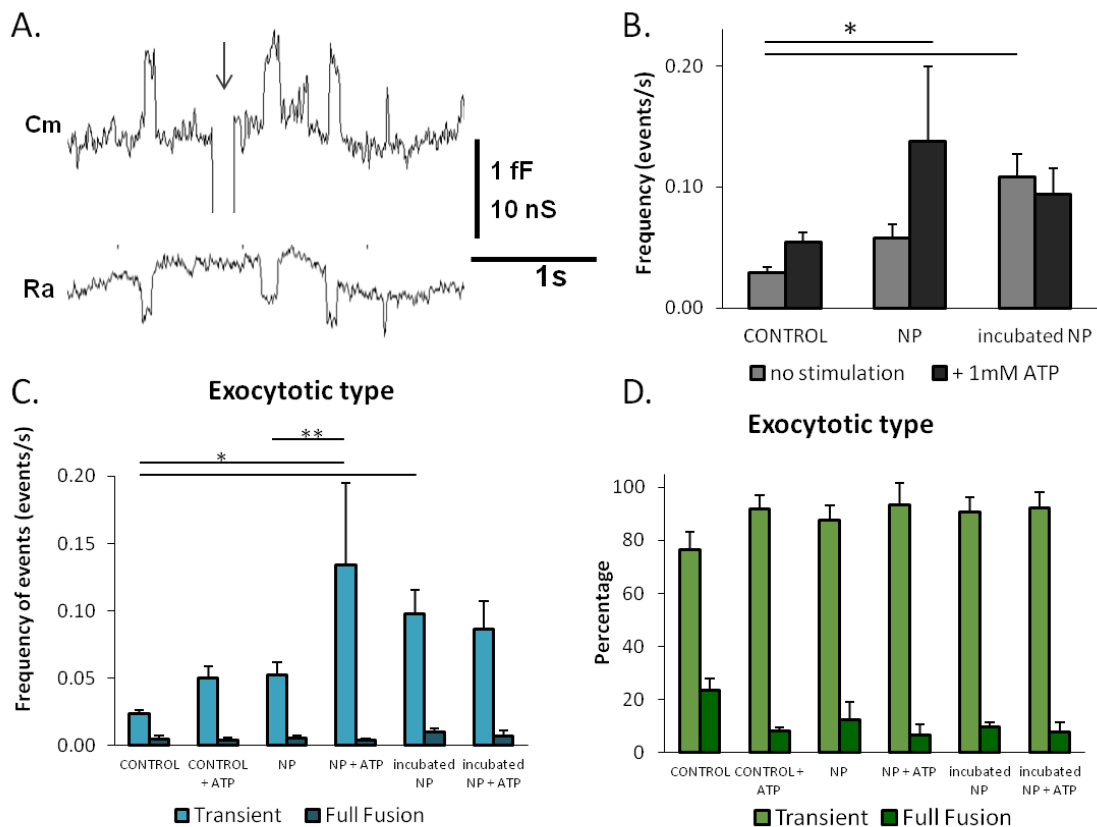
Figure 6 – A. Representative recording of reversible upward steps in the imaginary admittance trace (Im) and the corresponding real part of the admittance trace (Re), indicative of the formation of a transient type exocytotic vesicle. Arrow indicates a calibration pulse. **B.** Graphical representation of the average frequency of total exocytotic events in single astrocytes with stimulation of ATP when: (i) cultured in regular media (CONTROL); (ii) cultured in regular media and exposed to NP in the patch pipette solution during the recording (NP); and (iii) following 24 hours of incubation in MP-loaded CMCht/PAMAM dendrimer NP (incubated NP). **C-D.** Frequency (C) and percentage (D) of exocytosis type occurrence (transient or full fusion) in the above mentioned conditions; in the presence or absence of ATP stimulation. SEM are shown;* p<0.05; **<0.01.

Interestingly, the presence of both NPs and ATP inside astrocytes has a significant effect in exocytosis frequency. Conversely, ATP addition had no effect on the frequency of exocytosis when cells were incubated previously with NPs for 24 hours. In this case, it is believed that the exocytosis process was in a saturation level already and consequently there was no further possible boost in the frequency of exocytosis, even after stimulation with ATP.

To further dissect the exocytosis mechanisms occurring in astrocytes following NP interaction, we discerned between the two mechanisms of exocytosis (transient and full fusion) to investigate if the NPs were causing any alterations in its usual profile. As seen in Figures 6C and 6D, our findings reveal a prevalence of transient exocytosis events in all the conditions, with no alterations in the exocytotic subtype profile, even in the presence of NPs. Figure 6C indicates that the addition of ATP to the control astrocytes induced an approximate 2-fold increase in the frequency of transient events with only a modest decrease in the number of full fusion events. The same happened with the addition of NPs, suggesting once more that the presence of NPs stimulates exocytosis, in this case, in a similar proportion as the stimulant ATP. Equivalent frequency response was observed either in the presence of NPs or ATP, denoting that both ATP and NPs have similar exocytotic stimulant effects in astrocytes, particularly inducing transient event occurrence. When acute stimulation is provided to astrocytes, with ATP and NPs added simultaneously, the most significant boost in exocytosis frequency is observed. Nevertheless, no changes in the exocytotic subtype profile are detected (Figure 6D), with an approximately 90:10 ratio of transient:full fusion events taking place, and similar to the other conditions tested. The maintenance of the exocytotic subtype profile, with the same response after ATP or NP stimulation, might be an indicator that the interaction of NPs with astrocytes is not being deleterious or disturbing to the typical clearance mechanisms. Despite notorious frequency level variations, the ratio between the two exocytotic profiles is maintained.
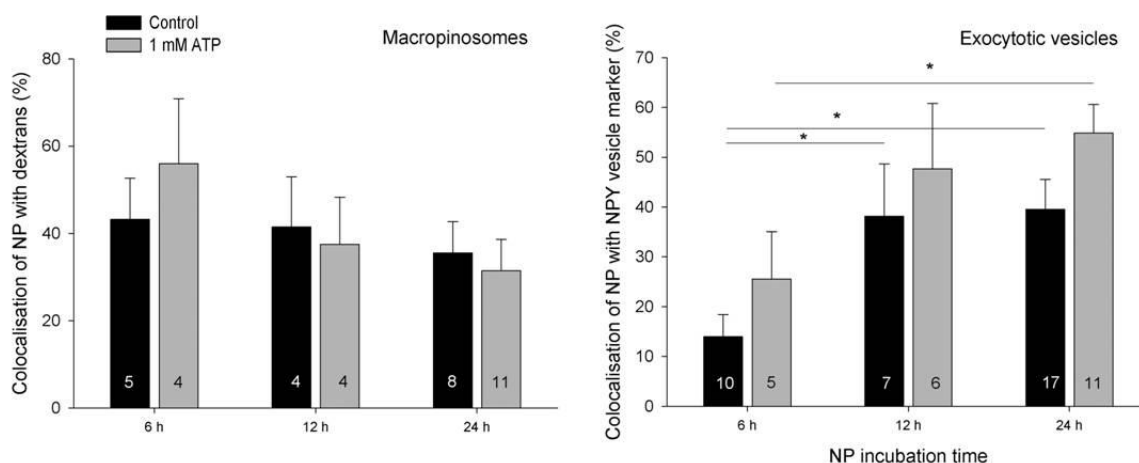
Figure 7 - NP co-localization with astrocyte vesicles (endocytotic and exocytotic) prior and after stimulation with 1 mM ATP. Co-localization coefficient of NPs in % with: macropinosomes labeled with Alexa Fluor® 546 dextrans (left); and mCherry-NPY labeled vesicles (right). Non-stimulated conditions (black columns) and 1 mM ATP astrocyte stimulation (gray columns) are represented. Error bars indicate SEM; numbers within columns indicate the number of analyzed cells. (* P< 0.05)

Finally, in an additional long-term study the astrocyte cultures were maintained for a week after an initial 24 hour exposure to the NPs. The media was replaced every day during a week to certify that no NPs were being exogenously added to the cells, besides the initial input, and all NPs present in the culture media were removed. Afterwards, both the endocytotic and exocytotic vesicles were labeled and the cells observed. As seen in Figure 8A, results demonstrate that FITC-labeled NPs were still present abundantly in the confluent astrocyte cultures with high retention rates in the cytosol. Nonetheless, very modest co-localization with endosomes was visualized and quantified (15±2%), which was significantly lower than after 24h of incubation (36±7%). On the other hand, co-localization of NPs with exocytotic vesicles was slightly increased one week after incubation (52±5% vs. 40±6%) and extensive co-localization spots were still observed. This is a strong indication that the NPs are still being cleared out of the astrocytes one week after internalization and with no NP renewal for a week, demonstrating a continuous clearance NP process. In addition, it was also confirmed that endocytosis is highly reduced under these circumstances, since no NPs are exogenously being added to the cells. The MP-loaded CMCht/PAMAM dendrimer nanoparticles seem to enter the astrocyte typical trafficking pathways, both endocytotic and exocytotic. More importantly, they are continuously cleared out from the cells even one week after the exposure.

121
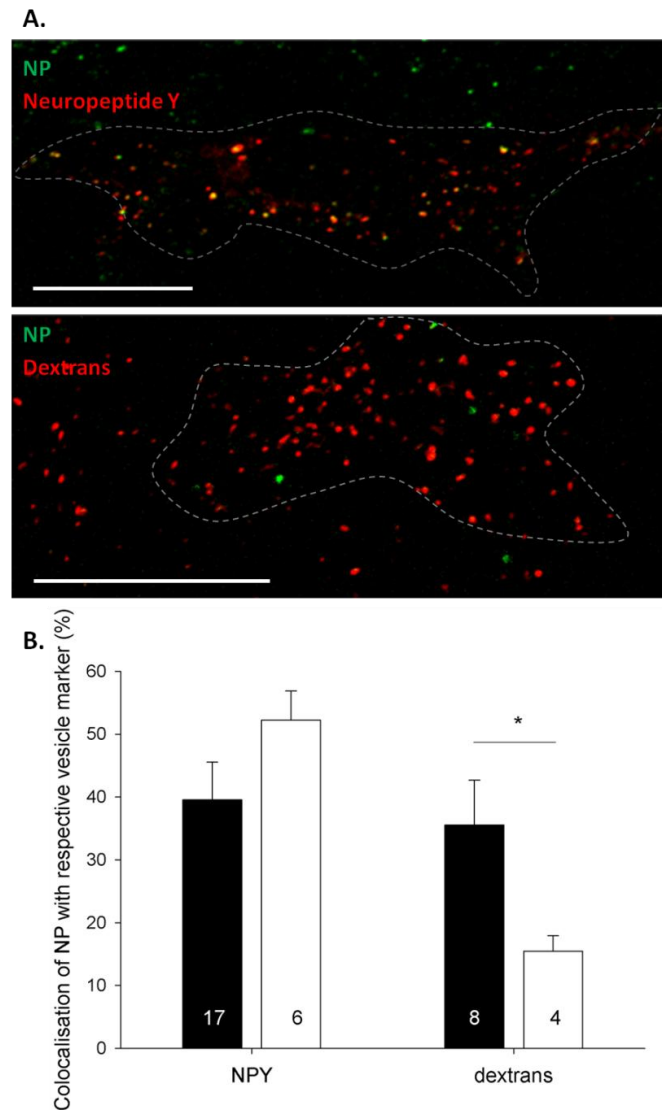
Figure 8 – A. Confocal micrographs of live astrocytes following mCherry-NPY transfection (above, exocytotic vesicles in red) or Alexa Fluor® 546 dextrans incubation (below, macropinosomes in red). FITC-labeled MP-loaded CMCht/PAMAM dendrimer NP (in green) were incubated for 24 hours and then removed from the media, with daily media change for one week. Co-localizations can be seen in yellow. Scale bars represent 20 μm**. B.** Co-localization coefficient of NP with membrane vesicles in % with the Alexa Fluor® 546 dextrans labeled macropinosomes and with the mCherry-NPY labeled vesicles immediately after 24h cell incubation with NP (black columns) and one week after (gray columns). Error bars indicate SEM, numbers in columns indicate numer of cells analyzed, asterisks denote statistically significant difference (* P< 0.05).

4. Conclusions

CMCht/PAMAM dendrimer NP have been showing many attractive features that renders them as great candidate nanocarriers to be used in biomedical applications, namely in CNS disorders. Despite biocompatibility and *in vivo* beneficial therapeutic effects have already been reported, the mechanisms underlying the interaction of the NPs with cells still remain unaddressed up to now. In this study, we thoroughly investigated the interaction of MP-loaded CMCht/PAMAM dendrimer NPs with astrocytes envisioning a potential targeted delivery to these cells following trauma or disease. The combination of the quantitative data obtained from patch-clamp electrophysiology readings and the live cell confocal imaging revealed to be appropriate to study endocytotic and exocytotic events, and have provided valuable and reliable information of the NP interaction and fate in astrocytes. It was noticed that endocytosis is slightly increased in the presence of the NPs, with a tendency to induce the formation of considerably larger vesicles. Confocal imaging confirmed the importance of macropinocytosis in the endocytotic uptake of the NPs and the time dependence of this uptake process. Exocytosis, on the other hand, is significantly increased following incubation with NPs suggesting that they are cleared out from astrocytes inside secretory vesicles. The reduction of the exocytotic vesicle diameter suggests that some degradation might have already occurred during the NPs intracellular trafficking. Live imaging of the astrocytes confirmed the presence of the NPs inside exocytotic vesicles, namely one week after incubation showing that this is a continuous and dynamic NP clearance process. There is an indication that NPs stimulate exocytosis, as ATP for instance, having similar effects on the exocytotic mechanism subtype profile, and reducing considerably the occurrence of full fusion events. The NPs were still found inside astrocytes one week after incubation, with more exocytotic transport occurring, while endocytosis was drastically decreased. The recycling of NPs, herein reported for the first time to occur via endocytosis and exocytosis, is relevant information providing new insights on the interaction of these NPs with nervous cells. No deleterious effects were detected during NP trafficking, confirming the suitability of these intracellular nanocarriers. Additionally, it is expected that the scientific community appreciates the potential relevance of patch-clamp measurements for studies involving nanomaterials and cell membrane interaction studies, given its high resolution and sensitivity.

5. Acknowledgements

References

1   Menjoge, A. R., Kannan, R. M. & Tomalia, D. A. Dendrimer-based drug and imaging conjugates: design considerations for nanomedical applications. *Drug Discovery Today* 15, 171-185 (2010).

2   Lee, D.-E. *et al.* Multifunctional nanoparticles for multimodal imaging and theragnosis. *Chemical Society Reviews* 41, 2656-2672 (2012).

3   Kimelberg, H. K. & Nedergaard, M. Functions of astrocytes and their potential as therapeutic targets. *Neurotherapeutics* 7, 338-353 (2010).

4   Potokar, M. *et al.* Astrocytic Vesicle Mobility in Health and Disease. *International journal of molecular sciences* 14, 11238-11258 (2013).

5   Nedergaard, M., Ransom, B. & Goldman, S. New roles for astrocytes: redefining the functional architecture of the brain. *Trends in neurosciences* 26, 523 (2003).

6   Parpura, V. *et al.* Glial cells in (patho)physiology. *Journal of Neurochemistry* 121, 4-27 (2012).

7   Oliveira, J. M., Salgado, A. J., Sousa, N., Mano, J. F. & Reis, R. L. Dendrimers and derivatives as a potential therapeutic tool in regenerative medicine strategies—a review. *Progress in Polymer Science* 35, 1163-1194 (2010).

8   Svenson, S. & Tomalia, D. A. Dendrimers in biomedical applications—reflections on the field. *Advanced drug delivery reviews* 57, 2106-2129 (2012).

9   Astruc, D., Boisselier, E. & Ornelas, C. Dendrimers designed for functions: from physical, photophysical, and supramolecular properties to applications in sensing, catalysis, molecular electronics, photonics, and nanomedicine. *Chemical Reviews* 110, 1857-1959 (2010).

10   Treuel, L., Jiang, X. & Nienhaus, G. U. New views on cellular uptake and trafficking of manufactured nanoparticles. *Journal of The Royal Society Interface* 10 (2013).

11   Albertazzi, L., Serresi, M., Albanese, A. & Beltram, F. Dendrimer internalization and intracellular trafficking in living cells. *Molecular Pharmaceutics* 7, 680-688 (2010).

12   Duan, X. & Li, Y. Physicochemical Characteristics of Nanoparticles Affect Circulation, Biodistribution, Cellular Internalization, and Trafficking. *Small* 9, 1521-1532 (2013).

13   Perumal, O. P., Inapagolla, R., Kannan, S. & Kannan, R. M. The effect of surface functionality on cellular trafficking of dendrimers. *Biomaterials* 29, 3469-3476 (2008).

14   Sahay, G., Alakhova, D. Y. & Kabanov, A. V. Endocytosis of nanomedicines. *Journal of controlled release* 145, 182-195 (2010).

15   Vasir, J. K. & Labhasetwar, V. Quantification of the force of nanoparticle-cell membrane interactions and its influence on intracellular trafficking of nanoparticles. *Biomaterials* 29, 4244-4252 (2008).

16   Gottstein, C., Wu, G., Wong, B. J. & Zasadzinski, J. A. Precise Quantification of Nanoparticle Internalization. *ACS nano* 7, 4933-4945 (2013).

17   Neher, E. & Marty, A. Discrete changes of cell membrane capacitance observed under conditions of enhanced secretion in bovine adrenal chromaffin cells. *Proceedings of the National Academy of Sciences* 79, 6712-6716 (1982).

18   Rituper, B. *et al.* High-resolution membrane capacitance measurements for the study of exocytosis and endocytosis. *Nat. Protocols* 8, 1169-1183 (2013).

19   Duncan, R. & Richardson, S. C. Endocytosis and intracellular trafficking as gateways for nanomedicine delivery: opportunities and challenges. *Molecular Pharmaceutics* 9, 2380-2402 (2012).

20   Oliveira, J. M. *et al.* Surface engineered carboxymethylchitosan/poly (amidoamine) dendrimer nanoparticles for intracellular targeting. *Advanced Functional Materials* 18, 1840-1853 (2008).

21   Cerqueira, S. R. *et al.* Microglia Response and In Vivo Therapeutic Potential of Methylprednisolone-Loaded Dendrimer Nanoparticles in Spinal Cord Injury. *Small* 9, 738-749 (2012).

22   Cerqueira, S. R. *et al.* Multifunctionalized CMCht/PAMAM dendrimer nanoparticles modulate the cellular uptake by astrocytes and oligodendrocytes in primary cultures of glial cells. *Macromolecular bioscience* 12, 591-597 (2012).

23   Pereira, V. H. *et al.* In vivo biodistribution of carboxymethylchitosan/poly (amidoamine) dendrimer nanoparticles in rats. *Journal of Bioactive and Compatible Polymers* 26, 619-627 (2011).

24   Pojo, M. *et al.* In vitro evaluation of the cytotoxicity and cellular uptake of CMCht/PAMAM dendrimer nanoparticles by glioblastoma cell models. *Journal of Nanoparticle Research* 15, 1-9 (2013).

25   Schwarts, J. P. & Wilson, D. J. Preparation and characterization of type 1 astrocytes cultured from adult rat cortex, cerebellum, and striatum. *Glia* 5, 75-80 (1992).

26   Lindau, M. & Neher, E. Patch-clamp techniques for time-resolved capacitance measurements in single cells. *Pflügers Archiv* 411, 137-146 (1988).

27   Salgado, A. J. *et al.* Carboxymethylchitosan/Poly (amidoamine) Dendrimer Nanoparticles in Central Nervous Systems-Regenerative Medicine: Effects on Neuron/Glial Cell Viability and Internalization Efficiency. *Macromolecular bioscience* 10, 1130-1140 (2010).

28   Fernandez, J., Neher, E. & Gomperts, B. Capacitance measurements reveal stepwise fusion events in degranulating mast cells. (1984).

29   Jorgačevski, J. *et al.* Hypotonicity and peptide discharge from a single vesicle. *American Journal of Physiology-Cell Physiology* 295, C624-C631 (2008).

30   Kitchens, K. M., Kolhatkar, R. B., Swaan, P. W. & Ghandehari, H. Endocytosis inhibitors prevent poly (amidoamine) dendrimer internalization and permeability across Caco-2 cells. *Molecular Pharmaceutics* 5, 364-369 (2008).

31   Ivanov, A. I. *Pharmacological inhibition of endocytic pathways: is it specific enough to be useful?*, (Springer, 2008).

32   Iversen, T.-G., Skotland, T. & Sandvig, K. Endocytosis and intracellular transport of nanoparticles: Present knowledge and need for future studies. *Nano Today* 6, 176-185 (2011).

33   Guček, A., Vardjan, N. & Zorec, R. Exocytosis in astrocytes: transmitter release and membrane signal regulation. *Neurochemical research* 37, 2351-2363 (2012).

34   Jiang, X. *et al.* Endo- and Exocytosis of Zwitterionic Quantum Dot Nanoparticles by Live HeLa Cells. *ACS nano* 4, 6787-6797 (2010).

35   Bartczak, D., Nitti, S., Millar, T. M. & Kanaras, A. G. Exocytosis of peptide functionalized gold nanoparticles in endothelial cells. *Nanoscale* 4, 4470-4472 (2012).

36   Panyam, J. & Labhasetwar, V. Dynamics of endocytosis and exocytosis of poly (D, L-lactide-co-glycolide) nanoparticles in vascular smooth muscle cells. *Pharmaceutical research* 20, 212-220 (2003).

37   Wang, Y. *et al.* A quantitative study of exocytosis of titanium dioxide nanoparticles from neural stem cells. *Nanoscale* 5, 4737-4743, doi:10.1039/c3nr00796k (2013).

38   Grigoriev, I. *et al.* Rab6, Rab8, and MICAL3 Cooperate in Controlling Docking and Fusion of Exocytotic Carriers. *Current Biology* 21, 967-974 (2011).

39   Colin, M. *et al.* Cell delivery, intracellular trafficking and expression of an integrin-mediated gene transfer vector in tracheal epithelial cells. *Gene therapy* 7, 139 (2000).

40   Mercer, J. & Helenius, A. Virus entry by macropinocytosis. *Nature cell biology* 11, 510-520 (2009).

CHAPTER V

Dendrimer nanoparticle diffusion in the rat brain parenchyma following intracisternal administration

CHAPTER V

Dendrimer nanoparticle diffusion in the rat brain parenchyma following intracisternal administration

Abstract

Drug delivery to the central nervous system (CNS) still is a challenge in biomedical research, with new exciting nanocarrier solutions arising from the nanotechnology field. Nonetheless, the real therapeutic applicability of nanoparticle (NP) systems can only be fairly predicted after its distribution properties in contact with live cells and biological tissues/organs are investigated. In this study, it was investigated the ability of fluorescein-labeled methylprednisolone (MP)–loaded CMCht/PAMAM dendrimer NPs to diffuse in the brain parenchyma following intracisternal administration in healthy rats. Confocal imaging revealed that the NPs were able to penetrate the nervous tissue, reaching areas such as the hippocampus, cerebellum and inner pre-frontal cortex parenchyma. The fluorescent NPs were detected intracellularly 72 hours post-administration. No morphological discrepancies were observed in astrocytes, suggesting no deleterious effects after administration of the NPs. The expression levels of glucocorticoid receptors (GR) in the brain following NP injection were also investigated. A decreased protein level of the GR following NP administration was detected, indicating that MP is being released from the NPs and acting intracellularly. Moreover, it was observed that NPs can be retained in the brain tissue while being able of delivering drugs, such as the corticosteroid MP. These findings provide new compelling arguments for the use of CMCht/PAMAM dendrimer nanoparticles as drug delivery nanocarriers for CNS.

1. Introduction:

In a progressively aging population it is expected that the incidence of neurodegenerative diseases will soon increase significantly.[1] The gradual loss of function and structure of neurons can be highly debilitating, leading to chronic disabilities that include failure to control movements, organ malfunctions as well as severe cognitive and emotional impairments. For these conditions, as for neurotraumatic episodes as well, there is no successful therapeutic intervention yet. Currently, clinicians still face a number of limitations and obstacles to treat central nervous system (CNS) disease, namely the inability of therapeutic drugs to cross the blood-brain barrier (BBB) and consistently target the affected tissue.[2] Since classical drugs are failing to succeed, also due to short half lives and unwanted side effects, alternative and more sophisticated vehicles are being developed and studied to reach the target sites and treat these disabilities in a more effective manner.[3] Nanotechnology, as the scientific field originating and engineering materials with dimensions from few to about 100 nanometers, is promising unique advances in biomedical applications, namely in neuroscience. These new nanomaterials can bring enhanced properties for use as drug carriers in regenerative strategies, namely: (i) increasing the drug bioavailability, with extended circulation times; (ii) the possibility to overcome the blood-CNS barriers; and (iii) the possibility to be functionalized, adding targeting, imaging or therapeutical features to the nanoparticle systems; while making use of traditional routes of administration. There is an immense set of nanoparticles recently proposed for use as nanocarriers for therapeutic applications, from classical linear polymers to novel spherical molecules. Dendrimers are particularly interesting monodisperse synthetic molecules with spherical morphology and highly ramified branches that resemble a tree.[4] They can be surface functionalized and its size thoroughly controlled, influencing its drug payload and targeting features.[5] Being the most investigated dendrimer molecules, poly(amido)amine (PAMAM) molecules have been recently suggested for use in central nervous system applications, mostly for malignant glioma therapies.[6] Functionalization of PAMAM dendrimers with targeting agents to allow transport across the BBB, such as transferrin, resulted in efficient distribution of the dendrimers in the brain tissue.[7] Furthermore, boronated-PAMAM dendrimers are also being explored for neuron boron capture therapies and already showed improved efficacy in rat glioma models.[8]

Recently, a new functionalization on PAMAM dendrimer nanoparticles was reported by grafting the dendrimer core with carboxymethylchitosan (CMCht), which led to an improvement in the

drug loading capacity and biocompatibility of the molecule.[9] The developed CMCht/PAMAM dendrimer NPs were suggested to be used as intracellular drug delivery vehicles, namely in CNS applications.[10] Moreover, these nanocarrier systems have already shown to be internalized by primary neuron and glial cell cultures without interfering with their viability and metabolic activity.[11] In another study, the corticosteroid methylprednisolone (MP) was shown to be able to be efficiently incorporated into the NPs.[12] These promising features led us to investigate further the NP distribution in the nervous tissue, namely in the brain, in order to have a preliminary insight on its dispersion properties and assess the potential applications *in vivo*. In a recent report, intravenous injections of fluorescently-labeled CMCht/PAMAM dendrimer NPs revealed their presence in peripheral organs and in the choroid plexus, while not intracellularly in the brain parenchyma.[13] This study has revealed that CMCht/PAMAM dendrimer NPs are not yet capable of crossing neither the BBB nor the blood-cerebrospinal fluid (CSF) barrier, located at the choroid plexus level, without further functionalization. Nonetheless, several direct administration techniques, such as intraparenchymal, intraventricular or subarachnoid injections have been used to target molecules directly in the nervous tissue and assess its ability to diffuse within it.[14] Injections in the *cisterna magna,* particularly, are considered substantially less invasive than intraventricular or intraparenchymal, and might subsequently be regarded for prospective clinical use.[15]

In the present study, it is aimed to assess the distribution of MP-loaded CMCht/PAMAM dendrimer NPs in the nervous tissue, and further investigate the MP intracellular release and action. The administration of fluorescently labeled NPs was performed directly into the CSF in the *cisterna magna* of Wistar rats in a simple and rapid procedure, as illustrated in Figure 1. Confocal imaging of relevant cerebral areas such as the hippocampus (HPC), pre-frontal cortex (PFC) and cerebellum (CB) was performed 72 hours post-injection to study the NP accumulation and distribution. Additionally, the intracellular action of the released MP, glucocorticoid receptor (GR) protein levels were analyzed in HPC, PFC and CB lysates using western blot analysis. Thus, it was both qualitative and quantitatively investigated the NP location in the brain following dispersion in the CSF, therefore adding new and valuable features for future studies and application in CNS conditions.

2. Materials and methods:

2.1. CMCht/PAMAM dendrimer nanoparticle synthesis and functionalization

Carboxymethylchitosan/poly(amidoamine) (CMCht/PAMAM) dendrimer NPs were produced as previously described.[9] Briefly, Starburst® PAMAM-carboxylic acid terminated dendrimers (PAMAM-CT) (generation 1.5, 20% w/v in methanolic solution) with an ethylenediamine core were purchased (Sigma, USA) and the following reactions were carried out: (i) increase in the PAMAM-CT generation; (ii) production of a PAMAM-methyl esther terminated dendrimer; (iii) condensation between the methyl esther and amine groups of PAMAM and CMCht; and (iv) conversion of the non-reacting methyl esther groups into carboxylic ones. MP was incorporated mixing an aqueous solution of CMCht/PAMAM dendrimer NP with an ethanolic MP solution with a final concentration of 5×10^{-4} M (w/w) and kept under vigorous agitation. Saturated sodium carbonate solution (Na_2CO_3, Sigma) and acetone (Pronalab, Portugal) were then added to the mixture. The precipitates were collected by filtration and dispersed in ultrapure water to undergo dialysis (cellulose tubing, benzoylated for separating compounds with a molecular weight of $\leq 1,200$, Sigma) for 48 hours. MP-loaded CMCht/PAMAM dendrimer NP were obtained by freeze-drying the solution (Telstar-Cryodos-80, Spain) during 1 week. Additionally, fluorescein isothyocianate (FITC, Sigma) labeled MP-loaded CMCht/PAMAM dendrimer NPs were prepared by covalently bonding the amine group of CMCht and the isothyocianate group from FITC.

2.2. Intracisternal nanoparticle administration

All experiments were carried out using male 10-week old Wistar rats (n=10) (Charles River, Spain). Animal handling and experiments were conducted in accordance with the Portuguese national authority for animal experimentation, Direção Geral de Veterinária (ID:DGV9457). Animals were kept in accordance with the guidelines for the care and handling of laboratory animals in the Directive 2010/63/EU of the European Parliament and Council. Animals were maintained for 12 hours in light/dark cycles at 22.5°C and 55% humidity, and fed with regular rodent's chow and tap water *ad libitum*.[16] The animals were anesthetized before surgery by intraperitoneal injection of 150 mg.Kg[-1] ketamine hydrochloride and 0.3 mg.Kg[-1] medetomidine. Then, the animals were placed in a stereotaxic frame with the head curved 45° downwards and

the dorsal base of the skull was shaved and soaked with ethanol and chlorohexidin. An occipito-cerebral midline incision was made and the muscles retracted until the meninges were visible. A small amount of CSF was withdrawn from the cistern magna and afterwards 15 µL of solution were injected with a Hamilton syringe (Hamilton, Switzerland). The animals were divided into two groups: (i) in the first, the animals received 0.9% saline injection; (ii) in the other, 5 mg.mL^{-1} FITC-labeled MP-loaded CMCht/PAMAM dendrimer NP. Following surgery, rats received analgesic (Butorphanol tartrate, 1 mg.mL^{-1}, Fort Dodge, Spain) and antibiotic (Enrofloxacine, 1 mg.mL^{-1}, Bayer, Germany) and were kept for 72 hours. After that, the animals were sacrificed and the brains were collected, freeze-sectioned and stained with rabbit GFAP antibody (Dako, Denmark, 1:500) and the secondary antibody Alexa Fluor 568 anti-rabbit (Molecular Probes, USA, 1:1000). The specimens were then observed under a confocal microscope (FV1000; Olympus, Germany).
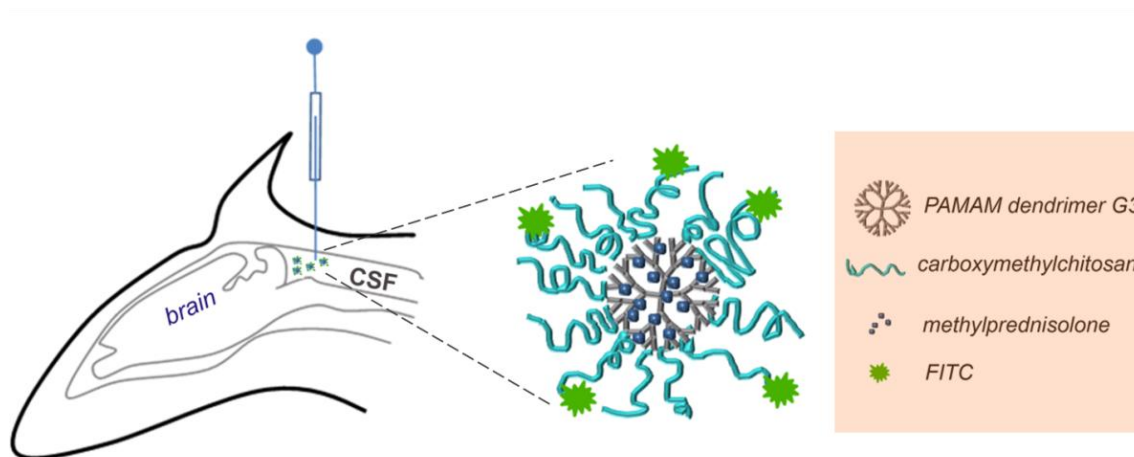
Figure 1 – Schematic representation of the intracisternal injection of fluorescent-labeled methylprednisolone-loaded CMCht/PAMAM dendrimer nanoparticles in healthy Wistar rats.

2.3. Western blot analysis

Proteins were extracted from the CB, HPC and PFC and homogenized in RIPA buffer (NaCl 0.1 M; tris(hydroxymethyl)aminomethane (Tris) pH 8.0, 0.01 M; EDTA pH 8.0, 0.001 M and complete protease inhibitor cocktail; Roche, Switzerland). Afterwards, sonication for 30 seconds in Laemmli buffer (SDS 4%, Tris pH 8, 0.12 M, glycerol 20% and dithiothreitol 0.2 M) was performed. Proteins were then quantified using the Bio-Rad protein assay (Bio-Rad, Hercules, USA). Samples were separated by SDS-PAGE (50 µg/lane) and then transferred into a

nitrocellulose membrane. Membranes were then stained with Ponceau S (Sigma) to confirm transfer efficiency; blocked with 5% skim milk in PBS and probed with anti-glucocorticoid receptor (GR) antibody (M-20) (Santa Cruz Biotechnology, USA, dilution 1:1000) at 4°C overnight. Membranes were washed and incubated with goat anti-rabbit IgG-HRP (Santa Cruz Biotechnology) and diluted to 1:10000. The blot was developed using the SuperSignal West Pico Chemiluminescent Substrate (PIERCE, USA) and exposed to X-ray film. Finally, the membranes were stripped with 2% SDS and 100 mM β-mercaptoetanol solution, warmed to 50°C for 30 minutes, thoroughly washed, blocked, re-blotted with mouse anti-alpha-tubulin (Santa Cruz Biotechnology) and diluted to 1:5000 to normalize for protein load.

2.4. Statistical analysis

Statistical evaluation was performed using the two-way analysis of variance test followed by Bonferroni post-test to assess the statistical differences between groups regarding the protein expression quantification. Statistical significance was defined for $p < 0.05$.

3. Results and discussion:

NP transport from the systemic circulation across the healthy CNS barriers is often restricted by the BBB and blood-CSF barriers, therefore limiting the current knowledge concerning their diffusion, retention and distribution in the nervous tissue.[17] Yet, in order to understand NP fate following *in vivo* administration and predict its therapeutic applicability these two parameters must necessarily be considered. In the present study, FITC-labeled MP-loaded CMCht/PAMAM dendrimer NPs were injected into the *cisterna magna* of healthy adult rats and its distribution in the nervous tissue was analyzed. Intracisternal administration is a straightforward method of accessing the CSF, merely requiring a small incision in the back of the neck of the animal, and after the visualization of the *dura mater* an injection can be easily performed. It can then be regarded as a less invasive technique than intraparenchymal injections, for instance, and as well suited for molecule diffusion studies in the CNS. Due to the growing interest in nanoparticle use as DDS, *in vivo* studies assessing the interaction of nanocarriers with living tissues is becoming essential in order to realize its potential clinical use.

Herein, FITC-labeled MP-loaded CMCht/PAMAM dendrimer NPs were administered intracisternally and tracked using confocal microscopy. Observation of the cryo-sectioned brain slices 72 hours following NPs injection, revealed a broad distribution of clear green fluorescent signals confirming intracellular localization of the NPs and consequently successful NP diffusion from the CSF to the brain tissue. Moreover, high magnification images (Figure 2) revealed preferential perinuclear localization inside astrocytes, that is comparable to previously reported *in vitro* observations.[12] Also, FITC-labeleb MP-loaded CMCht/PAMAM dendrimer NPs were also identified in other locations rather than in astrocytes, although in the present study those cells have not been identified. It is known, however, that other glial cells, such as microglia and oligodendrocytes do internalize these NPs as well, as shown *in vitro*.[12]
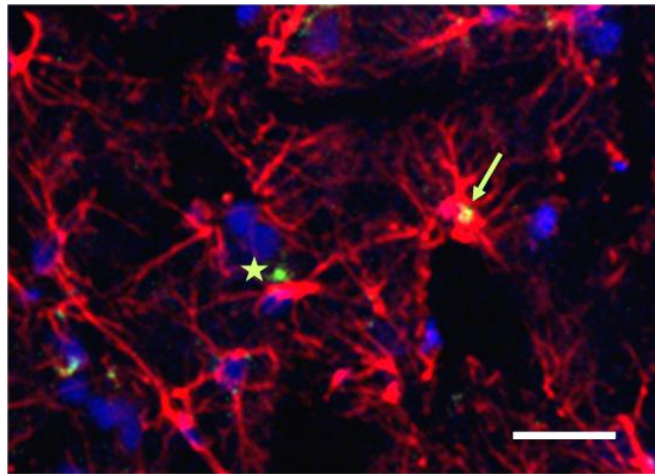
Figure 2 – High magnification confocal micrograph of the FITC-labeled NPs (in green) located intracellularly in astrocytes (arrow) and non-identified cell types (star), in rat hippocampus. DAPI (blue) designates cell nuclei and GFAP (red) identifies astrocytes. Scale bar corresponds to 20 µm.

The analysis of selected brain sections allowed the detection of internalized NPs not only in cortical areas of the PFC that are in close contact with the CSF but also, and more abundantly, in its inner parenchyma 72 hours post-injection (Figure 3). Control animals were injected with saline solution and did not display any green fluorescence, either in cortical or parenchyma PFC regions (Figures 3a,c). This observation confirms that the green fluorescent spots when detected are in fact due to the presence of FITC-labeled MP-loaded CMCht/PAMAM labeled NPs in the tissue (Figures 3b,d). Closer observation of the PFC tissue certifies a preferential inner distribution of the NPs 72 hours after injection, whereas the cortical areas reveal significantly less green fluorescent spots. This data indicates that following injection, the NPs followed a transport route

across the more superficial layers of the nervous tissue, allowing them to move to more internal levels. Following dispersion into the CSF of healthy animals, molecules are expected to exit this space through the CSF flow tracts to the blood stream.[18] The entry of substances into the brain parenchyma is typically mediated by a slow process which is diffusion. Only when molecules escape binding to efflux transporters and metabolism, they are able to be effectively diffused and retained in the brain parenchyma. The results herein presented indicated that diffusion of MP-loaded CMCht/PAMAM dendrimer nanoparticles effectively occurs and is fast enough to allow its retention in different layers of the brain 72 hours post-injection in the CSF. Under the tested conditions the NPs were able to traverse from the pial surface to the inner medullar areas, being preferentially retained in the latter. In pre-frontal cortex (PFC) preparations, only a reduced number of NP was found close to the pial membrane while the majority of the uptake was visible in deeper parenchymal areas (Figure 3e). This indicates that the NPs introduced in the CSF entered the cortical layers of the PFC and diffused crosswise, being most abundantly retained in the inner layers. Astrocyte labeling of the PFC sections showed no significant morphological or GFAP expression alterations between saline (control) and NP injected animals, suggesting that no astrogliosis is being induced by the presence of NPs (Figure 3a-d). Astrocytes are known to play a vital role in continuously monitoring the neuronal environment, and when an insult is detected these cells become reactive and initiate a protective mechanism designated astrogliosis.[19] During this process astrocytes become hypertrophic and are morphologically distinct from resting astrocytes. The presence of FITC-labeled MP-loaded CMCht/PAMAM NPs does not seem to induce astrocyte activation, even when NPs are internalized by astrocytes. These findings validate the therapeutic potential of CMCht/PAMAM dendrimer nanoparticles as carriers for astrocyte intracellular targeted delivery, which were recognized as important therapeutic targets in neuroinflammation and neurodegeneration.[20] Moreover, the fact that MP is an anti-inflammatory drug being transported inside the nanocarriers adds significance to astrocyte targeting, since this drug inhibits astrocyte activation and proliferation during inflammatory processes.

In terms of brain biodistribution, the NPs were also thoroughly found in other areas such as the choroid plexus, the lateral ventriculus and the HPC (Figure 4). Co-staining of GFAP and nuclear
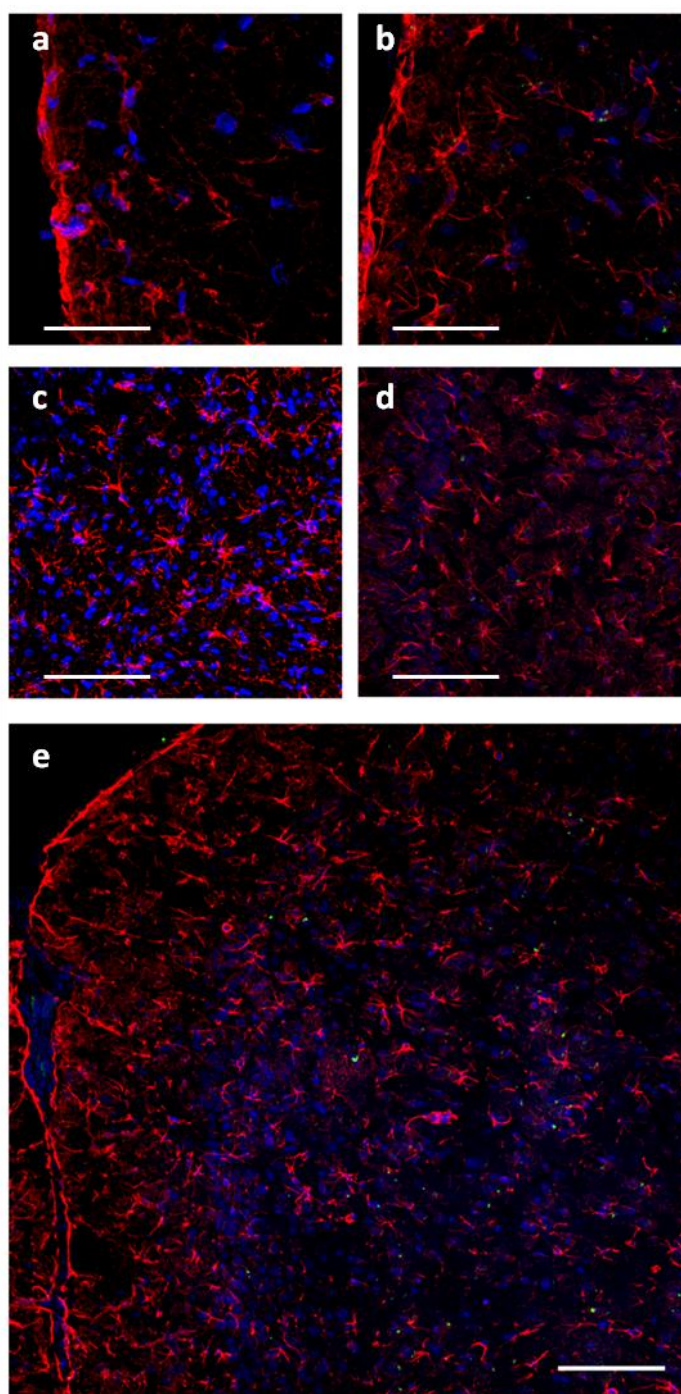
Figure 3 – Confocal microscope photographs of rat brain frozen sections stained for astrocytes (GFAP, in red) and nuclei (DAPI, in blue) following intracisternal injection. a,c) Controls with saline injection, no green fluorescence is observed. b,d) Following FITC-labeled MP-loaded nanoparticles injection, green fluorescence is observed both in the cortical and inner regions of the pre-frontal cortex parenchyma. e) Overview of a PFC brain slice following BP injection. Scale bar corresponds to 50 μm.

labeling indicated once more that the NP green fluorescence was located intracellularly in astrocytes but also in other cell types that were not yet identified and will be further investigated in future studies. From Figure 4, it is evident that the layers in contact with the CSF tend to possess significantly a decreased NP-related fluorescence (green color), suggesting an effective NP trafficking along the depth of the brain parenchyma.
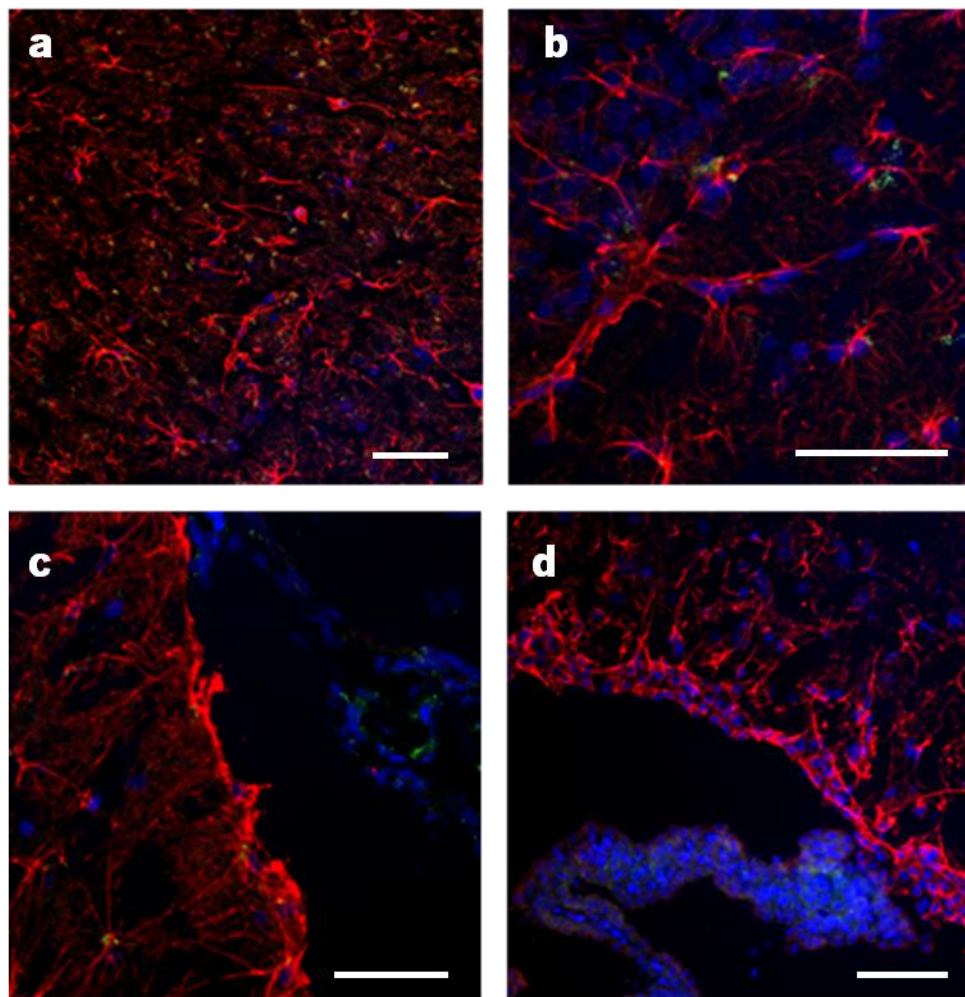
Figure 4 – Confocal microscope photographs of frozen sections from rat brain stained for astrocytes (GFAP, in red) and nuclei (DAPI, in blue) following NP intracisternal injection. Green fluorescence emitted by the FITC-labeled MP-loaded NP was found in: a) pre-frontal cortex; b) hippocampus; c) lateral ventricles (in the CSF side); and d) choroid plexus. Scale bars represent 50 μm.

Abundant NP retention was observed in the choroid plexus (Figure 4c,d). It is unclear however, whether the movement of the NPs from the CSF to the choroid plexus was through the epithelial layer or the blood flow. In this case, probable re-circulation of NPs through CSF and the blood flow could allow entry in the choroid plexus, since the capillaries within the choroid plexus are

fenestrated and not with the tight junctions that endothelial cells typically present in the CNS. The present study has demonstrated the ability of MP-loaded CMCht/PAMAM dendrimer NPs not only to diffuse but also be intracellularly retained in distinct areas of the brain.

CMCht/PAMAM dendrimer NPs were already shown to be easily internalized *in vitro* in primary neurons and glia whilst not affecting their normal metabolism.[11-12] Additionally, the present study revealed that if injected in the CSF there are no apparent morphological and structural differences in the nervous tissue, namely in astrocytes that are involved in the response to environment alterations.

It was recently shown by Albertazzi *et al.* that the surface properties of PAMAM dendrimers affect its diffusion in the brain following intraparenchymal and subarachnoid injection, therefore slight alterations in the dendrimer composition may dramatically change its uptake and distribution in the CNS.[21] Herein, our findings have demonstrated that the grafting of G3 PAMAM dendrimers with CMCht and subsequent MP incorporation do not hamper its ability to diffuse within the several layers of nervous tissue and to be internalized by astrocytes and other CNS cells.

Next, and in order to have a deeper insight on the MP release from the NP and intracellular action while retained in the brain tissue, protein expression of the GR was investigated. Two types of GR can be found in the rat brain: (i) the high-affinity mineralocorticoid receptor (MR) that is most densely present in the HC; and (ii) the ubiquitously distributed GR.[22] When glucocorticoids are exogenously administered in rats there is a typical down-regulation effect in the GR expression, with some regional and affinity differences.[23] These *in vivo* changes in GR expression in the rat brain were shown to be effectively quantified by western blot, without the need for prior adrenalectomy of the animals.[23-24] Figure 5 shows that the intracisternal administration of MP resulted in a down-regulation of the expression of the GR both in the HPC and the PFC, in relation to control animals injected with saline solution. Both in HP and PFC lysates an almost 2-fold significant decrease was noted in the presence of MP-loaded NPs. No alteration was observed in the CB however, which is explained by the fact that the density of GR in this particular area is lower than in the HP and PFC, thus resulting in an overall diminished protein expression (Figure 5B). Notably, the administration of FITC-labeled MP-loaded CMCht/PAMAM dendrimer NPs reached similar protein expression levels as the drug when administered alone, with statistically significant differences to the controls. As MP alone, NP administration induces significant GR expression down-regulation in the HPC and the PFC, though not as drastically as the administration of the corticosteroid solution. The analysis of the GR expression results thus

indicated that MP is indeed being released from the NPs and acting intracellularly via activation of its cytosolic GR, as predicted, and resulting in altered protein expression profiles.

The fact that MP-loaded CMCht/PAMAM dendrimer NPs show a broad distribution in the cerebral tissue along with a convenient intracellular retention, with no apparent astrogliosis, associated to the MP release and intracellular action renders this NP system attractive features with exciting prospects to be considered for therapeutic applications, namely as drug delivery systems in CNS disorders.
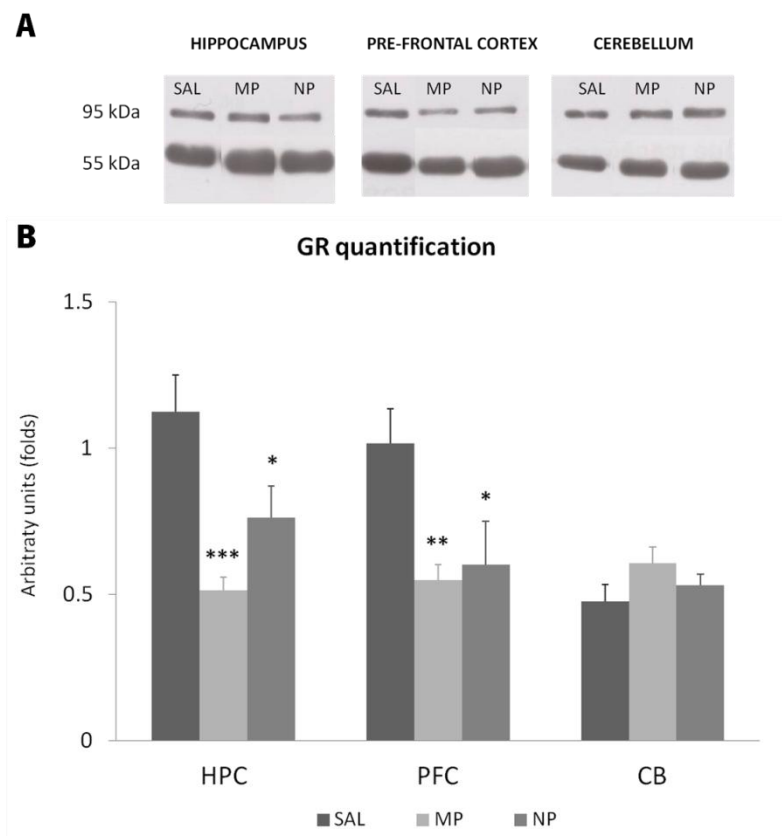
Figure 5 – Western-blot analysis of lysates (hippocampus – HPC; pre-frontal cortex – PFC; and cerebellum – CB) following intracisternal injection of saline (SAL), methylprednisolone solution (MP) or methylprednisolone-loaded CMCht/PAMAM dendrimer nanoparticles (NP). Bars show the quantification of the expression level of the 95 kDa glucocorticoid receptor (GR) compared with the expression of 55 kDa α-tubulin. Data expressed as mean ± SEM. $*p < 0.05$; $**p < 0.01$; $***p < 0.005$.

4. Conclusions:

This study demonstrated that MP-loaded CMCht/PAMAM dendrimer NPs broadly diffuse in the healthy rat brain following administration in the CSF. Our findings showed that the NPs are retained intracellularly in the choroid plexus, lateral ventricles, PFC and HPC, 72 hours post-administration. Moreover, histological observation of the brain tissue showed no morphological differences between control and NP injected animals suggesting no deleterious effects. Additionally, altered expression of GR receptors in PFC and HPC were detected following NP administration pointing to an intracellular drug release and action. These observations can open up new and exciting possibilities for the use of these NP as intracellular drug delivery carriers for the nervous system.

5. Acknowledgements

References

1. World Health Organization., *Neurological disorders : public health challenges*. World Health Organization: Geneva (2006).

2. Palmer, A. M., The role of the blood–CNS barrier in CNS disorders and their treatment. *Neurobiology of Disease 37* (1), 3-12 (2010).

3. Modi, G.; Pillay, V.; Choonara, Y. E., Advances in the treatment of neurodegenerative disorders employing nanotechnology. *Annals of the New York Academy of Sciences 1184* (1), 154-172 (2010).

4. Svenson, S.; Tomalia, D. A., Dendrimers in biomedical applications—reflections on the field. *Advanced drug delivery reviews 57* (15), 2106-2129 (2012).

5. Oliveira, J. M.; Salgado, A. J.; Sousa, N.; Mano, J. F.; Reis, R. L., Dendrimers and derivatives as a potential therapeutic tool in regenerative medicine strategies—A review. *Progress in Polymer Science 35* (9), 1163-1194 (2010).

6. Yang, H., Nanoparticle-mediated brain-specific drug delivery, imaging, and diagnosis. *Pharmaceutical research 27* (9), 1759-1771 (2010)

7. (a) Wu, G.; Barth, R. F.; Yang, W.; Kawabata, S.; Zhang, L.; Green-Church, K., Targeted delivery of methotrexate to epidermal growth factor receptor–positive brain tumors by means of cetuximab (IMC-C225) dendrimer bioconjugates. *Molecular cancer therapeutics 5* (1), 52-59 (2006); (b) He, H.; Li, Y.; Jia, X.-R.; Du, J.; Ying, X.; Lu, W.-L.; Lou, J.-N.; Wei, Y., PEGylated Poly (amidoamine) dendrimer-based dual-targeting carrier for treating brain tumors. *Biomaterials 32* (2), 478-487 (2011); (c) Ke, W.; Shao, K.; Huang, R.; Han, L.; Liu, Y.; Li, J.; Kuang, Y.; Ye, L.; Lou, J.; Jiang, C., Gene delivery targeted to the brain using an Angiopep-conjugated polyethyleneglycol-modified polyamidoamine dendrimer. *Biomaterials 30* (36), 6976-6985 (2009).

8. Yang, W.; Barth, R. F.; Wu, G.; Huo, T.; Tjarks, W.; Ciesielski, M.; Fenstermaker, R. A.; Ross, B. D.; Wikstrand, C. J.; Riley, K. J., Convection enhanced delivery of boronated EGF as a molecular targeting agent for neutron capture therapy of brain tumors. *Journal of neuro-oncology 95* (3), 355-365 (2009).

9. Oliveira, J. M.; Kotobuki, N.; Marques, A. P.; Pirraco, R. P.; Benesch, J.; Hirose, M.; Costa, S. A.; Mano, J. F.; Ohgushi, H.; Reis, R. L., Surface engineered carboxymethylchitosan/poly(amidoamine) dendrimer nanoparticles for intracellular targeting. *Adv Funct Mater 18* (12), 1840-1853 (2008).

10. Pereira, V. H.; Salgado, A.; Oliveira, J. M.; Cerqueira, S. R.; Frias, A.; Fraga, J.; Roque, S.; Falcão, A. M.; Marques, F.; Neves, N., In vivo biodistribution of carboxymethylchitosan/poly (amidoamine) dendrimer nanoparticles in rats. *Journal of Bioactive and Compatible Polymers 26* (6), 619-627 (2011).

11. Salgado, A. J.; Oliveira, J. M.; Pirraco, R. P.; Pereira, V. H.; Fraga, J. S.; Marques, A. P.; Neves, N.M.; Mano, J.F.; Reis, R.L.; Sousa, N., arboxymethylchitosan/Poly(amidoamine) Dendrimer Nanoparticles in Central Nervous Systems-Regenerative Medicine: Effects on Neuron/Glial Cell Viability and Internalization Efficiency. *Macromolecular Bioscience 10* (10), 1130-1140 (2010).

12.   Cerqueira, S. R.; Oliveira, J. M.; Silva, N. A.; Leite-Almeida, H.; Ribeiro-Samy, S.; Almeida, A.; Mano, J. F.; Sousa, N.; Salgado, A. J.; Reis, R. L., Microglia Response and In Vivo Therapeutic Potential of Methylprednisolone-Loaded Dendrimer Nanoparticles in Spinal Cord Injury. *Small 9* (5), 738-49 (2013).

13.   Pereira, V. H.; Salgado, A. J.; Oliveira, J. M.; Cerqueira, S. R.; Frias, A. M.; Fraga, J. S.; Roque, S.; Falcão, A. M.; Marques, F.; Neves, N. M.; Mano, J. F.; Reis, R. L.; Sousa, N., In vivo biodistribution of carboxymethylchitosan/poly(amidoamine) dendrimer nanoparticles in rats. *Journal of Bioactive and Compatible Polymers 26* (6), 619-627 (2011).

14.   Alam, M. I.; Beg, S.; Samad, A.; Baboota, S.; Kohli, K.; Ali, J.; Ahuja, A.; Akbar, M., Strategy for effective brain drug delivery. *European Journal of Pharmaceutical Sciences 40* (5), 385-403 (2011).

15.   Louboutin, J.; Reyes, B.; Agrawal, L.; Van Bockstaele, E.; Strayer, D., Intracisternal rSV40 administration provides effective pan-CNS transgene expression. *Gene therapy 19* (1), 114-118 (2011).

16.   National Research Council (U.S.). Committee for the Update of the Guide for the Care and Use of Laboratory Animals.; Institute for Laboratory Animal Research (U.S.); National Academies Press (U.S.), *Guide for the care and use of laboratory animals*. 8th ed.; National Academies Press: Washington, D.C., (2011).

17.   Wolak, D. J.; Thorne, R. G., Diffusion of Macromolecules in the Brain: Implications for Drug Delivery. *Molecular Pharmaceutics 10* (5), 1492-504 (2013).

18.   Pardridge, W., Drug transport in brain via the cerebrospinal fluid. *Fluids Barriers CNS 8* (1), 1-4 (2011).

19.   Sofroniew, M. V., Molecular dissection of reactive astrogliosis and glial scar formation. *Trends in Neurosciences 32* (12), 638-647 (2009).

20.   Hamby, M. E.; Sofroniew, M. V., Reactive Astrocytes As Therapeutic Targets for CNS Disorders. *Neurotherapeutics 7* (4), 494-506 (2010).

21.   Albertazzi, L.; Gherardini, L.; Brondi, M.; Sulis Sato, S.; Bifone, A.; Pizzorusso, T.; Ratto, G. M.; Bardi, G., In Vivo Distribution and Toxicity of PAMAM Dendrimers in the Central Nervous System Depend on Their Surface Chemistry. *Molecular Pharmaceutics 10* (1), 249-260 (2012).

22. Sousa, N.; Cerqueira, J. J.; Almeida, O. F. X., Corticosteroid receptors and neuroplasticity. *Brain Research Reviews 57* (2), 561-570 (2008).

23. Chiba, S.; Numakawa, T.; Ninomiya, M.; Richards, M. C.; Wakabayashi, C.; Kunugi, H., Chronic restraint stress causes anxiety- and depression-like behaviors, downregulates glucocorticoid receptor expression, and attenuates glutamate release induced by brain-derived neurotrophic factor in the prefrontal cortex. *Progress in Neuro-Psychopharmacology and Biological Psychiatry 39* (1), 112-119 (2012).

24. Spencer, R. L.; Kalman, B. A.; Cotter, C. S.; Deak, T., Discrimination between changes in glucocorticoid receptor expression and activation in rat brain using western blot analysis. *Brain research 868* (2), 275-286 (2000).

CHAPTER VI

Microglia response and *in vivo* therapeutic potential of methylprednisolone-loaded dendrimer nanoparticles in spinal cord injury

CHAPTER VI

Microglia response and *in vivo* therapeutic potential of methylprednisolone-loaded dendrimer nanoparticles in spinal cord injury

Abstract

The control and manipulation of cells that trigger secondary mechanisms following spinal cord injury (SCI) is one of the first opportunities to minimize its highly detrimental outcomes. Herein, we investigate the ability of surface engineered carboxymethylchitosan/polyamidoamine (CMCht/PAMAM) dendrimer nanoparticles to intracellularly deliver methylprednisolone (MP) to glial cells, allowing a controlled and sustained release of this corticosteroid in the injury site. The negatively-charged MP-loaded CMCht/PAMAM dendrimer nanoparticles comprising sizes of 109 nm enable a MP sustained release, which was detected for a period of 14 days by HPLC. *In vitro* studies in glial primary cultures show that incubation with 200 μg.mL^{-1} nanoparticles do not affect the cells' viability or proliferation, while allowing the entire population to internalize the nanoparticles. At higher concentrations microglial cells' viability was proved to be affected in response to the MP amounts released. Following lateral hemisection lesions in rats, we observed the nanoparticles uptake by the spinal tissue 3 hours upon administration. Moreover, significant differences in the locomotor output between the controls and the MP-loaded nanoparticles treated animals one month after the lesion were observed. Therefore, the MP-loaded CMCht/PAMAM dendrimer nanoparticles may prove to be useful in the reduction of the secondary injury following SCI.

1. Introduction

Trauma to the central nervous system (CNS) is still a major cause of disability worldwide. In the US alone 10,000 new spinal cord injury (SCI) cases are reported every year, bearing tremendous costs along with greater expenses of human suffering.[1] Given the complexity of the triggered events following SCI and the still poor understanding of the mechanisms underlying it, so far there are no fully restorative therapies for this condition.[2] As a consequence of the injury severe impairments can occur and loss of function, particularly associated to the motor and sensory levels, commonly lead to tetraplegia or paraplegia.[3] Therefore, the harsh economical and physical burdens of SCI emphasize the need to develop new therapeutic approaches aimed at improving these patients' quality of life.

The devastating consequences following SCI are the outcome of a two-step process that initiates with a mechanical insult to the spinal cord. The primary injury results in immediate cell death and vascular leakage, as well as disruption of ascending and descending pathways.[4a] These events lead to a subsequent cascade of secondary mechanisms that widen the magnitude of the initial lesion.[4] A complex response follows, extending from massive neuroinflammation reactions to the formation of a glial scar that inhibits axonal regeneration. The secondary phase is also characterized by the occurrence of different phenomena,[5] such as: (i) excitotoxic biochemical events, e.g., formation of free radicals and nitric oxide, glutamate and protease release; (ii) cellular responses, such as invasion by immune cells, neuronal and glial cell death and demyelination; and (iii) vascular changes, involving edema, ischemia and hypoxia. The extension of this secondary injury has significant implications in the lesion volume itself, as well as in the tissue potential for functional recovery. Therefore, one of the first opportunities to intervene after a SCI in an effort to minimize its detrimental outcomes is precisely the control of the negative impact of the secondary injury.

To the present, high dose methylprednisolone (MP) administration is still the only recommended neuroprotective route to prevent further secondary injury damage, which has been already tested in multicenter clinical trials.[6] MP is a synthetic corticosteroid with anti-inflammatory and antioxidant actions that when administered in a high dose systemic injection during the first hours post-injury has shown to reduce neurological deficits after SCI.[7] Although not completely unveiled yet, MP action mechanisms involve the modulation of inflammation at the injury site. This is achieved by astrocyte reactivity inhibition, down-regulation of inflammatory cytokine

150

production by microglia and also by an antagonistic effect on lipid peroxidation.[8] In addition to being a potent anti-inflammatory drug, recent studies suggest that methylprednisolone promotes its neuroprotective effects also via a selective anti-apoptotic mechanism on oligodendrocytes, which are essentially implicated in white matter injuries such as SCI.[9] Nevertheless, the necessary systemic high dose injections of MP also seriously aggravate adverse side effects such as wound infections, pneumonia and acute corticosteroid myopathy.[10] These undesired effects critically limit the drug's neuroprotective potential often inducing only modest overall improvements in the neurological functions.[11] As a result, its clinical use remains quite controversial.

A directed and sustained delivery of MP by means of using a controlled drug delivery system, as a nanoparticle-based system, could be extremely advantageous in these situations. With such a strategy the drug's action could be maximized in the affected nervous cells, enhancing its efficiency as an anti-inflammatory and neuroprotective agent, while eliminating its systemic negative side effects. The use of different nanoparticle formulations [e.g., cerium oxide,[12] monomethoxy PEG–poly(D,L-lactic acid),[13] PEG-silica,[14] poly(lactic-co-glycolic acid)[15]] has been recently investigated for SCI treatment. These nanoparticles were proposed to act in SCI neuroprotection either by sealing the damaged axonal membranes,[13,14] by an intrinsic antioxidant mechanism[12] and also as a MP drug delivery system[15] revealing some promising and satisfactory results. Within the present study we are proposing the use of a recently described dendrimer-based intracellular drug delivery system to act in the control of the secondary injury damage.[16] For SCI applications, this nanoparticle system will be loaded with MP and intracellularly delivered to glial cells, particularly microglia, which are in part responsible for the secondary events after SCI. From the vast range of nanocarriers, dendrimers are nature-inspired highly ramified and spherical synthetic nanoparticles that not only present precise and controlled architectures, but also possess tunable molecular weights and superior drug loading capacities.[17] Also, they have the potential to be further engineered to achieve higher functionalization degrees, such as targeting and imaging properties.[18] The water-soluble dendrimer nanoparticles developed by our group consist of a highly branched nanospherical poly(amidoamine) (PAMAM) dendrimeric core grafted with carboxymethylchitosan (CMCht), a natural biocompatible polymer.[16] This engineered macromolecular carrier has already shown to efficiently transport biological agents intracellularly to rat bone marrow stromal cells via the endocytic pathway.[16,19] Moreover, they were shown to be easily internalized by neurons and glial cells, while not evidencing any cytotoxicity, both *in vitro*

and *in vivo*.[20] Thus, in the present study we aim to produce MP-loaded CMCht/PAMAM dendrimer nanoparticles that have the potential to modulate the inflammatory reaction after CNS traumatic injury, namely by attenuating the microglial cell response. The corticosteroid is effectively incorporated in the nanoparticles and these are easily internalized by glial cells. We demonstrate that these nanoparticles are able to intracellularly release MP having an impact on microglial cell viability. Also, when administered locally following lateral hemisection lesions to the spinal cord of Wistar rats the MP-loaded nanoparticles significantly improved the locomotor outcome of the treated animals. These initial results lead us to consider this system as a potential promising therapy for SCI.

2. Materials and methods

2.1. CMCht/PAMAM dendrimer nanoparticle synthesis

Carboxymethylchitosan/ poly(amidoamine) (CMCht/PAMAM) dendrimer nanoparticles were produced in a stepwise manner, as previously described by Oliveira *et al*.[16] Starburst® PAMAM-carboxylic acid terminated dendrimers (PAMAM-CT) (generation 1.5, 20% w/v in methanolic solution) with an ethylenediamine core were purchased (Sigma, Germany) and the following reactions were carried out: (i) an increase in the PAMAM-CT generation; (ii) the production of a PAMAM-methyl esther terminated dendrimer; (iii) a condensation reaction between the methyl esther and amine groups of PAMAM and CMCht; and finally (iv) the conversion of the non-reacting methyl esther groups into carboxylic ones in the CMCht/PAMAM dendrimer nanoparticles. Afterwards, MP was incorporated in these molecules (Figure 2c) mixing an aqueous solution of CMCht/PAMAM dendrimer nanoparticles with an ethanolic MP solution with a final concentration of 5×10^{4} M (w/w) and kept under vigorous agitation. Saturated sodium carbonate solution (Na_2CO_3, Aldrich, Germany) and acetone (Pronalab, Portugal) were then added to the mixture. The resulting precipitates were collected by filtration and then dispersed in ultrapure water. Extensive dialysis (cellulose tubing, benzoylated for separating compounds with a molecular weight of $\leq1,200$, Sigma, Germany) was performed during 48 hours. Both CMCht/PAMAM dendrimer nanoparticles and MP-loaded CMCht/PAMAM dendrimer nanoparticles were obtained by freeze-drying (Telstar-Cryodos-80, Spain) for approximately one week, until the solvents were completely removed. Additionally, fluorescein isothyocianate (FITC,

Sigma, Germany) labeled MP-loaded CMCht/PAMAM dendrimer nanoparticles were prepared by covalently bonding the amine group of CMCht and the isothyocianate group from FITC.[16]

2.2. Nanoparticle characterization

Both the zeta potential and diameter of the CMCht/PAMAM dendrimer nanoparticles and the MP-loaded CMCht/PAMAM dendrimer nanoparticles were determined in a particle size analyzer (Zetasizer Nano ZS, Malvern, UK). At first, 1×10^{-3} mg.mL^{-1} solutions of each sample were prepared in ultrapure water for determination of the nanoparticles diameter. Each sample was filtered and placed in polystyrene cuvettes (Malvern, UK) to be analysed. For the zeta potential determinations, samples were prepared in three different buffer solutions: (i) citrate buffer (pH 5.0); (ii) phosphate buffer saline (PBS, pH 7.4); and (iii) sodium carbonate buffer (NaOH, pH 10.0). Each sample was filtered and slowly loaded to folded capillary cells for the zeta potential measurements. The efficiency of the MP incorporation into the CMCht/PAMAM dendrimer nanoparticles was assessed by Fourier transformed infrared (FTIR) spectrometry. To obtain the FTIR spectra of the samples, transparent potassium bromide (KBr, Pike Technologies, USA) pellets were prepared, containing the samples and after that, the analyses were run in an infra-red spectroscope (IR Prestige-21, Shimadzu, Japan). Also ^{1}H NMR spectroscopy was performed to assess the effectiveness of the FITC conjugation. For that purpose the samples were dispersed in deuterium oxide (D$_2$O, Aldrich, Germany) at a final concentration of 10 mg.mL^{-1}. The one-dimensional ^{1}H spectra were acquired in a Varian Unity Plus spectrometer at 300 MHz and 20°C.

2.3. *In vitro* methylprednisolone release studies

The amount of MP released from the CMCht/PAMAM dendrimer nanoparticles was quantified using the high performance liquid cromatography equipment (HPLC, Knauer Smartline, Germany) with an UV detector set at 250 nm. The mobile phase was composed of acetonitrile: ammonium phosphate buffer (0.1 M, pH 4.6) (50:50, v/v) at a flow rate of 1 mL.min^{-1}. Two distinct solutions were prepared: (i) 1 mg.mL^{-1} MP-loaded CMCht/PAMAM dendrimer nanoparticles in PBS solution (pH 7.4); and (ii) 1 mg.mL^{-1} MP-loaded CMCht/PAMAM dendrimer nanoparticles in citrate buffer solution (pH 5.0). These two solutions were prepared both in the absence and presence of 15% fetal bovine serum (FBS, Gibco, USA). Also 0.01% sodium azide

(Merck, Germany) was added to each solution. The *in vitro* release profiles were determined at 37°C and 60 rpm for times ranging from 1 hour up to 14 days. At each time point, samples were collected for analysis and the same volume replaced with the respective buffer solution. After collection at each time-point and preceding the analysis, the samples were centrifuged at 2000 rpm for 10 minutes and integrated in a solution of sample:acetonitrile:phosphate buffer (50:25:25, v/v) for further detection through a C_{18} analytical column (Atlantis T3, Waters, USA). The MP retention time was approximately 3 minutes. A calibration curve was previously acquired by diluting a MP stock solution to the final concentrations of 0.5, 2.5, 10, 25 and 100 $\mu g.mL^{-1}$ standards and the results were expressed as an average ± standard deviation, n=3.

2.4. Isolation and culturing of rat cortical glial and microglial cells

Neonatal rat cortices were isolated from P4 Wistar rat pups as previously described elsewhere.[34] Glial cells primary cultures were maintained at 37°C in a 5% CO_2 atmosphere, in Dulbecco's modified Eagle medium (DMEM, Gibco, USA) supplemented with 10% FCS and 1% antibiotic/antimycotic (Sigma, USA) for a week for further testing. Microglia cultures were obtained from these mixed glial cell cultures. For microglia isolation, glial cells were plated out at a density of 1×10^6 cells.cm^{-2} in polystyrene T_{75} flasks (Thermo Scientific, USA) previously coated with poly-L-lysine (Sigma, USA). The glial primary cultures were maintained in the same above referred conditions, with periodical media renewal. After two weeks of culturing, the cell flasks were agitated in an orbital shaker at 240 rpm during 4 hours. Following this, the medium containing detached microglia cells was collected and centrifuged at 1200 rpm for 5 minutes. The pellet was re-suspended and plated out at a density of 4×10^4 cells.cm^{-2} on coverslips previously coated with poly-L-lysine (Sigma, USA). Microglia cells primary cultures were then maintained at 37°C in a 5% CO_2 atmosphere, in DMEM medium (Gibco, USA) supplemented with 10% FBS (Gibco, USA) and 1% antibiotic/antimycotic (Sigma, USA) for 3 days for further testing.

2.5. *In vitro* cytotoxicity and proliferation assays

The viability and proliferation of the glial cells were tested and compared: (i) after a single addition of 200 μg of MP-loaded CMCht/PAMAM dendrimer nanoparticles to the wells in the first day of the experiment; or (ii) with periodical addition of 200 μg of MP-loaded CMCht/PAMAM

dendrimer nanoparticles, every 48 hours during a week. In both cases, the cell viability was verified after incubation of the cells at 37°C for 3 hours with (3-(4,5-dimethylthiazol-2-yl)-5-(3-carboxymethoxyphenyl)-2(4-sulfophenyl)-2H tetrazolium) (MTS, Promega, USA) in a 5:1 ratio. After the incubation, the optical density of each sample was read in a multiplate reader (Tecan Sunrise, Switzerland) at 490 nm. Also high dosages of CMCht/PAMAM and MP-loaded CMCht/PAMAM dendrimer nanoparticles were evaluated regarding in microglia cultures viability: 1000 and 1500 μg, as well as the corresponding MP amount released from the MP-loaded CMCht/PAMAM dendrimer nanoparticles (1.5 and 2.25 mg). The cell proliferation was ascertained in glial cell cultures using the 5-bromo-2'-deoxyuridine assay (BrdU, Roche, USA), which quantifies the BrdU incorporation during DNA synthesis in replicating cells. BrdU was added to the glial cell cultures for 24 hours and after that the medium was removed. The cells' DNA was denatured with FixDenat (Roche, USA), after which the anti-BrdU peroxidase antibody (Roche, USA) was added. The immune complexes were detected by the quantification of the substrate reaction product, measuring the optical density at 405 nm (reference filter set at 655 nm) in a multiplate reader (BioRad, USA).

2.6. Internalization study – immunocytochemistry

The glial cultures were incubated with 200 μg of FITC-labeled MP-loaded CMCht/PAMAM dendrimer nanoparticles for periods of 1, 3, 12, 18 and 24 hours (n=3/ time point). Subsequent to each incubation time, the cells were washed in 0.1 M PBS and fixed in a 4% paraformaldehyde solution for 30 minutes.[20a] The following primary antibodies were used: rabbit GFAP antibody (Dako, Denmark, 1:500, v/v) for astrocyte recognition; mouse CD11b antibody (BD Biosciences Pharmingen, USA, 1:100, v/v) was used in microglial cell identification; and mouse O4 antibody (R&D Systems, 1:50, v/v) for oligodendrocyte detection. Then, cells were incubated with the secondary antibodies: Alexa Fluor 594 anti-mouse and Alexa Fluor 568 anti-rabbit (both Molecular Probes, USA, 1:2000 in 10% FCS in PBS, v/v). Nuclei were stained with 4',6-diamidine-2-phenyl indole (DAPI, Thermo Scientific, USA, 1:2000, v/v). The FITC-labeled MP-loaded CMCht/PAMAM dendrimer nanoparticles internalization levels for each cell population were determined according to Equation (1) (n=3, 3 random fields/coverslip):

Equation (1): $I = \dfrac{Pc}{Tc} \times 100$

I: percentage of internalization;

Pc: number of positive cells for FITC-labeled MP-loaded CMCht/PAMAM dendrimer nanoparticles;

Tc: total number of each cell type.

Microglial cells in microglial cultures were also immunostained following a similar procedure to the described for glial cells. Mouse CD11b antibody (BD Biosciences Pharmingen, USA, 1:100, v/v) was incubated for an hour, followed by secondary antibody AlexaFluor 594 anti-mouse (Molecular Probes, USA, 1:2000 in 10% FCS in PBS, v/v) incubation. Nuclei were then stained with DAPI (Thermo Scientific, USA, 1:2000, v/v).

2.7. Hemisection SCI

8 weeks old male Wistar rats (n=15) from Charles River were housed in light and temperature controlled rooms and all the procedures involving the animals were in accordance with the Animal Care Guidelines.[35] Before the surgery, the animals were anesthetized by intraperitoneal injection of 150 mg.Kg-1 ketamine hydrochloride and 0.3 mg.Kg-1 medetomidine. The surgical area was shaved and soaked with ethanol and chlorohexidin. A laminectomy at T8-T9 level was performed to expose the spinal cord. After that, a unilateral defect was made on the cord by removing approximately 2 mm of the tissue. Immediately after the lesion, 5 µL of either: (i) saline (control group); (ii) CMCht/PAMAM dendrimer nanoparticles (NP group); (iii) MP-loaded CMCht/PAMAM dendrimer nanoparticles (NPmp group); and (iv) methylprednisolone, were injected circa 1 mm rostral and 1 mm caudal to the lesion. Both the methylprednisolone and the nanoparticles were prepared in 5 mg. mL-1 solutions. To stabilize the vertebral column in the lesion area, a semi tubular starch/poly-caprolactone (SPCL) scaffold was implanted in alignment with the vertebrae in all the animals.[36] The muscles and skin were sutured and disinfection was carried out with chlorohexidin. Following surgery rats were kept under heat lamps and received vitamins (Duphalyte, Farmoquil, Portugal), analgesic (Butorphanol tartrate, 1mg.mL-1, Fort Dodge, Spain) and antibiotic (Enrofloxacine, 1mg.mL-1, Bayer, Germany). Throughout the experimental period, animals were examined for symptoms of illness or potential reaction to the treatment. Animals were maintained for 4 weeks however an extra NP group (n=3) was sacrificed three hours after the lesion to assess the presence of the fluorescently labeled MP-loaded CMCht/PAMAM dendrimer nanoparticles in the tissue after the injection in the cord. The spinal

cords were collected, freeze-sectioned and stained with rabbit GFAP antibody (Dako, Denmark) and the secondary antibody Alexa Fluor 568 anti-rabbit (Molecular Probes, USA).

2.8. BBB locomotor assessment

Rats were allowed to move freely in the open-field arena and scored during a 4 min period for their ability to use their hindlimbs by two independent blinded observers. Joint movements, paw placement, weight support, and fore/hindlimb coordination were judged according to the 21-point BBB locomotion scale. A BBB score of 0 indicates no hindlimb movement. A BBB score of 1 through 8 indicates joint movement, but no weight support. A BBB score of 9 through 20 indicates an ability to support weight and use the limb for locomotion but with some degree of abnormality. A BBB score of 21 corresponds to the locomotion of a normal rat. Scores obtained by 2 independent observers were averaged for the left hindlimb.

2.9. Statistical analysis

Statistical evaluation was performed using the one-way analysis of variance test followed by the Tukey´s post-test to assess the statistical differences between groups in the viability and proliferation assays. For the BBB scores, significant differences between the groups were determined using two-way ANOVA repeated measures followed by the Bonferroni´s post-test. Statistical significance was defined for $p < 0.05$.

3. Results and Discussion

3.1. Characterization of the MP-loaded nanoparticles

The use of nano-sized carriers for the local delivery of therapeutic agents is an exciting and promising approach in CNS traumatic conditions, for which there are no therapeutic solutions yet. MP is the corticosteroid clinically administered in SCI cases but it presents low efficacy and occasionally devastating undesired side effects in patients. In an attempt to overcome these major impediments for the success of pharmacological therapies in SCI, we herein propose a nanoparticle-based system that incorporates MP to be intracellularly delivered to glial cells. The

design of such nano-vehicles for drug release purposes *in vivo*, demands assessing first of all its physicochemical properties and biological performance *in vitro*.

Following MP loading into the CMCht/PAMAM dendrimer nanoparticles we evaluated its new features, such as: size, zeta potential, morphology and drug loading efficiency. Figures 1a,b refer to the electron micrographs of the MP-loaded CMCht/PAMAM dendrimer nanoparticles, when freeze-dried or dispersed in solution. It is possible to discern its spherical morphology when dispersed in solution and an elongated nature after the solvents evaporation.

Sample	Diameter (nm)	Zeta potential (mV)		
		pH 5.0	pH 7.4	pH 10.0
PAMAM (G1.5)	2 ± 1	2.6 ± 1.0	-23.7 ± 7.0	-2.7 ± 0.8
CMCht/PAMAM	85 ± 38	2.2 ± 1.2	-14.7 ± 3.0	-13.4 ± 4.1
MP-loaded CMCht/PAMAM	109 ± 46	2.5 ± 2.2	-26.4 ± 1.7	-16.6 ± 6.4
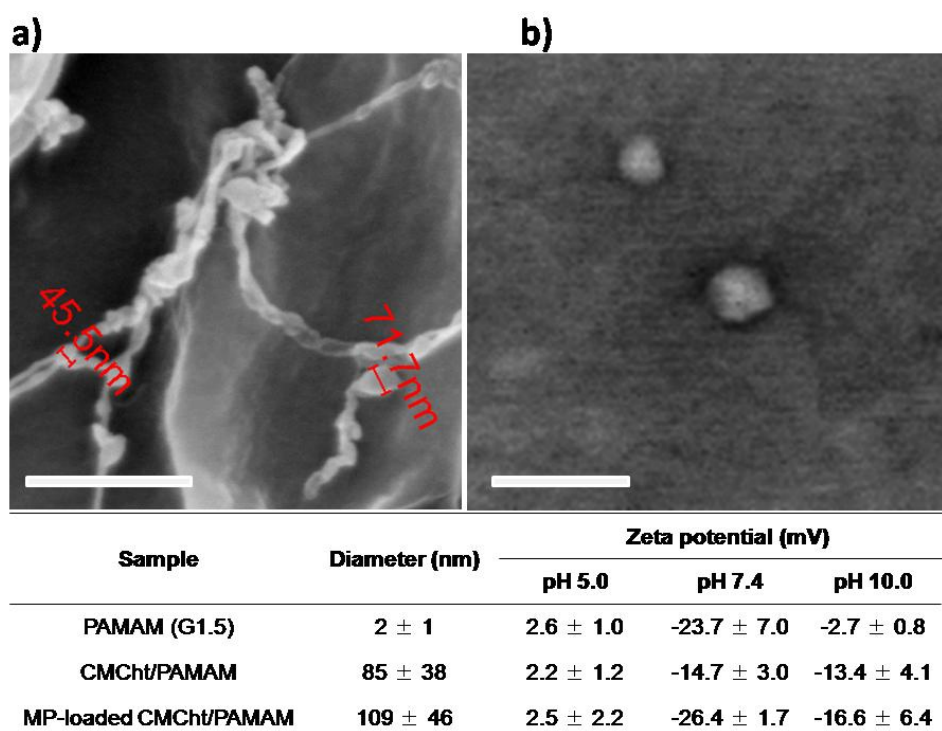
Figure 1. Electron micrographs of MP-loaded CMCht/PAMAM dendrimer nanoparticles. **a)** SEM image of the elongated freeze-dried MP-loaded CMCht/PAMAM dendrimer nanoparticles. **b)** S-TEM image of the spherical MP-loaded CMCht/PAMAM dendrimer nanoparticles dispersed in water. Scale bars represent 500 nm. Distributions of the diameter and zeta potential determined by DLS analysis are shown (n=6; mean ± SD).

Moreover, the average diameter determined by STEM observation was 125 ± 30 nm, which is in accordance with the Zetasizer determinations. The latter indicated that MP-loaded CMCht/PAMAM dendrimer nanoparticles dispersed in ultrapure water comprise average sizes of 109 nm, while the non-loaded samples disclose average sizes of 85 nm. Thus, the incorporation of MP into the CMCht/PAMAM dendrimer nanoparticles resulted in an average diameter increase of around 28%. Also, some aggregates were detected with average diameters of 334 nm and

2088 nm due to the interaction of the PAMAM amine groups with the CMCht carboxyl groups that favors electrostatic interactions. Since these results were obtained in water dispersion, we expect that this aggregation decreases in culture media and biological fluids dispersion due to the presence of proteins that dynamically interact with the nanoparticle corona, decreasing its reactivity.[21] Additionally, the zeta potential determination of these nanoparticles indicated that this parameter is strongly affected by pH, being that at physiological pH both CMCht/PAMAM dendrimer nanoparticles and MP-loaded CMCht/PAMAM dendrimer nanoparticles have stable negative net charges of -14.7 mV and -26.4 mV, respectively. The MP incorporation renders an increased stability to the CMCht/PAMAM dendrimer nanoparticles due to the new charge balance after the corticosteroid loading. As previously reported, CMCht possesses protonated amino groups in acidic conditions and negative carboxylic ions at physiological pH.[16] This fact is reflected in the nanoparticles' positive net charge measured at pH 5.0, while both at physiological pH and at pH 10.0 it remains negative. The effective MP incorporation into the nanoparticles was confirmed by the comparative analysis of the characteristic absorption band spectra in the infrared (IR) region of CMCht/PAMAM and MP-loaded CMCht/PAMAM dendrimer nanoparticles, as well as MP. From the IR spectra shown in Figure 2a it is possible to observe that MP-loaded CMCht/PAMAM dendrimer nanoparticles disclose an altered IR spectrum in relation to the CMCht/PAMAM dendrimer nanoparticles spectrum due to the MP characteristic peaks' appearance. Therefore, it was possible to detect characteristic absorption bands referable to both CMCht/PAMAM dendrimer nanoparticles, such as the 3580 cm^{-1} free OH group and the 2887 cm^{-1} CH stretching vibration associated bands, and MP by the 3420 cm^{-1} associated OH group and 2922 cm^{-1} CH_2 asymmetric stretching band. This result indicates the successful incorporation of the corticosteroid in the nanoparticle system.

Additionally, and in order to track the internalization of MP-loaded CMCht/PAMAM dendrimer nanoparticles *in vitro*, a green fluorescent probe (FITC) was conjugated to the nanocarriers. To investigate the effectiveness of the conjugation, ^{1}H NMR analysis of MP-loaded CMCht/PAMAM dendrimer nanoparticles and the FITC-labeled MP-loaded CMCht/PAMAM dendrimer nanoparticles was performed. From Figure 2b, it is possible to observe that the FITC-labeled MP-loaded CMCht/PAMAM dendrimer nanoparticles spectrum has new proton signals located at 6.68 ppm that are attributed to the aromatic ring of the FITC molecule. Therefore, the formation of this new signal is evident and strongly suggests that the conjugation of FITC actually occurred, by the formation of a new thiourea bond between the amine groups of CMCht/PAMAM and the

isothyocianate group of FITC. There were no other significant changes in the spectral profile of MP-loaded CMCht/PAMAM dendrimer nanoparticles.
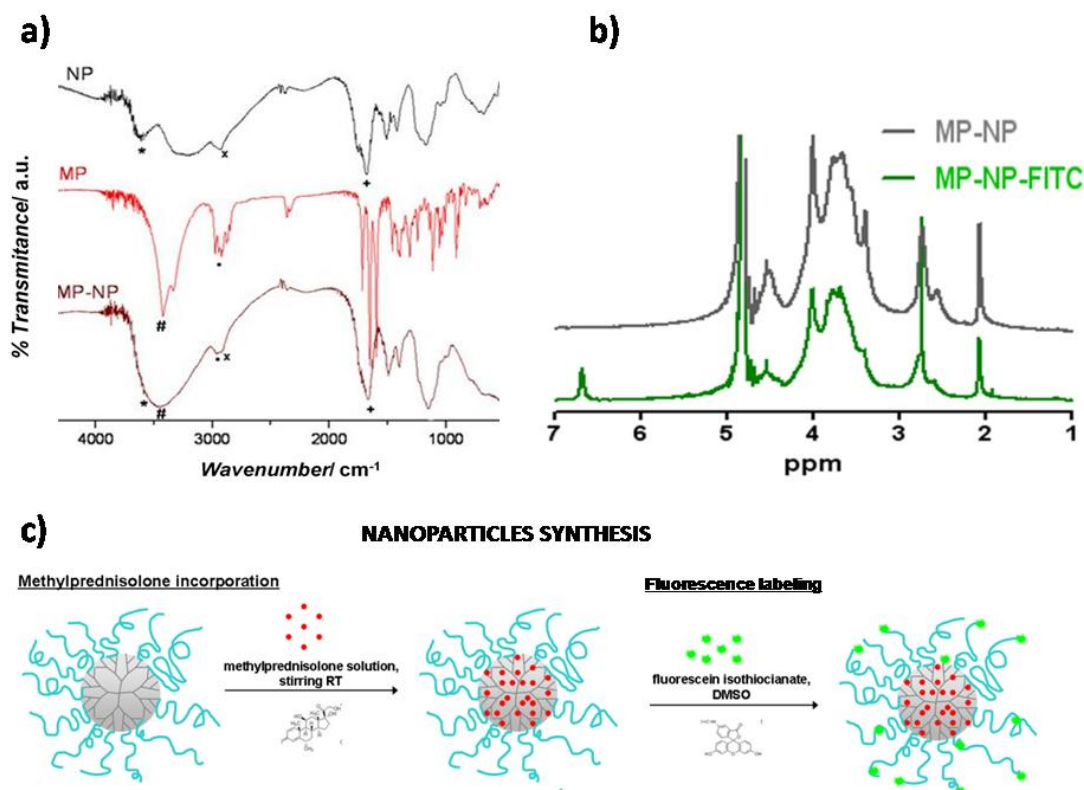
Figure 2. a) FTIR spectra of CMCht/PAMAM dendrimer nanoparticles (NP), methylprednisolone (MP) and MP-loaded CMCht/PAMAM dendrimer nanoparticles (MP-NP) evidencing the successful incorporation of MP in the nanoparticles. (*) 3580 cm-1 corresponds to OH group free, (#) 3420 cm-1 is attributed to OH group associated, (•) 2922 cm-1 corresponds to CH2 asymmetric stretching band, (#) 2887 cm-1 is attributed to CH stretching symmetric band, and (+) 1655-1630 cm-1 corresponds to amide I. **b)** 1H NMR spectra of MP-loaded CMCht/PAMAM dendrimer nanoparticles (MP-NP) and FITC-labeled MP-loaded CMCht/PAMAM dendrimer nanoparticles (MP-NP-FITC) demonstrating the successful conjugation of the fluorescent molecule. **c)** Schematic representation of the methylprednisolone loading into the CMCht/PAMAM dendrimer nanoparticles and the fluorescent labeling of these molecules.

The release of MP from the MP-loaded CMCht/PAMAM dendrimer nanoparticles was investigated after incubating the nanoparticles at 37°C under agitation. Two different buffer solutions were used at pH 5.0 and 7.4, each of which simulating the endocytic and cytoplasmic compartments which are acidic and physiological, respectively. On the other hand, the effect of proteins was also considered by adding 15% FBS to each solution in order to evaluate the contribution of these proteins in the MP release. At pre-determined times, samples from each condition were

collected, centrifuged and the supernatant analyzed by high performance liquid chromatography (HPLC). In all the four solutions tested the corticosteroid was released in a sustained manner, as displayed in Figure 3a. Moreover, the MP release followed a biphasic pattern characterized by an initial burst release in the first 24 hours followed by a slower sustained release phase that was observed during 14 days. In addition, the detected amount of MP as a free drug was shown to be affected both by the pH and the presence of serum in the buffer solution. In PBS buffer (pH 7.4) about 100 μg of the drug were released during the first 24 hours. In the presence of FBS there is a slight increase (125 μg), although not statistically significant. A slower sustained release is then observed in the following 6 days in a similar way both in the absence or presence of serum proteins. However, at day 14 in the presence of FBS a statistically significant higher MP quantity was detected. This data suggests that the presence of serum proteins can contribute to the release of higher amounts of drug from the nanoparticles. This is most likely related with possible nanoparticle degradation along time, the prevention of aggregation via protein adsorption to the nanoparticles corona or even due to the protein-drug interactions that facilitate the drug's release.[16,22a] Comparatively, the MP release rate from the nanoparticles was significantly inferior when dispersed in citrate buffer (pH 5.0) being only 30 μg of the corticosteroid released in the initial burst phase. As already reported, the relatively hydrophobic core of the PAMAM dendrimer molecules and the stronger interactions of drug molecules with the more protonated dendrimer tertiary amine groups at pH 5.0 can result in a minor release of the incorporated drug due to these stronger interactions.[23] Likewise, these protonated tertiary amines may produce more tightened intramolecular branched structures, restricting the MP release.[24] Nanoparticle aggregation is also more likely to occur under these circumstances, owing to the charge instability and it can prevent and diminish the MP release from the drug delivery system.[16] Interestingly, this acidic pH effect is completely eliminated in the presence of serum proteins with a significant and drastic increase in the MP release. Once again the interaction of the nanoparticles with proteins, namely by protein adsorption to its surface, was shown to affect the dendrimers' conformation and consequently its behaviour and responses.[22] The pH conformation alteration of the nanoparticles and protein interaction events can be used as a possible trigger for encapsulation and release of guest molecules given its effects in these nanoparticles behaviour. The different conformations that PAMAM dendrimers present according to the pH and independently of the molecule size were recently described.[24] Indeed, these pH-induced conformational changes occur revealing a "dense core" conformation of the dendrimer at high

pH while at low pH it emerges as a "dense shell" molecule, occurring an intermediate conformation when the pH remains neutral. Particularly in MP-loaded CMCht/PAMAM dendrimer nanoparticles, both the pH variation and the protein interaction affect the nanoparticles' conformation and consequently its drug release, being the higher amounts of MP detected in acidic pH in conjunction with serum proteins. This can possibly be translated in a triggering event being initiated inside the endocytic compartment during the nanoparticles internalization by cells. Therefore, this dendrimer nanoparticles system may display an inherent pH-responsive triggering mechanism for the drug release. However, one thing that will be investigated in the future is the extent of endosomal and lysosomal accumulation, since long exposure to highly acidic environments and hydrolytic enzymes can eventually become harmful to the drug, altering and degrading it.[25]
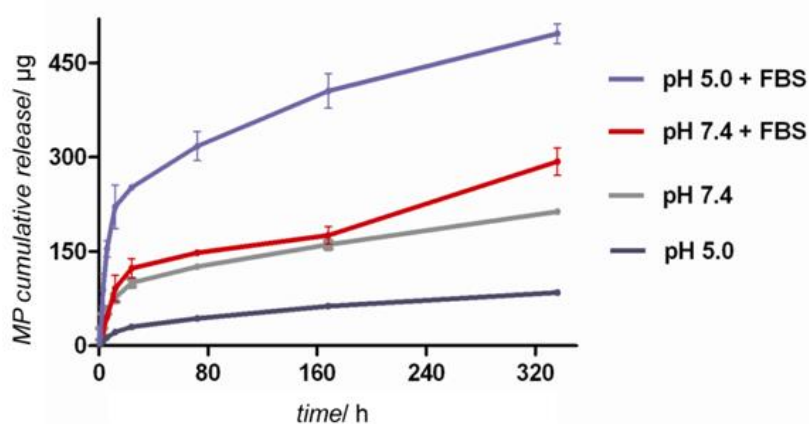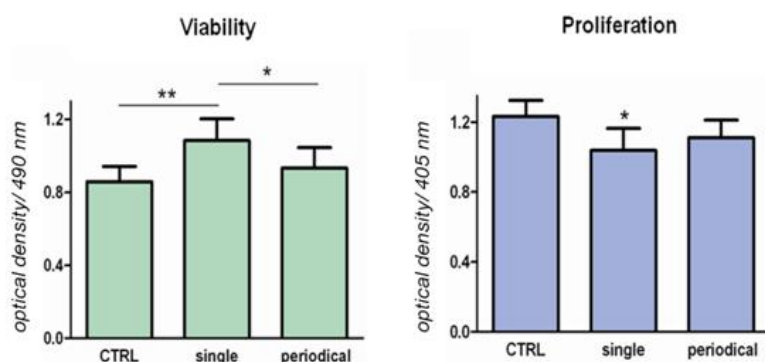
Figure 3. a) Methylprednisolone release from CMCht/PAMAM dendrimer nanoparticles, determined by HPLC. MP was detected for the period ranging from 1 hour up to 14 days. Solutions of 1 mg.ml-1 were prepared in PBS buffer solution (pH 7.4) or citrate buffer solution (pH 5.0), in the presence or absence of 15% FBS (n=3; mean ± s.d.). **b)** Percentage of cell viability and proliferation of cortical glial cell cultures after MP-loaded CMCht/PAMAM dendrimer nanoparticles' addition, using the MTS and BrdU assays, respectively. Single addition of 200 μg.ml-1 MP-loaded nanoparticles (single) and periodical addition every 48 hours (periodical) were performed (n=6, mean ± SD; * p<0.05, ** p<0.01)

3.2. Internalization of MP-loaded CMCht/PAMAM nanoparticles by glial cells

As initially stated, the MP-loaded CMCht/PAMAM dendrimer nanoparticles are proposed to be used in the modulation of inflammatory events lead by glial cells, acting as a MP release system and therefore protecting the nervous tissue from further damage. Glial cells play an important role in the secondary events that follow CNS traumatic injury, namely by the inflammatory actions of astrocytes and microglia. Previous studies have already demonstrated that void CMCht/PAMAM dendrimer nanoparticles are efficiently internalized by glial cells and neurons, while not affecting these cells' viability.[17,20a] To further investigate the influence of the MP-loaded nanoparticles in the metabolic activity of glial cells, primary cultures were exposed to 200 μg.mL^{-1} MP-loaded CMCht/PAMAM dendrimer nanoparticles for 7 days: (i) after one single addition on day 1; and (ii) following periodical additions every 48 hours. As evidenced in Figure 3b, MP-loaded CMCht/PAMAM dendrimer nanoparticles do not negatively affect the cells' viability, for a period of 7 days. In both cases large amounts of a brown formazan product were formed during the MTS viability assay indicating normal cell metabolic activity. Additionally, the observed increase in metabolic activity after the nanoparticles addition, namely in the single addition group when compared to the control group, can be interpreted as the result of an activation of microglial cells that leads to a subsequent metabolic activity increase. In line with these results, we are able to report that the MP-loaded CMCht/PAMAM dendrimer nanoparticles are not cytotoxic over primary cultures of glial cells in the concentration range tested. Then, in order to explore the effect of the nanoparticles on proliferation, cells were subjected to the same exact before mentioned conditions. After nanoparticles incubation, bromodeoxyuridine (BrdU) was added and maintained in the last 24 hours of culturing. This nucleoside is incorporated during DNA synthesis and can be quantified providing a direct indication of cell proliferation. Our results revealed similar proliferation rates in the nanoparticles addition groups and in the control group not exposed to the nanoparticles. However, a statistically significant decrease in proliferation after a single addition of nanoparticles was observed. Nevertheless, this was not confirmed following periodical additions of the same MP-loaded CMCht/PAMAM dendrimer nanoparticles. Since an increase in the metabolic activity also occurred after a single nanoparticles addition, this can indicate that in this situation the cells are more committed to metabolic processes than in its proliferation. Yet, the MP-loaded CMCht/PAMAM dendrimer nanoparticles do not significantly

interfere in the regular glial cells' proliferation and metabolic activity at a concentration of 200 µg.mL^{-1}.

After this initial screening of the nanoparticles possible cytotoxic effects and interference in the cell proliferation, we decided to evaluate the dynamics of the nanoparticles uptake by each glial cell type. The cells were cultured with the FITC-labeled MP-loaded CMCht/PAMAM dendrimer nanoparticles and their uptake was assessed both by fluorescence and confocal microscopy observation following immunocytochemistry. Each cell type in the glial mixed population was stained with the appropriate primary antibody: GFAP for astrocytes; O4 for oligodendrocytes; and CD11b for microglia. The number of cells for each subpopulation internalizing green FITC-labeled MP-loaded CMCht/PAMAM dendrimer nanoparticles were counted at different time-points for a maximum of 24 hours. All cell types revealed to be amenable to the nanoparticle internalization having all reached the maximum internalization during this time period. Moreover, as seen in Figure 4b the accumulation of the nanoparticles inside the cells did not affect the normal morphology of the astrocytes and oligodendrocytes, whereas in microglia an increase in volume and in cytoplasmic extensions was evident. The microglia subpopulation of cells also internalized the nanoparticles at a higher rate due to its well-known phagocytic nature.[26] Approximately 50% of the observed microglial cells accumulated FITC-labeled MP-loaded CMCht/PAMAM dendrimer nanoparticles in its intracellular compartment after 1 hour of culturing. The entire subpopulation of microglial cells had internalized nanoparticles 12 hours after its addition and these levels were maintained at 24 hours. On the other hand, oligodendrocytes showed a linear growing internalization rate along time, starting with about 20% of oligodendrocytes internalizing FITC-labeled MP-loaded CMCht/PAMAM dendrimer nanoparticles one hour after its addition and reaching 85% of nanoparticles internalization at 24 hours. Still, astrocytes take longer to recognize the nanoparticles and initiate the internalization process. This is showed by the fact that they evidenced lower percentage rates of nanoparticle-bearing cells both at one and three hours after incubation with figures around 15% (Figure 4a). However, 12 hours after FITC-labeled MP-loaded CMCht/PAMAM dendrimer nanoparticles exposure a 50% increase in nanoparticle internalizing cells was observed. Eventually, more than 90% internalization by astrocytes was achieved 24 hours after nanoparticles addition, as in the other cell types. The lower astrocytic nanoparticle internalization rates can be related to the low cell division rates and also lower endocytic activity in comparison to the other glial cell types.[27] In previous works, PAMAM dendrimer nanoparticles were pointed to be mainly internalized by the endocytic pathway and

possessing an inherent buffering capacity provided by its amine groups that allows endosomal escape.[25,28] CMCht/PAMAM dendrimer nanoparticles were already proved to be mainly internalized by the endocytosis.[16] The observable regular distribution of the MP-loaded nanoparticles over the cells' cytoplasm suggests that they already escaped the endosomal route of internalization being widespread in the cytoplasm. Despite some particular variations in the initial time-points it was clear that 24 hours after incubation with the nanoparticles all glial cells were internalizing the nanoparticles present in the media.
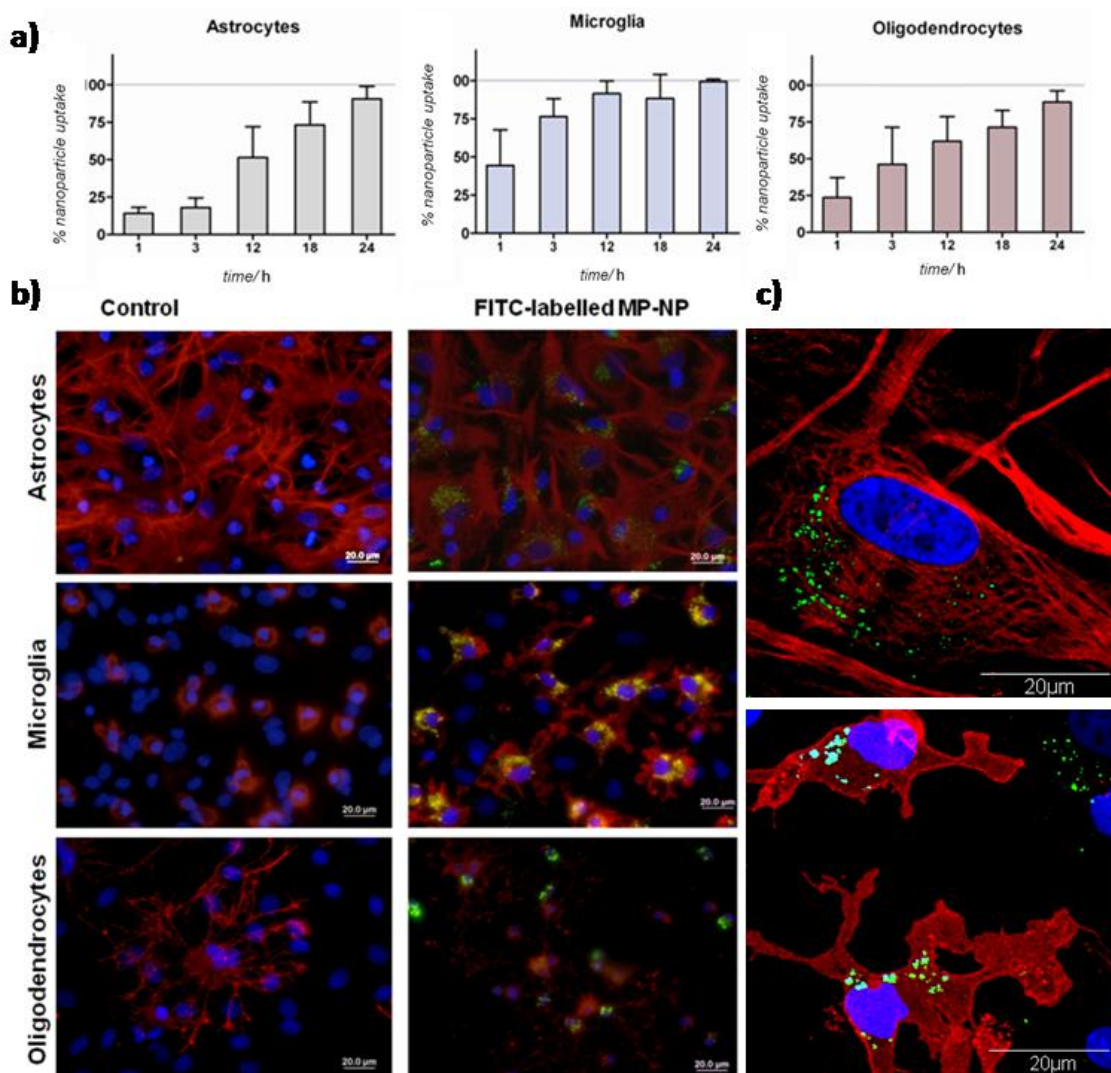
Figure 4. a) Percentage uptake rates of FITC-labeled MP-loaded CMCht/PAMAM dendrimer nanoparticles in each glial cell type (n=3; mean ± s.d.). **b)** Representative immunocytochemistry images of astrocytes, microglia and oligodendrocytes, after 1 week of culturing before (control) and after the nanoparticles addition (FITC-labeled MP-NP). Images obtained by fluorescence and confocal microscopy observation. **c)** Astrocytes and microglia confocal z-stack images demonstrating that intracellular localization of the accumulated nanoparticles.

3.3. Impact of the MP released from CMCht/PAMAM nanoparticles on microglial cell cultures

Following this, we strived to obtain a first *in vitro* insight of a possible therapeutic action of this new system. We decided to study the MP effects in the viability and metabolic activity of the microglia after being released into the cytoplasm from the MP-loaded CMCht/PAMAM dendrimer nanoparticles. To observe such an effect, we tested higher dosages of MP-loaded CMCht/PAMAM dendrimer nanoparticles in glial and microglial cultures knowing from previous works that MP can exert drastic effects in these populations above certain doses, namely affecting astrocytic and microglial viability.[8c,29] Subsequent to a range concentration test of different dosages of MP-loaded nanoparticles in glial cells (supplementary information), we decided to proceed with experiments considering MP-loaded CMCht/PAMAM dendrimer nanoparticles concentrations above 1000 μg.mL^{-1}. Above this concentration the cultures started to display variations in the viability assay results that were performed. To investigate the cause of this alteration we also treated the cultures with void CMCht/PAMAM nanoparticles, in order to see if the effect was due to the released corticosteroid action or the nanoparticles formulation itself. Additionally, we added a MP concentration similar to the one being released by the MP-loaded CMCht/PAMAM dendrimer nanoparticles estimating from the previously obtained MP release profile (supplementary information). Figure 5a reveals that in mixed glial cultures the addition of CMCht/PAMAM dendrimer nanoparticles to the culture medium had no effect in the cells' metabolic activity in the two high dosages tested. However, a significant decrease after MP and MP-loaded CMCht/PAMAM dendrimer nanoparticles exposure was observed. In view of the fact that a significant decrease on cell viability in relation to the control group occurred after MP and MP-loaded CMCht/PAMAM dendrimer nanoparticles addition, we can assume that MP is the main factor responsible for affecting the glial cells' viability. However, these glial cultures are mixed cultures and it is known that MP has differential effects in the different subpopulations of nervous cells.[8c,9b,29] As a result, the overall variations detected in the glial cells response are, in fact, a balance of the possible different responses of each cell type. It has been pointed out in the literature that the more drastic effects of MP in viability occur in microglial cells, via an apoptotic induction mechanism.[29] For that reason, the exact same previously referred conditions were evaluated in pure microglial cells' cultures. The addition of CMCht/PAMAM dendrimer nanoparticles both at 1000 μg.mL^{-1} and 1500 μg.mL^{-1} to microglia induced an augment in the

cells' metabolic activity rates. This increase is probably related to the activation of these phagocytic cells which in response to the presence of the nanoparticles change from a resting state to an activated state, becoming metabolically more active.[26b,30] On the contrary, addition of MP to microglia significantly affected its viability. In this case, a 30% decrease was verified in the higher concentration.
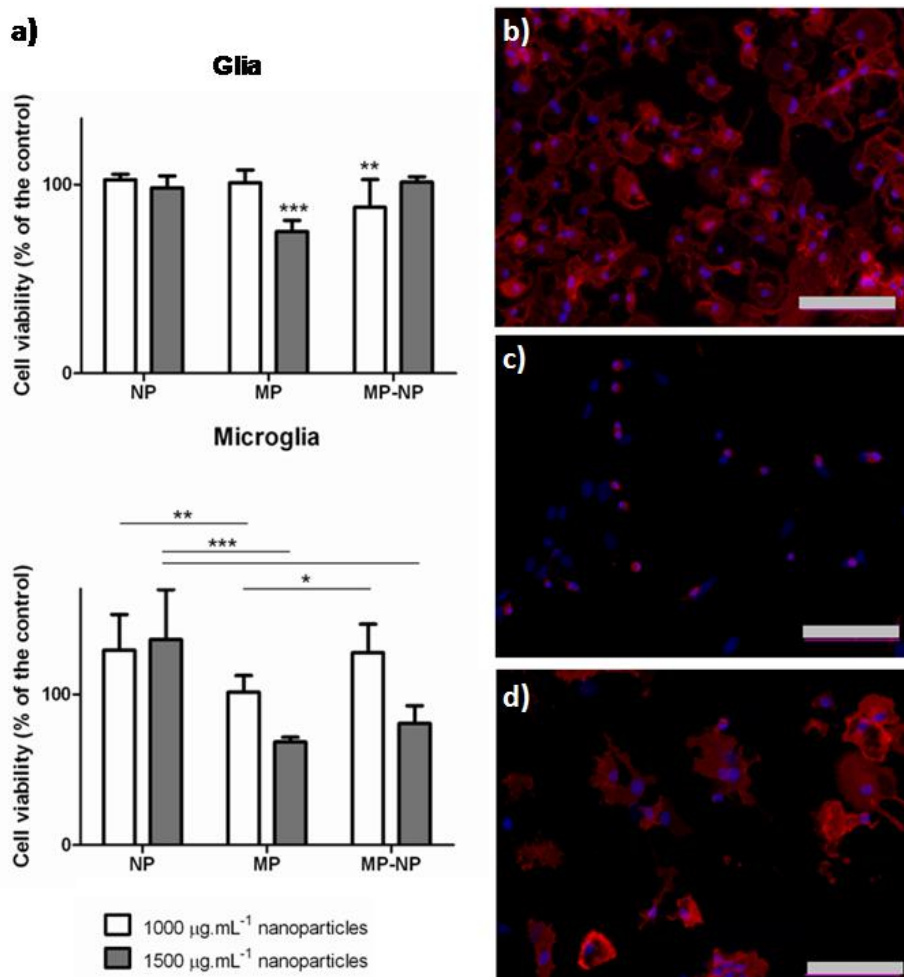
Figure 5. a) Percentage cell viability of glial and microglial cultures after 1000 and 1500 μg addition of CMCht/PAMAM (NP) and MP-loaded CMCht/PAMAM (MP-NP) dendrimer nanoparticles, and the corresponding acute MP addition (MP) (n=3, mean ± SD; * $p<0.05$, ** $p<0.01$, *** $p<0.001$). b-d) Representative immunocytochemistry images of microglia after exposure to 1500 μg addition of NP **(b)**, MP **(c)** and MP-NP **(d)** are shown. It is evident the negative effect of MP acute addition to microglial population (MP), which is attenuated by the sustained release from the nanoparticle system (MP-NP). Images were obtained by fluorescence microscopy. Scale bars represent 100 nm.

The MP-loaded CMCht/PAMAM dendrimer nanoparticles addition also induced differences in microglia metabolic activity when at 1500 μg.mL^{-1}, having this a significant 20% reduction effect.

However, the MP released from the 1000 μg.mL^{-1} addition of MP-loaded CMCht/PAMAM dendrimer nanoparticles is not sufficient to induce significant alterations in the viability of microglial cells. This seems to be evidence that the MP effects are distinct according to the drug formulation itself, whether via an acute or prolonged delivery when released from the nanoparticles. We also proved that the MP-loaded CMCht/PAMAM dendrimer nanoparticles negative effect in microglial cells viability is due to the toxic action of the MP released from the nanoparticles. The control CMCht/PAMAM dendrimer nanoparticles did not induce any noxious effects in microglia indicating that the nanoparticles *per se* have no influence in these alterations. These findings were further confirmed by observation of the cultures after immunostaining the microglia. It is evident in Figure 5b-d that in the higher dosage both the MP solution and the MP-loaded CMCht/PAMAM dendrimer nanoparticles induce observable differences in the microglial cells' cultures. The MP acute addition not only significantly reduced the number of cells in culture but also caused visible morphological changes in microglia, decreasing its volume and inducing a more rounded morphology (Figure 5c). On the other hand, the MP-loaded CMCht/PAMAM dendrimer nanoparticles appears to preferentially affect the microglial cells in its density, clearly reducing the cell number while not apparently affecting its morphological state.

3.4. *In vivo* evaluation of the therapeutic potential of MP-loaded CMCht/PAMAM dendrimer nanoparticles

In order to have a preliminary insight of the therapeutic potential of these MP-loaded nanoparticles *in vivo* we tested its local administration in a rat model of lateral hemisection. The dorsal left side of the rats' spinal cords was surgically removed around T8-9 vertebrae, while the right side remained intact. This partial spinal cord laceration disconnects the ascending and descending axonal tracts at the left thoracic spinal cord level impairing the animals' locomotion. In this study, these functional deficits and its potential recovery were the main parameters to be analyzed in a first assessment of our therapeutic intervention. The Basso, Beattie and Bresnahan open-field locomotor rating scale was chosen to assess both the degree of functional deficits upon the injury and the extent of recovery, once it can be correlated with the amount of spared white matter.[31]

Initially, using confocal microscope imaging we were able to detect the presence of green FITC-labeled nanoparticles around the lesioned tissue site 3 hours upon local injection (Figure 6a). The

assessment of the efficacy of the lesion was demonstrated in the obtained BBB scoring of the rats one week after the lesion. In all groups, the animals scored below 5 revealing only modest movement of the joints with no stepping or plantar placement in the injured paw. These scores are indicative of the severity of the induced thoracic unilateral lesion that accurately distressed the axonal traits, namely the corticospinal tract and consequently affecting the animals' locomotion. During the subsequent three weeks only slight improvements but not significant differences were observed in the locomotor performance of the control group, as well as the NP and MP injected animals (Figure 6b). However, we registered a statistically significant improvement in the functional outcome of the rats receiving the MP-loaded CMCht/PAMAM dendrimer nanoparticles, standing out from all the other groups (Figure 6b). The MP-loaded nanoparticles injected animals achieved an average score of 9 revealing extensive movement of the three hindlimb joints as well as plantar placement of the left foot with weight support in stance. This score is significantly different from all the other animal groups, indicating that the animals that received the therapeutic intervention are less impaired and more prone to recovery 4 weeks after the lesion. This restoration of function after hemisection injuries was pointed out to be achieved by two possible mechanisms: via regeneration of severed axons or by the formation of alternative pathways.[32] The axon re-growth can be enhanced in a suitable environment in the presence of growth factors and absence of inhibitory molecules, such as the ones derived from the inflammatory response. Our findings reveal no apparent spontaneous recovery in our control animals 4 weeks after injury. Interestingly, it seems that the MP-loaded nanoparticles create a more suitable environment in the lesioned area that allows visible improvements in the overall functional outcome of the affected paws. The mechanisms underlying this are most likely due to the action of the MP being released in a sustained manner from the nanoparticles, modulating the inflammation following the injury, namely by affecting the microglial population density, as we have shown *in vitro*. The microglial activity modulation in conjunction with astrocyte activation inhibition,[8c] also contributes to the suppression of inhibitory molecules formation during the inflammatory response and, not only decreases cell death after injury but also allows the axon re-growth process.[32] It was already shown by several authors that although necessary, if one minimizes the inflammation mediators' action around the lesion site the tissue degeneration can be prevented and the functional outcomes can improve.[33]
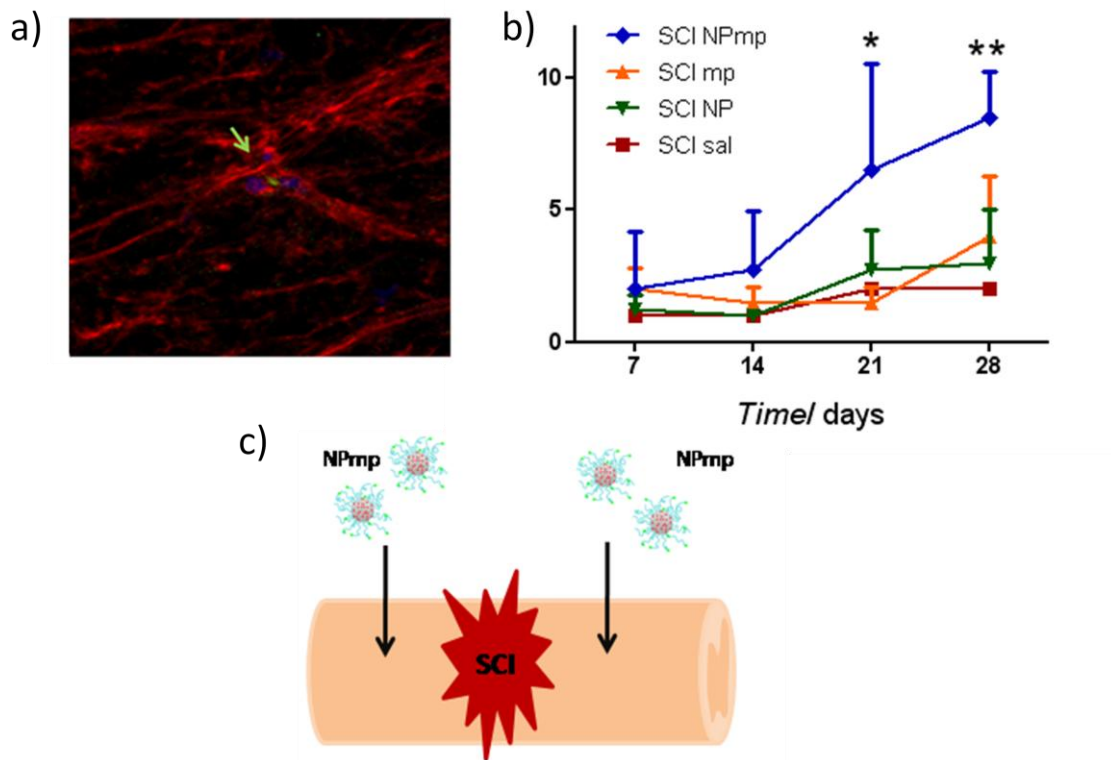
Figure 6. a) Internalized nanoparticles in the lesioned spinal tissue 3 hours after the lesion (blue – nuclei; green – MP-loaded NPs; red - astrocytes). **b)** BBB scoring of the hemisected animals from 7 to 28 days post-surgery. Rats injected with MP-loaded nanoparticles were significantly different from the other groups (mean BBB scores ± s.d., *p<0.05, **p<0.01). **c)** Schematic representation of the local injections performed after the hemisection.

Within the present study, we demonstrated the feasibility and applicability of the developed dendrimer nanoparticles for drug delivery in central nervous system therapies, particularly in the control of the secondary injury events that follow neurotraumatic conditions such as SCI. These MP-loaded nanoparticles exhibit interesting and promising potential in applications involving the modulation of inflammation upon spinal injuries and future studies aiming at the comprehension of the specific mechanisms occurring in this therapeutic intervention are of the utmost importance.

4. Conclusions

In this study we report a new approach to modulate inflammation after neurotrauma, using MP-loaded CMCht/PAMAM dendrimer nanoparticles. It was demonstrated the effective loading of MP into the nanoparticles and a sustained release of this drug during 14 days. Our studies further indicate that the MP-loaded nanoparticles possess a sphere-like shape and an average diameter range of 109 ± 46 nm with negative zeta potential. These nanoparticles are easily internalized by astrocytes, oligodendrocytes and microglia. The nanoparticles were found to be non-cytotoxic and they do not interfere with the cells' morphology or proliferation when added at concentration of 200 µg.mL^{-1}. The intracellular internalization of high concentrations of MP-loaded CMCht/PAMAM dendrimer nanoparticles modulates the metabolic activity of microglia cells, by the action of MP. In an *in vivo* study the MP-loaded nanoparticles proved to be effective in improving the functional outcome of partially hemisected rats, after administration and internalization in the spinal tissue. We foresee that these nanoparticles can still undergo additional surface modifications in order to render them a cell targeted profile. Therefore, these nanoparticles may provide a new opportunity for the treatment and modulation of secondary events following SCI, limiting the damage extent and providing neuroprotection to the lesioned tissue.

5. Acknowledgements

References

1   a) Hawryluk, G. W., Rowland, J., Kwon, B. K. & Fehlings, M. G. Protection and repair of the injured spinal cord: a review of completed, ongoing, and planned clinical trials for acute spinal cord injury: A review. *Neurosurgical focus* 25, E14 (2008). b) McDonald, J. W. & Sadowsky, C. Spinal-cord injury. *The Lancet* 359, 417-425 (2002).

2   Hyun, J. K. & Kim, H.-W. Clinical and experimental advances in regeneration of spinal cord injury. *Journal of tissue engineering* 1 (2010).

3   Becker, D., Sadowsky, C. L. & McDonald, J. W. Restoring function after spinal cord injury. *The neurologist* 9, 1-15 (2003).

4   a) Sekhon, L. & Fehlings, M. Epidemiology, demographics, and pathophysiology of acute spinal cord injury. *Spine* 26, S2-12 (2001). b) Hausmann, O. Post-traumatic inflammation following spinal cord injury. *Spinal Cord* 41, 369-378 (2003).

5   a) Ramer, L., Ramer, M. & Steeves, J. Setting the stage for functional repair of spinal cord injuries: a cast of thousands. *Spinal Cord* 43, 134-161 (2005). b) Donnelly, D. J. & Popovich, P. G. Inflammation and its role in neuroprotection, axonal regeneration and functional recovery after spinal cord injury. *Experimental neurology* 209, 378-388 (2008). c) Fleming, J. C. *et al.* The cellular inflammatory response in human spinal cords after injury. *Brain* 129, 3249-3269 (2006).

6   Sayer, F. T., Kronvall, E. & Nilsson, O. G. Methylprednisolone treatment in acute spinal cord injury: the myth challenged through a structured analysis of published literature. *The Spine Journal* 6, 335-343 (2006).

7   a) Bracken, M. B. *et al.* A randomized, controlled trial of methylprednisolone or naloxone in the treatment of acute spinal-cord injury: results of the Second National Acute Spinal Cord Injury Study. *New England Journal of Medicine* 322, 1405-1411 (1990). b) Lee, H.-C., Cho, D.-Y., Lee, W.-Y. & Chuang, H.-C. Pitfalls in treatment of acute cervical spinal cord injury using high-dose methylprednisolone: a retrospect audit of 111 patients. *Surgical neurology* 68, S37-S41 (2007).

8   a) Kwon, B., Fisher, C., Dvorak, M. & Tetzlaff, W. Strategies to promote neural repair and regeneration after spinal cord injury. *Spine* 30, S3-13 (2005). b) Xu, J. *et al.* Methylprednisolone inhibition of TNF-α expression and NF-kB activation after spinal cord injury in rats. *Molecular brain research* 59, 135-142 (1998). c) Liu, W. L. *et al.*

Methylprednisolone inhibits the expression of glial fibrillary acidic protein and chondroitin sulfate proteoglycans in reactivated astrocytes. *Glia* 56, 1390-1400 (2008).

9   a) Sun, Y.-Y. *et al.* Glucocorticoid Protection of Oligodendrocytes against Excitotoxin Involving Hypoxia-Inducible Factor-1α in a Cell-Type-Specific Manner. *The Journal of Neuroscience* 30, 9621-9630 (2010). b) Lee, J.-M. *et al.* Methylprednisolone protects oligodendrocytes but not neurons after spinal cord injury. *The Journal of Neuroscience* 28, 3141-3149 (2008). c) Xu, J. *et al.* STAT5 mediates antiapoptotic effects of methylprednisolone on oligodendrocytes. *The Journal of Neuroscience* 29, 2022-2026 (2009).

10   Baptiste, D. C. & Fehlings, M. G. Update on the treatment of spinal cord injury. *Progress in brain research* 161, 217-233 (2007).

11   a) Chvatal, S. A., Kim, Y.-T., Bratt-Leal, A. M., Lee, H. & Bellamkonda, R. V. Spatial distribution and acute anti-inflammatory effects of methylprednisolone after sustained local delivery to the contused spinal cord. *Biomaterials* 29, 1967-1975 (2008). b) Duksal, F., Kilic, I., Tufan, A. C. & Akdogan, I. Effects of different corticosteroids on the brain weight and hippocampal neuronal loss in rats. *Brain research* 1250, 75-80 (2009).

12   Das, M. *et al.* Auto-catalytic ceria nanoparticles offer neuroprotection to adult rat spinal cord neurons. *Biomaterials* 28, 1918-1925 (2007).

13   Shi, Y. *et al.* Effective repair of traumatically injured spinal cord by nanoscale block copolymer micelles. *Nature nanotechnology* 5, 80-87 (2009).

14.   Cho, Y., Shi, R., Borgens, R. & Ivanisevic, A. Repairing the damaged spinal cord and brain with nanomedicine. *small* 4, 1676-1681 (2008).

15.   Kim, Y.-t., Caldwell, J.-M. & Bellamkonda, R. V. Nanoparticle-mediated local delivery of methylprednisolone after spinal cord injury. *Biomaterials* 30, 2582-2590 (2009).

16.   Oliveira, J. M. *et al.* Surface engineered carboxymethylchitosan/poly (amidoamine) dendrimer nanoparticles for intracellular targeting. *Advanced Functional Materials* 18, 1840-1853 (2008).

17.   Oliveira, J. M., Salgado, A. J., Sousa, N., Mano, J. F. & Reis, R. L. Dendrimers and derivatives as a potential therapeutic tool in regenerative medicine strategies—a review. *Progress in Polymer Science* 35, 1163-1194 (2010).

18   Yellepeddi, V. K., Kumar, A. & Palakurthi, S. Surface modified poly (amido) amine dendrimers as diverse nanomolecules for biomedical applications. (2009).

19   Oliveira, J. M. *et al.* The osteogenic differentiation of rat bone marrow stromal cells cultured with dexamethasone-loaded carboxymethylchitosan/poly (amidoamine) dendrimer nanoparticles. *Biomaterials* 30, 804-813 (2009).

20   a) Salgado, A. J. *et al.* Carboxymethylchitosan/Poly (amidoamine) Dendrimer Nanoparticles in Central Nervous Systems-Regenerative Medicine: Effects on Neuron/Glial Cell Viability and Internalization Efficiency. *Macromolecular bioscience* 10, 1130-1140 (2010). b) Pereira, V. H. *et al.* In vivo biodistribution of carboxymethylchitosan/poly (amidoamine) dendrimer nanoparticles in rats. *Journal of Bioactive and Compatible Polymers* 26, 619-627 (2011).

21   Maiorano, G. *et al.* Effects of cell culture media on the dynamic formation of protein–nanoparticle complexes and influence on the cellular response. *ACS nano* 4, 7481-7491 (2010).

22   Lynch, I. & Dawson, K. A. Protein-nanoparticle interactions. *Nano Today* 3, 40-47 (2008).

23.   Wang, Y., Guo, R., Cao, X., Shen, M. & Shi, X. Encapsulation of 2-methoxyestradiol within multifunctional poly (amidoamine) dendrimers for targeted cancer therapy. *Biomaterials* 32, 3322-3329 (2011).

24   Liu, Y., Bryantsev, V. S., Diallo, M. S. & Goddard Iii, W. A. PAMAM dendrimers undergo pH responsive conformational changes without swelling. *Journal of the American Chemical Society* 131, 2798-2799 (2009).

25   Saovapakhiran, A., D'Emanuele, A., Attwood, D. & Penny, J. Surface modification of PAMAM dendrimers modulates the mechanism of cellular internalization. *Bioconjugate chemistry* 20, 693-701 (2009).

26   a) Kreutzberg, G. W. Microglia: a sensor for pathological events in the CNS. *Trends in neurosciences* 19, 312-318 (1996). b) Streit, W. J. Microglia as neuroprotective, immunocompetent cells of the CNS. *Glia* 40, 133-139 (2002).

27   Lamprecht, A. & Benoit, J.-P. Etoposide nanocarriers suppress glioma cell growth by intracellular drug delivery and simultaneous P-glycoprotein inhibition. *Journal of controlled release* 112, 208-213 (2006).

28   a) Albertazzi, L., Serresi, M., Albanese, A. & Beltram, F. Dendrimer internalization and intracellular trafficking in living cells. *Molecular Pharmaceutics* 7, 680-688 (2010). b) Kitchens, K. M., Kolhatkar, R. B., Swaan, P. W. & Ghandehari, H. Endocytosis inhibitors

prevent poly (amidoamine) dendrimer internalization and permeability across Caco-2 cells. *Molecular Pharmaceutics* 5, 364-369 (2008).

29   Chan, A., Papadimitriou, C., Graf, W., Toyka, K. V. & Gold, R. Effects of polyclonal immunoglobulins and other immunomodulatory agents on microglial phagocytosis of apoptotic inflammatory T-cells. *Journal of neuroimmunology* 135, 161-165 (2003).

30   a) Hutter, E. *et al.* Microglial response to gold nanoparticles. *ACS nano* 4, 2595-2606 (2010). b) Vilhardt, F. Microglia: phagocyte and glia cell. *The international journal of biochemistry & cell biology* 37, 17-21 (2005).

31   a) Basso, D. M., Beattie, M. S. & Bresnahan, J. C. A sensitive and reliable locomotor rating scale for open field testing in rats. *Journal of neurotrauma* 12, 1-21 (1995). b) Basso, D. M. Behavioral testing after spinal cord injury: congruities, complexities, and controversies. *Journal of neurotrauma* 21, 395-404 (2004).

32   Deumens, R., Koopmans, G. C. & Joosten, E. A. Regeneration of descending axon tracts after spinal cord injury. *Progress in neurobiology* 77, 57-89 (2005).

33   a) Beattie, M. S. Inflammation and apoptosis: linked therapeutic targets in spinal cord injury. *Trends in molecular medicine* 10, 580-583 (2004). b) Alexander, J. K. & Popovich, P. G. Neuroinflammation in spinal cord injury: therapeutic targets for neuroprotection and regeneration. *Progress in brain research* 175, 125-137 (2009).

34.   Chen, Y. *et al.* Isolation and culture of rat and mouse oligodendrocyte precursor cells. *Nature protocols* 2, 1044-1051 (2007).

35.   Resources, I. o. L. A. *Guide for the Care and Use of Laboratory Animals*. (National Academies Press, 1996).

36.   Silva, N. A. *et al.* Development and characterization of a Novel Hybrid Tissue Engineering–based scaffold for spinal cord injury repair. *Tissue Engineering Part A* 16, 45-54 (2009).

CHAPTER VII

Biocompatibility and functionality studies of MP-loaded CMCht/PAMAM dendrimer nanoparticles in Schwann cell cultures

CHAPTER VII

Biocompatibility and functionality studies of MP-loaded CMCht/PAMAM dendrimer nanoparticles in Schwann cell cultures

Abstract

Schwann cells have been investigated for SCI transplantation, since they have been shown to promote axonal regeneration and myelination following injury. Combination of Schwann cell transplantation and the systemic administration of the corticosteroid methylprednisolone (MP) has been also reported to improve repair and function in SCI animal models. However, there is a lot of controversy surrounding MP administration in human patients, since high dosage systemic administration is required, thus severely affecting other peripheral organs and causing undesired side effects. One way of circumventing this issue is to use adequate drug delivery systems that can act specifically and more effectively in the target tissue. In the present study, it is aimed to investigate the interaction of MP-loaded nanoparticles with Schwann cells, namely assessing the uptake profile and possible interference in its myelination ability. Incubation of MP-loaded nanoparticles in Schwann cell cultures have revealed straightforward internalization in a time dependent profile, reaching maximum internalization levels 24 hours post-incubation. Additionally, the presence of nanoparticles has not significantly affected co-cultures of Schwann cells with dorsal root ganglia neurons, particularly the axon myelination function of Schwann cells. Extensive myelination was observed following nanoparticle incubation, with no significant differences to the controls. The conjugation of Schwann cell transplantation and MP-loaded nanoparticle administration may therefore be reasonable in the development effective therapeutic strategies for SCI repair.

1.   Introduction:

Spinal cord injury (SCI) frequently follows a mechanical trauma that damages the spinal tissue. It has severe consequences associated with it, which dramatically affect the victims quality of life.[1] Following this primary insult where massive cell death and vascular leakage occur, a chain of biochemical and cellular secondary reactions is initiated broadening the lesion impact and altering the environment surrounding the injury.[2] In brief, the secondary injury is dominated by excitotoxicity, hemorrhage and edema, infarction, reactive oxygen species (ROS) production, lipid peroxidation, axonal disruption and degeneration, and further cell necrosis and apoptosis, particularly in neurons and oligodendrocytes.[3,4] The post-lesion environment thus becomes extremely inhibitory for axonal growth and reconnection. In a chronic phase, regeneration becomes even more difficult to manage due to the formation of a glial scar.[5] Consequently, patients suffering from severe SCI commonly develop several motor, respiratory and cardiac dysfunctions, among others.[6] Therefore, therapeutic options that can modulate the post-lesion environment and create more permissive conditions for repair to occur are urgently needed.

The clinically recommended, and still very controversial, pharmacological agent to treat SCI is the corticosteroid methylprednisolone (MP).[7] MP is a potent anti-inflammatory and antioxidant drug that has been shown to improve motor and sensory functioning, following high dosage systemic administration to SCI patients.[8] Although the range of MP action mechanisms is not yet completely understood, it is known to involve astrocyte and microglia proliferation inhibition, as well as anti-apoptotic oligodendrocyte protection.[9,10] However, simultaneous occurrence of severe wound infections, gastric bleeding, sepsis, pneumonia, pulmonary embolism and even death have also been described following high dosage systemic MP administration, questioning the safety and effectiveness of this option.[11]

Tissue engineering as an interdisciplinary field that aims at restoring, maintaining or improving tissue function merging the knowledge of different scientific fields, is bringing new hopes for more effective neural regeneration strategies.[12] It suggests the use of cell transplantation, biomolecular therapies and/or biomaterial-based advanced strategies in order to provide more suitable conditions for regeneration to occur.[13] Several cell types are currently under investigation for SCI repair, amongst them autologous Schwann cell (SC) transplantation is believed to be one of the more promising approaches.[14] SCs are the myelinating cells of the peripheral nervous system and they have been shown not only to myelinate central axons after transplantation into SCI animal

models, but also to provide a more permissive substrate environment for axon regeneration.[15] These cells have proved to enhance the invasion of host SCs into the lesioned area, which favorably contributes to regeneration.[16] SC transplantation combined with MP administration has also demonstrated improved axonal regeneration following SCI in rat models.[17] In this study, it is proposed the use of an innovative drug delivery system for MP administration, allowing a local and sustained release and eliminating the severe side effects of systemic high dose administration, in conjunction with SC culturing. Biocompatibility assays involving biomaterials and Schwann cells have mostly been assessed for guidance conduits for SC aligned growth, either using nanofibers[18] or polymer macrostructures.[19] To our knowledge, there have been no reports on drug delivery nanocarriers compatibility with SCs.

From the variety of recently developed nanoparticles (NPs), dendrimers possess extraordinary features that make them ideal vehicles for the controlled and sustained delivery of drugs.[20] Dendrimers possess a spherical highly branched structure that can entrap molecules, and from which emanate external surface groups that can be further functionalized.[21] Poly(amidoamine) (PAMAM) dendrimers, the most extensively used for biomedical applications, have been recently surface grafted to carboxymethylchitosan (CMCht), in order to enhance biocompatibility and drug payload capabilities.[22] MP has also been successfully incorporated in the surface engineered CMCht/PAMAM dendrimers, demonstrating a sustained and controlled release *in vitro*.[23] The interaction of MP-loaded CMCht/PAMAM dendrimer NPs with primary cultures of SC, as well as co-cultures of SC with dorsal root ganglia neurons (DRGN) was investigated in the present report. Following NP exposure to pure SC cultures, fluorescence microscopy studies were conducted to assess the NP uptake profile and possible morphological/spatial distribution discrepancies. Transmission electron microscopy analysis was performed to investigate the cell ultrastructure after MP-loaded CMCht/PAMAM dendrimer nanoparticles uptake. Finally, co-cultures of SC and DRG were also exposed to NPs and the myelination ability of SC quantified, following immunocytochemistry and Sudan black staining.

2. Materials and methods

2.1. Nanoparticle synthesis

Carboxymethylchitosan/polyamidoamine (CMCht/PAMAM) dendrimer nanoparticles were produced as previously reported by Oliveira *et al.* [22] Generation 1.5 Starburst® PAMAM-carboxylic acid terminated dendrimer solution (PAMAM-CT) in 20% methanol (w/v) were purchased from Sigma (Germany). The following reactions were carried out: (i) increase in the PAMAM-CT generation; (ii) production of a PAMAM-methyl esther terminated dendrimer; (iii) condensation reaction between the methyl esther and amine groups of PAMAM and CMCht; and (iv) conversion of the non-reacting methyl esther groups into carboxylic ones in the CMCht/PAMAM dendrimer nanoparticles. Initially, the methanol was removed from the PAMAM-CT dendrimers by evaporation under nitrogen gas. The remaining compound was re-dissolved in ultra-pure water in a final concentration of 10 mg.mL^{-1} and the pH was corrected to 6.5. Then, 1-ethyl-3-(3-dimethylaminopropyl) carbodiimide hydrochloride (EDC, Fluka, Slovakia) was added under agitation for 30 minutes at room temperature. Ethylenediamine (EDA, Sigma, Germany) was added at the same molar ratio of EDC, and the solution let to react for 4 hours under vigorous agitation. The solution was subsequently dialyzed against ultrapure water in order to remove the exceeding EDC (cellulose tubing, benzoylated for separating compounds with a molecular weight of ≤1,200, Sigma, Germany). The obtained amine terminated PAMAM dendrimers (PAMAM-AT) were mixed with methanol (Sigma, Germany) and methyl methacrylate (Fluka, Germany), and kept under agitation in a water bath at 50°C for further 24 hours. After methanol removal under nitrogen gas, appropriate volumes of hydrochloric acid (HCl, Panreac, Portugal) and trifluoroacetic acid (TFA, Sigma, Germany) were added to the solution. Meanwhile, 1 g of CMCht was dissolved in 50 mL of water. The PAMAM methyl esther terminated dendrimers were dissolved in a 20/80 water/methanol solution and the CMCht was added and kept under agitation for 72 hours, after which the CMCht/ PAMAM dendrimer nanoparticles with carboxylic-terminated groups were obtained.

2.2. Methylprednisolone incorporation into the CMCht/PAMAM dendrimer nanoparticles

Methylprednisolone (MP, Sigma, Germany) was incorporated in the nanoparticles by mixing an aqueous solution of CMCht/PAMAM dendrimer nanoparticles with an ethanolic solution containing methylprednisolone in a final concentration of 5×10^{-4} M (w/w). Saturated sodium carbonate solution (Na_2CO_3, Aldrich, Germany) and acetone (Pronalab, Portugal) were then added to the mixture and kept under vigorous agitation. The resulting precipitates were collected by filtration and then dispersed in ultrapure water. Extensive dialysis (cellulose tubing, benzoylated for separating compounds with a molecular weight of ≤1,200, Sigma, Germany) was performed during 48 hours. Both CMCht/PAMAM dendrimer nanoparticles and MP-loaded CMCht/PAMAM dendrimer nanoparticles were obtained by freezing the final solution at -80°C and freeze-drying (Telstar-Cryodos-80, Spain) the samples for approximately 7 days, until the solvents were completely removed.

2.3. Fluorescent labeling of MP-loaded CMCht/PAMAM dendrimer nanoparticles

Fluorescein isothiocyanate (FITC) labeled MP-loaded CMCht/PAMAM dendrimer nanoparticles conjugates were prepared by covalently bonding the amine group of CMCht and the isothiocyanate group from FITC. A 10 mg.mL^{-1} FITC (Sigma, Germany) solution was prepared in dimethyl sulfoxide anhydrous (DMSO, Riedel-de Haen, Germany) in the dark. Simultaneously, a 10 mg.mL^{-1} MP-loaded CMCht/PAMAM dendrimer nanoparticles solution was set in carbonate-bicarbonate coupling buffer (pH 9.2). Afterwards, 50 μL of the FITC/DMSO solution were added per each mL of the MP-loaded CMCht/PAMAM dendrimer nanoparticles buffered solution, under agitation. The resulting solution was kept in the dark at 4°C for 8 hours. The FITC-labeled MP-loaded CMCht/PAMAM dendrimer nanoparticle solution was then dialyzed (cellulose tubing, benzoylated for separating compounds with a molecular weight of ≤1,200, Sigma, Germany) for 48 hours against ultrapure water in order to remove the FITC molecules that did not react. Finally, the solution was frozen at -80°C and subsequently freeze-dried (Telstar-Cryodos-80, Spain) until the solvents were completely removed.

2.4.   Schwann cell cultures

SCs were obtained from adult male Fischer rats and isolated from the sciatic nerves as previously reported.[24] In brief, the sciatic nerves from five rats were cut into small 1–2 mm pieces and placed into 35 mm uncoated tissue culture dishes. Every week nerve segments were re-plated, until after 3 weeks in culture (the nerve segments were now essentially depleted from fibroblasts) SCs were enzymatically and mechanically dissociated before transferring to new dishes for SC expansion in the presence of mitogens (20 µg/mL bovine pituitary extract and 2 µM forskolin). SC purity was between 95 and 98%.

2.5.   Dorsal root ganglia cultures

DRGs were dissected from embryonic P15 Sprague-Dawley rats and incubated in trypsin (Worthington Biochemical Corporation, USA). The tissue was centrifuged and the pellet was re-suspended in serum-containing medium. Following mechanical dissection, the pellet was re-suspended in NLA medium (neurobasal medium and B27 (Invitrogen, USA)) supplemented with nerve growth factor (NGF, Invitrogen, USA). One drop of DRG cell suspension in NLA medium was plated in the center of collagen-coated dishes. Approximately 5,000–7,000 neurons were plated per culture. After the cells attached to the collagen, the cultures were flooded and treated with NLA medium containing fluorodeoxyuridine (FUDR, Sigma, Germany) on days 2 to 4, 6 to 8, and 10 to 12, to exclude the non-neuronal cells (fibroblasts, SCs, and phagocytes). After the anti-mitotic treatment, the resulting DRGN cultures were maintained on NLA medium for at least 1 week to ensure that no residual FUDR remained when SCs were added.

2.6.   Immunocytochemistry

Cultures were stained with antibodies against S100, neurofilament (NF) and myelin basic protein (MBP) to identify SCs, neurons and myelin, respectively. Cultures to be stained for S100 were rinsed with L-15 before fixing in 4% PFA in 0.1 M PBS for 10 min at room temperature. The cells were permeabilized with 4% PFA and 0.2% Triton X-100 for 10 minutes. The rabbit S100 polyclonal primary antibody (Dako, USA, 1:400) was incubated for one hour at room

temperature. After incubation, the cultures were rinsed three times with 0.1 M PBS containing 10% serum. The secondary antibody, goat anti-rabbit AlexaFluor 594 (Invitrogen, USA, 1:500) was applied for 30 minutes. Cultures were rinsed three times in 0.1 M PBS containing 10% serum. Cultures to be stained for MBP or NF were fixed in 4% PFA in 0.1 M PBS at room temperature. The cultures were permeabilized for 15 min with 4% PFA containing 0.2% Triton X-100 in 0.1 M PBS at room temperature. The cultures were then treated with ice-cold 50% acetone for 2 minutes, ice-cold 100% acetone for 2 minutes, and 50% acetone for 2 minutes. Cultures were then rinsed twice with 0.1 M PBS for 5 minutes each and incubated with mouse monoclonal anti-MBP (SMI 94, Sternberger Monoclonals, Inc., USA, 1:1000) or mouse monoclonal anti-neurofilament (SMI 31, Sternberger Monoclonals, Inc., USA, 1:1000). After washing in PBS, secondary antibody goat anti-mouse Alexa Fluor 594 or 488 (Invitrogen, USA, 1:500) was added for 30 minutes. Coverslips were then mounted in Citifluor containing Hoechst 33342 (Pierce, USA).

2.7.   Myelination in SC/DRGN co-cultures

For myelination experiments, co-cultures were prepared by adding 50,000 SCs to purified DRGN cultures. The DRGN co-culture media was replaced every other day with NLA medium for 2 weeks. For inducing myelination, the co-culture media was replaced by medium containing ascorbic acid (NLA medium + ascorbic acid). All cultures were then maintained for an additional 2 weeks, with regular media renewal every 2–3 days. The total period of co-culturing was 4 weeks. Myelination was observed as expected in SC/DRGN cultures before the end of the co-culturing period.

2.8.   Sudan black staining

Co-cultures of DRGN/SCs were fixed for 15 minutes in 4% PFA, rinsed in PBS, and further fixed in 0.1% OsO4 for 1 hour. The cultures were then rinsed washed in PBS followed by dehydration in 25, 50, and 70% ethanol, each for 5 minutes. The 0.5% Sudan black in 70% ethanol solution was applied for 1 hour. The cultures were rehydrated in ethanol (70%, 1 minute; 50%, 5 minutes; 25%, 5 minutes) and then rinsed in PBS and mounted. Myelinated axons were counted using a

square grid eyepiece during three scans across the coverslip. The number of Sudan black-stained myelin sheaths crossing the scan line was counted.

2.9. Transmission electron microscopy

The cultures were maintained in 2% phosphate buffered glutaraldehyde with 100 mM sucrose overnight at 4°C. Afterwards they were placed in 2% buffered OsO4 for 1 hour at room temperature. Cultures were further processed for EMbed plastic (Electron Microscopy Sciences, Fort Washington, USA) embedding. Areas were chosen for semi-thin sectioning; the 1 µm sections were stained with toluidine blue/methylene blue/sodium borate. Thin sections, stained with uranyl acetate and lead citrate, were examined in a Philips CM-10 electron microscope (FEI Company, USA). Sections were cut perpendicular to the plane of the coverslip.

2.10. Statistical analysis

Statistical analysis was done to compare the myelin quantification using one-way ANOVA followed by the Bonferroni post-test between groups to assess statistical differences. Statistical significance was defined for $p < 0.05$.

3. Results and discussion

The emergence of new nanotools for regenerative medicine can have tremendous future impact in the design of new enhanced reparative strategies, namely for complex pathologies such as neurological diseases. In particular, SCI treatments can benefit from more effective drug delivery systems (DDS), with prolonged and sustained profiles as the ones provided by recently developed nanocarriers. Moreover, combination of biomaterial-based DDS with cell transplantation can provide better means to reach the proper environment for successful SCI repair and regeneration. More effective delivery of therapeutic agents, such as MP, that modulate the inflammatory/inhibitory lesion site, associated with SC transplantation strategies intended at replacing the cell population and supporting axonal regeneration may prove to be valuable therapeutic approaches. In fact, it is now widely accepted that such combinatorial strategies will

186

more likely overcome the complexity of SCI pathology, dealing simultaneously with several of the events that make the environment so harsh for regeneration.

In the present study, it was investigated the *in vitro* interaction of MP-loaded CMCht/PAMAM dendrimer NPs with Schwann cells foreseeing a combined tissue engineering strategy for nerve regeneration. In order to do so, the effect of the MP-loaded CMCht/PAMAM dendrimer NPs in the SC myelinating capacity was evaluated, as well as the spatio-temporal uptake profile. Primary rat SC cultures were exposed to 200 µg.mL^{-1} FITC-labeled MP-loaded CMCht/PAMAM dendrimer NPs to assess intracellular distribution and quantify NP cell uptake at different culturing times. During the incubation periods, proliferation and density of SC cultures was followed, and no observable differences to control SCs grown in regular media were detected. These NPs have been previously tested in primary glial cultures with no reported differences in metabolic activity or proliferation rates of the NP incubated cells, thus no cytotoxicity was expected to occur in primary SCs as well.[23] Figure 1 shows the fluorescence microscopy images of the temporal NP uptake profile in pure SC cultures. Assessment of NP intracellular distribution following immunocytochemistry and fluorescence microscopy observation pointed out, similarly to what it has been previously observed for glial cultures, to a preferential intracellular localization in the perinuclear region. This was verified for all the different incubation periods tested, for a maximum of 24 hours. Figure 1 also indicates that the internalization of FITC-labeled MP-loaded CMCht/PAMAM dendrimer NPs by SCs is a time-dependent process that reaches a saturation point 24 hours following incubation, denoting that at this time point each SC in culture has internalized NPs. The levels of internalization are maintained for at least 7 days of culturing showing that the NPs can be intracellularly retained in SCs, which can be advantageous for drug delivery therapeutic purposes. In fact, SCs have the additional possibility to act also as NP carriers in a combined transplantation strategy due to the dynamic cellular NP transport, namely through transcytosis or exocytosis.[25] Moreover, all the cultures exposed to NPs have revealed the typical SC bipolar morphology and longitudinal orientation, with parallel arrangement, indicating that NP do not disturb the SC typical distribution in the culture dish.[24] Observation of the obtained SC cultures indicated high levels of purity, with no fibroblast contamination and successful expansion and extension of SC processes, as the obtained fluorescence images confirm.
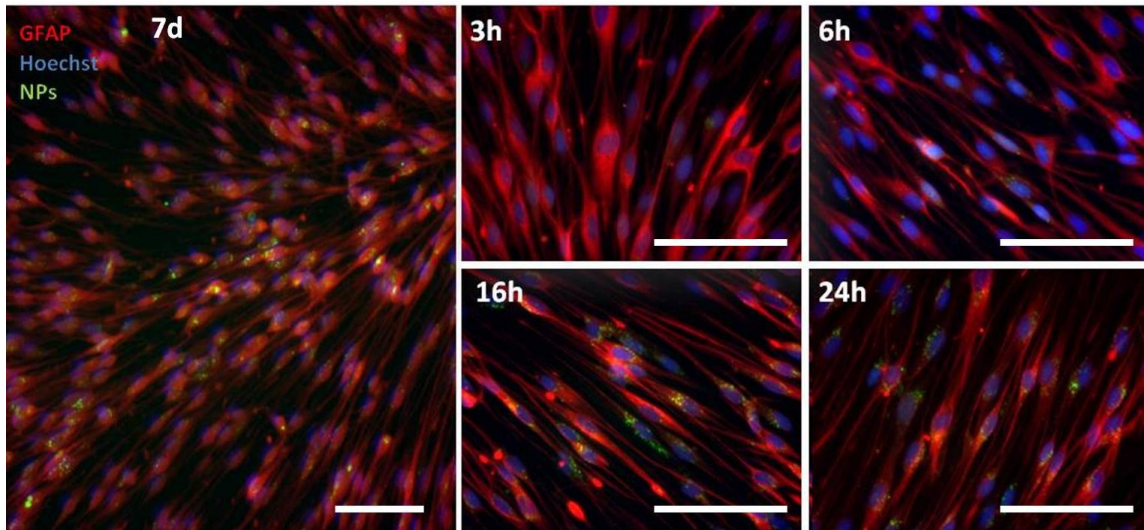
Figure 1 – Primary Schwann cell cultures incubated with MP-loaded FITC-labeled CMCht/PAMAM dendrimer nanoparticles. Nuclei are stained with Hoescht (blue), and SC with GFAP (red). Nanoparticles are visible in green.

Additionally, at each time-point cells were fixed and the number of SCs displaying fluorescent-NP uptake was quantified. Figure 2 shows the graphical representation of the quantification of NP uptake in SC cell cultures, confirming its time dependence. The rate of NP uptake has shown to be relatively slow with modest internalization rates during the first 6 hours of incubation with NPs reaching around 30% culture uptake after this time period. The dynamics seems to follow a linear progression trend reaching the maximum internalization figures 24 hours following NP incubation with practically all SCs presenting internalized NPs. This internalization profile corroborates the previously reported observations for the uptake of astrocytes and oligodendrocytes in glial primary cultures that display a very similar trend.[23] Since SCs are the myelinating glial cells from the peripheral nervous system, a similar response from the CNS glia is expectable after NP uptake, particularly oligodendrocytes. The mechanism leading to MP-loaded CMCht/PAMAM dendrimer internalization in astrocytes has been recently confirmed to be associated with endocytotic mechanisms. Considering the observed NP uptake profile similarities for these two cell types – SCs and astrocytes - it is likely that SCs also display the same intracellular transport mechanisms, however additional studies are needed to confirm that hypothesis. NP binding and interaction with the cell membrane have been shown to be highly dependent not only on the NP characteristics (e.g., size, shape, and charge), but also on the target cell type.[26] In the present study, it was unveiled the MP-loaded CMCht/PAMAM dendrimer NPs particular uptake profile by SCs.
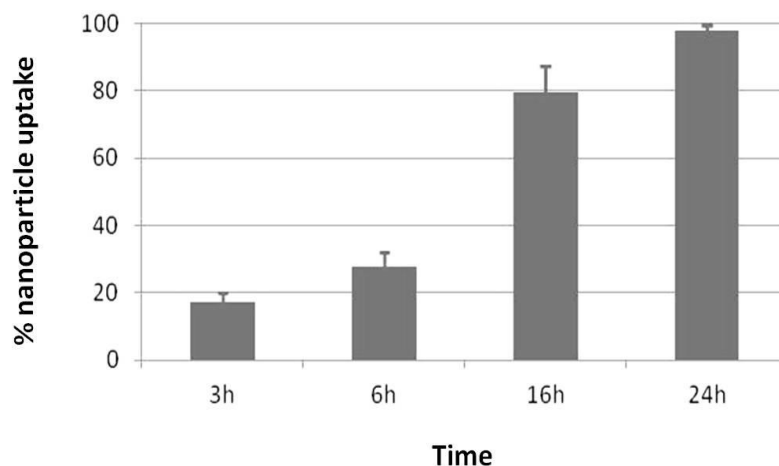
Figure 2 – Percentage uptake rates of FITC-labeled MP-loaded CMCht/PAMAM dendrimer NPs in rat primary Schwann cells (n=3; mean ± SD).

In this investigation, co-cultures of SCs and DRG neurons have also been established by means of plating the previously obtained SCs onto established DRGN cultures. As seen in Figure 3, that shows the fluorescence images of the co-cultures, the SCs were successfully plated onto DRG neurons and promptly aligned along the axon, even in the presence of MP-loaded CMCht/PAMAM dendrimer NPs. A particular feature of SCs is precisely the affinity relation for axons, typically associating with the neurites and extending its processes to migrate along the neurites, when co-cultured with DRGN. This was thoroughly observed in the SC/DRGN co-cultures, as it is shown in Figure 3. Functionally *in vitro* SCs are capable of forming a myelin sheath around cultured axons, mimicking the *in vivo* SC function. Thus, these SC/DRGN co-cultures are commonly used for investigation of the myelination mechanism, as well as testing of new strategies in nerve regeneration.[27,28] Herein, it was investigated if MP-loaded CMCht/PAMAM NPs do affect SC myelination capacity on DRGN neurites. In the presence of FITC-labeled MP-loaded NPs, SCs normally lined up along the neurites extending their processes along the axons signaling the initiation of the myelination process. No differences in the co-cultures, with or without NP incubation, were observable regarding this.
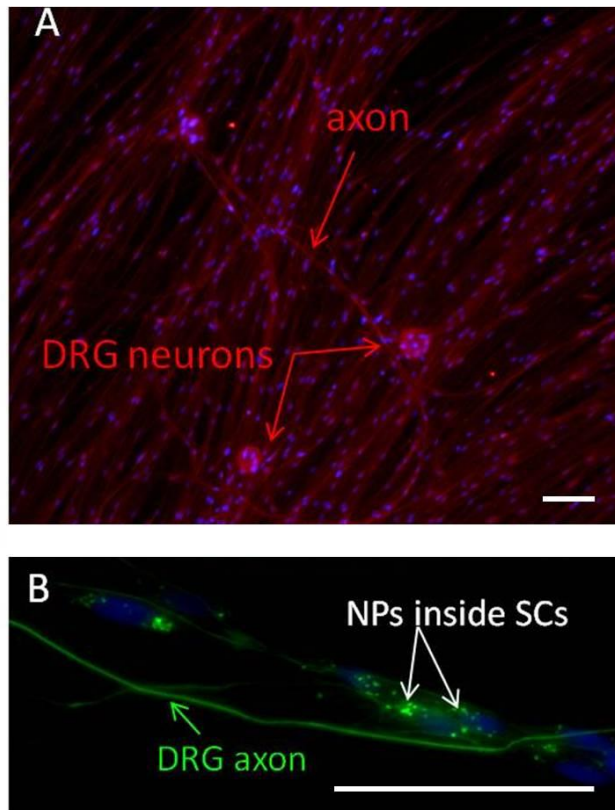
Figure 3 — A. Co-cultures of Schwann cells and dorsal root ganglia neurons, labeled with S100 (red). **B.** Detail of a labeled DRGN axon (labeled with NF) and the lined up Schwann cells with internalized FITC-labeled MP-loaded CMCht/PAMAM dendrimer nanoparticles (green spots). Scale bars correspond to 50 μm.

Additionally, the co-cultures of SC and DRGN axons were observed under a TEM microscope (Figure 4), in order to investigate if ultrastructural differences in the cells were observable after NP exposure. Cross-sections of the cultures allowed the visualization of SCs attached to the collagen matrix, and in close proximity with the DRGN axons that abundantly surrounded the SC cell body (Figure 4A). The same distribution and cell proximity was observed in the presence of NPs (Figure 4B). Initiation of the axon typical encirclement process by a SC is also suggested by the observation of evaginations of the SC membrane around the DRGN axons (arrows in Figure 4). No apparent morphological differences between the cells in the two different conditions were detected, indicating that NPs are not exerting any deleterious effects in the co-cultures. Additionally, the 109 nm diameter NPs were not distinguishable, even at higher magnification images, from the spherical vesicles and organelles. In future studies, conjugation to a contrast agent (such as phosphotugstic acid) will be done, since it was noticed that this is required for NP discrimination and identification via electron microscopy methodologies.
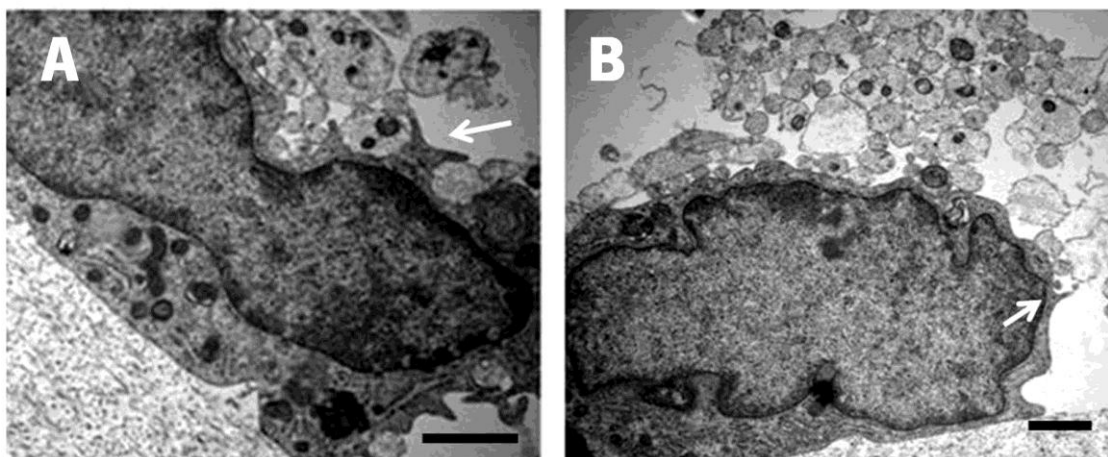
Figure 4 – Electron micrographs of cross-sections of co-cultures of Schwann cells and dorsal root ganglia neurons (non-myelinating conditions), in control (A) and NP exposure (B) conditions. Initiation of DRGN axon by a SC is visible (arrow). Scale bars correspond to 1 μm.

More importantly, SC functionality was assessed by means of adding myelination media to the co-cultures.[29] In order to visualize the formed myelin two different treatments were performed: Sudan black staining and anti-myelin-basic protein (MBP) immunolabeling. Figure 5 shows the microscopy images after SC/DRGN cultures were subjected to Sudan black staining, and the myelin identification is visible. Myelin was abundantly formed and positively stained in both conditions, i.e., in regular myelination media with and without NP previous exposure. Sudan black staining reveals thickened phase-dark segments that appear along the neurites and correspond to myelin formation (Figure 5A). From both micrographs (control and NP stimulated), along the myelinated axons it is possible to discern the SC bodies enwrapping the neurites and extending the processes beside them. Once again, it can be observed that SCs displayed the typical behavior when in contact with neurons following MP-loaded CMCht/PAMAM dendrimer NP incubation. Moreover, the myelinated axon quantification has showed no statistical differences between the two culturing conditions, with very similar average figures (Figure 5B). From TEM analysis and Sudan black staining data, both visual observation and myelinated axon quantification, it was confirmed that neither the SC contact with DRGN or myelin production were affected by the presence of NPs in culture.
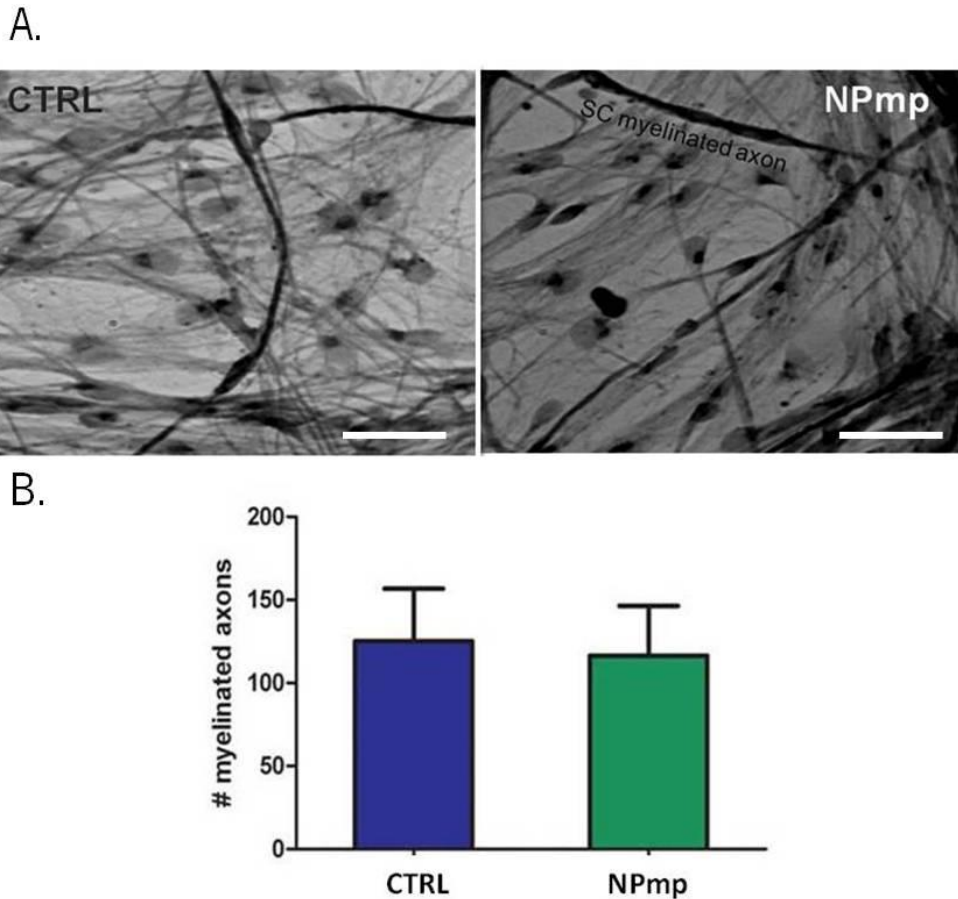
Figure 5 – A. Bright field micrographs, after Sudan black staining for myelin visualization. Co-cultures of Schwann cells and dorsal root ganglia neurons cultured in myelinating media, in control conditions (CTRL) and following MP-loaded CMCht/PAMAM dendrimer NP incubation (NPmp). Scale bars represent 50 μm. **B.** Graphical representation of the myelinated axon quantification in control conditions (CTRL) and following MP-loaded CMCht/PAMAM dendrimer NP incubation (NPmp).

To validate the previous findings, immunostaining for MBP, a myelin specific marker, has also been performed. Figure 6 shows the fluorescence microscopy images of the co-cultures of SC and DRGN following myelin (anti-MBP antibody) and SC (anti-S100 antibody) labeling. This experiment has revealed that extensive myelination has occurred in the absence and presence of NPs, thus confirming that SCs are functionally active in the presence of MP-loaded CMCht/PAMAM dendrimer NPs. These results also confirm the presence of the FITC-labeled MP-loaded dendrimer NPs in the co-culture, as it can be seen from the green spots appearing inside the cells. Moreover, in both conditions SCs visibly proliferated in the DRGN culture, and closely aligned along the axons while forming myelin sheaths. Therefore, it was once more demonstrated that despite the presence of NPs and the extended period in culture that myelination studies

require, the interaction of NPs with SCs do not affect myelin sheath production, which is these cells foremost function and essential in nerve regeneration.
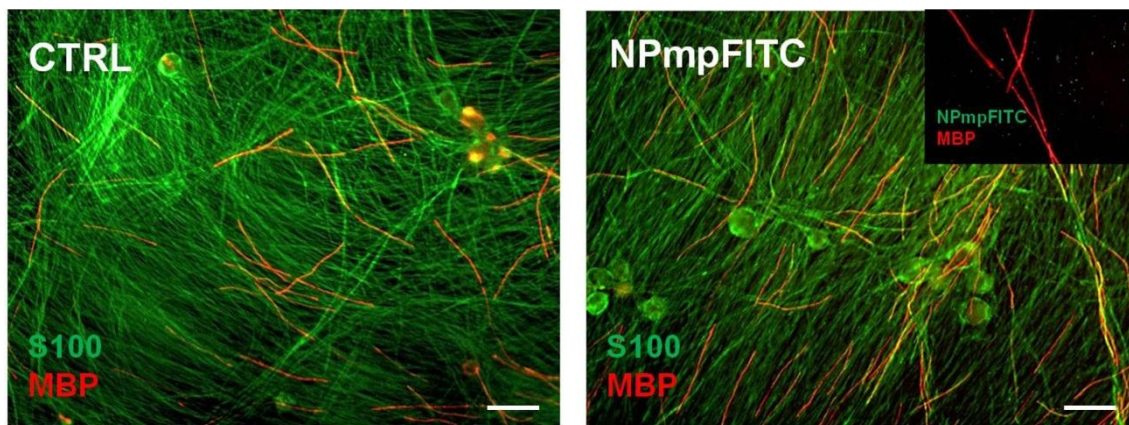

Figure 6 – Fluorescence microscopy images of Schwann cells and dorsal root ganglia neurons following myelination induction, in control conditions (CTRL) and following FITC-labeled MP-loaded CMCht/PAMAM dendrimer NP incubation (NPmpFITC). Immunolabeling was performed with S100 for SC identification (green) and MBP for myelin (red). A detailed image is presenting showing myelinated axons (in red) and the dispersion of NPs in the culture (green spots). Scale bars correspond to 50 μm.

The present study corroborates that combined therapies with the investigated MP nanocarrier and SC transplantation are encouraging and may be an applicable strategy for SCI management after pre-clinical and subsequent clinical validation. The conjunction of an appropriate sustained and specific delivery of MP - that will modulate inflammation while reducing oligodendrocyte death[10] - with SC transplantation - which supports nerve growth and provides neurotrophic factors - seems an attractive and potentially successful strategy for SCI repair. Potentiating beneficial actions while reducing undesired side effects will hopefully maximize tissue healing in a safer and more effective approach.

4. Conclusions

In the present work, MP-loaded CMCht/PAMAM dendrimer NPs and SC interactions were investigated. SCs were able to easily internalize MP-loaded NPs in a time dependent manner. Results have also shown that NPs do not affect the typical SC morphology or spatial arrangement

in culture. Moreover, when in contact with DRGN, the NP-incubated SCs profusely encircle and myelinate the axons, confirming that the cells function in not altered by the presence of the NPs. This study confirm the suitability of combining the two proposed tissue engineering strategies envisioning the development of more effective SCI therapies. In a near future, *in vivo* testing of this approach should be conducted in lesion models.

5. Acknowledgements

References

1   Simpson, L. A., Eng, J. J., Hsieh, J. T., Wolfe & the Spinal Cord Injury Rehabilitation Evidence Research Team, D. L. The health and life priorities of individuals with spinal cord injury: a systematic review. *Journal of neurotrauma* 29, 1548-1555 (2012).

2   Kwon, B. K., Tetzlaff, W., Grauer, J. N., Beiner, J. & Vaccaro, A. R. Pathophysiology and pharmacologic treatment of acute spinal cord injury. *The Spine Journal* 4, 451-464 (2004).

3   Profyris, C. *et al.* Degenerative and regenerative mechanisms governing spinal cord injury. *Neurobiology of disease* 15, 415-436 (2004).

4   Donnelly, D. J. & Popovich, P. G. Inflammation and its role in neuroprotection, axonal regeneration and functional recovery after spinal cord injury. *Experimental neurology* 209, 378-388 (2008).

5   Hu, R. *et al.* Glial scar and neuroregeneration: histological, functional, and magnetic resonance imaging analysis in chronic spinal cord injury: Laboratory investigation. *Journal of Neurosurgery: Spine* 13, 169-180 (2010).

6   Grossman, R. G. *et al.* Incidence and severity of acute complications after spinal cord injury. *JNS: Spine Special Supplements* 17, 119-12 (2012).

7   Bracken, M. B. Steroids for acute spinal cord injury. *Cochrane Database Syst Rev* 1 (2012).

8   Bracken, M. B. *et al.* A randomized, controlled trial of methylprednisolone or naloxone in the treatment of acute spinal-cord injury: results of the Second National Acute Spinal Cord Injury Study. *New England Journal of Medicine* 322, 1405-1411 (1990).

9   Liu, W. L. *et al.* Methylprednisolone inhibits the expression of glial fibrillary acidic protein and chondroitin sulfate proteoglycans in reactivated astrocytes. *Glia* 56, 1390-1400 (2008).

10   Xu, J. *et al.* STAT5 mediates antiapoptotic effects of methylprednisolone on oligodendrocytes. *The Journal of neuroscience* 29, 2022-2026 (2009).

11   AANS/CNS. Pharmacological therapy after acute cervical spinal cord injury. *Neurosurgery* 50, S63-72 (2002).

12   Langer, R. & Vacanti, J. P. Tissue engineering. *Science* 260, 920-926 (1993).

13   Schmidt, C. E. & Leach, J. B. Neural tissue engineering: strategies for repair and regeneration. *Annual review of biomedical engineering* 5, 293-347 (2003).

14   Wiliams, R. R. & Bunge, M. Schwann cell transplantation: a repair strategy for spinal cord injury? *Progress in brain research* 201, 295-312 (2011).

15   Tetzlaff, W. *et al.* A systematic review of cellular transplantation therapies for spinal cord injury. *Journal of neurotrauma* 28, 1611-1682 (2011).

16   Hill, C. E., Moon, L. D., Wood, P. M. & Bunge, M. B. Labeled Schwann cell transplantation: cell loss, host Schwann cell replacement, and strategies to enhance survival. *Glia* 53, 338-343 (2006).

17   Chen, A., Xu, X. M., Kleitman, N. & Bunge, M. B. Methylprednisolone administration improves axonal regeneration into Schwann cell grafts in transected adult rat thoracic spinal cord. *Experimental neurology* 138, 261-276 (1996).

18   Chew, S. Y., Mi, R., Hoke, A. & Leong, K. W. The effect of the alignment of electrospun fibrous scaffolds on Schwann cell maturation. *Biomaterials* 29, 653-661 (2008).

19   Hurtado, A. *et al.* Poly (D, L-lactic acid) macroporous guidance scaffolds seeded with Schwann cells genetically modified to secrete a bi-functional neurotrophin implanted in

the completely transected adult rat thoracic spinal cord. *Biomaterials* 27, 430-442 (2006).

20   Svenson, S. & Tomalia, D. A. Dendrimers in biomedical applications—reflections on the field. *Advanced drug delivery reviews* (2012).

21   Oliveira, J. M., Salgado, A. J., Sousa, N., Mano, J. F. & Reis, R. L. Dendrimers and derivatives as a potential therapeutic tool in regenerative medicine strategies—a review. *Progress in Polymer Science* 35, 1163-1194 (2010).

22   Oliveira, J. M. *et al.* Surface engineered carboxymethylchitosan/poly (amidoamine) dendrimer nanoparticles for intracellular targeting. *Advanced Functional Materials* 18, 1840-1853 (2008).

23   Cerqueira, S. R. *et al.* Microglia Response and In Vivo Therapeutic Potential of Methylprednisolone-Loaded Dendrimer Nanoparticles in Spinal Cord Injury. *Small* (2012).

24   Morrissey, T. K., Kleitman, N. & Bunge, R. P. Isolation and functional characterization of Schwann cells derived from adult peripheral nerve. *The Journal of neuroscience* 11, 2433-2442 (1991).

25   Cerqueira, S. R. *et al.* Electrophysiological quantification of cellular internalization, retention and exocytosis of drug-loaded dendrimer nanoparticles in astrocytes. *submitted* (2013).

26   Shin, E. *et al.* Membrane potential mediates the cellular binding of nanoparticles. *Nanoscale* (2013).

27   Fernandez-Valle, C., Fregien, N., Wood, P. M. & Bunge, M. B. Expression of the protein zero myelin gene in axon-related Schwann cells is linked to basal lamina formation. *Development* 119, 867-880 (1993).

28   Paino, C., Fernandez-Valle, C., Bates, M. & Bunge, M. Regrowth of axons in lesioned adult rat spinal cord: promotion by implants of cultured Schwann cells. *Journal of neurocytology* 23, 433-452 (1994).

29   Oudega, M., Xu, X. M., Guénard, V., Kleitman, N. & Bunge, M. B. A combination of insulin-like growth factor-I and platelet-derived growth factor enhances myelination but diminishes axonal regeneration into Schwann cell grafts in the adult rat spinal cord. *Glia* 19, 247-258 (1997).

SECTION IV

CHAPTER VIII

General Conclusions and Final Remarks

Chapter VIII

General Conclusions and Final Remarks

Tissue engineering as the field that brings together physics, materials science, biology, chemistry and medicine is promising the development of enhanced strategies to restore, maintain and improve tissue function. One of the major challenges in regenerative medicine nowadays is central nervous system (CNS) repair, due to the complexity of the nervous tissue as well as the cascade of reactions that follow injury and disease. However, the body of knowledge regarding neurodegeneration following neurotrauma has considerably evolved in the last decades, unraveling new therapeutic targets and providing a more complete understanding of the spatiotemporal post-injury processes. Based on tissue engineering concepts and approaches a novel strategy to protect the spinal cord following injury, while providing an appropriate environment for regeneration has been proposed in this work. In order to overcome the current constraints on drug delivery to CNS, particularly following spinal cord injury (SCI), it has been proposed the use of a drug delivery system that can act intracellularly on glial cells. Glial cells, particularly astrocytes and microglia, are some of the main responsible cells for the deleterious and inhibitory reactions that follow SCI and obstruct nerve regeneration. A concerted strategy that tackles specific modulation of these cells could improve the lesion environment and provide the means for regeneration to occur.

The main aim of this thesis was to design and explore the potential of a dendrimer-based multifunctional nanocarrier in SCI protection and repair. Drug delivery targeting neuroprotection during secondary injury reactions is the main point of action for the developed nanoparticle system, since this is the first opportunity to act on the lesion site in an attempt to prevent further damage. Thus, the therapeutic potential of MP-loaded CMCht/PAMAM dendrimer nanoparticles as intracellular drug delivery systems has been assessed both *in vitro* and in relevant animal models. MP has shown to promote functional recovery following SCI, but it presents serious adverse side effects in patients. In order to overcome this problem, MP was incorporated in a nanoparticle-based DDS to intracellularly deliver the corticosteroid to glial cells. The main

objective of this approach is the maximization of neuroprotection and repair, while at the same time minimizing peripheral damage.

In the work herein described, the CMCht/PAMAM dendrimer nanoparticles were initially multi-functionalized: (i) with a targeting ligand, to evaluate desired targeting features; (ii) loading MP and evaluating the profile release of the drug; and (iii) binding a fluorescent probe to allow intracellular tracking of the nanoparticles.

In Chapter III the conjugation and characterization of CD11b antibody functionalized nanoparticles was performed. For the first time CMCht/PAMAM dendrimers were successfully linked to a cell-targeting agent, in this case specifically recognizing microglia cell membrane receptors. The addition of CD11b antibody was confirmed by spectroscopic techniques, and revealed to be biocompatible in primary glial cell cultures. Significant differences in the NP uptake profile were found after CD11b antibody conjugation. Preferential internalization in microglial cells was observed, with visible reduction of the NP internalization in astrocytes and oligodendrocytes. It was thus provided an initial proof-of-concept for the targeted drug delivery using this nanoparticle system, reporting for the first time altered uptake of the multifunctional CMCht/PAMAM dendrimer nanoparticles. In the case of MP delivery for SCI application this can be of utmost relevance, since this corticosteroid has already shown to have the ability to modulate astrocyte and microglia inflammatory actions.

Next, in Chapter IV the analysis of the interaction of MP-loaded CMCht/PAMAM dendrimer nanoparticles with the astrocyte cell membrane, in order to investigate endocytic and exocytotic transport, has been performed. Patch-clamp electrophysiology has demonstrated to be a relevant technique to take into consideration for similar studies, providing reliable quantitative temporal information on the formation and fusion of vesicles in the cell membrane following NP incubation. From the obtained data, it was observed that incubation with MP-loaded CMCht/PAMAM dendrimer nanoparticles contribute to the stimulation of exocytotic vesicle formation, indicating that after its intracellular action the nanoparticles are extensively cleared out from the target cells. This fact decreases the possibility of eventual long-term nanoparticle toxicity, which brings additional advantages for the therapeutic use of this nanoparticle system. Live astrocyte confocal imaging confirmed that the NPs are indeed transported in exocytotic vesicles, being the first time that it has been directly reported. Investigation of the intracellular NP trafficking mechanisms provides essential information in understanding how these nanocarriers interact with biological

systems, and may open up new possibilities for therapeutic actions in SCI repair. It has been proposed an innovative combination of a reliable quantitative technique (patch-clamp electrophysiology) and a visual qualitative methodology (live confocal imaging) to thoroughly investigate uptake and NP clearance. It is expected that more studies using these techniques and profoundly investigating nanoparticle intracellular trafficking will be performed in the future.

From these *in vitro* results, a CNS biodistribution study was conducted in healthy rats to predict where the NPs tend to accumulate when dispersed in the cerebrospinal fluid (CSF), in direct contact with the CNS, overcoming the BBB. In chapter V, we demonstrate that the MP-loaded CMCht/PAMAM dendrimer nanoparticles broadly diffuse in the brain parenchyma and are intracellularly retained 72 hours post-CSF injection. Moreover, protein expression analysis has revealed up-regulation of the glucocorticoid receptor confirming MP intracellular release and action through the expected GR activation pathway. No visible morphological alterations were detected in the brain tissue. The obtained data have confirmed the functionality of MP-loaded CMCht/PAMAM dendrimer nanoparticles as efficient nanocarriers that not only transport MP intracellularly but also preserved its integrity thus allowing intracellular action. Its broad diffusion in the brain brings the possibility of additional therapeutic applications, namely in brain neurodegenerative disorders and traumatic brain injury or stroke.

An *in vivo* proof-of-concept in an animal model of SCI was then performed following an initial physicochemical evaluation of the MP-loaded CMCht/PAMAM dendrimer nanoparticles, as described in Chapter VI. MP-loaded nanoparticles proved to be stable in physiological conditions. Furthermore, a prolonged and sustained release of MP was measured during 14 days using chromatographic analysis. Internalization in primary glia was confirmed, and successful modulation of microglia proliferation was possible testing higher dosages of the MP-loaded CMCht/PAMAM dendrimer nanoparticles added to pure primary cultures. Finally, MP-loaded nanoparticles were locally administered following spinal thoracic hemisection and significant locomotor improvements were detected in the treated animals. The MP-loaded nanoparticles have induced faster and more prominent hind-limb motor recovery, confirming the benefits of delivering MP in a local sustained manner, via a nanoparticle drug delivery system such as the one proposed herein.

Based on these encouraging results, Chapter VII addresses a preliminary assessment of the potential therapeutic combination of MP-loaded CMCht/PAMAM dendrimer nanoparticle

administration and Schwann cell transplantation. It is proposed the simultaneous use of these two strategies aiming at: (i) modulating the secondary injury inflammatory reactions; and (ii) providing the trophic needs and support that Schwann cells have shown to supply, for regeneration to occur. MP-loaded CMCht/PAMAM dendrimer nanoparticles do not alter Schwann cell morphology or typical arrangement when cultured. Moreover, nanoparticle internalization profile has resembled the previously described glia uptake profile. Myelination studies in co-cultures of Schwann cells and dorsal root ganglia neurons exposed to MP-loaded CMCht/PAMAM dendrimer nanoparticles have revealed extensive myelination was, with no differences to the control conditions. The combination of these two strategies may prove to be useful in more effective treatments for SCI.

As final remarks, the work performed and described in this thesis presents an innovative tissue engineering-based strategy for SCI neuroprotection suggesting that a sustained local MP delivery via specifically designed nanocarriers can bring tremendous advantages in SCI repair and tissue regeneration. It is expected that more studies following the herein proposed strategy will follow, to confirm the suitability of nanotechnology-based strategies in drug delivery to the injured spinal cord. Moreover, an original combination of methodologies to investigate NP intracellular trafficking has been presented that may impact the field prompting its use in the scientific community in order to obtain more robust data on this matter. Finally, therapeutic assessment of this system in more relevant injury models, such as rodent contusion models and primate pre-clinical testing, should be performed next to validate the herein obtained results. Moreover, nerve regeneration and reconnection should be further investigated in the previously referred models as well as motor recovery and sensory testing, to fully evaluate the recovery following SCI. Finally, the investigation of the proposed combination of nanoparticle administration and Schwann cell transplantation could bring new benefits in SCI therapies and should also be more thoroughly addressed.